Mechanistic regulation of gastroesophageal junction and role of retinoic acid in the development of Barrett's esophagus

Mechanistische Regulierung des gastroösophagealen Übergangs und die Rolle der Retinsäure bei der Entwicklung des Barrett-Ösophagus.

Doctoral thesis for a doctoral degree
at the Graduate School of Life Sciences,
Julius-Maximilians-Universität Würzburg,
Section Infection and Immunity

Submitted by
Naveen Kumar Nirchal

From
Nirchal, Kerala, India

Würzburg October 2022

Submitted on:

.....

Office stamp

Members of the Thesis Committee

Chairperson:	Prof. Dr. Christian Janzen
Primary Supervisor:	Dr. Cindrilla Chumduri
Supervisor (Second):	Prof. Dr. Markus Engstler
Supervisor (Third):	Prof. Dr. Thomas F. Meyer
Supervisor (Fourth):	Prof. Dr. med. F. Seyfried

List of Contents

1 Zusammenfassung

Der gastroösophageale Übergang (GEJ), der die Region abgrenzt, in der der distale Ösophagus auf die proximale Magenregion trifft, ist bekannt für die Entwicklung pathologischer Zustände, wie Metaplasie und Adenokarzinom des Ösophagus (EAC). Es ist wichtig, die Mechanismen der Entwicklungsstadien zu verstehen, die zu EAC führen, da die Inzidenzrate von EAC in den letzten 4 Jahrzehnten um das 7-fache gestiegen ist und die Gesamtüberlebensrate von 5 Jahren 18,4 % beträgt. In den meisten Fällenwird die Diagnose im fortgeschrittenen Stadium ohne vorherige Symptome erstellt. Der Hauptvorläufer für die Entwicklung von EAC ist eine prämaligne Vorstufe namens Barrett-Ösophagus (BE). BE ist der metaplastische Zustand, bei dem das mehrschichtige Plattenepithel des nativen Ösophagus durch ein spezialisiertes einschichtiges Säulenepithel ersetzt wird, das die molekularen Eigenschaften des Magen- sowie des Darmepithels aufweist. Zu den wichtigsten Risikofaktoren für die Entwicklung von BE gehören die chronische gastroösophageale Refluxkrankheit (GERD), eine veränderte Mikrobiota und veränderte Retinsäure-Signalwege (RA). Es ist unklar, welche Zelle der Ursprung für BE ist, da es keine eindeutigen Beweisen für den Prozess der BE-Initiation gibt. In dieser Arbeit habe ich untersucht, wie die GEJ-Homöostase in gesundem Gewebe durch stammzellregulatorische Morphogene aufrechterhalten wird, welche Rolle der Vitamin-A (RA-Signalübertragung) spieltund wie ihre Veränderung zur BE-Entwicklung beiträgt.

Im ersten Teil meiner Dissertation habe ich anhand von Einzelmolekül-RNA in situ-Hybridisierung und Immunhistochemie eindeutig das Vorhandensein von zwei Arten von Epithelzellen nachweisen können, dem Plattenepithel in der Speiseröhre und dem Säulenepithel imMagenbereich des GEJ. Mittels Abstammungsanalysen im Mausmodell konnte ich zeigen, dass die Epithelzellen des Ösophagus und des Magens von zwei verschiedenen epithelialen Stammzelllinien imGEJ abstammen. Die Grenze zwischen Plattenepithel und Säulenepithelzellen im SCJ des GEJ wirddurch gegensätzliche Wnt-Mikroumgebungen streng reguliert. Plattenepithelstammzellen des Ösophagus werden durch das Wnt-hemmende Mikroumgebungssignal aufrechterhalten, während Magensäulenepithelzellen durch das Wnt-aktivierende Signal aus dem Stromakompartiment erhalten

werden. Ich habe die *in vivo* Erhaltung der Epithelstammzellen des GEJ mit Hilfe eines *in vitro* Epithel-3D-Organoidkulturmodells rekonstruiert. Das Wachstum und die Vermehrung von Magensäulenepithel-Organoiden hängen von Wnt-Wachstumsfaktoren ab, während das Wachstum von Plattenepithel-Organoiden von Wnt-defizienten Kulturbedingungen abhängt. Darüber hinaus zeigte die Einzelzell-RNA-Sequenzanalyse (scRNA-seq) der aus Organoiden gewonnenenEpithelzellen, dass der nicht-kanonische Wnt/ planar cell polarity (PCP) Signalweg an der Regulierung der Plattenepithelzellen beteiligt ist. Im Gegensatz dazu werden säulenförmige Magenepithelzellen durch den kanonischen Wnt/beta-Catenin- und den nicht-kanonischen Wnt/Ca^{2+}-Weg reguliert. Meine Daten zeigen, dass die SCJ-Epithelzellen, die am GEJ verschmelzen, durch entgegengesetzte stromale Wnt-Faktoren und unterschiedliche Wnt-Weg-Signalee in den Epithelzellen reguliert werden.

Im zweiten Teil der Dissertation untersuchte ich die Rolle der bioaktiven Vitamin A Verbindung RA auf Ösophagus- und Magenepithelstammzellen. Die In-vitro-Behandlung von epithelialen Organoiden der Speiseröhre und des Magens mitRA oder seinem pharmakologischen Inhibitors BMS 493 zeigte, dass jeder Zelltyp unterschiedlich reguliert wurde. Ich beobachtete, dass eine verstärkte RA die Differenzierung von Stammzellen und den Verlust der Schichtung förderte, während die RA-Hemmung zu einer verstärkten Stammzellbildung und Regeneration im mehrschichtigen Epithel der Speiseröhre führte. Im Gegensatz zur Speiseröhre ist der RA-Signalweg in Magen-Organoiden aktiv, und die Hemmung von RA hat ein reduziertes Wachstum von Magen-Organoiden. Globale transkriptomische Daten und scRNA-seq-Daten zeigten, dass derRA-Signalweg einen Ruhephänotyp in den Ösophaguszellen induziert. Dagegen führt das Fehlen von RA in Magenepithelzellen zur Expression von Genen, die mit BE assoziiert sind. Daher isteine räumlich definierte Regulation der Wnt- und Retinsäure-Signalgebung amGEJ entscheidend für eine gesunde Homöostase, und ihre Störung führt zur Entwicklung von Krankheiten.

2 Abstract

Gastroesophageal junction (GEJ), demarcating the region where the distal esophagus meets with the proximal stomach region, is known for developing pathological conditions, including metaplasia and esophageal adenocarcinoma (EAC). It is essential to understand the mechanisms of developmental stages which lead to EAC since the incidence rate of EAC increased over 7-fold during the past four decades, and the overall five years survival rate is 18.4%. In most cases, patients are diagnosed in the advanced stage without prior symptoms. The main precursor for the development of EAC is a pre-malignant condition called Barrett's esophagus (BE). BE is the metaplastic condition where the multilayered squamous epithelium of the native esophagus is replaced by specialized single-layered columnar epithelium, which shows the molecular characteristics of the gastric as well as intestinal epithelium. The main risk factors for BE development include chronic gastro-esophageal acid reflux disease (GERD), altered microbiota, and altered retinoic acid signaling (RA). The cell of origin of BE is under debate due to a lack of clear evidence demonstrating the process of BE initiation. Here, I investigated how GEJ homeostasis is maintained in healthy tissue by stem cell regulatory morphogens, the role of vitamin A (RA signaling), and how its alteration contributes to BE development.

In the first part of my thesis, I showed the presence of two types of epithelial cells, the squamous type in the esophagus and the columnar type in the stomach region in the GEJ, using single-molecule RNA in situ hybridization (smRNA-ISH) and immunohistochemistry. Employing lineage tracing in the mouse model, I have demonstrated that the esophageal epithelial and stomach epithelial cells derived from two distinct epithelial stem cell lineages in the GEJ. The border between squamous and columnar epithelial cells in the Squamo-columnar junction (SCJ) of GEJ is regulated by opposing Wnt microenvironments. The regeneration of stomach columnar epithelial stem cells is maintained by Wnt activating signal from the stromal compartment while squamous epithelial stem cells of the esophagus are maintained by the Wnt inhibitory signals. I recapitulated the *in vivo* GEJ epithelial stem cell maintenance by using *in vitro* epithelial 3D organoid culture model. The growth and propagation of stomach columnar epithelial organoids depend on Wnt

growth factors, while squamous epithelial organoids' development needs Wnt-deficient culture conditions.

Further, single-cell RNA sequence (scRNA-seq) analysis of organoid-derived epithelial cells revealed the non-canonical Wnt/ planar cell polarity (PCP) pathway involvement in regulating the squamous epithelial cells. In contrast, columnar stomach epithelial cells are regulated by the canonical Wnt/ beta-catenin and non-canonical Wnt/Ca^{2+} pathways. My data indicate that the SCJ epithelial cells that merge at the GEJ are regulated by opposing stromal Wnt factors and distinct Wnt pathway signaling in the epithelial cells.

In the second part of the thesis, I investigated the role of Vitamin A-derived bioactive compound RA on esophageal and stomach epithelial stem cells. *In vitro* treatment of esophageal and stomach, epithelial organoids with RA or its pharmacological inhibitor BMS 493 revealed that each cell type was regulated distinctly. I observed that enhanced RA promoted esophageal stem cell differentiation and loss of stratification, while RA inhibition led to enhanced stemness and regeneration of the esophagus stratified epithelium. As opposed to the esophagus, RA signaling is active in the stomach organoids, and inhibition of RA reduces the growth of stomach organoids. Global transcriptomic data and scRNA-seq data revealed that RA signaling induces dormancy phenotype in the esophageal cells. In contrast, the absence of RA in stomach epithelial cells induces the expression of genes associated with BE. Thus, spatially defined regulation of Wnt and RA signaling at GEJ is critical for healthy homeostasis, and its perturbation leads to disease development.

3 Introduction

3.1 Gastroesophageal junction in the human and mouse

The esophagus is a hollow tube that connects the upper throat to the stomach. The function of the esophagus involves the passage of food and liquid to the stomach by esophageal muscular contraction called peristalsis. The average length of the esophagus in adult humans from the distal upper esophageal sphincter to the proximal lower esophageal sphincter is 21.2cm (Marshall et al. 1999), and in mice, 2.8 cm (Breuer, Neuhuber, and Wörl 2004). The esophagus consists of four layers, Mucosa, Submucosa, Muscularis propria, and Adventitia/Serosa (Figure 1A). The mucosal layer consists of stratified squamous epithelium, lamina propria, and muscular mucosae. The submucosal layer consists of esophageal glands (in humans but not rodents), blood vessels, and nerve plexus. Muscularis propria consists of inner circular and outer longitudinal muscle fibers composed of smooth and striated muscles. The composition of the type of muscle varies from the upper region of the esophagus to the lower part. The upper region consists of two layers of striated muscle, the middle region consists of a mixture of striated muscle and smooth muscle, and the lower region consists of two layers of smooth muscle (Yazaki and Sifrim 2012). These muscle layers are involved in the peristalsis during the swallowing process. The adventitial layer forms the connective tissue surrounding the esophagus above the diaphragm, and the serosa layer present below the diaphragm contains lymphatic vessels and nerve fascicles (Staller and Kuo 2013).

The stomach is a J-shaped muscular sac between the esophagus and the lower duodenum. Broadly stomach is divided into four regions, cardia, fundus, body, and pylorus. Microscopically, the stomach consists of layers similar to the esophagus, including mucosa, submucosa, muscularis externa, and serosa (Figure 1B). The mucosa consists of the gastric pit, single-layered columnar epithelial cells, lamina propria, and muscular mucosae. The submucosa is made of connective tissues consists nerve plexus, whereas muscularis externa consists of oblique (innermost), circular (middle), and longitudinal (outer) muscle layers along with myenteric nerve plexus. The outermost region, serosa, consists of mesothelium and connective tissue (Chaudhry SR 2021).

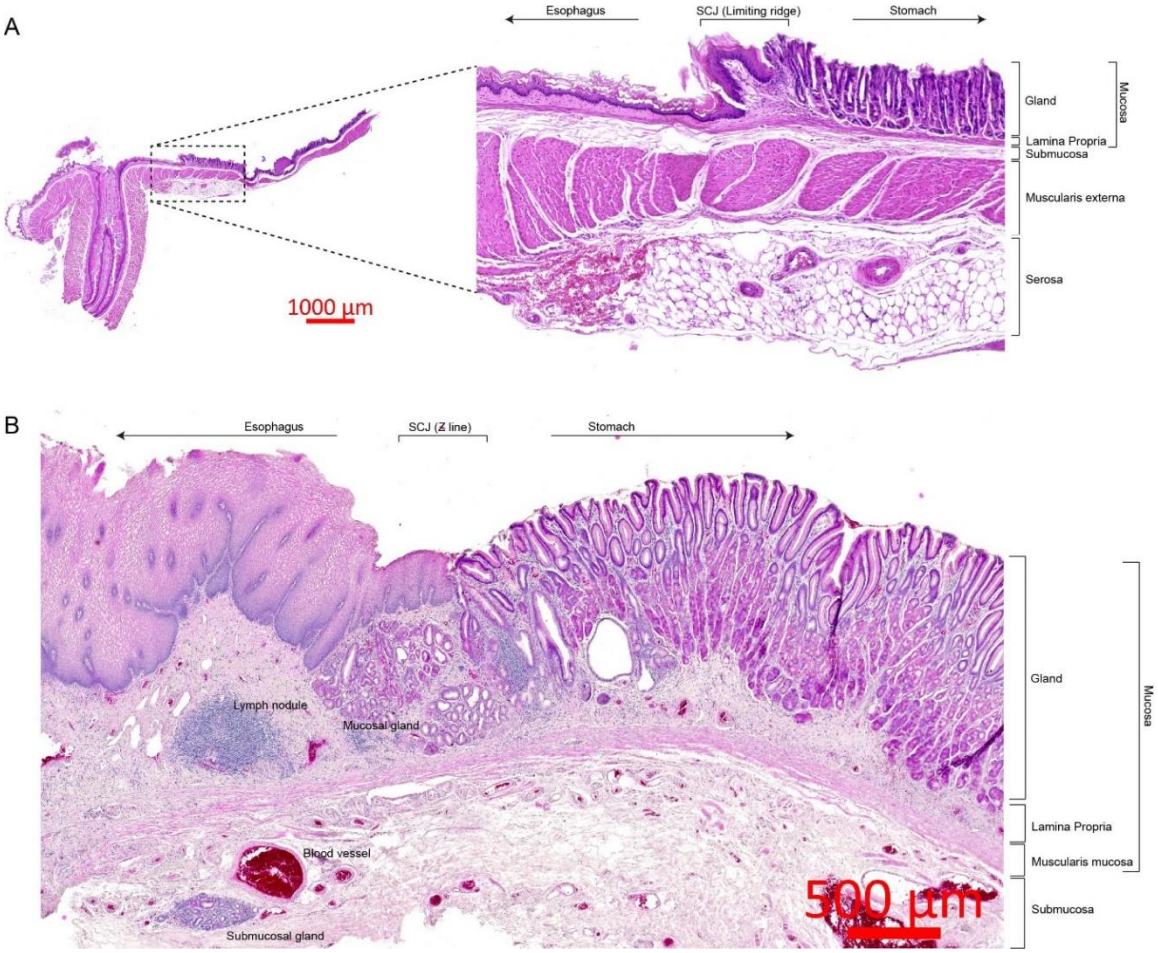

Figure 1. Histological anatomy of mouse and human GEJ. (A) H&E stained GEJ of mouse depicting the esophagus and stomach regions with limiting ridge containing SCJ. The tissue is anatomically divided into upper mucosa containing epithelial cell layers and muscularis mucosa, submucosa, muscularis externa, and serosa. The esophagus tissue is devoid of the submucosal gland and contains cornified layers in the uppermost region of the mucosa. **(B)** H&E stained the GEJ of humans depicting the esophagus and stomach regions with a Z line containing an SCJ. The mucosa of the esophagus consists of 20 to 30 layers of stratified squamous epithelium while the stomach consists of columnar epithelial glandular units. In the SCJ region lamina propria contain mucosal glands and submucosa contain submucosal glands.

3.2 Epithelial cells.

The inner lining of the esophagus is covered by multilayered squamous epithelial cells. Their thickness in humans varies from 20 to 30 layers, while in mice, 4 to 6 layers (Zhang et al. 2017). Turnover of epithelial cells in humans is approximately 11 days, while in mice, it is every 3.5 days. The epithelial

layers are broadly categorized into basal, parabasal, suprabasal, and terminally differentiated regions. The basal region consists of a single-layered stem cell population generally p63+ and KRT5+ which occasionally divides by asymmetric division, giving rise to one basal daughter cell and differentiating daughter cells in response to cues from the underlying basement membrane (Seery and Watt 2000). It was proposed that these basal layers either contain single progenitor cells (homogenous) or different cells expressing distinct stem cell markers (heterogenous) (Zhang et al. 2021). The parabasal layer consists of proliferating cells and cells undergoing terminal differentiation forming the active epithelial compartment. The superficial layer contains terminally differentiated cells that are undergoing enucleation and exfoliation. In the case of mice, the proliferating cells and stem cells are confined only to the basal region. The terminally differentiated cells in the mice undergo cornification and form a protective layer in the esophagus lumen, which is absent in the human esophagus (Deo and Deshmukh 2018). In rodents, the squamous epithelium extends and covers part of the stomach forming the forestomach.

The inner lining of the esophagus is covered with mucous secreted by the esophageal submucosal glands that lie in the submucosa connective tissue, which is absent in the mice. The mucous defends the epithelial against gastroesophageal reflux by neutralizing acid. Mucus comprises bicarbonate, non-bicarbonate buffer, mucin, prostaglandin E2, EGF, and TGFa, which neutralize acid and pepsin (Sarosiek and McCallum 2000). The submucosal gland consists of duct cells, oncocytes, mucous acini, and myoepithelial cells (al Yassin and Toner 1977). Ductal cells consist of squamous epithelial cells expressing p63+KRT5+KRT7+, oncocytes containing columnar type cells expressing KRT8+KRT7+, and mucous acini containing cells expressing KRT8+KRT7+MUC5b. Myoepithelial cells expressing α-SMA+p63+KRT5+ (Nowicki-Osuch et al. 2021) cover mucous acini and oncocytes.

The stomach surface region is covered with single-layered KRT8+ columnar epithelial cells, which are invaginated into a glandular unit creating deep depressions called pits on the surface (Figure 2). Two types of glandular units are found in the stomach, the cardia or pyloric gland in the gastric cardia and pylorus region and the gastric gland in the body and fundus. The columnar epithelial cell types change along the region of the stomach gland. The stomach

glands are divided into base, neck, isthmus, and pit regions. The basal region comprises mucous-secreting cells, digestive-enzyme-secreting chief cells, hormone-secreting endocrine cells, and stem cells. The neck region consists of mucous neck cells and acid-secreting parietal cells, while the isthmus region consists of undifferentiated proliferating cells involved in the continuous turnover of epithelia. The larger portion of the gland unit is covered on the surface by differentiated mucous-secreting pit /foveolar cells. In the case of the pyloric gland, they are shorter in length and have fewer parietal cells than the gastric gland, and parietal cells are absent in the mouse antrum (Choi et al. 2014, Willet and Mills 2016).

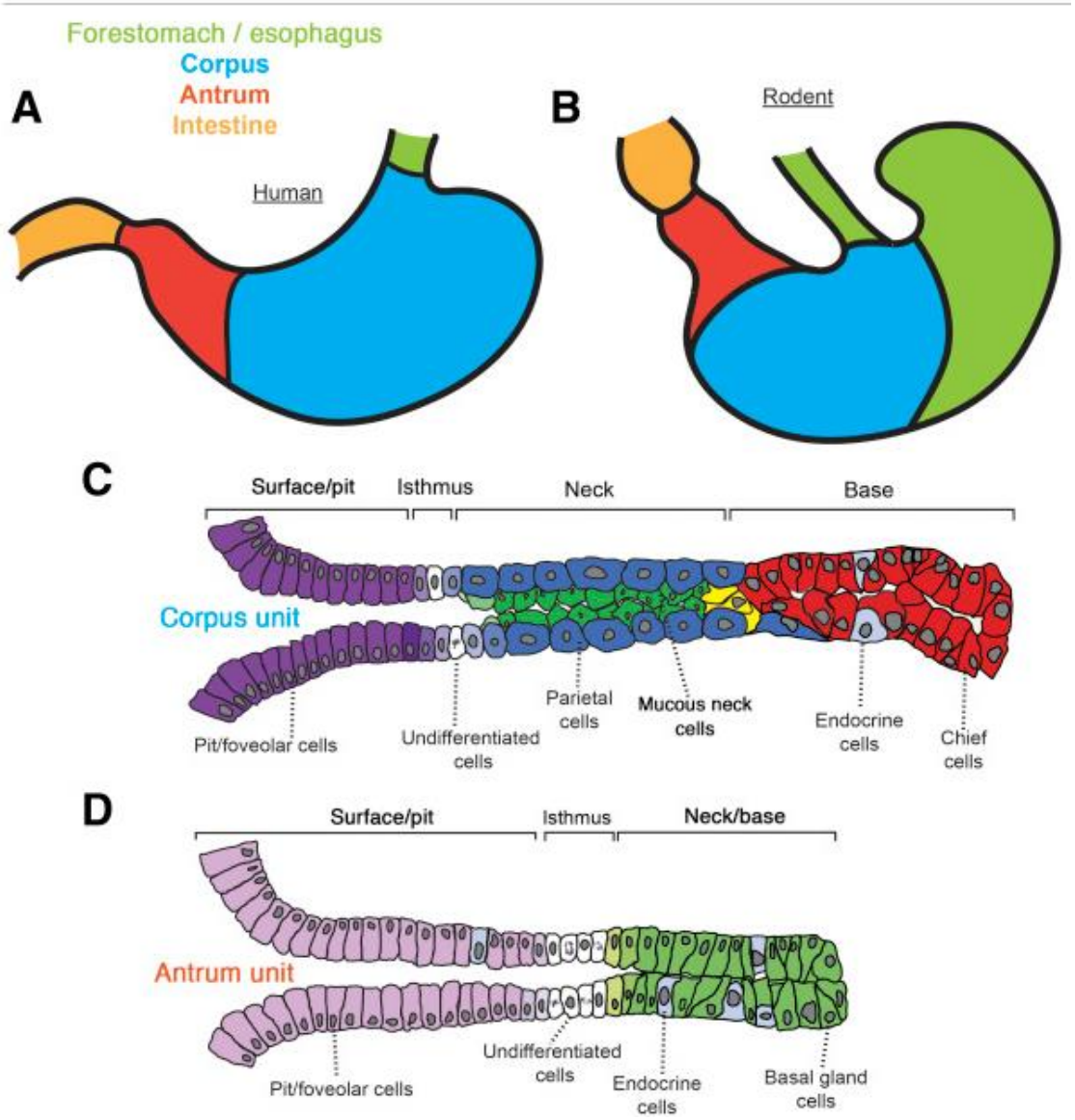

Figure 2. Cellular composition of stomach glands. (A-B) Diagram showing human stomach (A) with entire region covered by columnar epithelial glandular units (blue) and rodent stomach

(B) containing both squamous epithelia lined forestomach (green) and columnar epithelial glandular units (blue). **(C)** Cellular composition of corpus epithelial glandular unit containing base stem cell region, mucous and acid-secreting neck cell region, proliferative isthmus region, and the differentiated cell containing pit region. **(D)** Cellular composition of antral gland unit containing Neck/base, isthmus, and pit regions. Source: (Willet and Mills 2016)

3.3 Gastroesophageal junction

GEJ is the epithelial transition region of the multilayered squamous epithelium of the esophagus with the single-layered columnar epithelium of the stomach. The meeting point of squamous epithelium and columnar epithelial cells is called the SCJ or Z line in humans and "limiting ridge" or "gastric grove" in rodents (Luciano and Reale 1992, Eberle et al. 2013). The position of Z-line changes in pathological conditions such as GERD and BE (Odze 2005). The epithelial cells in the SCJ are shown to contain specialized progenitor types of cells. These cells include either residual embryonic origin cells expressing KRT7+ (Wang et al. 2011) or the presence of transitional basal cells expressing p63+KRT5+KRT7+ markers (Jiang et al. 2017). The squamous epithelial cells in the SCJ show higher expression of KRT7 in mice which is not observed in the human SCJ, instead it is present near the submucosal gland in the human GEJ (Jiang et al. 2017), (Nowicki-Osuch et al. 2021). The first columnar stomach gland in the GEJ, called the cardiac gland, has mucous-secreting cells and lacks parietal cells. A similar gland was also shown in the rodents, which lack parietal cells and consist of cells expressing MUC4, EPCAM, and DCLK1 (O'Neil, Christine P Petersen, et al. 2017). This gland may involve the secretion of hormones and paracrine sensory signaling (Eberle et al. 2013).

3.4 Development of esophagus and stomach

The esophagus and stomach are derived from the early foregut region. During the early stage of development, the esophagus and lung originate from the anterior foregut endoderm tube, which is later separated by the respiratory-

esophageal separation (RES) process (Que 2015) (Figure 3). The expression pattern of *Sox2* in the dorsal region and *Nkx2.1* in the ventral region of the anterior foregut specify future esophagus and lung, respectively (Trisno et al. 2018, Que et al. 2007). The BMP pathway inhibition by antagonist *Noggin* expressed by endodermal cells is required to regulate *Sox2* expression, thereby specification into the esophagus. In contrast, *Sox2* suppression by BMP specifies lung in the early anterior foregut (Que et al. 2006, Domyan et al. 2011). The canonical Wnt pathway genes *Wnt2*, *Wnt2*b, and *Barx1* are regulated by SHH secreted by endodermal cells. Further, RA regulates endodermal SHH and ventral mesodermal *Wnt2* and *Wnt2b* expression to induce differentiation of the ventral foregut into the lung (Rankin et al. 2016). The active Wnt signaling inhibits esophageal specification. This was shown by conditional deletion of the β-catenin gene (*Ctnnb1*), resulting in only *Sox2* expressing esophageal progenitor cells in the foregut tube. In contrast, conditional Wnt activation induces lung progenitor cells in the esophagus and stomach (Goss et al. 2009, Harris-Johnson et al. 2009). Supporting this, *Barx1*, which induces Wnt inhibitor *Sfrp1*, *Sfrp2* is highly expressed in the esophagus and stomach mesoderm and is involved in the early separation of the esophagus from the lung (Woo et al. 2011). The dorsal mesodermal expression *Fgf10* regulates RES separation by upregulating *Nkx2.1* and down-regulation of *Sox2* (Que et al. 2007). Further, the transcription factor *Isl1* also plays a critical role in RES by regulating *Nkx2.1* expression (Kim et al. 2019).

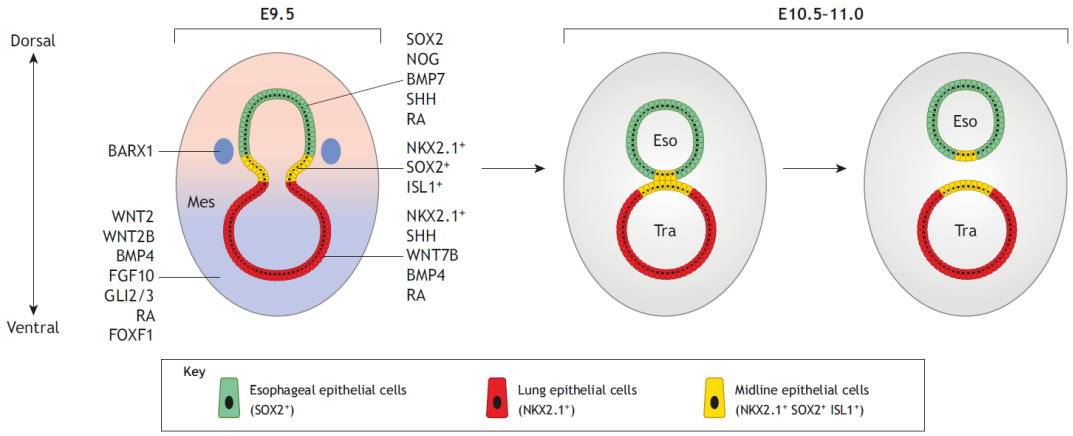

Figure 3. Signaling regulating the specification of the esophagus in the foregut. At E9.5, dorsal endoderm is specified by the expression of *Sox2, Nog, Bmp7, Shh,* and RA signaling, while ventral endoderm is specified by the expression of *Nkx2.1, Shh, Wnt7b, Bmp4,* and RA

signaling from epithelial and *Wnt2/2b, Bmp4, Fgf10, Gli2/3, Foxf1,* and RA signaling from mesenchymal cells. Middle-line epithelial cells co-express *Nkx2.1, Sox2,* and *Isl1* while dorsal mesenchymal cells express *Barx1.* At E10.5-11.0, dorsal and ventral endoderm separated into esophagus and trachea respectively. Source: (Zhang et al. 2021)

Initially, on an embryonic day E9.5, the entire esophagus region is lined by columnar-type esophageal epithelial progenitor cells expressing KRT8+p63-. Between embryonic days E10.5 and E14.5, the inhibition of BMP by *Noggin* and low Wnt activity induce progenitor cells to express p63 and squamification. This is supported by the observation that deletion of *Noggin* induces columnar lined glandular units in the esophagus (Rodriguez et al. 2010). However, active BMP signaling is required to differentiate stratified layers of squamous epithelial cells. The loss of expression of suprabasal markers loricrin and involucrin was observed in the conditional deletion of BMPr1a (Rodriguez et al. 2010). The Notch pathway is also involved in the stratification of esophageal epithelial cells. The Notch ligands Jag1, Jag2, and receptors are shown to express in the early esophagus, where inhibition of the Notch pathway reduces the esophageal stratification.

Like the esophagus, the stomach region is lined by single-layered columnar gastric progenitor cells in the early embryonic days. The regional identity of the stomach region is demarcated by the patterned expression of *Sox2*, *Gata4*, and *Pdx1* transcription factors in the gastric progenitor cells. *Sox2* expression in the entire foregut region governs the development of the lung, esophagus, and stomach. However, the boundary between the esophagus and stomach is defined by the expression of *Gata4*, which specifies the glandular stomach—deleting *Gata4* results in the squamous epithelium in the stomach region (Jacobsen et al. 2002). The SHH ligand Indian hedgehog (*Ihh*), specifically expressed in the precursor cells of stomach epithelial cells, creates the forestomach-hind stomach SHH-IHH boundary by regulating mesenchymal *Hoxa5* (Aubin et al. 2002, Kolterud et al. 2009).

Similarly, the stomach duodenal boundary is regulated by *Sox2* and *Cdx2* transcription factors. The expression of *Sox2* in intestinal progenitor cells differentiates them into stomach cell phenotype, whereas deletion of *Cdx2* induces oesophageal epithelial cell specification in the intestine, but not

stomach epithelial cells (Raghoebir et al. 2012, Gao, White, and Kaestner 2009). Further, the antrum region is specified by the transcription factor *Pdx1*, which is also involved in the differentiation of other tissues, such as the anterior duodenum, pancreatic bud, and biliary system (Offield et al. 1996). *Pdx1* expression is regulated by the *Tcf2/Hnf1b*, whose deletion is shown to down-regulate the *Pdx1* expression and deregulates the stomach specification (Haumaitre et al. 2005). The epithelial and stromal cross-interaction also regulates the homeostasis and regulation of growth of both regions. The BMP and *Fgf10* secreted by the stromal region are required for epithelial proliferation and gland development. Similarly, the SHH/IHH singling from epithelial cells regulates stromal cell differentiation and growth (Zhang and Que 2020, Nyeng et al. 2007, Spencer-Dene et al. 2006, Ramalho-Santos, Melton, and McMahon 2000). In mice, the initiation of gland formation and lineage differentiation of stomach epithelial progenitor cells begins from E-14.5. It results in the appearance of parietal cells, chief cells, mucous neck cells, and enteroendocrine cells (Nyeng et al. 2007).

3.5 Gastroesophageal junction disease: Types and pathology

Esophageal cancer (EC) represents the seventh most common cancer by incidence rate and sixth most common by mortality rate worldwide. EC most commonly occurs in males and is frequently reported in eastern and southern African countries (Bray et al. 2018). Esophageal cancer can be broadly divided into two categories based on histological types: esophageal squamous cell carcinoma (ESCC) and esophageal adenocarcinoma (EAC). The squamous type of epithelial cells characterizes ESCC. ESCC occurs in the upper and middle part of the esophagus tube and rarely in the GEJ. ESCC is mainly associated with alcohol consumption and smoking; however, the trend in incidence rate declined globally (Wang et al. 2018).

As opposed to ESCC, the EAC incidence rate is increasing at an alarming rate and is associated with GERD and obesity. EAC incidence is frequently observed in high-income countries where ESCC is shown to have a reduced incident rate (Arnold et al. 2017). EAC occurs in the GEJ region of the lower part of the

esophageal tube. The incidence rate of EAC increased over 7-fold during the past four decades, and the overall five years survival rate is 18.4% (Cook and Thrift 2021, Cook and Thrift 2021). The EAC is most commonly observed in males over 50 years, and in most cases, the EAC is diagnosed in the later stage. EAC is characterized by the columnar type of epithelial cells and the presence of specialized intestinal metaplasia (IM) (Spechler et al. 2011). The main risk factor for EAC development is the presence of a metaplastic condition called BE in the GEJ (Curtius et al. 2020). Considering the rapidly increasing rate of EAC incidence since the 1970s, it is an important task to delineate the mechanism of BE development (Hur et al. 2013).

3.6 Barrett's esophagus epidemiology and pathogenesis

BE is the metaplastic condition where the squamous epithelial cells of the distal esophagus are replaced by the columnar-type epithelial cells in response to chronic GERD, obesity, and microbiota alterations. Initially, in 1950, Norman Barrett described the metaplastic condition as a 'peptic ulcer of esophagus lined by columnar epithelium; later, it was named after his name (BARRETT 1950). The main risk factor for BE development is GERD. BE is an adaptive response to the esophageal injury caused by the harsh contents of GERD refluxate. The mucous-secreting BE epithelia withstand the harsh environment of GERD than squamous epithelial cells, thereby giving more advantage of protection for mucosal lining (Reid, Kostadinov, and Maley 2011, Odze et al. 2021). Even though BE is asymptomatic, the prevalence in the general population ranges from 1.6% to 6.8% (Gilbert et al. 2011) and approximately 15% of people with chronic GERD (Johansson et al. 2005). According to the British Society of Gastroenterology, American College of Gastroenterology, and the European Society of Gastrointestinal Endoscopy, the presence of ≥1 cm long columnar mucosa above the GEJ in the distal esophagus is considered BE. The segment ≥3 cm and <3 cm considered long segment BE and short segment BE, respectively (Shaheen et al. 2016, Fitzgerald et al. 2014, Weusten et al. 2017, Weusten et al. 2017). The progression of BE to EAC occurs through dysplasia,

low-grade dysplasia, and high-grade dysplasia, with progression towards EAC at the rate of 0.598%, 1.69%, and 6.58% per year, respectively (Goldblum 2003, Wani et al. 2009).

BE metaplasia is broadly classified into fundic type, oxyntic type, and intestinal type, where patients present either one of the types or a mixture of gland types (McDonald, Graham, et al. 2015). The fundic or oxyntic type of cells expressing *Tff1, Tff2, Muc5ac,* and *Muc6* gradually acquire intestinal marker *Cdx2* expression along with *Tff3* and *Muc2*. Intestinal type of metaplasia can either be found as incomplete intestinal metaplasia (mixture of gastric and intestinal type) or complete intestinal metaplasia with absorptive enterocyte, paneth, and goblet cells which contains MUC2 similar to the small intestine (McDonald, Lavery, et al. 2015).

3.7 Genetic aberrations and microbiome in Barrett's esophagus

BE occurs due to an adaptive response to GERD without any driver mutation. However, through progression to dysplasia and adenocarcinoma, it acquires gene amplification or deletion events. In low-grade dysplasia, it was shown to have P53 mutation or amplification of proto-oncogenes and receptor tyrosine kinases (Yamamoto et al. 2016). Further, BE is associated with inherited genetic risk genes such as *Crtc1, Barx1, Foxp1, Foxf1, Tbx5, Gdf7, Mrsa, Aldh1a2,* and MHC shown (Gharahkhani et al. 2016), (Palles et al. 2015, Levine et al. 2013, Su et al. 2012). The analysis of 25 paired BE and EAC samples revealed the presence of *Tp53* mutation as an early event followed by a genome doubling event to acquire amplification of oncogenic genes (Stachler et al. 2015).

Recently infection of certain pathogenic bacteria has been related to the increased risk of cancer due to their oncogenic proteins and/or direct or indirect alteration of the host's inflammatory and immunological responses (Duijster et al. 2021). In the case of GERD patients with or without BE, a shift in microbiota from normal Gram-positive bacteria to a more pathogenic gram-negative bacterial population has been observed. The LPS produced from the gram-negative bacteria can induce inflammation, boosting GERD-induced

inflammation and cancer initiation (Yang et al. 2009). A similar observation was also found in the BE to EAC progression with increased potentially pathogenic bacteria (Snider et al. 2019). However, *Helicobacter pylori* (*H. pylori), a* potential causative agent of gastric cancer, has an inverse effect on BE and EAC development. This is due to the acid-neutralizing capacity of *H. pylori* and reduced ghrelin synthesis, thereby preventing obesity and reducing GERD (Xie et al. 2013). However direct involvement of pathogenic bacteria in the BE and EAC development is not well studied.

3.8 Origin and development of Barrett's esophagus

Histologically, BE shows one or a mixture of histological types such as multilayered epithelium (MLE), cardiac type metaplasia, oxyntic type metaplasia, intestinal metaplasia, submucosal glandular hyperplasia, and squamous island in the metaplastic region (Shields et al. 2001, Chandrasoma 2005, Chandrasoma 2005, Spechler and Souza 2014, Lörinc and Öberg 2012, Eleftheriadis et al. 2013). Thus, based on kind of histological types, BE shows the presence of a heterogeneous type of cell population which obscured finding the cell of origin in BE initiation. Yet, several studies postulated different hypotheses concerning the origin of cells for BE (Figure 4).

3.8.1 Esophageal squamous cell origin

Owing to the presence of columnar-lined epithelium in the esophagus region, many studies emphasized squamous epithelial cells as the source of BE by a trans-differentiation process (Tosh and Slack 2002, Tata, Chow, and Tata 2021). The MLE, characterized by the presence of a mixture of the squamous and columnar epithelium, has been shown as a precedent of columnar metaplasia (Shields et al. 1993). The MLE expresses squamous marker KRT13 and columnar markers KRT7, KRT8/KRT18, KRT19, KRT20, and mucins, suggesting cell phenotype similarity with BE cells (Glickman et al. 2001). Supporting this, MLE is specifically shown to present in the short segment BE, indicating the intermediate stage of squamous to columnar trans-differentiation (Upton et al. 2006). The expression of columnar cells related to markers KRT7 and KRT20 was also induced in the squamous epithelial cells

treated with BMP4, which is known to be upregulated in the BE (Milano et al. 2007). Stromal and epithelial signaling interactions are also involved in the trans-differentiation process. The action of acid and bile on squamous epithelial cells revealed its ability to induce the secretion of hedgehog (Hh) ligands to the stromal cells. Stromal cells, in turn, secrete BMP4 and induce the expression of *Sox9*, a transcription factor shown to be involved in the columnar differentiation in the squamous epithelial cells (D. H. Wang et al. 2010, Minacapelli et al. 2017). The conversion of the squamous to the intestinal epithelium was shown by conditional activation of *Shh*, which induced the expression of transcription factor *Foxa2*, which induced the expression of goblet-specific mucin *Muc2* and mucin processing protein *Agr2* (Wang et al. 2014). Recently it was shown that activation of HH signaling in the squamous epithelial cells induced dedifferentiation into embryonic-like esophageal progenitor cells through chromatin remodeling and *Sox9* expression (Vercauteren Drubbel et al. 2021). The transcription factor CDX2 is essential for the development and function of the lower gastrointestinal tract from the duodenum to the anus. *Cdx2* expression is commonly expressed in the later stage and intestinal metaplasia of BE. Expression of *Cdx2* under squamous cell-specific *Krt14* promotor-induced transitional type cells with secretory features resembling BE cells. The treatment of *Krt14-Cdx2* mice with DNA methyltransferase inhibitor results in the expression of BE-associated genes (*Cdx2, Cdx1, Slc26a3*) indicating that chromatin remodeling or DNA epigenetic changes might be involved in BE initiation (Kong et al. 2011).

Similarly, treatment of cultured primary keratinocytes with bile and acid increased the expression of *Bmp4*, which induced the expression of intestinal markers *Cdx2*, *Viln1* (Zhou et al. 2009). The Hepatocyte nuclear factor 4α (*HNF4α*), shown to be required for goblet cell maturation, is also expressed in BE. Its ectopic expression in mouse esophageal cells induces the expression of BE markers like *Cdx2, Tff3, Krt8*, and *Cdh1*, indicating its vital role in the initiation of BE from esophageal epithelial cells (Colleypriest et al. 2017, Singh et al. 2022). The combined overexpression of *Myc* and *Cdx1* and *Notch* inhibition induced trans-differentiation of esophageal cells towards BE through the KLF4 transcriptional factor (Vega et al. 2014). Another group postulated that inflammation induced by GERD might reprogram the squamous epithelial

cells to undergo trans commitment to BE-like cells (Minacapelli et al. 2017). Recently the loss of *Spt6* in squamous epithelial cells has been shown to reduce the differentiation into stratified epithelia and induce transdifferentiation into intestinal-like cells (Vo et al. 2021).

3.8.2 Squamo-columnar junction regional cell origin

Several studies focused on the presence of specialized cells in SCJ and proposed that these cells have the property to give rise to columnar-type cells upon injury by gastroesophageal refluxate. It was postulated that the residual embryonic progenitor epithelial cells expressing KRT7 and CAR4 are retained in the adult GEJ. These cells expand as a repair mechanism upon injury and are responsible for initiating BE. (Wang et al. 2011). Recently another group reported the presence of transitional columnar epithelium with distinct basal progenitor cells (p63+KRT5+KRT7+) at the SCJ of GEJ. *Cdx2* expression in these transitional cells under *Krt5* promotor in mice induced formation of MLE and BE phenotype. Interestingly, *Lgr5*, a known stem cell marker of stomach and BE, didn't contribute to BE development in this setup (Jiang et al. 2017). As opposed to the above theories, gastric acid stress specifically allowed the proliferation of KRT5+K15+ cells and initiation of squamous tumor from the SCJ of the forestomach region, but not from KRT7+ cells in the SCJ, which remained intact suggesting KRT7 expressing cells may not play a role in BE development during GERD (Moon et al. 2019).

3.8.3 Submucosal gland cell origin

The esophageal submucosal gland (ESMG) responsible for the mucous secretion in the esophagus is only found in higher animals but not in rodents. The canine gastroesophageal reflux model demonstrated that the newly created columnar epithelium was due to expanded ESMG but not proximal migration of cardia cells (Gillen et al. 1988). In an organotypic culture, treatment of differentiation-inducing RA induced the formation of the glandular esophagus, possibly due to the expansion of ESMG duct cells (Chang et al. 2007). Mutational analysis of BE crypt revealed that a p16 mutation arising from the ESMGs duct's squamous epithelium was also present in BE crypt

(Leedham et al. 2008). It was shown that the reserve progenitor cells present in the ESMG might give rise to columnar or squamous mucosa after damage to epithelial cells (von Furstenberg et al. 2017). Further, single-cell RNA sequencing analysis of the normal human esophagus, BE, stomach, and duodenum revealed a transcriptional similarity between the esophageal gland and BE but not with the stomach or duodenum. Moreover, genes *Lefty1* and *Olmf4* found in normal ESMG cells transcriptionally overlapped with BE but not the stomach in the duodenum, which suggests that ESMG may be the source of BE (Owen et al. 2018).

3.8.4 Stomach/ cardia origin

As mentioned earlier, the first gland of the stomach in the GEJ is distinct from the corpus gland (lacks parietal cells and chief cells) and slightly similar to the antral gland. The first gland consists of progenitor cells similar to the antral gland expressing *Lgr5* and *Cd44v9*. Intestinal mucin *Muc4*, BE marker *Epcam*, and spasmolytic polypeptide-expressing metaplasia (SPEM) marker clusterin express strongly and specifically in the first gland. The presence of progenitor and BE markers in the first gland indicates its role in repair after mucosal injury and as a cell of origin for BE (O'Neil, Christine P Petersen, et al. 2017). L2-*IL-1β* overexpression in the esophagus of mice induced initiation of esophagitis and BE. It is associated with the migration of *Lgr5*+ cells from the cardia to the distal esophagus with increased Notch activation (Quante et al. 2012).

Further L2-*IL-1β* expression in the mouse model increased the expression of cholecystokinin-2-receptor (*Cck2r*) in the cardia progenitor cell and increased the progression to BE-like metaplasia in the esophagus upon hypergastrinemia induction (Lee et al. 2017). A recent study indicates that the inactivation of *Trp53* and *Rb1* in *Lgr5*+ cells induces the formation of gastric cancer, especially in the GEJ. The epithelial proliferation was facilitated by the *Cd44* cells in the SCJ, which express CD44 ligand osteopontin (*O*PN), known to increase the stemness of epithelial cells (Fu et al. 2020). Recently, *c-Myc* and *Hnf4a* transcription factors were shown to drive cardia cells to acquire BE phenotype and undifferentiated BE likely origin for the EAC (Nowicki-Osuch et al. 2021). However, in most studies, *in vivo* model of esophagojejunostomy in mice or rats was used to demonstrate BE development. Interestingly, in this model,

the columnar-lined esophagus developed from the wound-healing process of jejunal cells due to its competitive advantage over squamous epithelium (Agoston et al. 2018).

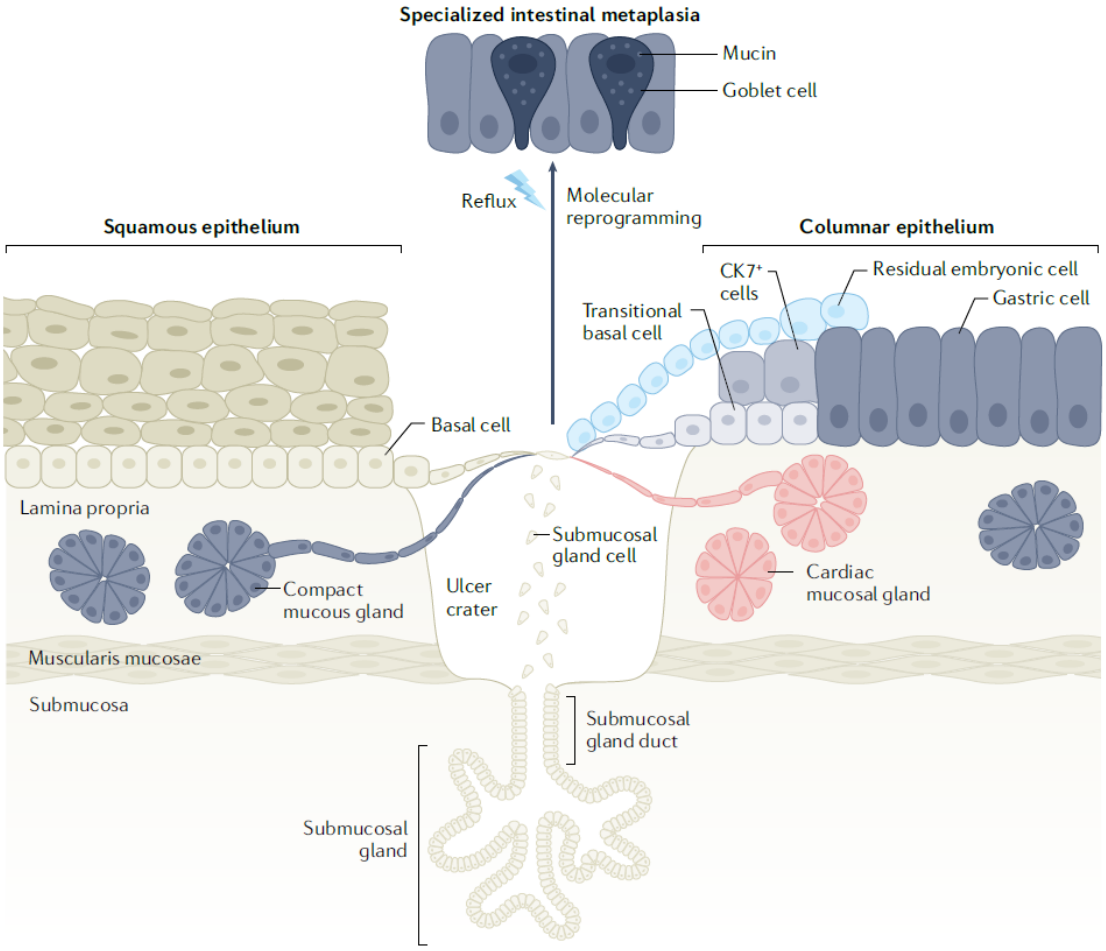

Figure 4. Figure depicting different theories for the origin of BE and IM. Chronic GERD induces injury to the esophageal epithelial cells which can be repaired by various postulated cell types which give rise to columnar metaplastic BE. The cellular origin for the development of BE could originate from squamous epithelium by transdifferentiation, mucosal and submucosal gland and duct cells, transitional basal cells, residual embryonic cells, and gastric epithelial cells. The molecular reprogramming of metaplastic columnar epithelial cells gives rise to acidic mucin-secreting goblet cells similar to intestinal epithelial cells. Source: (Souza and Spechler 2022)

3.9 Wnt pathway signaling and regulation

The Wnt pathway is essential for embryonic development and tissue homeostasis, and its deregulation is implicated in various cancers. The Wnt pathway is mediated by secreted glycoprotein Wnt ligands, which regulate cell proliferation, differentiation, and cell polarity during embryonic development and tissue homeostasis. The Wnt family consists of 19 secreted ligands which are glycosylated in the endoplasmic reticulum and acylated by O-acetyltransferase porcupine (*Prcn*) during its secretion (Mikels and Nusse 2006, Willert and Nusse 2012). The glycosylation and acetylation of Wnt are essential for its secretion and activity (Franch-Marro et al. 2008, Komekado et al. 2007). Secreted Wnt acts as a morphogen delivered to short-distance or long-distance target cells through diffusion. Broadly, the Wnt pathway is divided into two categories: the β-catenin-dependent canonical Wnt pathway and the β-catenin-interdependent non-Canonical Wnt pathway.

3.9.1 Canonical Wnt signaling pathway

In the canonical Wnt pathway, the Wnt ligand binds to heterodimeric complex receptors, which contain two types of receptor family, the Frizzled (FZD) seven-pass transmembrane receptors and the low-density lipoprotein receptor-related proteins (LRP5/LRP6) (Tamai et al. 2004) (Figure 5). Fzds are involved in both canonical and non-canonical Wnt pathways, whereas LRPs are involved in the canonical Wnt signaling pathway. Wnt binding to FZD, LRP receptor recruits components of the β-catenin destruction complex, such as Dishevelled (DVL) and AXIN 1 to the plasma membrane, thereby abrogating degradation of β-catenin. In the absence of Wnt, the destruction complex, consisting of an assembly of DVL, AXIN, GSK3β, and CK1α, phosphorylates cytoplasmic β-catenin and targets it to proteasomal degradation (Yang et al. 2018). In the presence of Wnt, the accumulated cytoplasmic β-catenin translocate into the nucleus, where it binds to the transcription factor T cell factor/lymphoid enhancer- binding factor (TCF/LEF) and promotes the transcription of Wnt target genes. The Wnt activity is maintained by negative feedback regulation by Wnt target genes *Axin 2*, *Rnf43*, and *Znrf3*. AXIN 2 activates the destruction complex and degradation of β-catenin, thereby inhibiting Wnt activity. Similarly, Wnt target proteins RNF43 and ZNRF3 are

localized to the surface membrane, where they ubiquitylate and degrade the Wnt receptors, thereby preventing Wnt ligand binding and Wnt activity (Bugter, Fenderico, and Maurice 2021). In contrast, R-spondin family proteins (RSPO 1 to 4) bind to their receptor LGRs (LGR4/5/6) and promote the degradation of RNF43 and ZNRF3. This allows the accumulation of Wnt receptors on the surface and potentiates the β-catenin-mediated Wnt activity (Hao et al. 2012).

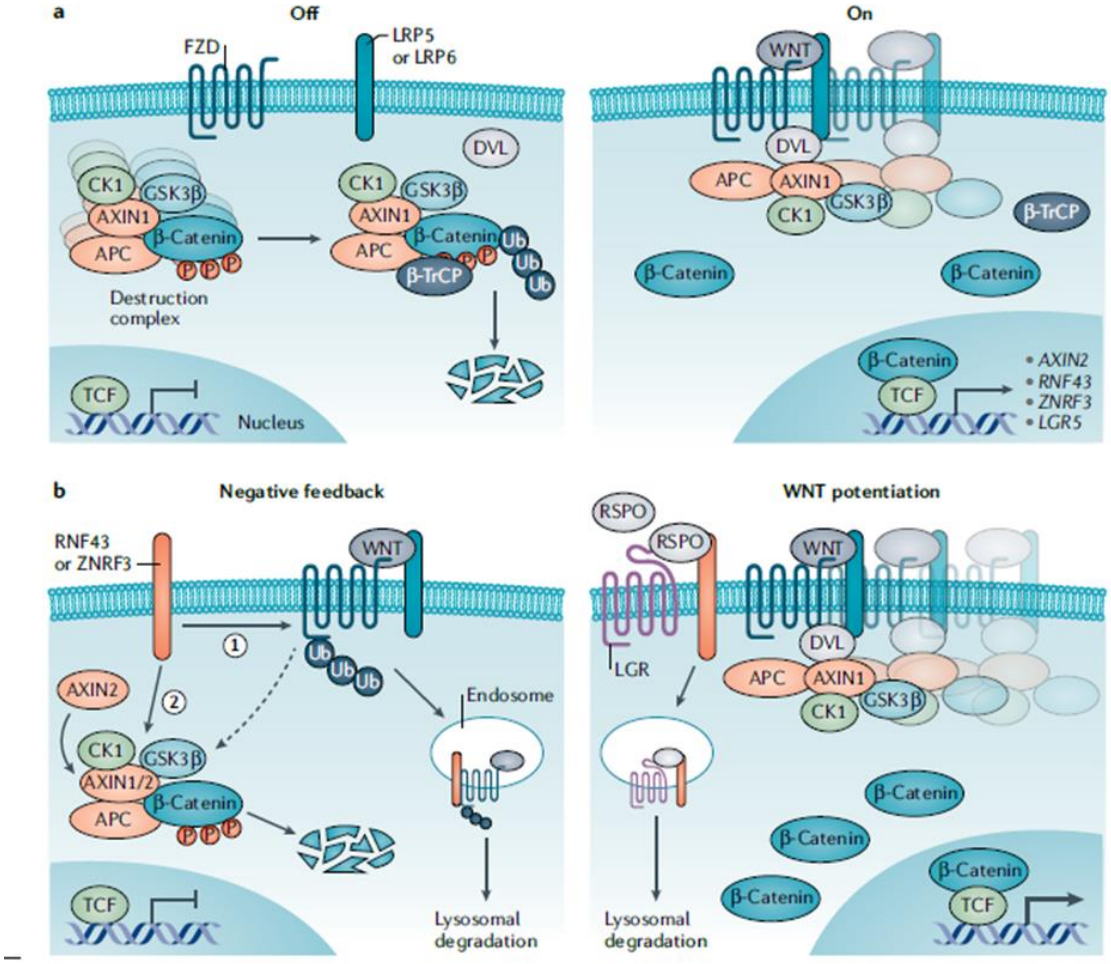

Figure 5. Canonical Wnt pathway regulation. (A) Left: In the absence of Wnt ligands, the destruction of complex proteins (APC, GSK3B, AXIN1, CK1) continuously degrades the cytosolic beta-Catenin by phosphorylation, ubiquitination, and proteasomal degradation. Right: In the presence of Wnt ligands, ligand binding activates Frizzled (FZD) receptor and co-receptor LRP5/LRP6 which recruits Dishevelled (DVL) to the plasma membrane. DVL promotes the recruitment of components of the destruction complex which allow inhibition of proteasomal degradation of beta-Catenin. The accumulated cytoplasmic beta-Catenin translocates into the nucleus where it induces the expression of Wnt target genes in association with TCF/LEF transcription factors. **(B)** Left: Wnt target proteins RNF43/ZNRF3 ubiquitylate FZD and allow

endocytosis and lysosomal degradation which allows fewer Wnt receptors available to bind. RNF43/ZNRF3 also allows the activation of the destruction complex and AXIN2 allow the accumulation of the destruction complex leading to the inactivation of Wnt signaling. Right: Rspondins bind to their receptor LGR4/LGR5/LGR6 and RNF43/ZNRF3 which allows clearance of RNF43/ZNRF3 and potentiation of Wnt signaling. Source: (Bugter et al. 2021)

3.9.2 Non-canonical Wnt signaling pathway

The non-canonical Wnt signaling pathway involves the absence of β-catenin-mediated signaling where Wnt binds to FZD without the participation of LRPs (Figure 6). There are two types of known non-canonical Wnt signal pathways, WNt/PCP and the Wnt/Ca^{2+} pathways. The primary function of the Wnt/PCP signaling pathway is to establish cell polarity and regulate cell migration. In the Wnt/PCP signaling pathway, Wnt ligands bind to FZD, ROR, RYK, and VANGL co-receptors which interact with each other inter and intracellularly. This recruits DVL that activates downstream small GTPases (Rho, Rac, cdc42), Rho-associated kinase (ROCK), and c-Jun N-terminal kinase (JNK) signaling cascades. This results in the cytoskeletal rearrangement and/or induction of gene transcription through the activation of AP1 (Jun-ATF-2)(Zhan, Rindtorff, and Boutros 2017.

In Wnt/Ca^{2+} pathway, the Wnt ligand induces the release of intracellular Ca^{2+}, subsequently Ca^{2+}-dependent cell signaling. This results in the regulation of cell attachment and migration. In the Wnt/Ca^{2+} pathway, the binding of Wnt ligands to FZD leads to phospholipase C (PLC) activation. PLC cleaves PIP2 into PIP3, which regulates the release of Ca^{2+} from the endoplasmic reticulum and to the cytoplasm. The released Ca^{2+} activates calcium-sensitive enzymes (CAMKII) and calcineurin which subsequently activate NF-κB, CREB, and NFAT transcription factors (Lojk and Marc 2021).

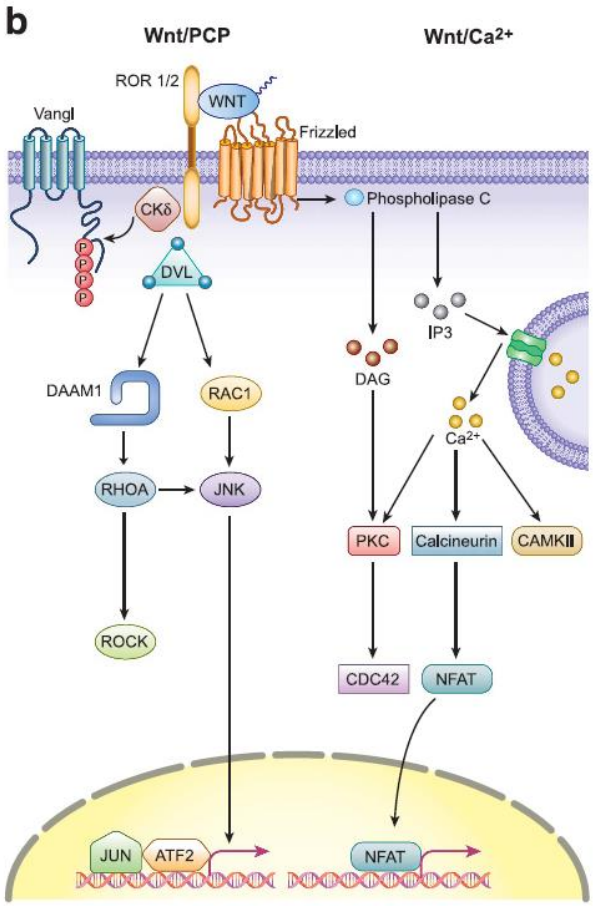

Figure 6. Non-canonical Wnt pathway. In Wnt/PCP pathway, the Wnt ligand binds to FZD and ROR1/2 receptors facilitating the recruitment and activation of DVL or VANGL. DVL bind and activate RHOA, and RAC1 leading to downstream activation of ROCK, JNK, and transcription of genes associated with cell motility and cell polarity. In Wnt/Ca^{2+} pathway, FZD activate PLC leading to calcium efflux and activation of PKC, CAMKII, Calcineurin, and NFAT transcription factor leading to the expression of genes associated with cell fate and cell migration. Source: (Zhan et al. 2017).

3.9.3 Wnt signaling pathway modulators

WNT pathway can be modulated or antagonized by the several secreted protein families. The secreted Frizzled related proteins (sFRPs) bind to FZD receptors while Wnt inhibitory factor (WIF) binds to Wnt ligands; therefore, these two families of proteins inhibit both canonical and non-canonical Wnt pathways (Bovolenta et al. 2008, Surmann-Schmitt et al. 2009). Whereas the Dickkopf protein family (DKKs) and the Wise/SOST family bind to LRPs, which specifically inhibit the canonical Wnt pathway. DKKs bind to Kremen 1 and 2 receptors, which potentiate the binding of DKKs to LRPs and inhibition of the Wnt pathway (Li et al. 2005, Niehrs 2006). However, DKK2 alone acts as a Wnt

activator because DKK binding to LRP6 blocks the autoinhibition and activates LRP6. In the presence of Kremen 2, DKK2 binds LRP6 and internalizes the LRP6 receptor and thus inhibiting Wnt signaling (Mao and Niehrs 2003). The other known Wnt pathway inhibitors include Notum, TIKI, IGFBP4, and glypicans, which bind Wnt ligands or FZD receptors and inhibit Wnt activation (Zhang et al. 2015, Zhu et al. 2008, Li et al. 2019). As mentioned above, the RSPO family, which potentiates the canonical Wnt pathway, also enhances Wnt/PCP pathway by binding to SDC4 and activating JNK (Ohkawara, Glinka, and Niehrs 2011). Like Wnt ligands, Norrin binds to FZD4 to form a ternary complex with LRP5/6 and activates TCF/LEF transcription factor (Chang et al. 2015).

3.10 Retinoic acid pathway

RA is the active metabolite of Vitamin A (Retinol) which play an essential role in the biological processes during development and adult tissue homeostasis (Ghyselinck and Duester 2019). Since the human body cannot synthesize RA, it is mainly sourced from the diets such as plant-derived pro-vitamin A, called β-carotene, or retinol from animal food sources. Intestinal enterocyte cells absorb β-carotene, retinol, and retinyl ester from the lumen. From enterocytes, they are transported either to liver cells for storage or target cells by incorporating retinol into the chylomicron. From the liver, retinol is transported through the blood to the target cells. Metabolized retinol is secreted either into bile or to the blood, where it binds to retinol-binding protein (RBP) and transthyretin (TTR) which are taken up later by the target cells expressing membrane receptors: stimulated by retinoic acid 6 (STRA6) and STRA6-like receptor, also known as RBP4 receptor-2 (RBPR2) (Bohn et al. 2019) (Figure 7).

Inside target cells, retinol is stabilized by the cellular retinol-binding proteins (CRBPs). Initially, retinol is reversibly oxidized to retinaldehyde (Retinal) by cytosolic alcohol dehydrogenases (ADHs) or retinol dehydrogenase (RDH). However, excess retinal can be reversibly converted into retinol by the dehydrogenase/reductase 3 (DHRS3) enzyme. Retinal is further irreversibly oxidized into RA by a reaction catalyzed by the enzyme

retinaldehyde dehydrogenase (RALDH/ALDH). The synthesized RA is transported to the nucleus by cellular retinoic acid binding proteins (CARBPs), where it binds to hetero dimers of nuclear retinoic acid receptors (RAR-RXRs) bound to retinoic acid responsive elements (RARE) within the promoters of target genes. The binding of RA induces conformational changes in the RAR-RXR complex, which releases co-repressor complexes (NCoR/SMRT) with histone deacetylase activity and allows the recruitment of co-activator complexes with histone acetylase activity and histone methyl transferase activity, thus allow transcription of target genes (al Tanoury, Piskunov, and Rochette-Egly 2013). RA can act in an autocrine or paracrine manner, where it can diffuse into neighbor cells. However, the excessively produced RA can be hydroxylised by the cytochrome P450 subfamily 26 (CYP26) enzymes, either present in the cells or expressed as a negative feedback mechanism into less biologically active polar metabolites (Roberts 2020).

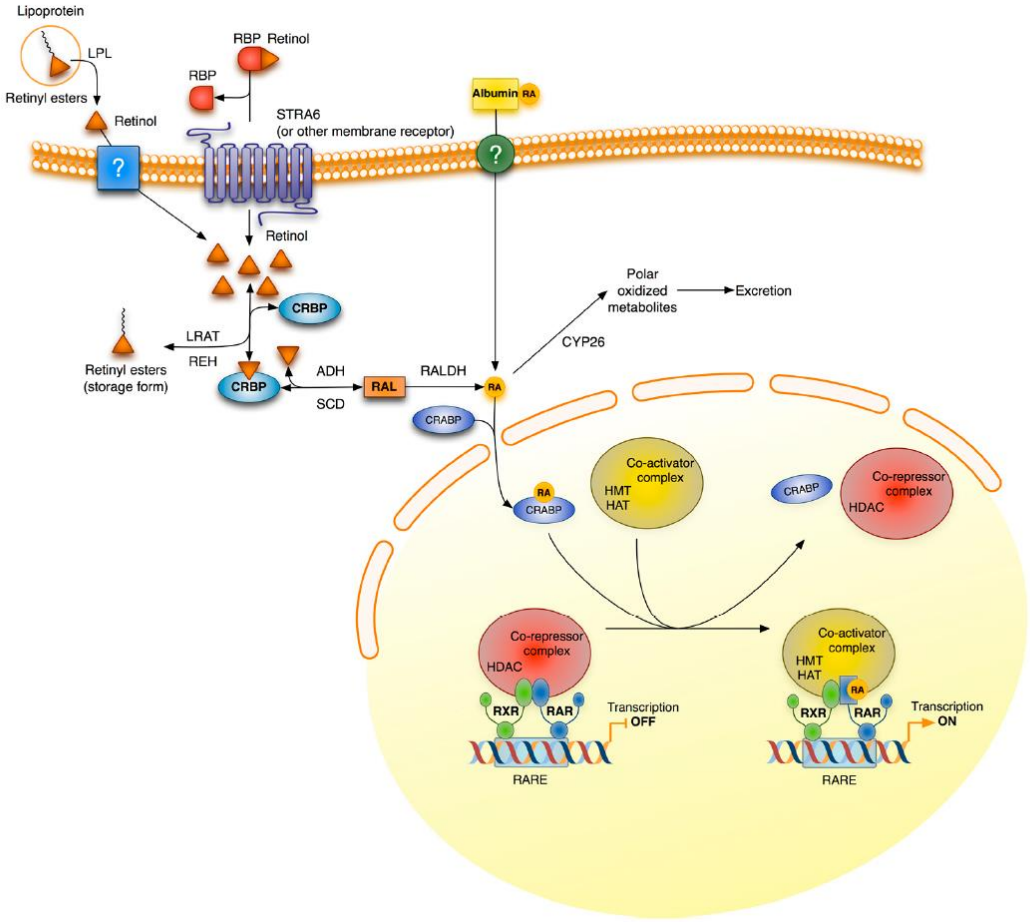

Figure 7. Retinoic acid signaling pathway. Lipoprotein or RBP-bound retinol may enter the cell through passive diffusion or by binding to the STRA6 cell receptor. Retinol is either stored

as retinyl ester or metabolized into RA by undergoing two-step oxidation involving Alcohol dehydrogenase (ADH) and retinaldehyde dehydrogenase (RALDH) enzymes. RA is either degraded by CYP26 family proteins or translocated into the nucleus by cellular retinoic acid binding protein (CRABP). In the nuclease, binding of RA to the RAR-RXR receptor complex allows the replacement of the co-activator complex with the co-repressor complex and transcription of target genes. Source: (Barber et al. 2014)

Deregulation of the RA signaling pathway is implicated in various cancers, and RA is shown to induce differentiation of cancer cells and act as an anti-tumor agent (Tang and Gudas 2011, Costantini et al. 2020, Hunsu et al. 2021). Retinol is shown as an antioxidant that scavenges lipid free radicals and protects DNA from oxidative damage, and its deficiency leads to an increased risk for esophageal and gastric cancer (Abnet et al. 2003, Persson et al. 2008). Meta-analysis shows intake of β-carotene has a protective effect on EAC and gastric adenocarcinoma (Kubo and Corley 2007). In BE, the activity of RA was shown to increase in the initial stage, and treatment of ectopic cultured BE tissue with RA replaced the squamous epithelium with columnar epithelium (Chang et al. 2008, Chang et al. 2007). This is partly due to the differentiation and exfoliation of squamous epithelial cells and the replacement of submucosal gland columnar epithelial cells. Reduced RA was observed in the gastric during the progression of inflammation, atrophy, and intestinal metaplasia (Matsumoto et al. 2005). However, gastric carcinoma stem cells show a high activity of ALDH, even though the treatment of RA reduces the ALDH activity, cancer cell stemness, and tumor growth inhibition (Moreb et al. 2005, Nguyen et al. 2016). This reflects that ALDH is involved in the RA synthesis and the regulation of other oncogenic signaling pathways that regulate stemness and cancer (Poturnajova, Kozovska, and Matuskova 2021). There is also an implication of RA deficiency in the development of intestinal metaplasia. RA can decrease the master regulator of goblet cell differentiation gene KLF4 expression and RARa deficiency, increasing the goblet cell number in the distal bowel of mice (Jijon et al. 2018). Yet, RA involvement in epithelial homeostasis and intestinal development is less understood.

3.11 Organoid models

The organoid model is a recent advance in the primary epithelial culture method. The organoid mimics morphological, structural, and functional similarity to *in vivo* epithelial mucosa. In past decades, studies used 2D cell lines, which are either derived from tumor cells or genetic manipulation. Therefore they lack the physiological similarity of normal epithelial cells and differentiated types of cells, which is necessary to understand tissue physiology and disease development (Schutgens and Clevers 2020). In contrast, the organoid model recapitulates *in vivo* conditions such as epithelial cell polarity, cell-cell interaction, and signaling requirement for stemness and differentiation of different epithelial cell types (Huch and Koo 2015). This allows for long-term culture of primary epithelial cells and enables an understanding of the molecular mechanisms involved in organ functionality, adult tissue maintenance, and disease development. The organoid culture model was initially developed from patient-derived intestinal epithelial cells. Later, the model was applied to epithelial cells from other tissues such as the stomach, colon, fallopian tube, lung, and cervix (Sato et al. 2009, Schlaermann et al. 2016, Sato et al. 2011, Kessler et al. 2015, Dye et al. 2015, Chumduri et al. 2021). Different studies have grown organoid models for esophageal epithelial cells from mice, human adult tissue stem cells, and human IPSC (DeWard et al. 2014, Kasagi et al. 2018, Trisno et al. 2018), yet the long-term expansion of human esophageal organoids is not yet achieved. Fine-tuning of growth signaling components needs to be addressed for the human esophageal organoid model, which differs from columnar epithelial-derived organoid models (Trisno et al. 2018). The cell-cell interaction and spatiotemporal signal are achieved in organoid culture by use of ECM Matrigel produced from murine Engelbreth-Holm-Swarm sarcomas, which provide basement support for epithelial polarization and compartmentalization (Kleinman et al. 1986). The composition of growth components in the organoid culture medium depends on the tissue of origin, which shows signaling heterogeneity in the maintenance of epithelial stem cells of different tissue origins (Kim, Koo, and Knoblich 2020). The advantage of the organoid model is the physiological relevance to the epithelial tissue compartment, rapid establishment and scale-up with genomic stability, amenable to genetic manipulation, host-microbe interaction studies,

and development of personalized medicine. However, the organoids lack the stromal, immune, and blood vessel compartments and optimum signals from these compartments, which makes it hard to study the organ-level cell-cell interactions (Kim et al. 2020, Schutgens and Clevers 2020).

3.12 Epithelial cell heterogeneity and single-cell RNA sequencing

The single cell represents the building block unit of multicellular organisms with cell type-specific gene expression and function. In the tissue, the single cells are heterogeneous concerning differentiation trajectories and spatial position (Arendt et al. 2016). For example, in the stomach gland, epithelial heterogeneity varies from the base of the gland (stem cell compartment) to the surface (terminally differentiated compartment). However, normal homeostasis is maintained by region-specific epithelial-epithelial cell and epithelial-stromal cell interactions (Willet and Mills 2016, Zagami et al. 2022). Understanding cellular heterogeneity and its networks can be achieved by transcriptional profiling using the scRNA-seq technique. Compared to the bulk RNA sequence, this provides an in-depth analysis of the cellular developmental process of various tissues, lineage trajectory, cellular heterogeneity in the normal and matched cancer tissues, and identification of novel cell types (He et al. 2020, L. Han et al. 2020, X. Han et al. 2020, He et al. 2021, Plasschaert et al. 2018). scRNA-seq was initially performed by Tang et al. in 2009 by manual single-cell isolation and sequencing, which later developed into various improved high throughput scRNA-seq techniques (Tang et al. 2009, Jovic et al. 2022). The scRNA-seq analysis involves basic steps like isolation of viable single cells, isolation of total mRNA and conversion into cDNA by reverse transcriptase, library preparation with unique molecular identifiers (UMI) for next-generation sequencing (NGS), and sequencing using sequencing flatforms. There are different scRNA-seq-seq methods available that could amplify full-length (Smart-seq2, SUPeR-seq, and MATQ-seq) or partial transcripts from 3' end or 5' end mRNA (Drop-seq, Seq-Well, and DroNC-seq, SPLiT-seq, STRT-seq) (Chen, Ning, and Shi 2019). Single-cell separation is done by limiting dilution, microfluidic/microplate

methodology, and fluorescence-activated cell sorting (FACS) methods that result in low isolation efficiency (Gross et al. 2015). This problem has been overcome by the use of Drop-seq, where microdroplets containing UMI barcodes and cDNA synthesizing bases, oligos can capture single cells, which increases the single cell isolation capacity and enables simultaneous analysis of a large number of cells (Macosko et al. 2015). Further, multiplexing different samples with barcoded antibodies or lipid oligos allows the analysis of many cells from different samples in one library preparation and sequencing. This allows for replicating samples in one experiment, removing multiplets, and significantly reducing experimental costs (Kang et al. 2018, Mylka et al. 2022). Recent advances in the scRNA-seq-seq technology also made it possible to analyze the epigenetic changes occurring at the single-cell level by using an assay for single-cell transposase-accessible chromatin using sequencing (scATAC-seq) and single-cell nucleosome, methylation, and transcription sequencing (scNMT-seq) (Buenrostro et al. 2015, Clark et al. 2018). Thus scRNA-seq analysis allows understanding the cell heterogeneity, lineage prediction, gene function, and epigenomic function at the level of single cells derived from the patients, animal models, and *in vitro* organoid models.

4 Aim of the study

The GEJ, where the esophagus's multilayered squamous epithelium meets with the stomach's single-layered columnar cells, is the hotspot for dysbiosis, BE and carcinogenesis. BE is an adaptive state where the esophagus epithelium is replaced by metaplastic columnar cells predisposed to dysplasia and adenocarcinoma. Several studies postulated various theories concerning the cell of origin for the development of BE. Despite this, the mechanisms, and the role of the tissue microenvironment in BE development remain largely unknown.

Understanding normal cellular homeostasis and microenvironmental signaling, which maintains a healthy SCJ, is a prerequisite to understanding perturbations during infections, metaplasia development, and its progression to cancer. Therefore, my first aim was to decipher the epithelial subcellular composition and the stem cells of the squamous epithelium-lined esophagus and columnar epithelium-lined stomach and how the tissue microenvironment governs the maintenance of these two epithelial cell borders in the normal GEJ.

My second aim focused on the study of the role of RA, which is associated epidemiologically with BE development, on the esophagus and stomach epithelial stem cell regeneration and model the BE development.

These aims will be achieved by using mouse models and advanced *in vitro* organoid cultures that mimic *in vivo* architecture, subcellular heterogeneity, and function together with bulk and single-cell transcriptomics.

5 Materials

5.1 Mice strains used in this study

Table 1. Mice strains and sources

Mouse strain	Description	Reference/Source
C57bl/6	Wild type mice	Charles River Laboratory
C57bl/6-*Krt5CreErt2/Rosa26-tdTomato*	Cre recombinase is expressed under the promotor of *Krt5*. Upon activation by Tamoxifen, *Krt5*-expressing cells will be lineage traced with Rosa26tdTomato.	(Rock et al. 2009, Madisen et al. 2010)
C57bl/6-*Krt8CreErt2/Rosa26-tdTomato*	Cre recombinase is expressed under the promotor of *Krt8*. Upon activation by Tamoxifen, *Krt8*-expressing cells will be lineage traced with Rosa26tdTomato.	(van Keymeulen et al. 2011, Madisen et al. 2010)
C57bl/6-*Axin2CreErt2/Rosa26-tdTomato*	Cre recombinase is expressed under the promotor of *Axin2*. Upon activation by Tamoxifen, *Axin2*-expressing cells will be lineage traced with Rosa26tdTomato.	(Choi et al. 2013)

5.2 Cells and cell lines

Table 2. Cell lines and their sources

Cell line	Description	Source
3T3-J2	Mouse embryonic fibroblast line used as the feeder cells for the human esophagus squamous epithelial 2D culture, Culture Medium: DMEM (10% FCS, 2 mM L-Glutamin, 1 mM Na-Pyruvate)	(Rheinwald and Green 1975)
L Wnt-3a	Mouse fibroblasts cell line, secrete biologically active Wnt3a protein, selection marker G418; Culture Medium: DMEM, 10% FCS, 1 mM Na-Pyruvate, 2 mM L-Glutamin, 0,4 mg/mL G418	Clevers Lab, Netherlands/Utrecht; ATCC® CRL-2647TM; Departmental collection #C-0705
293T HA Rspo1-Fc	Human; 293T cell line stably transfected to express murine R-spo1 with an N-terminal HA epitope tag and fused to a C-terminal murine IgG2a Fc fragment; Culture Medium: DMEM (10% FCS, 2 mM L-Glutamin, 1 mM Na-Pyruvate)	Clevers Lab, Netherlands/Utrecht; Departmental collection #C-0005
293T WntR	Human; 293 T cell line transformed with Lentivirus containing Wnt GFP reporter (7TGC), stably integrated expression plasmid with inducible GFP (Wnt-dependent); Culture Medium: DMEM/Ham's F12+ 10% FCS	Clevers Lab, Netherlands/Utrecht; Departmental collection #C-0001

5.3 Antibodies

Table 3. Primary antibodies used for immunofluorescence and western blot

Protein	Donor species	Supplier	Cat No	Dilution
Cytokeratin 5	Rabbit	Abcam	ab52635	1:5000 (WB)
Cytokeratin 7	Rabbit	Abcam	ab181598	1:1000 (WB)
Cytokeratin 5-Alexa 488	Rabbit	Abcam	ab193894	1:300 (IF)
Cytokeratin 7-Alexa 555	Rabbit	Abcam	ab209601	1:300 (IF)
Cytokeratin 8	Rabbit	Abcam	ab59400	1:1000 (WB) 1:200 (IF)
Cytokeratin 17	Rabbit	Abcam	ab109725	1:100 (IF)
Cytokeratin 6	Mouse	Abcam	ab18586	1:200 (IF)
p63	Mouse	Abcam	ab375	1:200 (IF)
p63	Rabbit	Abcam	Ab53039	1:1000 (WB)
E-Cadherin	Mouse	BD Biosciences	610181	1:200 (IF)
E-Cadherin-488	Mouse	BD Biosciences	560061	1:100 (IF)
Ki67	Rabbit	Abcam	ab16667	1:200 (IF)
Muc5Ac	Mouse	Abcam	ab212636	1:500 (IF)
c-Jun	Mouse	Abcam	ab280089	1:1000 (IF)
β-Actin	Mouse	Sigma Aldrich	A5441	1:10,000 (WB)
Ki67-FITC				

IF= Immunofluorescence, WB= Westernblot

Table 4. Secondary antibodies used for immunofluorescence and western blot

Protein	Host species	Supplier	Cat No	Dilution
Donkey anti-mouse-Alexa Fluor 488	Mouse	Jackson Immuno Research	715-454-151	1:150 (IF)
Donkey anti-rabbit-Cy3	Rabbit	Jackson Immuno Research	711-166-152	1:150 (IF)
Donkey anti-rabbit–Alexa Fluor 647	Rabbit	Jackson Immuno Research	711-605-152	1:150 (IF)
Donkey anti-mouse–Cy5 AffiniPure	Mouse	Jackson Immuno Research	715-175-151	1:150 (IF)
Sheep anti-mouse IgG-HRP	Mouse	Amersham	NA931	1:2000 (WB)
Donkey anti-rabbit IgG-HRP	Rabbit	Amersham	NA934	1:2000 (WB)

IF= Immunofluorescence, WB= Western blot

5.4 Primers and Probes

Table 5. Primers used for the qRT-PCR

All the primers listed below are used for the qRT-PCR. The primers were designed using the online program Primer3 (v.0.4.0). The melting temperature was set to 60°C with product sizes ranging between 100 bp to 200 bp. All the

primers were ordered from Sigma Aldrich and were diluted to 10 µM final concentration with water.

Gene name	**Primer Sequence (5' – 3')**	**(Accession No)**
Krt8	FW- GGCTTCAGCTACGGAATGAG RV- CGACATCAGAAGACTCGGACA	NM_031170.2
Krt7	FW- GGCCTATTCCATCAAGACCA RV- TTTTTAGCCGATGCAGCTCT	NM_033073.3
Tfgb3	FW- AAGCAGCGCTACATAGGTGGCA RV- GGCTGAAAGGTGTGACATGGAC	NM_009368.3
Cyp26b1	FW- CAAGGGCTGGAGTGTCATGT RV- TTCAGGAACAGCTTGGCCAA	NM_175475.3
Rarb	FW- TGACTGACCTTGTGTTCACCTT RV- CTTCCAGCAGTGGTTCTTGG	NM_001289762.1
Id2	FW- TCACCAGAGACCTGGACAGAAC RV- TGCTATCATTCGACATAAGCTCAG	NM_010496.3
Bmp2	FW- AACACCGTGCGCAGCTTCCATC RV- CGGAAGATCTGGAGTTCTGCAG	NM_007553.3
Sox2	FW-ATGGGCTCTGTGGTCAAGTC RV- GCCGCTCTGGTAGTGCTG	NM_011443
Tff3	FW- TCTGGCTAATGCTGTTGGTG RV- CAGGGCACATTTGGGATACT	NM_011575

Table 6. Probes used for the smRNA Hybridisation (smRNA-scope)

All the probes were ordered from the Advanced Cell Diagnostics company

Gene name	**Target region**	**Cat No**
Mm-*Ppib*	98 - 856	313911
DapB	414 - 862	310043
Mm-*Krt5*	666 - 2086	415041
Mm-*Krt8*	4 - 1799	424521

Mm-*Krt7*	2 - 1588	511801
Mm-*Axin2*	330 - 1287	400331
Mm-*Dkk2*	781 - 1645	404841
Mm-*Lgr5*	2165 - 3082	312171
Mm-*Rspo3*	2 - 2331	429861

5.5 Commercial kits

Table 7. Commercial kits and their sources

Kit	**Application**	**Supplier**	**Cat No**
Agilent High Sensitivity DNA Kit	Library quality check	Agilent	5067-4626
AllPrep DNA/RNA Mini Kit	RNA and DNA extraction	QIAGEN	80204
Chromium Single Cell 3' Library & Gel Bead Kit v3	Single-cell library preparation		PN-120237
Chromium Single Cell A Chip Kit	Single-cell sequencing	10X Genomics	PN-120236
NovaSeq6000 S1 Reagent Kit (100 cycles)	Single-cell sequencing	Illumina	20012865
RevertAid First Strand cDNA Synthesis Kit	cDNA synthesis	Thermo Fisher Scientific	K1621
RNA Nano 6000 microfluidics kit	RNA quality check	Agilent Technologies	5067-1511
RNAscope 2.5 HD Reagent Kit- RED	smRNA-ISH	Advanced Cell Diagnostics	322350
RNeasy Mini Kit	RNA extraction	QIAGEN	74104

5.6 Laboratory instruments

Table 8. Laboratory instruments and their sources

Equipment	Application	Manufacturer
Agilent 2100 Bioanalyzer	RNA quality control	Agilent technologies
Axioscan Imager	Immunofluorescence and smRNA-ISH	Carl Zeiss Microscopy
Cam-XC30	Camera	Olympus
CKX41	Fluorescence microscope	Olympus
Cryostat Leica Biosystems	Immunofluorescence and smRNA-ISH	Leica
Drying oven	Immunofluorescence and smRNA-ISH	Thermo Fisher Scientific
Eppendorf centrifuge 5417R	RNA isolation	Eppendorf
Eppendorf centrifuge 5810R	Primary cell culture	Eppendorf
FACSymphony™ A5	FACS	BDbiosciences
Agilent G2565CA Microarray Scanner System	Microarray	Agilent Technologies
Gammacell® 40 Exactor	Gamma Irradiation System	MDS Nordion
GeneGenius	Gel documentation	Syngene
Genomics Chromium Controller	scRNA-sequence	10X Genomics
Hera Safe Cell 150	Primary cell incubator	Thermo Scientific
Heraeus Hera Safe	Microbiology laminar flow chamber	Thermo Scientific
HybEZ Oven	smRNA-ISH	ACD

Leica TCS SP8	Confocal microscope	Leica Microsystems GmbH
Leica TP1020	Tissue processor	Leica biosystems
Microm AP250	Paraffin Embedding station	Microm
Microm HM315	Paraffin Rotation Microtome	Microm
Mini Trans-Blot® Cell	Western blot	Bio-Rad
Mini-PROTEAN tetra cell	SDS-PAGE/ Western blot	Bio-Rad
Mini-PROTEAN© Tetra Handcast Systems	SDS-PAGE	Bio-Rad
NanoDrop 1000 UV-Vis spectrophotometer	RNA concentration	Paq lab Biotechnologies
pH meter	pH measurement and adjustment	Mettler-Toledo
PowerPac™ HC	Power supply	Bio-Rad
Sorvall™ RC 6 Plus	sorvall centrifuge and rotor	Thermo Scientific
StepOnePlus™	Real-Time PCR System	Applied Biosystems
Tabletop Orbital Shaker incubator	Tissue digestion	Thermo Scientific
Thermomixer comfort	Boiling protein lysates	Eppendorf
Waterbath	Prewarming medium	GFL

5.7 Software

Table 9. Software

Software	Application	Company
Adobe Illustrator CS4	Data presentation	Adobe
Adobe Photoshop	Image Processing	Adobe
BD FACSDiva™ Software	FACS analysis	BD Biosciences
CellSensEntry	Image processing	Olympus
ImageJ1.47v	Image processing/quantification	Open source
Mendeley	Literature	Elsevier
MS Office 2010 (Word, Excel, PowerPoint)	Documentation, data analysis	Microsoft
Prism® 7.03	Statistical data analysis	GraphPad
R	Bulk and single-cell RNA-seq data analysis	Open source
R Studio	Bulk and single-cell RNA-seq data analysis	RStudio, Inc.
StepOneTM Software (version 2.3)	qRT-PCR analysis	Life Technologies
Zen 3.2 (Blue edition)	Axioscan image analysis	ZEISS Microscopy

5.8 Chemicals

Table 10. Chemicals

Chemical	Supplier	Cat No.
30% Acrylamide/Bisacrylamid (37.5:1)	Roth	3029.1
7 AAD	BD Pharmingen™	559925
Amersham Hyperfilm ECL	GE Healthcare Life Sciences	28906835

Ammonium hydroxide	Sigma-Aldrich	221228
Ammonium persulfate	Sigma-Aldrich	A3678-25G
Beta Mercaptoethanol	Roth	4227.1
Bovine serum albumin (BSA)	Biomol	1400.1
Bromophenol blue	AppliChem	A2331,0005
Corn oil	Sigma-Aldrich	C8267
DAPI	Merck	D9542
Dimethyl Sulfoxide-DMSO	Sigma	D2660-100ML
DNA gel loading dye (6X)	Fermentas	R0611
DNase/RNase-free water	Sigma	W4502-6x1l
dNTPs	Thermo Scientific	R0182
Donkey Serum	Jackson Immuno Research	17000121
DRAQ 5	Cell signaling technology	4085
Eco mount	Biocare	EM897L
Ethanol	Merck	1.00983.2511
Glycerol	Roth	3783.2
Glycine	Biomol	49.432.500
Glycine	Roth	3187.4
Green master mix (2x) high ROX	Genaxxon	M3052.0500
HCl	Roth	9277.2
Hematoxylin Solution, Gill No. 1	Sigma-Aldrich	GHS1128
HistoBond® microscope slides	Marienfeld	810000
Hoechst	Sigma-Aldrich	B2261
Isopentane	Roth	3926.1
Isopropanol	Merck	1.09634.2511
KCl	Merck	1049360500
KH2PO4	Roth	3904.1
Methanol	Roth	8388.6

MgCl2	Promega	A351H
Mowiol® 4-88	Sigma	81381
Na2HPO4	Roth	X987.1
NaCl	VWR	27810.364
Non-fat dried Milk powder	PanReac AppliChem	A0830,0500
OCT compound	Sakura Finetek USA	4583
PageRuler™ Plus Prestained Protein Ladder, 10 - 250 kDa	Thermo Scientific	26619
Paraformaldehyde (PFA)	Sigma-Aldrich	4441244
PVDF membrane Polyscreen ®	PerkinElmer™	NEF100200
Sodium dodecyl sulfate (SDS)	Roth	CN30.3
Tamoxifen	Sigma-Aldrich	T5648
Target retrieval solution (10x)	Dako	S1699
TEMED	Roth	8142.1
Tris base	Roth	4855.2
TRIzol® reagent	Invitrogen™	15596026
Triton X-100	Roth	3051.4
Tween 20	Roth	9127.2
Western Lightning Chemiluminescence Reagents	Perkin Elmer	NEL103001E
Xylene	Roth	9713.2

5.9 Buffers and compositions

Table 11. Buffers and compositions

Buffer	**Composition**	**Concentration**
Collagen I solution	PBS Collagen Type 1	 0.04%

Collagenase II solution	Hank's balanced salt solution (HBBS) Collagenase Type II	 0.05%
Electrophoresis buffer (10X Stock)	Tris base Glycine SDS Makeup volume with distilled H2O, pH 8.3	240 mM 1.9 M 0.1 %
FACS buffer	BSA in PBS, sterile filtered	0.1%
FACS permeabilization buffer	BSA Triton X-100 in PBS, sterile filtered	0.1% 0.1%
Immunofluorescence blocking solution (IFB)	BSA FCS in PBS, sterile filtered	1% 2%
Immunofluorescence permeabilization solution	BSA FCS Triton X-100 in PBS, sterile filtered	1% 2% 0.2%
Laemmli buffer (6x)	Glycerol Beta-mercaptoethanol SDS Stacking gel buffer Bromophenol blue 10 mL distilled H2O pH 6.8	3 mL 1.5 mL 10% 3.75 mL Pinch 10 mL
Mowiol mounting solution	Mowiol® 4-88 Glycerol Tris base Makeup volume with distilled H2O, pH 8.5	20% (w/v) 25% (w/v) 100 mM

Paraformaldehyde 3.7%	Distilled H2O at 60°C Paraformaldehyde 10xPBS pH 7.4	900 mL 3.7 g 100 mL
PBST	PBS Tween 20	 0.05% (v/v)
Phosphate-buffered saline (PBS)	NaCl KCl KH2PO4 Na2HPO4 x 2 H2O Makeup volume with distilled H2O, pH 7.4	137 mM 2.7 mM 1.8 mM 10 mM
Resolving Gel buffer (1M)	Tris base Distilled H2O Adjust pH 8.8 (with HCl)	30.2 g 250 mL
Resolving Gel solution (12%)	Resolving gel buffer Acrylamide/Bis-acrylamide 30%/0.8% (w/v) solution 10% SDS solution 10% (w/v) ammonium persulfate (APS) TEMED Distilled H2O	1.88 mL 1.95 mL 50 µL 40 µL 4 µL 1.23 mL
Stacking Gel buffer (1M)	Tris base Distilled H2O Adjust pH 6.8 (with HCl)	30.2 g 250 mL

Stacking Gel solution	Stacking gel buffer Acrylamide/Bis-acrylamide 30%/0.8% (w/v) solution 10% SDS solution 10% (w/v) ammonium persulfate (APS) solution TEMED Distilled H2O	250 µL 500 µL 20 µL 20 µL 2 µL 1.21 mL
1X Tris-buffered saline (1X TBS)	Tris base NaCl pH to 7.5 Makeup volume with distilled H2O	20 mM 140 mM
1X TBST	1X TBS Tween20	 0.05% (v/v)
Western blot-blocking solution	1X TBST Non-fat dried Milk powder	5% (w/v)
Wet blot transfer buffer	Glycine Tris base Methanol Makeup volume with distilled H2O, pH 8.0	14.4 g/L 3 g/L 20% (v/v)
Tamoxifen solution	Tamoxifen Corn oil Dissolve at 37°C overnight in a shaker	20 mg 1 mL

5.10 Primary cell culture growth factors and supplements

Table 12. Primary cell culture growth factors and supplements

Reagent	Working concentration	Supplier	Cat. No.
A-83-01 (TGF-β RI Kinase Inhibitor IV)	2 µM	Calbiochem	616454
ATRA (all trans retinoic acid)	1 µM	Sigma	R2625
B27 supplement (50x)	1%	Gibco	17504044
BMS 493 (Pan-retinoic acid receptor (pan-RAR) inverse agonist)	2 µM	Tocris	3509
EGF (human)	10 ng/mL	Invitrogen Biosource	PHG0311
EGF (Mouse)	50 ng/mL	Invitrogen Biosource	PMG8043
Fetal calf serum (FCS)	5% or 10%	Biochrom	S0115
FGF-10 (human)	100 ng/mL	Peprotech	100-26-B
Forskolin	10 µM	Sigma	F6886
Gastrin	100 µM	Sigma	G9145
GlutaMax (100x)	1%	Gibco	35050-038
HEPES (1M)	12 mM	Gibco	15630-056
Hydrocortisone	0.5 µg/mL	Sigma	H0888-1G
IWP2 inhibitor	5 mM	Tocris	3533
L-Glutamine	2 mM	Gibco	25030-024
N2 supplement (100x)	1%	Gibco	17502048
N-acetyl-L-cysteine (NAC)	1.25 mM	Sigma	A9165-5G
Na-pyruvate	1mM	Sigma-Aldrich	S8636

Nicotinamide (NIC)	10 mM	Sigma-Aldrich	N0636
Noggin (human)	100 ng/mL	Peprotech	120-10C
Noggin (Mouse)	100 ng/mL	Peprotech	250-38-100
Penicillin/Streptomycin	1%	Gibco	15140-122
R-spondin1 (RSPO1) conditioned media	25%	In house	The protocol described by (Willert et al. 2003, Farin, van Es, and Clevers 2012)
SB202190 (p38 Inhibitor)	10 µM	Sigma	S7067
WNT3A conditioned media	25%	In house	The protocol described by Willert et al. 2003, Farin et al. 2012)
Y-27632 dihydrochloride monohydrate (ROCK inhibitor)	10 µM	Sigma-Aldrich	Y0503

5.11 Cell culture reagents

Table 13. Cell culture reagents

Reagent	Supplier	Cat No
Advanced DMEM/F12 (ADF)	Gibco	12634
Collagen type I (solution from rat tail)	Sigma-Aldrich	C3867
Collagenase type II (0.5 mg/mL)	Calbiochem	234155
Cryo-SFM	PromoCell	C-29910
DMEM	Gibco	10938-025
Dulbecco's phosphate-buffered saline (DPBS), without Ca^{2+} and Mg2+	Gibco	14190-169
Matrigel (basement membrane matrix, Growth factor reduced)	Corning	356231
TrypLE™ Express	Gibco	12605-028

5.12 Cell culture medium

Table 14. Composition of complete DMEM

Reagent	Volume (mL)
DMEM/F12	500
Na-pyruvate	5
L-Glutamine	5
FCS	5 (10%)

Table 15. Composition of WNT3A/RSPO1 cell growth conditioned medium

Reagent	Volume (mL)
DMEM/F12	500
Na-pyruvate	5

L-Glutamine	5
FCS	5(10%)
Zeocin	0.125

Table 16. Composition of WNT3A/RSPO1 harvesting medium

Reagent	**Volume (mL)**
DMEM/F12	500
Na-pyruvate	5
L-Glutamine	5
FCS	2.5 (5%)

Table 17. Composition of ADF++ medium

Reagent	Volume (mL)
Advanced DMEM/F12	500
GlutaMax	5
HEPES	6
FCS	2.5 (5%)

Table 18. Composition of primary culture medium

Medium	**Composition**	**Volume (µL)**
Human esophagus primary cell media	ADF++	937.5
	Hydrocortisone (50 µg/mL)	10
	Human-EGF (100 µg/mL)	1 (1:10)
	Human-FGF-10 (100µg/mL)	1
	Human-Noggin (100µg/mL)	1
	B27 supplement (50x)	20
	N2-supplement (100x)	10
	N-acetylcysteine (500 mM)	2.5
	Nicotinamide (1 M)	10
	TGF-β inhibitor (0.5 mM)	4

	Rock inhibitor (3 mM)	3
	Forskolin (10 mM)	1
Human stomach primary cell media	ADF++	445.5
	Gastrin (5 mM)	1 (1:10)
	Human-EGF (100 µg/mL)	1 (1:10)
	Human-FGF-10 (100 µg/mL)	1
	Human-Noggin (100 µg/mL)	1
	B27 supplement (50x)	20
	N2-supplement (100x)	10
	N-acetylcysteine (500 mM)	2.5
	Nicotinamide (1M)	10
	TGF-β inhibitor (0.5 mM)	4
	Rock inhibitor (3 mM)	3
	WNT3A (100%)	250
	RSPO1 (100%)	250
	p38 Inhibitor (100 mM)	1 (1:10)
Mouse esophagus primary cell media	ADF++	946.5
	Mouse-EGF (500 µg/mL)	1 (1:10)
	Human-FGF-10 (100µg/mL)	1
	Mouse-Noggin (100 µg/mL)	1
	B27 supplement (50x)	20
	N2-supplement (100x)	10
	N-acetylcysteine (500 mM)	2.5
	Nicotinamide (1 M)	10
	TGF-β inhibitor (0.5 mM)	4
	Rock inhibitor (3 mM)	3
	Forskolin (10 mM)	1
	ADF++	446.5
	Gastrin (5 mM)	1 (1:10)
	Mouse-EGF (500 µg/mL)	1 (1:10)
	Human-FGF-10 (100 µg/mL)	1
	Mouse-Noggin (100 µg/mL)	1
	B27 supplement (50x)	20

Mouse stomach primary cell media	N2-supplement (100x)	10
	N-acetylcysteine (500 mM)	2.5
	Nicotinamide (1M)	10
	TGF-β inhibitor (0.5 mM)	4
	Rock inhibitor (3 mM)	3
	WNT3A (100%)	250
	RSPO1 (100%)	250

5.13 Quantitative Reverse Transcription -PCR

Table 19. QRT-PCR reaction mixture set up for one sample

Components	**Final concentration**	**volume**
Forward+Reverse primer mix (100 µM)	20 µM	4 µL
Green master mix (2x) high ROX	1X	10 µL
DNase/RNase-free water	-	1 µL
cDNA template	2.5 ng/ µL	5 µL
Total volume	-	20 µL

Table 20. QRT-PCR cycling conditions

Stage	**Step**	**Temperature**	**Time**
Holding	Denaturation	95°C	10 min
Cycling (40 cycles)	Denaturation	95°C	15 sec
	Annealing/Extension	60°C	1 min
Melt curve	Denaturation	95°C	15 sec
	Annealing	60°C	15 sec
	Denaturation	95°C	15 sec

6 Methods

6.1 Cell culture

All the primary and cell line culture was performed under a Laminar air flow chamber in a sterile condition. Unless otherwise stated, commercially available media components are used and cultured in different formats of plastic culture vessels with a respective volume of media. Cells were incubated inside the humidified incubator with 5% CO_2 at 37°C.

6.2 Cell line culture

3T3-J2 fibroblast cell line, L Wnt-3a cells (ATCC® CRL-2647™), 293T HA Rspo1-Fc cells or L cells (ATCC® CRL-2648TM), Wnt reporter cell line (293T WntR) were cultured in a complete medium containing Dulbecco's Modified Eagle Medium (DMEM) (Gibco, # 10938-025) supplemented with heat-inactivated 10% fetal calf serum (FCS) (Biochrome, #S0115), 2 mM L-glutamine (Invitrogen, #25030081) and 1 mM sodium pyruvate (Sigma, # S8636) at 37°C under a humidified incubator containing 5% CO2. To L Wnt-3a cells (ATCC® CRL-2647™), 293T HA Rspo1-Fc cells, additionally 1.25 µL/mL Zeocin (Invitrogen, #R25001) was added for the selection and propagation of cells. Cells were propagated in 25 cm^2/75 cm^2 flasks at a 70-80% confluence every 2-4 days. For passaging, adherent cells were washed twice with warm 5-10 mL of 1x PBS (Gibco, # 14190-094), followed by incubation with warm 1-3 mL trypsin (Gibco, #25300-096) for approximately 3-5 minutes at 37°C. Detached cells were resuspended and washed with a culture medium by centrifugation (300 xg, 6 min, 4°C). The cell pellet was resuspended in an appropriate volume of growth medium and transferred into fresh cell culture flasks in a 1:4 dilution.

6.3 RSPO1 and WNT3a conditioned media preparation

WNT3A and RSPO1 conditioned culture media used for complete 3D organoid media was prepared from L Wnt-3a cells (ATCC® CRL-2647™), 293T HA Rspo1-Fc cells, or L cells (ATCC® CRL-2648TM) respectively. Both conditioned media were prepared with the following same protocol.

On Day 1, one million L Wnt-3a cells/ 293T HA Rspo1-Fc cells were seeded in a T75 flask in 12 mL of growth medium (Table 15) and cultured for 2 days. On Day 3, cells were washed with PBS, treated with TrypLE, and split into two T150 flasks at a 1:4 ratio in a 20 mL growth medium (Table 15). Cells were cultured for another 3 days. On day 6, cells were split into a 1:4 ratio and cultured in eight T150 flasks for another 3 days. On day 9, cells were expanded to forty-eight T150 flasks at 1:4 ratio splitting. On day 11, the media was changed to 20 mL of harvesting media (Table 16) and incubated for 5 days. Conditioned media was collected as harvest-1 in a Sorvall centrifuge tube, and floating cells were pelleted by centrifugation (1500 xg, 10 min, 4°C). Conditioned media was filter-sterilized by passing through a 0.2 µm filter and stored at 4°C until pooling. Flasks were replenished with fresh harvesting media. This harvesting procedure was repeated another 3 times to get a total of 4 harvested conditioned media. The activity of WNT3A and RSPO1 conditioned media was tested using a reporter cell line (293T WntR) which expresses GFP upon Wnt pathway activation by conditioned supernatant. The quality of conditioned media was evaluated by quantifying the number of cells expressing GFP fluorescence using microscopy.

6.4 Mouse primary cell isolation and culture in the 3D organoid model

6.4.1 Tissue dissection

Mice were euthanized by cervical dislocation, and the whole mouse was surface sterilized by spraying 70% ethanol. Mice dissection was performed using sterile forceps and scissors in sterile conditions under a Laminar airflow chamber. The intact esophagus and stomach organs were removed aseptically and

transferred to a 10 mm Petri dish. Connective tissue and fat contents were removed using bent forceps. The esophagus and stomach organs were cut open longitudinally. Food particles were removed and washed thrice with ice-cold PBS. The organ was separated into the esophagus, gastro-esophagus junction, and corpus. Forestomach and antrum part was eliminated. Cut tissues were disinfected by incubation with 5 mL of 0.04% sodium hypochlorite solution at RT for 15 min. Tissues were washed with ice-cold PBS and processed for epithelial cell isolation.

6.4.2 Esophagus primary cell isolation

Esophagus and gastro-esophagus junction tissues were minced into small pieces in a separate 10 mm Petri dish. Minced tissue was transferred to a 15 mL conical tube containing 3 mL of warm Collagenase type II (Calbiochem, 234155) solution (Table 11) and incubated for 30 min at 37°C in a shaker at 180 rpm in a horizontal position to enzymatically digest tissue and dissociate the epithelial cells. The tissue was mechanically disrupted by pipetting up and down 10 times using a 1 mL pipette tip and centrifuged (1000 xg, 6 min, 4°C). The supernatant was discarded, and the pellet was resuspended in 3 mL of warm TryplE solution and incubated for 30 min at 37°C in a shaker at 180 rpm in a horizontal position. The tissue was mechanically disrupted by pipetting up and down 10 times using a 1 mL pipette tip and diluted to 10 mL with ADF++. Tissue debris was filtered by passing the solution through a 70 µm cells strainer (Falcon, 352350), and the collected solution was centrifuged (1000 xg, 6 min, 4°C) to wash TrypLE. Pellet was resuspended in 3 mL of ADF++, and the cell number was counted using the Neubauer chamber (Carl Roth, T728.1).

6.4.3 Growing esophagus organoids

Isolated cells were mixed with ice-cold Matrigel (Corning, 356231) to get a cell concentration of 10,000 cells /40 µL Matrigel per well and added as one droplet in a pre-warmed 24-well plate to culture 3D organoid. After incubation for 5 min at RT, 24 well plate was incubated inside a CO_2 incubator for 15 min at 37°C. After the polymerization of Matrigel, 500 µL of warm complete mouse esophagus primary cell media (Table 18) was added and incubated at 37 °C, 5% CO_2 in a humidified incubator. The media was changed every 3 to 4 days.

6.4.4 Propagation of esophagus organoids

For propagation of epithelial cells, 8 days old 3D organoids were harvested into a 15 mL falcon tube using ice-cold ADF++. Organoids were pelleted by centrifugation (300 xg, 6 min, 4°C). The organoid pellet was resuspended in 200 µL warm TrypLE and incubated for 20 min at 37°C in a shaker at 180 rpm to dissociate single cells. The solution was diluted to 10 mL with ADF++, and the cell suspension was centrifuged (300 xg, 6 min, 4°C). The cell pellet was resuspended in 5 mL of ADF++, and the cell number was counted. The required number of cells was pelleted by centrifugation and mixed with ice-cold Matrigel to get a cell concentration of 5000 cells/40 µL Matrigel. Matrigel was added to the pre-warmed 24-well plate. Media supernatant and Matrigel were discarded. After polymerization of Matrigel at 37°C, 500 µL of warm esophagus media was added, and the plate was incubated at 37°C, 5% CO_2 in a humidified incubator. The media was changed every 3 to 4 days.

6.4.5 Stomach primary cell isolation

After disinfection as above, corpus tissue was incubated in a 15 mL falcon tube wrapped in aluminum foil with 10 mL of 0.5 mM DTT/3 mM EDTA in PBS solution for 90 min at RT on a roller platform to weaken the intercellular junction and to release glands. After incubation, tissue was once rinsed with ice-cold PBS and transferred to a 15 mL falcon tube containing 10 mL of ice-cold PBS. The Falcon tube was shaken vigorously for 1 minute to release the glands. Residual tissue was discarded, and the solution containing glands was centrifuged (300 xg, 6 min, 4°C). The gland pellet was resuspended in 1 mL of ADF++, and the number of glands was counted under a microscope using the Neubauer chamber. Depending on the number of wells to seed, the required volume of solution containing glands was centrifuged (300 xg, 6 min, 4°C). The gland pellet was resuspended in ice-cold Matrigel to get a concentration of 100 glands/40 µL Matrigel per well. 40 µL of Glands with Matrigel was added per well of a pre-warmed 24-well plate and incubated at 37°C for 15 min in a 5% CO_2 incubator. After the polymerization of Matrigel, 500 µL of complete mouse stomach primary cell media (Table 18) was added and incubated at 37°C in a 5% CO_2 incubator. The media was changed every 3 to 4 days.

6.4.6 Propagation of stomach organoid

For propagation of stomach organoids, on day 8, organoids were split into 1:2 to 1:4 ratios depending on the size and the number of organoids per well. Matrigel organoid suspensions from 3 to 4 wells were pooled into a 15 mL falcon tube using ice-cold ADF++. Organoids were pelleted down by centrifugation, and Matrigel and supernatant were discarded. The organoid pellet was resuspended with 1 mL of pre-warmed TypLE and incubated in a shaking water bath (100 rpm) at 37°C for 5 min. Organoids were broken down by pipetting up and down 5 times with a 200 µL pipette tip. The broken organoid-containing solution was diluted with 5 mL of ADF++ and centrifuged. Pellet was mixed with the required volume of Matrigel; 40 µL Matrigel drop was seeded per well in a pre-warmed 24-well plate and incubated at 37°C for 15 min to allow solidification of Matrigel. After the polymerization of Matrigel, 500 µL of mouse stomach primary cell media (Table 18) was added and incubated at 37°C in a 5% CO_2 incubator. The media was changed every 3 to 4 days.

For organoid efficiency calculation, harvested organoids were incubated with 1 mL warm TrypLE for 10 min in a shaking water bath (100 rpm) at 37°C. Organoids were made into single cells by gentle pipetting up and down 20 times with a 200 µL pipette tip. The solution was diluted to 5 mL with ADF++, and cells were pelleted down by centrifugation. The cell pellet was resuspended in 2 mL of ADF++, and the cell number was counted. The required volume of cell suspension was centrifuged, and the pellet was resuspended in ice-cold Matrigel to get a concentration of 5000 cells /40 µL Matrigel. 40 µL of Matrigel was added per well of a pre-warmed 24-well plate and incubated at 37°C for 15 min in a 5% CO2 incubator. After the polymerization of Matrigel, 500 µL of complete mouse stomach primary cell media (Table 18) was added and incubated at 37°C in a 5% CO2 incubator. The media was changed every 3 to 4 days.

6.5 Human primary cell isolation and culturing in 3D model

Human esophagus or stomach biopsies were collected from the patients undergoing endoscopic surveillance for BE or cancer. Normal human esophagus and cardia tissue samples were obtained from the patients who had undergone surgeries. The informed consent form was obtained from the patients, and experiments were conducted under the Ethics permission number EA4/034/14, approved by the ethics committee of Charité University Medicine, Berlin, Germany.

Tissue samples were processed to isolate epithelial cells within 2 hr of surgery. The tissue was washed thrice with ice-cold PBS and minced into small pieces using sterile scissors and forceps. Minced tissues were transferred into a 15 mL falcon tube containing 5 mL of pre-warmed Collagenase II solution (Table 11). Falcon tubes were incubated for 2 hr at 37°C in a shaker at 180 rpm in a horizontal position to digest tissue and dissociate the epithelial cells enzymatically. Hereafter, the isolation of epithelial cells was performed as above.

6.5.1 Esophagus epithelial 2D culture

Human esophagus cells were maintained in 2D by co-culturing with mouse fibroblast 3T3-J2. After isolating single cells, cells were seeded on collagen-coated one well of 6 well plates in the human esophagus primary cell medium (Table 18) and incubated at 37°C in a 5% CO_2 incubator. The media was changed every 3 to 4 days. After reaching nearly 75% to 80% confluence, the monolayer of cells was washed with warm PBS. Differential trypsinization was performed by adding 2 mL of pre-warmed TrypLE to the monolayer and incubating for 2 min at 37°C in a 5% CO_2 incubator to detach nonepithelial cells, which usually detach earlier than epithelial cells. After incubation, detached cells were aspirated, then 3 mL of TrypLE was added; cells were incubated for 10 min at 37°C in a 5% CO_2 incubator. Cell clumps were made into single cells by pipetting up and down using a 5 mL pipette, and cells were transferred to a 15 mL falcon tube containing 7 mL of ADF++. Cells were then centrifuged, and the pellet was resuspended with 3 mL of ADF++ and used for seeding either for 2D co-culture with mouse fibroblast or 3D organoid culture.

6.5.2 Esophagus epithelial 2D co-culture

Mouse fibroblast cell line 3T3-J2 used as a feeder cell was grown to 90% to 95% confluence using a complete DMEM medium (Table 14) in a T25 flask. 3T3-J2 containing flask was lethally irradiated (30Gy, 36 min irradiation), and media was washed with PBS. Harvested esophagus cells were added on top of irradiated feeder cells in the human esophagus primary cell medium (Table 18) and incubated at 37°C in a 5% CO_2 incubator. After esophagus cells reached 75% confluence, cells were washed with PBS, and epithelial cells were detached by the differential trypsinization method as above.

6.5.3 Esophagus epithelial 3D organoid culture

Esophagus epithelial cells harvested from 2D culture were used to generate 3D organoid culture. Approximately 10,000 cells were used in 40 µL Matrigel per well. Matrigel was overlaid with 500 µL of human esophagus primary cell media (Table 18) and cultured as described above for mouse esophagus organoids.

6.5.4 Stomach epithelial organoid culture

Isolated stomach epithelial cells from tissue were directly cultured in Matrigel to generate organoids using human stomach primary cell media (Table 18). Splitting and propagation of stomach organoids were performed as described above for mouse stomach organoids.

6.6 Freezing and thawing primary cells

For cryopreservation of primary epithelial-derived organoids, epithelial cells were grown into organoids until day 3 or 4, and organoids were harvested as above. one well-worth of the organoid pellet was resuspended in 500 µL Cryo-SFM medium and transferred to labeled cryovials. For 2D cells, isolated cells from one T25 flask were transferred into 3 cryovials. Cryovials were slowly frozen (-1°C/min) inside a freezing container filled with isopropanol overnight at -80°C. For short-term storage, vials were kept at -80°C, and for long-term storage, vials were stored in a liquid nitrogen tank.

For thawing organoids, the cryovial was immersed in a water bath at 37°C without touching the rim of the vial cap. The thawed organoid with the freezing

the medium was transferred to a 15 mL falcon tube, and 5 mL of ADF++ was added dropwise and centrifuged. The organoid pellet was resuspended in ice-cold Matrigel, seeded on pre-warmed 24 well plates, and a complete 3D medium was added.

6.7 Organoid-forming efficiency and size analysis

Epithelial cells were counted, and a defined number of cells were resuspended in 40 µL of Matrigel to generate organoids as described above. One week after seeding, whole well images were acquired, and the number of organoids formed was counted. Organoid formation efficiency was calculated by determining the percentage of organoids formed from the number of cells seeded. The size of organoids was determined by measuring the diameter of organoids using Image J software.

6.8 Lineage tracing of mice and organoids

The lineage tracing of esophagus squamous epithelial cells and stomach columnar epithelial cells was performed using C57/bl6 mice either containing *Krt5-CreERT2; Rosa26-tdTomato* or *Krt8-CreERT2; Rosa26-tdTomato*. To activate Cre, Tamoxifen solution was freshly prepared (Table 11) and the solution was injected intraperitoneally to get a final concentration of 0.2 mg/g body weight of a mouse. The injection was repeated 2 times in subsequent days. To analyze the lineage-traced cells, mice were euthanized between 14 weeks and 20 weeks according to ethically approved procedures. Tissues were freshly frozen as described below (in 6.10.5) for further use.

To trace epithelial lineage invitro, esophagus or stomach epithelial cells were isolated from the C57/bl6 mice either containing *Krt5-CreERT2; Rosa26-tdTomato* or *Krt8-CreERT2; Rosa26-tdTomato*. Organoids were cultured as described above. To induce lineage tracing, 4OH-Tamoxifen was added at a final concentration of 800 nM for 2 days from the beginning of the culture.

6.9 Microscopy

Fluorescence images were acquired with the confocal fluorescent microscope SP5/SP8. Whole slide images were acquired with an Axio scan imager with a tiling function performed at Microscopy Core Facility, Max Planck Institute for Infection Biology (MPIIB), Berlin. Routine phase-contrast images were acquired using the Olympus CKX41 inverted cell culture microscope.

6.10 Immunofluorescence histochemistry

6.10.1 Fixation and paraffinization of tissue

Human and mouse tissue samples were washed with PBS and fixed with 3.7% PFA overnight at 4°C. Tissues were washed 3 times with PBS and subjected to sequential dehydration followed by paraffinization. Tissues were passed through alcohol series (70%, 80%, 90%, 100%), isopropanol, xylene, and molten paraffin, 60 min each using a Tissue processor (Leica TP1020) machine. The paraffin block was prepared using a paraffin embedding station (Microm AP250) and stored at RT.

6.10.2 Fixation and paraffinization of organoids

Organoids along with Matrigel were harvested from the well using 5 mL of ice-cold 0.1% BSA in PBS into a 10 mL glass tube previously rinsed with 0.1% BSA in PBS. Organoids were allowed to settle down by gravity by keeping tubes on ice for 15 min. The upper layer of the supernatant was removed without disturbing settled organoids. Organoids were mixed with 5 mL of ice-cold 0.1% BSA and allowed to settle down on the ice. The process was repeated 3 to 4 times until no visible Matrigel was observed inside the tube. The last wash was performed with ice-cold PBS to remove 0.1% BSA. Organoids were fixed with 5 mL of 3.7% PFA for 1 hr at RT. PFA was washed with PBS, and organoids were subjected to dehydration in a series of ethanol (70%, 80%, 90%, 100%) followed by isopropanol and acetone wash twice each with 20 min incubation. Approximately 1 mL of acetone was retained and proceeded for the paraffinization immediately or stored at 4°C for one week until use.

Parffinsation of organoids was performed manually. The embedding metal jar was preheated to 65°C using a heating plate. Organoids along with acetone were transferred to the heated metal jar and allowed to evaporate the acetone. When there was a still residual amount of acetone, molten paraffin was added to the organoids and incubated for 15 min to penetrate the paraffin inside the organoids. The metal jar was transferred to a cooling pad for a few seconds to solidify paraffin; the plastic cassette was placed on top and overlaid with more molten paraffin, incubated at -8°C for 1 hr to solidify.

6.10.3 Deparaffinization and rehydration

Paraffinized tissue or organoid sections of 5 µm thickness were cut using a microtome (Microm HM315) and spread on top of water preheated to 40°C. Sections were transferred to high-binding adhesion slides (Thermo Scientific™ SuperFrost Plus©, J1800AMNZ) and dried at RT. For tissue sections, slides were heated to 60°C for 1 hr before proceeding to deparaffinization and rehydration. Deparaffinization was performed by passing the slides through xylene twice with incubation of 10 min each, followed by rehydration performed with a series of ethanol (2 times each with 100%, 90%, 70%, and 50 % ethanol) and water for 2 min each. Hydrated sections were subjected to antigen retrieval by heating slides in antigen retrieval solution (Dako, # S1699) at 95°C for 30 min.

6.10.4 Antibody staining and imaging

Slides were washed with running tap water and by adding PBS to the tissue. A circular barrier was drawn surrounding the section using a Pap pen. PBS was removed, and 50 to 100 µL blocking solution was added (Table 11), followed by 60 min incubation at RT. The blocking solution was replaced by primary antibodies diluted in the blocking solution and incubated overnight at 4°C inside the humidified chamber. The antibody was discarded, and sections were washed 5 times by incubation with PBS for 2 to 3 min each. Added fluorochrome tagged secondary antibodies diluted in blocking solution along with diluted DNA binding dye Hoechst or DAPI or Draq5 and incubated for 60 min at RT.

For directly tagged antibodies, sections were stained with secondary antibodies without adding DNA dye. After washing with PBS 5 times, sections were

blocked for 1 hr at RT. Directly tagged primary antibody diluted in blocking solution was added along with DNA dye of choice for 2 hr at RT.

Following incubation, sections were washed with PBS 5 times as above, and a final wash with water. Sections were mounted on Mowiol mounting solution (Table 11), covered with a glass coverslip, and dried at RT. Images were acquired either with a Leica TCS SP8 confocal microscope (Leica Microsystems GmbH) or an AxioScan imager for tiled images. Images were processed using Image J, ZEISS ZEN blue edition image software, or Adobe Photoshop.

6.10.5 Fresh frozen block preparation and staining

For lineage-traced mice, tissues were fixed with 2 % PFA for 1 hr at RT in the dark. Tissues were washed thrice with PBS. The freezing apparatus was prepared by keeping a small plastic box filled with 5 mL of isopentane on top of a 1:1 mixture of dry ice and isopropanol. Excess liquid from the tissue was wiped with tissue paper and placed on a plastic cryomold. The tissue was overlaid with OCT medium, and the cryomold was placed on pre-chilled isopentane for solidification. The frozen blocks were either sectioned using a cryostat microtome (Thermo Microm HM525 NX) or stored at -80°C.

Sections were air-dried at RT overnight in the dark. Before antibody staining, sections were kept at 40°C for 20 min and washed 5 times with PBS to remove the OCT medium. After drawing a barrier circle around the section, tissue was permeabilized by adding 50 µL to 100 µL Immunofluorescence permeabilization solution (Table 11) and incubated for 1 hr at RT. DNA dye or antibody staining was performed as above, except the blocking solution was replaced by an Immunofluorescence permeabilization solution wherever applicable.

6.11 Standard protein methods

6.11.1 Sample preparation

To extract proteins, organoids were harvested by washing them with ice-cold PBS. The organoid pellet collected in Eppendorf was dissolved in 100 µL of 1: 3 diluted 6X Laemmli buffer (Table 11) and mixed well using a 200 µL pipette

tip. The lysate was boiled at 95°C for 10 min at 1000 rpm and stored at -20°C until use.

6.11.2 Sodium dodecyl-sulfate polyacrylamide gel electrophoresis (SDS-PAGE)

Stacking (7%) and resolving gel (12%) solutions were prepared from Acrylamide/ Bisacrylamid depending on the size of the protein of interest. The gel solution was prepared according to Table 11.

To prepare the gel, the resolving gel was poured until a quarter of two SAS-PAGE glass plates and covered with a thin layer of isopropanol. After polymerization, isopropanol was washed with water and overlaid with freshly prepared stacking gel. Immediately comb was inserted into the stacking gel and allowed to polymerize. Polymerized gel with plate was inserted in 1X SDS-PAGE running buffer (Electrophoresis buffer) (Table 11). 10 µL of protein lysate and 5 µL prestained protein ladder was loaded into the gel. Protein was run for 15 minutes at 70 V, followed by 90 minutes at 120 V.

6.11.3 Western blot

Separated proteins in the gel were transferred onto the PVDF membrane to detect specific proteins by an antibody. For this, the PVDF membrane was activated by soaking in 100% methanol for a few seconds, followed by washing with wet blot transfer buffer (Tabel 11). A sandwich of wet blot buffer (Table 11) soaked trans-blot sponge, Whatman paper, PVDF membrane, gel with separated proteins, and Whatman paper, a trans-blot sponge was prepared. The sandwich assembly was inserted inside Mini Trans-Blot® Electrophoretic Transfer Cell (Bio-Rad) filled with wet blot transfer buffer (Tabel 11) and an ice pack. Proteins were transferred to the membrane by applying 250 mA, 400 V, and 4°C under constant stirring for 2 hr. After transfer, the membrane was washed with 1X TBS (Table 11) for 5 min in a shaker, followed by blocking with western blot blocking solution (Table 11) at RT. A primary antibody diluted in western blot blocking solution was added to the membrane and incubated overnight in the shaker at 4°C. The primary antibody was washed 3 times with 1X TBST (Table 11) for 10 min each on a shaker at RT. Next, an appropriate secondary antibody tagged with peroxidase diluted in western blot blocking

the solution was added and incubated for 1 hr at RT on a shaker. The secondary antibody was washed 3 times with 1XTBST and one time with 1XTBS. The membrane was kept between the thin plastic sheet. The membrane was covered with a chemiluminescence reagent (Amersham Hyperfilm ECL or Perkin Elmer) for 1 min at RT. Excess liquid was removed, and the signal was developed using either Hyperfilm (Amersham Biosciences) and a developer machine in a dark room or a gel imager.

6.12 Flow cytometry

Organoids were harvested as described above to analyze the percentage of cells in different stages of the cell cycle. Organoids were treated with TrypLE at 37°C for 10 min in a shaking water bath. Organoids were made into single cells and passed through a 40 µm cell strainer. Cells were fixed with 2% PFA for 20 min. Cells were washed and permeabilized by incubating with FACS permeabilization buffer (Table 11) for 30 min on ice. Cells were stained by incubating with a FITC-tagged Ki67 antibody and 7 AAD (1:20 dilution) solution for 30 min on ice. Cells were washed and resuspended in 200 µL of 0.1% BSA in PBS. Cells were acquired with BD FACS Aria and analyzed with BD FACSDiva software. Cell debris, singlet, and aggregate were excluded by applying SSC and FSC gates. Further FSC area and FSC height ratio were used to select single cells. Fluorophores were excited by an excitation laser with 488 nm wavelength and the signal was detected by their corresponding detectors: FITC (502LP-530/30), 7 AAD (655LP-695/40). Approximately 20,000 single cells were acquired, and data were analyzed using BD FACSDiva software.

6.13 RNA analysis technologies

6.13.1 Single-molecule RNA in situ hybridization

To detect the expression of genes in the tissue, smRNA-ISH was performed using the RNAScope kit (Advanced Cell Diagnostics, 322350) according to manufacturer protocol with some modifications. Briefly, tissues or organoids

were deparaffinized as described above. 10 µm thick sections were cut using a microtome (Microm HM315) and transferred onto superfast slides (Thermo Scientific™ SuperFrost Plus©, J1800AMNZ). Slides were dried at 37°C for 1 hr and baked at 60°C for 1 hr. Deparaffinization was performed by incubating for 5 min with xylene two times, followed by two-time incubation with 100% ethanol for 1 min each. Slides were air-dried, and hydrogen peroxide was applied for 10 min at RT. After washing with distilled water, antigen retrieval was performed by incubating slides in boiling antigen retrieval solution for 20 min. Slides were washed with distilled water and 100% ethanol and air-dried at RT. After drawing hydrophobic barriers surrounding the sample, protease plus was applied and incubated inside humidified HybEZ oven at 40°C for 20 min. After washing with distilled water, slides were incubated with hybridization probes (Table 6) and amplification probes. Initially, slides were incubated with a hybridization probe for 2 hr at 40°C, then 30 min at 40°C with AMP1, 15 min at 40°C with AMP2, 30 min at 40°C with AMP3, 15 min at 40°C with AMP4. Slides were incubated with AMP5 and AMP6 at RT for 45 and 15 min, respectively. Between each incubation step, slides were washed with wash buffer two times for 2 min at RT. Sections were incubated with Fast Red solution for 10 min at RT to develop a signal. After washing slides with distilled water, sections were counterstained with 50% Hematoxylin solution for 2 min. After washing with water, slides were incubated with 0.02% ammonia, followed by a wash with distilled water. Slides were air-dried and dipped with xylene solution, and sections were covered with Eco mount solution, placed in coverslip, and allowed to dry at RT before microscopy. Images were acquired with an Axio Scan imager at 10X magnification and processed by ZEN Blue imaging software.

6.13.2 Isolation of RNA and qRT-PCR

The organoid pellet from two wells was used for RNA isolation using Qiagen RNeasy Mini or Allprep Kit according to manufacturer protocol under RNAse free environment. RNA quality and quantity were measured using NanoDrop® ND-1000 Spectrophotometer (Kisker). RNA was stored at -80°C until further use.

1 µg of RNA was treated with DNase I and was reverse transcribed into cDNA using the RevertAid First Strand cDNA Synthesis Kit (Thermo Fisher Scientific, K1621) according to manufacturer protocol. cDNA was diluted to a 1:20 ratio and mixed with a qRT-PCR reaction mixture (Table 19). QRT-PCR was run in triplicates per sample on RTCR applied biosystem machine with the program mentioned in Table 20. The expression level of the housekeeping gene *Gapdh* was used to normalize the relative expression level of genes. Fold changes of genes were calculated using the $2^{-\Delta\Delta Ct}$ method by normalizing endogenous *Gapdh* gene expression and relative to the untreated control (Livak and Schmittgen 2001).

6.13.3 Microarray expression analysis

Organoids were harvested using ice-cold PBS as triplicates, and the pellet was dissolved with a 1 mL Trizol® reagent. All steps from RNA isolation from Trizol® samples up to array scanning were performed in the MPIIB, Berlin, Germany, Microarray Core Facility. Microarray analysis was performed with help from Christian Wentland, Chumduri group, University of Wurzburg. Total RNA was isolated using Allprep DNA/RNA Mini Kit (QIAGEN, #80204) according to manufacturer protocol. The quantity of RNA was measured using a NanoDrop 1000 UV-Vis spectrophotometer (Kisker), and quality was assessed by Agilent 2100 Bioanalyzer with an RNA Nano 6000 microfluidics kit (Agilent Technologies). Microarray experiments were performed as single-color hybridizations on Agilent- 028005 SurePrint G3 Mouse GE 8x60K, and Agilent Feature Extraction software was used to obtain probe intensities. The extracted single-color raw data files were background corrected, quantile normalized, and further analyzed for differential gene expression using R and the associated BioConductor package limma (Ritchie et al. 2015).

To compare esophagus and stomach gene expression, an unpaired t-test was performed. Genes with a p-Value < 0.05 and log2 fold change of − 0.5849625 and 0.5849625, corresponding to a 1.5-fold decrease, or increase in abundance, respectively, were considered differentially expressed. For corresponding replicates (condition vs. control in the same animal), a paired t-test was used within animals. Otherwise, an unpaired t-test was used. For each comparison, genes with a p-Value < 0.05 and an absolute log2 fold change >

1.5 were considered differentially expressed. All statistical analysis was performed with R unless stated otherwise.

6.13.4 Gene set enrichment analysis (GSEA)

A pre-ranked GSEA with 5000 permutations was performed using the associated R package fgsea (Ritchie et al. 2015). For each comparison, probes were converted to Human orthologues and ranked by their t-statistics. Enrichment was computed on Molecular Signature Database (MSigDB) (Subramanian et al. 2005) gene sets from the Hallmark (h.all.v7.0.symbols.gmt), Curated (c2.all.v7.0.symbols.gmt), GO_BP (c5.bp.v7.0.symbols.gmt), regulatory target (c3.all.v7.0.symbols.gmt), oncogenic (c6.all.v7.0.symbols.gmt) and immunologic (c7.all.v7.0.symbols.gmt) category and additional custom gene sets. For further analysis, the false discovery rate (FDR) was computed using the Benjamini-Hochberg method (Benjamini and Hochberg 1995), and gene sets with an FDR < 0.05 were considered significantly enriched.

6.13.5 Overrepresentation analysis of microarray data

The over-representation analysis (OA) was performed using the function compareCluster from the R package ClusterProfiler (The Gene Ontology Consortium 2019). Significantly differentially expressed genes between the stomach (3234 genes) and esophagus (3415 genes) with a valid Entrez ID, were used as input for the analysis

6.13.6 Sample preparation for single-cell RNA sequence

To prepare single cells from the organoids, Matrigel was completely removed by washing thrice with ice-cold PBS, and centrifugation (5 min, 300 xg, 4°C). Single cells from organoids were dissociated by incubating with warm TrypLE in a shaker (15 min, 37°C, 180 rpm) and pipetting up and down 20 times using a 1 mL pipette. To remove cell clumps dissociated cells were filtered through a 40 µm cells strainer to obtain suspension of single cells, and the cells were washed with 0.1% BSA in 1X PBS.

6.13.7 Multiplexing individual samples for single-cell RNA sequencing

Single-cell suspension was subjected to multiplexing of samples according to the MULTI-seq protocol (McGinnis et al. 2019). The cell multiplexing and scRNA seq of organoids were performed in collaboration with Dr. Antoine-emmanuel Saliba group, Helmholtz Institute for RNA-based Infection Research Würzburg, Germany. The cells number were counted, and a total of 1×10^6 cells/sample were pelleted at 1000 xg for 5 min. The pellet was resuspended in 180 µL of 3X SSC buffer with 1%BSA. To this 20 µL of 20X lipid-modified DNA oligonucleotide (LMO) anchor: with a unique "sample barcode" oligonucleotides mix (20X= 4µM) to be multiplexed, with each sample receiving a different sample barcode, was added. After incubation of samples on ice for 5 min, 20 µL of 20X (20X= 4µM) common lipid-modified co-anchor was added to stabilize the membrane residence of barcodes. Samples were incubated on ice for an additional 5 min. Added 500 µL of ice-cold 3X SSC containing 1% BSA to the samples, pelleted by centrifugation (1000 g for 5 min at 4°C), and the supernatant was removed. The cell pellet was rewashed with 500 µL of ice-cold 3X SSC+1% BSA, and the pellet was resuspended in 150 µL of ice-cold 0.125X SSC + 0.04% BSA. The resuspended cells from individual samples were counted. The samples were pooled together in equal ratios, and cell numbers were adjusted to 1000 cells/µL.

6.13.8 Single-cell RNA sequence library preparation and MULTI-seq

The single cells were partitioned into nanolitre-scale Gel-Bead-In-EMulsions (GEMs) beads using a 10x Chromium Controller. To prepare the library, single-cell suspended in GEMs were processed for reverse transcription, cDNA amplification, and construction of the gene expression libraries using the 10x Genomics Single Cell 3′ v3.1 RNA-seq kit and accompanying protocol. The cDNA amplification and reaction incubations were performed on SimpliAmp Thermal Cycler (Applied Biosystems) and Libraries were quantified by QubitTM 3.0 Fluorometer (ThermoFisher), and quality was checked using a 2100 Bioanalyzer with a High Sensitivity DNA kit (Agilent). Using Novaseq 6000 sequencer (Illumina), sequencing was performed in paired-end mode with an S1 100-cycles kit.

6.13.9 Processing of raw sequencing data

Raw data processing and downstream bioinformatic analysis of scRNA-sequence data were performed together with Pon Ganish Prakash, Chumduri group, University of Wurzburg. CellRanger (v3.1.0) software from 10x Genomics was used to process the raw sequencing data. Using default parameters and mm10 build of the mouse genome as a reference, FASTQ file generation, UMI counting, and generation of the feature barcode matrix were achieved using the commands "cell ranger mkfastq" and "cell ranger count".

6.13.10 Single-cell RNA sequence sample De-Multiplexing

The generated MULTI-seq FASTQ files were processed using the R package deMULTIplex (v1.0.2) (https://github.com/chris-mcginnis-ucsf/MULTI-seq) to determine the sample origin of each cellular barcode. This resulted in a sample barcode UMI count matrix data which was then used by the MULTI-seq sample classification pipeline to group the cells from the same samples together. Cells that are positive for more than one sample barcode were classified as doublets. To overcome the non-ideal situation in the sample multiplexing process where usually a small group of cells can remain 'negative' without falling into any of the sample groups, a semi-supervised negative cell reclassification was used using the functions 'findReclassCells' and 'rescueCells' to rescue the negative cells and add them back to their respective predicted sample groups. Finally, complete information regarding the sample group (including negatives and doublets) for each cell was utilized for downstream analysis.

6.13.11 Single-cell RNA-seq data quality control, normalization, and clustering

The digital gene expression matrix was analyzed using R software (v.4.0.3) with the Seurat (Hao et al. 2021) package (v.4.0.0). Previously demultiplexed sample barcode UMI information was incorporated into the metadata. Negatives and doublets were excluded from the data for further analysis. Then, cells were filtered using the condition where barcodes with less than 100 genes, more than 8500 genes, and more than 80,000 UMI counts were suspected potential doublets. Broken or low-quality cells with <20% of the UMIs derived from the mitochondrial genome were excluded. Ultimately, Individual Seurat

objects were created based on each sample. Normalization and variance stabilization of these objects was performed using the SCtransform package (v.0.3.2) (Hafemeister and Satija 2019), which also identified the highly variable genes. Mitochondrial mapping percentage and cell cycle scores were regressed during normalization. Dimensionality reduction of the data was performed using the RunPCA function with default parameters. Clustering was done on the top 30 principal components using the FindNeighbors and FindClusters functions, which were then visualized by implementing a nonlinear dimensionality reduction with the RunUMAP function. A set of mixup cells/doublets with erroneously annotated sample barcodes and cells, with substantial and coherent expression profiles of a hybrid transcriptome based on columnar and squamous epithelial marker gene expression (Krt8/18 and Krt5/14/6a/13, respectively) were identified and excluded in the analysis. Reclustering of esophagus and stomach cell clusters separately unraveled the different subpopulations present within both epithelia.

6.13.12 Cell-Type Annotation and differential gene expression identification

The identified cell clusters were annotated based on specific canonical marker genes. Additionally, to identify highly differentiated genes across clusters, the FindAllMarkers command was used with the default Wilcoxon rank-sum test in Seurat.

6.13.13 Trajectory Inference/Pseudotime Analysis

Developmental trajectories in the data were modeled using the Slingshot package (v.1.6.1) (Street et al. 2018). Global lineage structure and pseudotime values were calculated using get lineage and getCurves functions with default parameters.

7 Results

7.1 Gastroesophageal junctional and the mucosal lining

To investigate the disease development at the GEJ, it is critical to understand the GEJ homeostasis and signaling mechanisms that regulate the GEJ. The adult human esophageal mucosa is lined with stratified squamous epithelium that meets the columnar epithelium-lined stomach at the GEJ (Figure 8 A). Esophagus epithelial cells are structured into basal stem cell populations, parabasal populations consisting of proliferative cells, and suprabasal differentiated cells. The human esophagus epithelium meets with columnar epithelial cells-lined cardia in the distal stomach region at GEJ. In the mouse, the esophagus opens into the stomach that comprises two regions- a glandular stomach and stratified squamous epithelium-lined fore-stomach similar to the esophagus (Figure 8 B).

Besides the highly similar architecture between mice and human esophageal epithelium, most of the mice's esophageal basal cells proliferate, while in humans, only very few basal cells and many parabasal cells proliferate (Hayakawa et al. 2021). Further, the mouse esophagus contains superficial cornified layers, which are absent in the human esophagus. Multi-layered squamous epithelial cells are much thicker (20 to 30 layers) than mouse esophagus (4 to 6 layers) (Zhang et al. 2017). The human esophagus consists of submucosal glands while it is absent in the mouse.

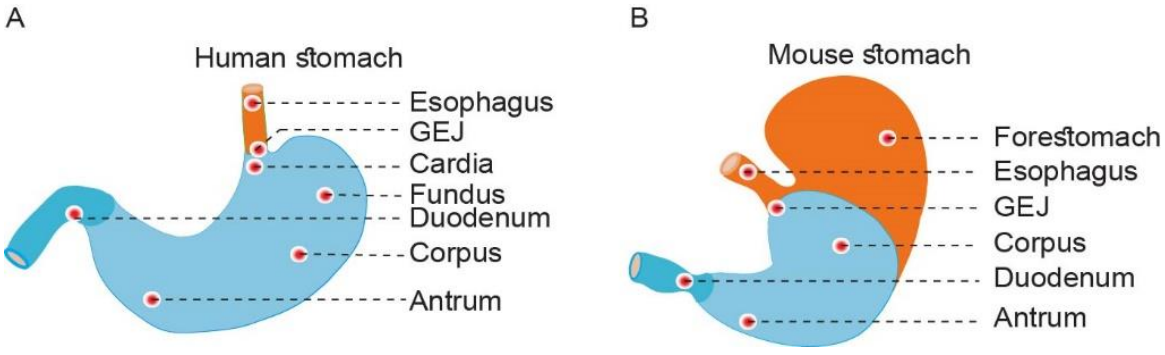

Figure 8. Human and mouse esophagus and stomach anatomy. (A) The human esophagus's distal region joins with the stomach's proximal region forming GEJ. **(B)** In the mouse, the esophagus is continuous with the forestomach having squamous epithelial cells joined with columnar epithelial cells of the stomach form GEJ around the mid-region of the stomach.

7.2 Embryonic Development of gastroesophageal epithelium

To gain insights into the development and establishment of the postnatal epithelial cells at the GEJ, I analyzed the mucosal lining of the GEJ at different embryonic stages and in adult tissues. For this, the entire esophagus and stomach, including GEJ tissues from mouse embryonic days 13 (E13), E16, E19, and an adult, were fixed with paraformaldehyde and embedded with paraffin. The tissue sections were made from paraffin block and analyzed by immunohistochemistry for the cytokeratin and p63 transcription factor. On E13, the entire mucosal lining of the stomach consists of columnar-type progenitor epithelial cells without squamous epithelium-lined foregut observed in adult mice stomachs. These progenitor cells express columnar-specific marker protein cytokeratins ($KRT8^+KRT7^+$) and show no expression of squamous cell markers (KRT5 and p63) (Figure 9 A, B). The esophagus's distal region was lined by columnar-type progenitor epithelial cells. In contrast, the proximal region consisted of multi-layered cells with basal-type cells expressing squamous epithelia specific p63. These $p63^+$ cells were present below the columnar-type progenitor epithelial cells. These proximal esophageal cells, although they express p63, but do not express KRT5, indicating that at this stage, progenitor cells differentiation to multi-layered epithelium involves the p63. No proper epithelial glandular structure is formed in the stomach region at this stage.

On E16, esophagus and forestomach cells express p63 below the $KRT8^+KRT7^+$ columnar epithelial cells. At this stage, these subcolumnar $p63^+$ cells also expressed KRT5 in the esophagus and forestomach. The columnar progenitor cells were superimposed over the multi-layered p63 expressing squamous epithelial cells. However, at the junctional region, some of the $KRT8^+KRT7^+$ progenitor columnar cells express p63 without KRT5 expression ($KRT8^+KRT7^+p63^+KRT5^-$) (Figure 9 A, B). In the stomach region, glandular structure formation of columnar epithelial cells began indicating the differentiation of progenitor columnar epithelial cells into different functional columnar epithelial cell types.

By E19, proper squamous multilayered $p63^+KRT5^+$ epithelial cells that are distinct from $KRT8^+KRT7^+$ columnar cells, lined the esophagus and forestomach

mucosa. In this embryonic stage, columnar epithelial that are $KRT8^{+}KRT7^{+}$ but $p63^{-}KRT5^{-}$ attained glandular structure in the stomach region (Figure 9 A, B). The columnar progenitor cells were shedding from the esophagus and forestomach, leaving visibly demarcating squamous and glandular mucosal areas of the esophagus and stomach. In the GEJ region, $KRT7^{+}KRT8^{+}p63^{+}KRT5$- cells subsequently gain KRT5 expression and lose KRT8 expression creating a clear border between squamous and columnar epithelia.

In summary, in the E13 stage, the distal esophagus and entire stomach mucosa are lined with progenitor columnar-type epithelial cells. During E13 to E19 progression, these progenitor columnar-type epithelial cells gradually achieve squamous features with emerging ($p63^{+}KRT5^{+}$) at the sub-columnar position in the esophagus region. This process proceeds from the proximal esophagus towards the distal esophagus until the formation of the SCJ at E19. From E16 until E19, progenitor epithelial cells covering the stomach mucosa start to invaginate and develop glandular structures indicating terminal differentiation to different gastric cell types.

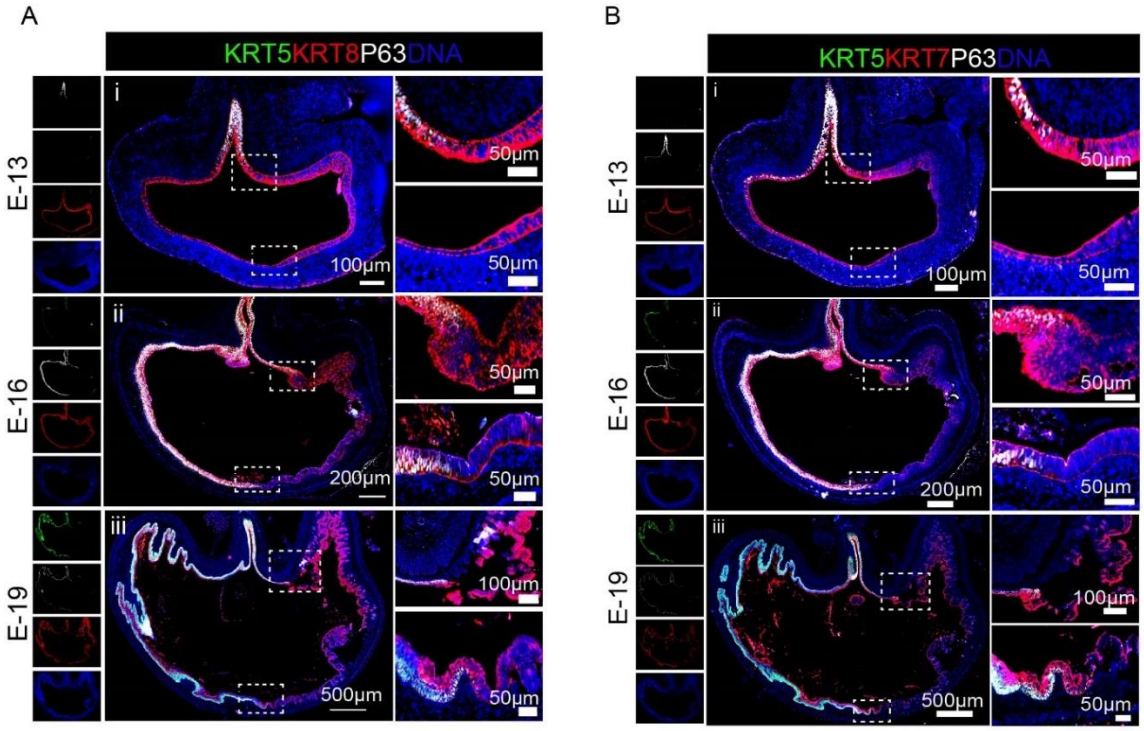

Figure 9. Development of gastroesophageal epithelium in embryonic stages. (A-B) Tiled images of tissue sections from mouse esophagus and stomach from embryonic day 13

(E-13) (i), E-16 (ii), and E-19 (iii) stained with KRT5 (green), KRT8 (red)/KRT7 (red), p63 (white). Nuclei are stained with DAPI (blue). Enlarged images from the dotted box are shown in the right panel of each image.

7.3 Adult gastroesophageal junction comprises two distinct epithelial lineages

Next, I analyzed the epithelial lining of the GEJ mucosa in the adult mouse and human tissue. I used deparaffinized tissue sections from 8 to 10 weeks old mice and normal adult human gastroesophageal junctional tissue samples. In humans, basal cells express high levels of p63 that decrease with differentiation towards parabasal to suprabasal cells (Figure 10 A). In the mouse esophagus, p63 expression is restricted to the basal cell layer (Figure 10B). KRT5 expression was observed in all the squamous multilayered epithelial cells of the esophagus in mice and humans. Esophageal squamous epithelium is $p63^{+}KRT5^{+}$ while stomach columnar epithelial cells are $KRT8^{+}KRT7^{+}$(Figure 10A-D). These two epithelial types meet at GEJ.

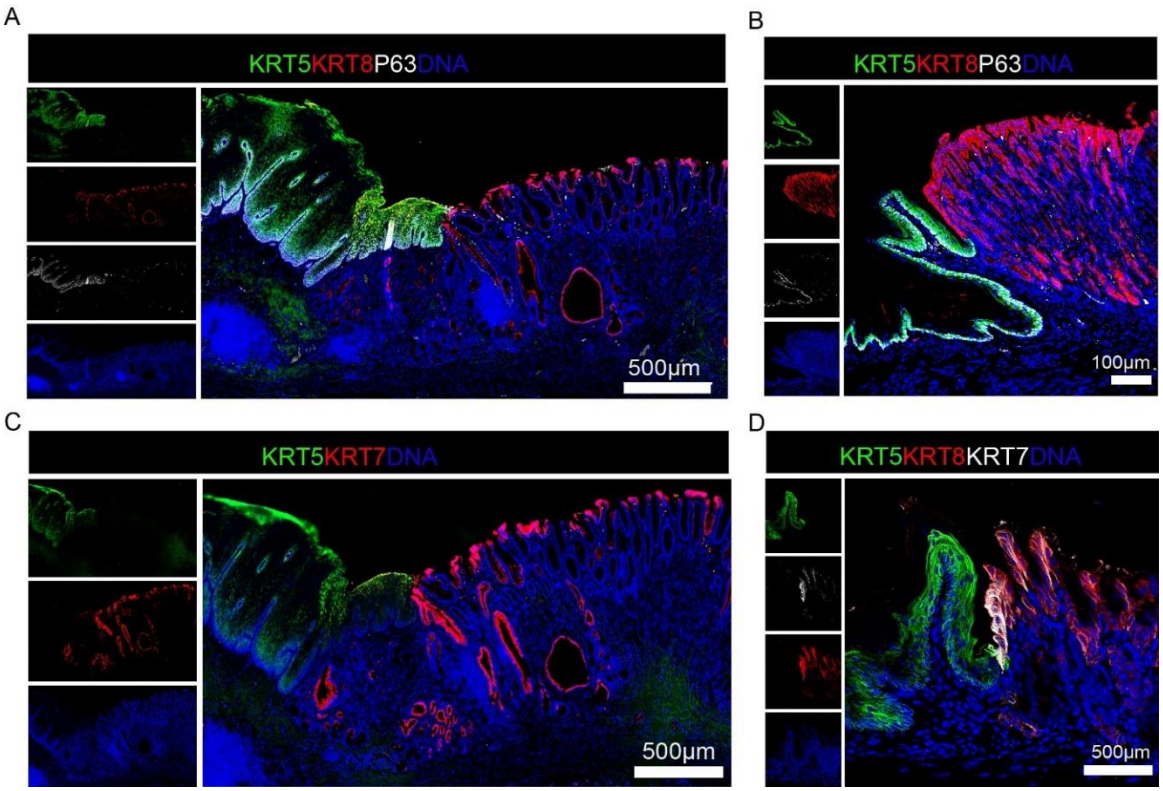

Figure 10. Distinct cytokeratin expression in human and mouse GEJ. (A-B) Tiled images of tissue sections from human (A) and mouse (B), esophagus, and stomach stained with KRT5 (green), KRT8 (red), and p63 (white). **(C-D)** Tiled images of tissue sections of the esophagus

and stomach stained with KRT5 (green), KRT7 (red) for humans (C), and KRT5 (green), KRT8 (red), KRT7 (white) for the mouse (D). Nuclei are stained with DAPI (blue).

7.4 KRT7 expression is not restricted to junctional cells

In recent years KRT7 expression has been attributed to the GEJ transitional epithelial cells with clinical importance. High expression of KRT7 is observed in the BE (Cabibi et al. 2009). It was postulated that its expression is restricted only to the residual embryonic cells or transitional basal cells in the GEJ but not adjacent esophagus squamous and columnar cells of cardia cells in the mouse and humans (Wang et al. 2011), (Jiang et al. 2017). Moreover, it was also proposed that these junctional $KRT7^{+}$ cells are the precursor for the initiation of BE during chronic GERD conditions (Jiang et al. 2017). To analyze whether such $KRT7^{+}$ cells are present only in the junctional epithelial cells, I performed smRNA-ISH for the *Krt5*, *Krt7,* and *Krt8* mRNA in mice tissues to evaluate the expression of these genes. This analysis revealed that *Krt5* and *Krt8* expression were restricted to the esophagus squamous epithelial cells and stomach columnar epithelial cells, respectively (Figure 11 A, B). Of note, the *Krt7* expression is not confined only to the junctional region; instead, the *Krt7* gene is highly expressed in the entire columnar epithelium of the stomach and, to a lesser extent, also in the basal cells of the esophagus (Figure 11 C). As observed previously by immunofluorescence, the expression of KRT7 is very high in the squamous epithelial cells near the junction and columnar cells of the cardia in mice (Figure 10 D). But the KRT7 expression was absent in the basal squamous epithelial cells of the human esophagus near the junction. All the columnar cells of human stomach epithelial cells expressed KRT7 (Figure 10 C). Thus, the KRT7 expression pattern differs between mouse and human GEJ, and its expression is not confined to the junctional cells.

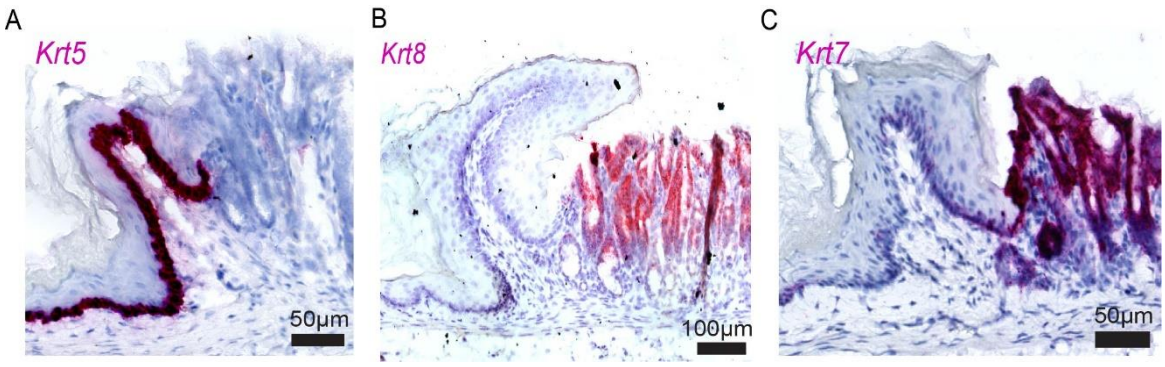

Figure 11. Distinct cytokeratin expression in mouse GEJ by smRNA-ISH. (A-C) Tiled images of mouse GEJ tissue probed with *Krt5, Krt8,* and *Krt7*. Nuclei are labeled with blue.

7.5 Adult gastroesophageal junction homeostasis is maintained by two distinct epithelial stem cells

Next, I investigated if the epithelial regeneration of the esophagus and stomach at the GEJ depends on common stem cells or terminally differentiated unipotent adult stem cells. Here I employed *in vivo* lineage tracing of proliferating KRT5 and KRT8 cells to track the daughter cells. Epithelial lineage tracing was performed in mice expressing squamous specific *Krt5-CreERT2; Rosa26-tdTomato* or columnar specific *Krt8-CreERT2; Rosa26-tdTomato* mice (Figure 12 A). Lineage was induced by injecting Tamoxifen intraperitoneally to activate Cre recombinase and expression of tdTomato under the promotor of cytokeratin specific to either squamous epithelium of the esophagus (*Krt5*) or columnar epithelia of the stomach (*Krt8*). Tissue from GEJ was isolated after 14 to 20 weeks post-tamoxifen induction. Tissues were freshly frozen, and sections of GEJ were analyzed for the fluorescent labeling of epithelial cells by microscopy. Lineage tracing revealed that KRT5 only traced for the squamous epithelium in the entire region of the esophagus but not adjacent columnar epithelial cells (Figure 12 B). In contrast, the KRT8 lineage is traced exclusively in the columnar epithelial cells of the stomach (Figure 12 C) but not in the squamous epithelial cells of the esophagus. Importantly, KRT8+ junctional cells that also express high KRT7 did not give rise to the esophageal or multilayered epithelium. This suggests that two different epithelial stem cells give rise to the KRT5^{+} squamous lineage and KRT8+ columnar lineage that meet at GEJ, and no residual embryonic cells exist that give rise to both epithelium regeneration in the adult GEJ.

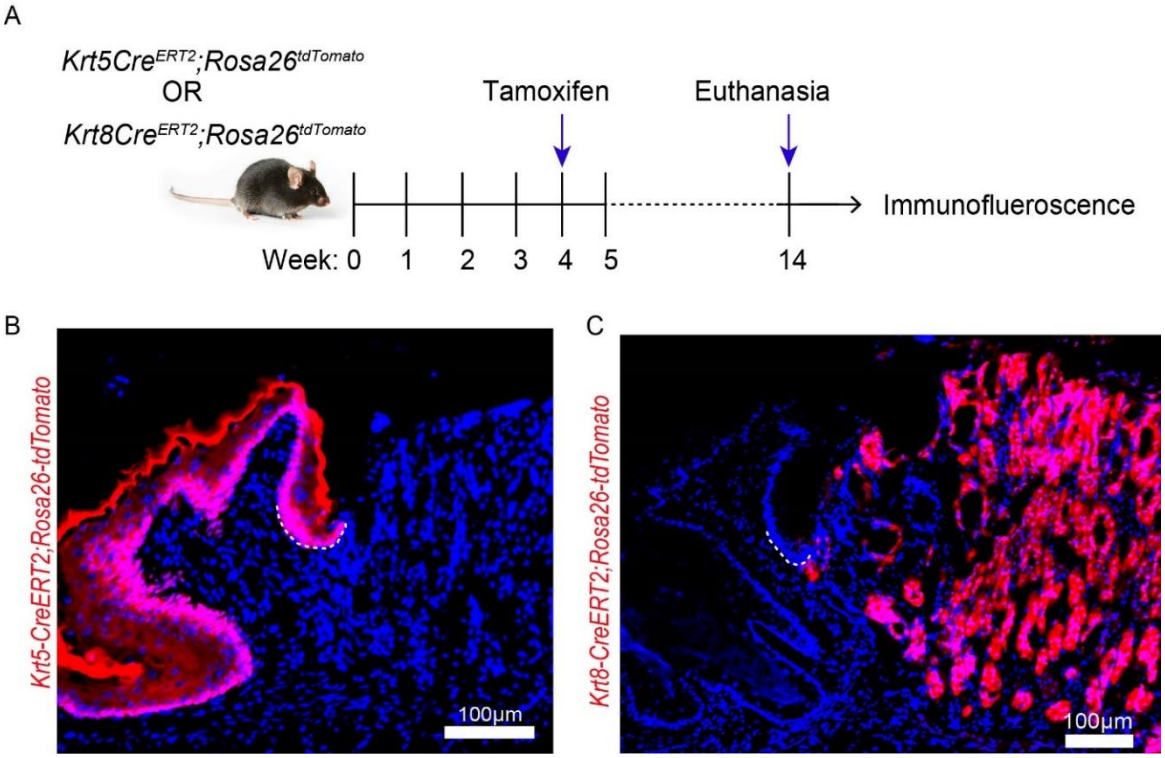

Figure 12. Lineage tracing of mouse GEJ reveals two distinct epithelial stem cells instead of a common progenitor for regeneration of the esophagus or stomach epithelium. (A) Tamoxifen treatment scheme for lineage tracing of mice epithelial cells either expressing *Krt5-CreERT2; Rosa26-tdTomato* or *Krt8-CreERT2; Rosa26-tdTomato*. Lineage in epithelial cells in mice was induced by activating Cre recombinase by administering tamoxifen intraperitoneally at the age of 4 weeks on two consecutive days. Mice were euthanized in the 14th week, and gastroesophageal tissues were fixed for immunofluorescence. **(B)** Tiled images of GEJ from tissue sections of 14 weeks *old Krt5-CreERT2; Rosa26-tdTomato* lineage traced in the squamous epithelial cells of the esophagus, **(C)** *Krt8-CreERT2; Rosa26-tdTomato* lineage traced in the columnar epithelial cells of the stomach after Tamoxifen induction at the age of 4 weeks. Nuclei stained with DAPI (blue). The white dotted line indicates the basal cells of squamous epithelial cells in the esophagus near GEJ.

7.6 The opposing Wnt pathway regulates gastroesophageal epithelial homeostasis

Epithelial homeostasis is maintained by continuous self-renewal and differentiation of epithelial stem cells. This is governed by the autocrine or paracrine signaling between epithelial cells and /or non-epithelial cells. Stromal cells are known to regulate epithelial homeostasis of the mucosal lining. The Wnt pathway is known to maintain the stemness of glandular stomach

epithelial cells. The Wnt morphogen R-spondin3 (RSPO*3*) from the stromal cells contributes to the regeneration of the stomach epithelium (Sigal et al. 2017). However, how the Wnt pathway maintains the esophagus and GEJ epithelial cells is not well known. Therefore, further understanding of the complete microenvironmental Wnt signaling surrounding GEJ epithelial cells is essential. For this purpose, spatial expression analysis of different Wnt pathway agonistic and antagonistic factors was performed in mice GEJ tissue using smRNA-ISH.

Known stem cell marker of stomach Leucine-rich repeat-containing G-protein coupled receptor 5 (*Lgr5)* specifically expressed at the base of stomach glands (Barker et al. 2010, Leushacke et al. 2017) but not expressed in the esophagus epithelial cells (Figure 13 A, B). The *Axin2* gene is a downstream target of the Wnt- beta-catenin signaling pathway (Jho et al. 2002), expressed at the base of stomach glands and sporadically in the muscular layers of the esophagus tissue but not in the epithelial layers of the esophagus (Figure 13 C, D). To further understand whether the Wnt pathway is involved in the stem cell regeneration in both squamous and columnar epithelial cells at GEJ, lineage tracing for AXIN2 was performed using *Axin2-CreERT2/Rosa26-tdTomato mice*. AXIN2 lineage tracing resulted in the tracing of columnar epithelial cells of the stomach but not the squamous epithelium of the esophagus (Figure 13 E, F). This suggests that a Wnt-independent mechanism regulates the epithelial stem cells of the esophagus.

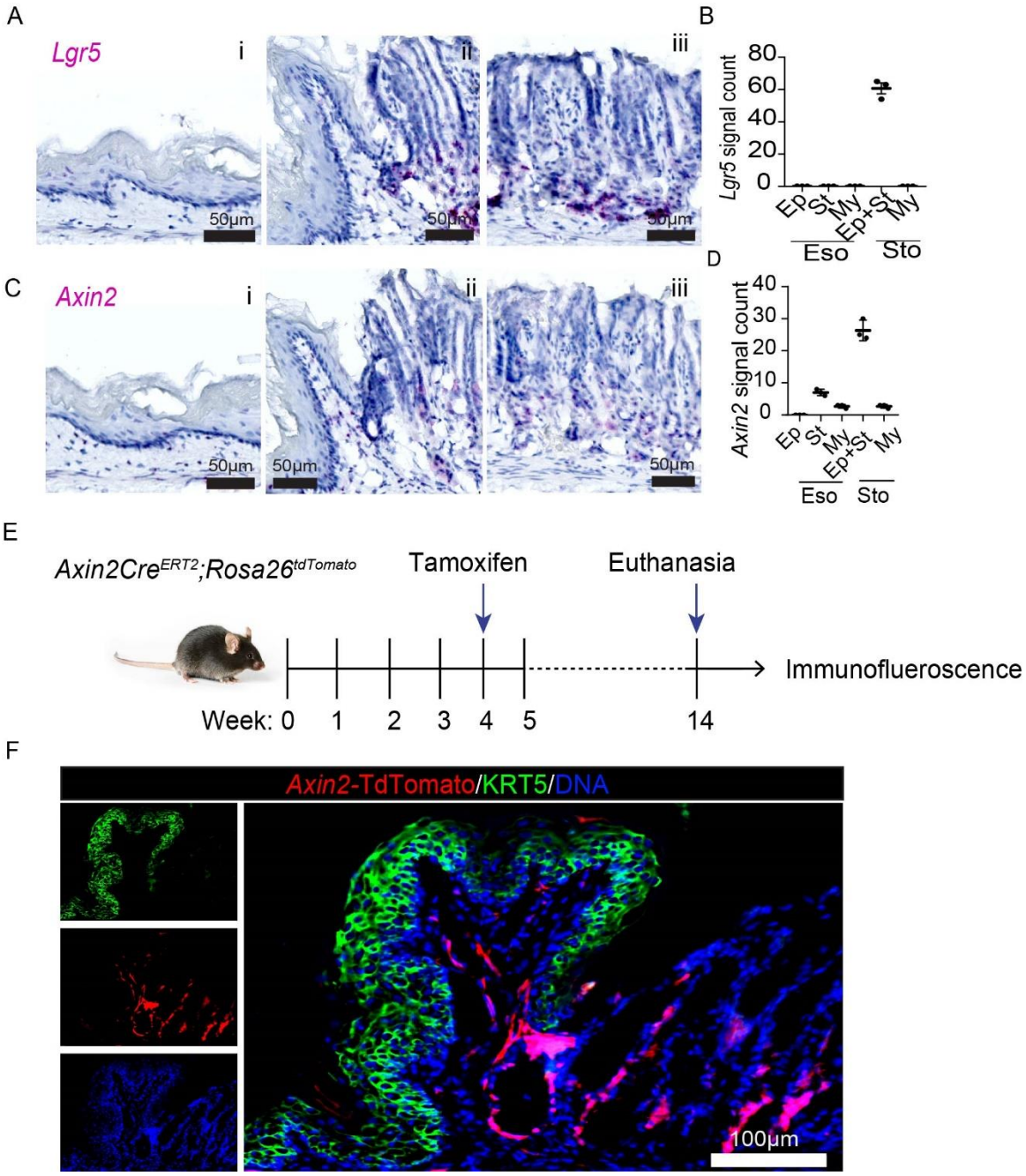

Figure 13. Spatial expressions pattern of Wnt pathway genes in the mouse GEJ. (**A-D**) Tiled images of mouse GEJ tissue probed for the Wnt pathway genes *Lgr5* (A), and *Axin2* (C) in the mouse esophagus tissue (i), GEJ (ii), and stomach glands (iii). Nuclei were labeled with blue. Quantification of *Lgr5* (B), and *Axin2* (D) signal counts in Epithelia (Ep), stroma (St), and Myofibroblast (My) in the mouse GEJ tissue regions. Signal counts were performed from three non-overlapping 100 µm^2 areas of the image. Images are representative of n=3 mice. Tiled images were acquired with an AxioScan imager. Tamoxifen treatment scheme for lineage tracing of mice epithelial cells expressing *Axin2-CreERT2; Rosa26-tdTomato*. (**E-F**) Lineage tracing in epithelial cells was induced by activating Cre recombinase by administering tamoxifen intraperitoneally at the age of 4 weeks on two consecutive days. Mice were euthanized in the

14th week, and gastroesophageal tissues were fixed for immunofluorescence (E). Tissues were stained with squamous epithelial marker KRT5 (green) and DNA was stained with Hoechst (F).

Myofibroblasts are characterized by the expression of the microfilament α-smooth muscle actin (α-SMA) and vimentin known to present between the lamina propria and epithelial compartment of the gastrointestinal tract (Roulis and Flavell 2016). These cells regulate epithelial proliferation and regeneration by secreting various paracrine morphogens (Roulis and Flavell 2016). In the stomach, these myofibroblast cells are known to secrete one of the Wnt activating factors, *Rspo3* (Sigal et al. 2017). The expression of *Rspo3* was observed in the myofibroblast (Myo) of both the esophagus and stomach tissue (Figure 14 A, B). However, the proximity of *Rspo3* signals from myofibroblast cells to the epithelial stem cell compartment of the esophagus and stomach is dissimilar. In the stomach, myofibroblasts are located near the stem cells of the stomach glands, while in the esophagus, the stromal region separates basal epithelial stem cells and myofibroblast cells. Thus, the average distance of the *Rspo3* signals to the epithelia is greater in the esophagus than in the stomach (Figure 14 C), indicating that Rspo3 activates the Wnt pathway in the stem cells of the stomach gland but not in the esophagus.

Next, I analyzed how the Wnt inhibitor *Dkk2* gene was expressed and distributed in the mouse GEJ tissue. Previously in our lab, it was shown that *Dkk2*, one of the Wnt pathway inhibitors, is expressed highly in the stromal cells directly underlying squamous epithelial cells of the ectocervix and thus inhibiting Wnt activity (Chumduri et al. 2021). To find whether a similar type of Wnt inhibition by DKK2 is present in the esophagus, the expression pattern of *Dkk2* was analyzed in the mouse GEJ. The Wnt pathway inhibitor *Dkk2* was highly expressed in the esophagus stroma and myofibroblast cells and to a significantly lesser extent in myofibroblast cells in the stomach (Figure 14 D, E). However, the average distance between the *Dkk2* signal and the epithelial cell was less in the stomach than in the esophagus (Figure 14 F). This implies that the absence of Wnt activating molecules in the esophagus and higher expression of DKK2 enhances the Wnt inhibition in the esophagus. Whereas in the stomach, low levels of DKK2 might act as a Wnt inhibitor for the slow recycling of stem cells.

The overall analysis of Wnt regulator gene expression suggests that the homeostasis of esophagus and stomach epithelium at GEJ is regulated by 1: opposing Wnt signaling, where stomach epithelial cells were regulated by the Wnt activating factors while the Wnt independent mechanism regulated esophagus epithelial cells. 2: The spatial distribution, proximity, and signal concentrations of Wnt agonists and antagonists in the stromal cells are critical in maintaining Wnt activating or inhibitory microenvironment. Thus, the adult squamous and columnar epithelium at GEJ is maintained by spatially defined opposing Wnt microenvironments.

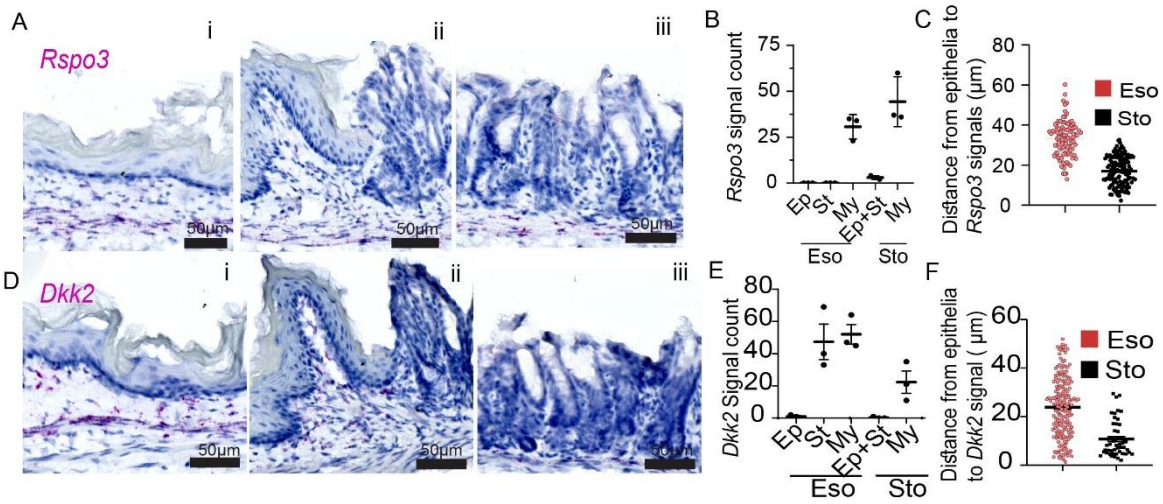

Figure 14. Spatial expressions pattern of Wnt pathway regulating genes in the mouse GEJ. Tiled images of mouse GEJ tissue probed for the Wnt pathway regulating genes *Rspo3* (A), and *Dkk2* (D) in the mouse esophagus tissue (i), GEJ (ii), and stomach glands (iii). Nuclei were labeled with blue. Quantification of *Rspo3* (B), and *Dkk2* (E) signal counts in Epithelia (Ep), stroma (St), and Myofibroblast (My) in the mouse GEJ tissue regions, and distance (µm) from epithelia to *Rspo3* (C) and *Dkk2* signals (F). Signal counts were performed from three non-overlapping 100 µm^2 areas of the image. Images are representative of n=3 mice. Tiled images were acquired with an AxioScan imager.

7.7 Differential Wnt dependency of esophagus and stomach epithelial organoids

The stem cell-derived 3D organoid culture model allows the understanding of different cellular and functional aspects of healthy and disease epithelial cells. This model recapitulates *in-vivo* tissue of origin in terms of morphological features and requirement of growth factors. They can self-renew and

differentiate to form self-organized mature epithelial organoids when cultured in the solubilized basement membrane matrix (Matrigel) and allow long-term expansion of primary epithelial cells (Clevers 2016). Furthermore, sub-epithelial stromal cells play a crucial role in epithelial stem cell maintenance by signaling cross talk and paracrine effect (Gnecchi et al. 2008). Since organoids are devoid of other cell types, it is essential to understand in-depth the critical growth factors and the signaling requirement for squamous and columnar epithelial stem cell regeneration and homeostasis of the GEJ. Thus, a 3D organoid culture model of these epithelial types was established. To generate organoids, epithelial cells from the esophagus and stomach tissue were isolated and cultured in the Matrigel. The growth kinetics, morphology, and passaging ability were monitored throughout the culture of organoids.

Wnt signaling is known to play a critical role in the maintenance of adult stemness and organoid generation. To know whether Wnt signaling is essential for the GEJ epithelial regeneration, the organoids were generated from the esophagus and stomach adult stem cells from the GEJ region in the media supplemented with or without Wnt activating ligands WNT3A and RSPO1 along with other growth factors as base components. Based on our previous and other studies the composition of the base components was optimized; that includes epidermal growth factor (EGF), BMP pathway inhibitor Noggin, fibroblast growth factor-10 (FGF10), Nicotinamide, Forskolin, and transforming growth factor-β receptor kinase inhibitor (A83-01) and rho-associated kinase inhibitor (Rocki) (Chumduri et al. 2021, Schlaermann et al. 2016, Sato et al. 2009) Apart from the Wnt components, stomach media included gastrin, and p38 inhibitor, and excluded Forskolin compared to the esophagus media. The inclusion of hydrocortisone increased the size of esophagus organoids but did not influence the longevity of organoid cultures.

Mouse esophagus epithelial organoids could grow in the presence and absence of WNT3A, and RSPO1 conditioned media, suggesting Wnt signaling is dispensable for the growth of the esophagus squamous epithelial cells (Figure 15 A, upper panel). Interestingly when human esophagus cells were supplemented with WNT3A and RSPO1 in the 3D culture media, cells could not generate organoids (Figure 15 B, upper panel). This Wnt inhibitory effect on human esophagus organoids was found in all human esophagus epithelial cells

tested (n=6). In the case of both mouse and human stomach organoids, the presence of WNT3A and RSPO1 in the media was essential for forming organoids (Figure 15 A, B, lower panel). In some cases, stomach organoids were generated in lesser numbers in the absence of Wnt signaling, but they could not regrow in the subsequent passage. This suggests that, as previously shown (Barker et al. 2010), Wnt singling is essential for stomach epithelial organoid growth.

Next, organoid formation efficiency was estimated by seeding the single epithelial cells to generate organoids in Wnt proficient and deficient conditions. In mouse organoid formation efficiency was calculated at passages 8 and 12 in Wnt proficient and deficient conditions (Figure 15 C). Even though there was a growth of the esophagus organoid in the presence of the Wnt activating media, the organoid formation efficiency was reduced from passage 8 to passage 12. In contrast, organoid formation efficiency was maintained from passages 8 to 12 in the absence of Wnt growth factors. This indicates that the presence of Wnt activity reduces squamous epithelial stemness. In the case of stomach organoids, as previously published (Barker et al. 2010, Schlaermann et al. 2016), the efficiency of organoid formation was maintained in both passages in the Wnt proficient media (Figure 15 C).

To understand the ability of epithelial cells to grow for the long term, organoids were passaged at equal cell seeding density. Esophagus organoids could be passaged for more than 22 passages (>7 months) in the absence of Wnt media, whereas they showed growth arrest at passage 13 when grown in the presence of Wnt media (Figure 15 D). Similarly, human esophagus epithelial organoids could grow only in Wnt deficient conditions for up to 6 passages. On the contrary, stomach organoids could be expanded for more than 22 passages (>7 months) in the presence of Wnt media, whereas they underwent growth arrest by the 4^{th} passage in the absence of Wnt growth factors (Figure 15 D). Thus, the Wnt signaling factors are not essential for the establishment, long-term culturing, and expansion of esophagus squamous epithelial organoids as opposed to stomach columnar organoids.

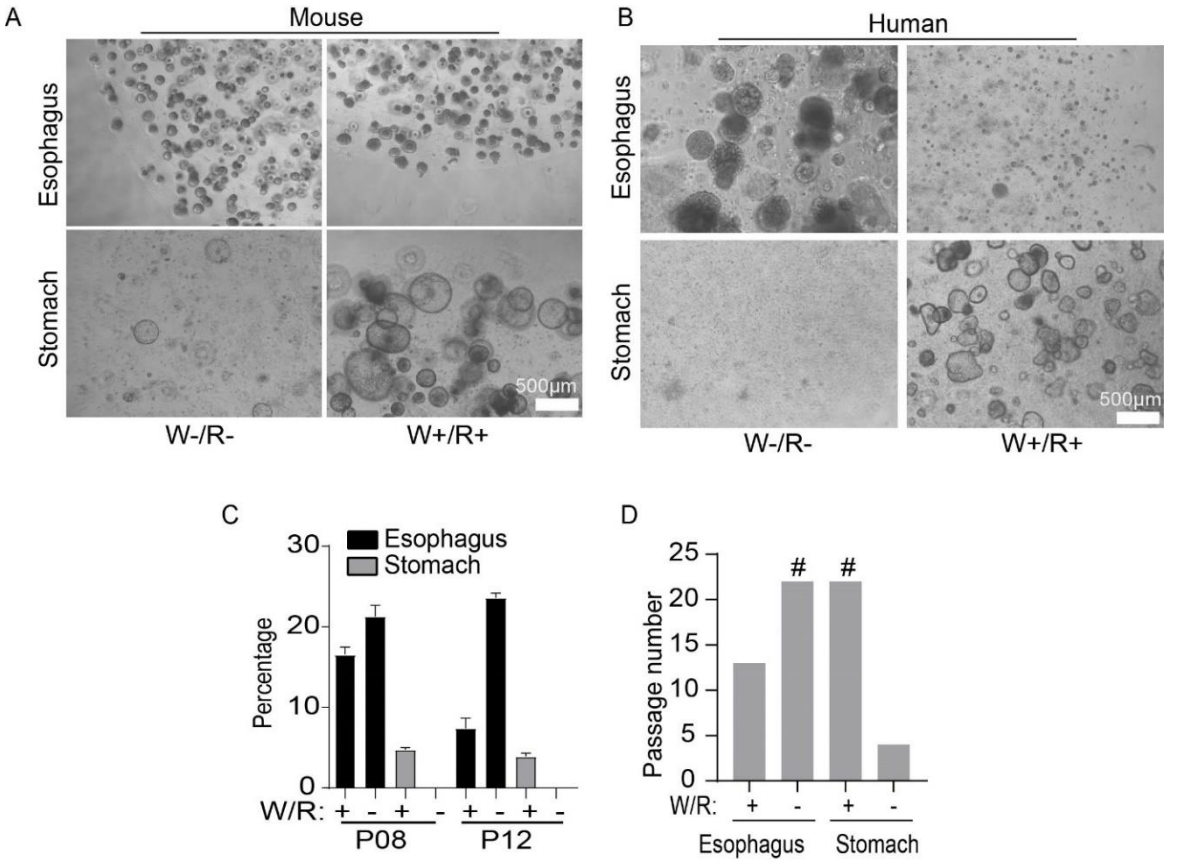

Figure 15. Distinct Wnt signaling requirement for GEJ epithelial organoid growth. (A-B) Bright-field images of the mouse (A) and human (B) esophagus (upper panel) and stomach (lower panel) epithelial organoids grown in the presence or absence of WNT3A (W) and RSPO1(R). **(C)** Bargraph showing percentage of organoids formed from esophagus and stomach epithelial cells in the presence or absence of WNT3A and RSPO1 (W-/R- or W+/R+) at indicated passage number. n= mean+/-SD of three biological replicates. **(D)** Bargraph showing the passage number of esophagus and stomach epithelial organoids cultured in the presence or absence of WNT3A and RSPO1 (W-/R- or W+/R+).'#' indicates organoids retained passaging ability beyond the indicated number.

7.8 Epithelial organoids recapitulate tissue of origin

To explore whether organoids resemble *in vivo* tissue of origin, the morphology of mature organoids was analyzed (Figure 16 A, B). Morphologically, esophagus organoids consist of multi-layered stratified squamous epithelial cells. The innermost lumen consists of cornified epithelial cells in the case of the mouse and differentiated cells in the human. To understand the morphology in detail, organoids were fixed with PFA and manually paraffinized.

Organoid sections were probed with epithelial-specific marker proteins by immunofluorescence. Organoids derived from mouse and human adult stomachs consist of single-layered columnar epithelial cells, forming a hollow sphere with a lumen containing cell debris and secreted mucous. Squamous marker KRT5 was expressed only in the multi-layered esophagus organoids but not in the single-layered stomach organoids. While the columnar marker KRT8 was expressed in the stomach but not in the esophagus organoids. The squamous epithelial marker p63 was only expressed at the basal cells of the esophagus organoids resembling *in vivo* tissue (Figure 16 C, D). These results indicate that cultured organoids maintain lineage specificity and morphology of tissue of origin.

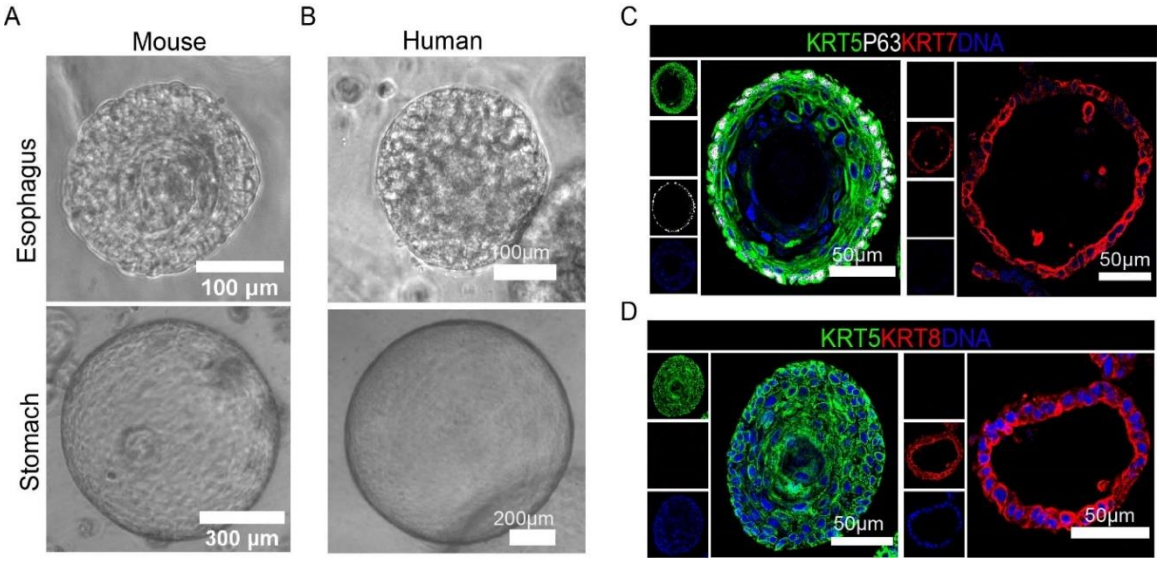

Figure 16. Esophagus and stomach epithelial organoids recapitulate the tissue of origin. (A-B) Bright-field images of the mouse (A) and human (B) esophagus (upper panel) and stomach (lower panel) organoids grown in the absence and presence of WNT3A and RSPO1, respectively. **(C-D)** Confocal images of esophageal organoid (left panel) and stomach organoid (right panel) immunostained for KRT5 (green), KRT7 (Red), p63 (white) (C), KRT5 (green), KRT8 (Red) (D) proteins, and nuclei stained with DAPI (blue.)

7.9 Altered Wnt growth condition doesn't induce transdifferentiation between adult squamous and columnar epithelium

Several studies support the transdifferentiation of squamous epithelium to the columnar epithelium in the GEJ due to several GERD-related factors (Clemons et al. 2012, Vega et al. 2014, Minacapelli et al. 2017, D. H. Wang et al. 2010, Wang et al. 2014). In the BE, the presence of specialized columnar epithelial cells in the esophagus region may indicate that active Wnt activity transdifferentiates squamous epithelium to specialized columnar epithelium. Since squamous and columnar epithelium lies next to each other in the GEJ junction, I analyzed whether activating the Wnt signaling in squamous epithelium induces transdifferentiation into columnar epithelium by using organoid technology. For this, mature esophagus and stomach organoids derived from the GEJ region were paraffined, sectioned, and subjected to smRNA-ISH for the Wnt signaling genes *Lgr5* and *Axin2* (Figure 17 A, B). The expression of *Lgr5* was only found in a few epithelial cells of the stomach organoids as a cluster of signals which are absent in the esophagus organoid. Similarly, *Axin2* was expressed only in the stomach organoids but not in the esophagus organoids. This again shows that active Wnt signaling is present only in the stomach but not in the esophagus.

To investigate whether the Wnt signals induce transdifferentiation of squamous to the columnar epithelium, epithelial lineage tracing was induced by Tamoxifen in mice expressing either squamous specific *Krt5-CreERT2; Rosa26-tdTomato,* or columnar specific *Krt8-CreERT2; Rosa26-tdTomato*. Lineage-marked epithelial cells were isolated from the esophagus and stomach and cultured into organoids in the presence or absence of Wnt-conditioned media (Figure 17 C). Mature organoid analysis by fluorescent microscope showed that the KRT5 labeled squamous organoids in the presence of Wnt media didn't transdifferentiate to KRT5 columnar epithelium (Figure 17 D). Similarly, KRT8 labeled columnar epithelial organoids did not transdifferentiate to KRT8 squamous epithelium (Figure 17 E). In summary, stem cells of the esophagus and stomach are terminally committed to two distinct adult stem cell lineages that cannot transdifferentiate into another lineage with the modulation of Wnt

signaling. Further, these results imply that the Wnt-driven transdifferentiation process of the squamous epithelium to columnar epithelium doesn't occur in the BE pathology.

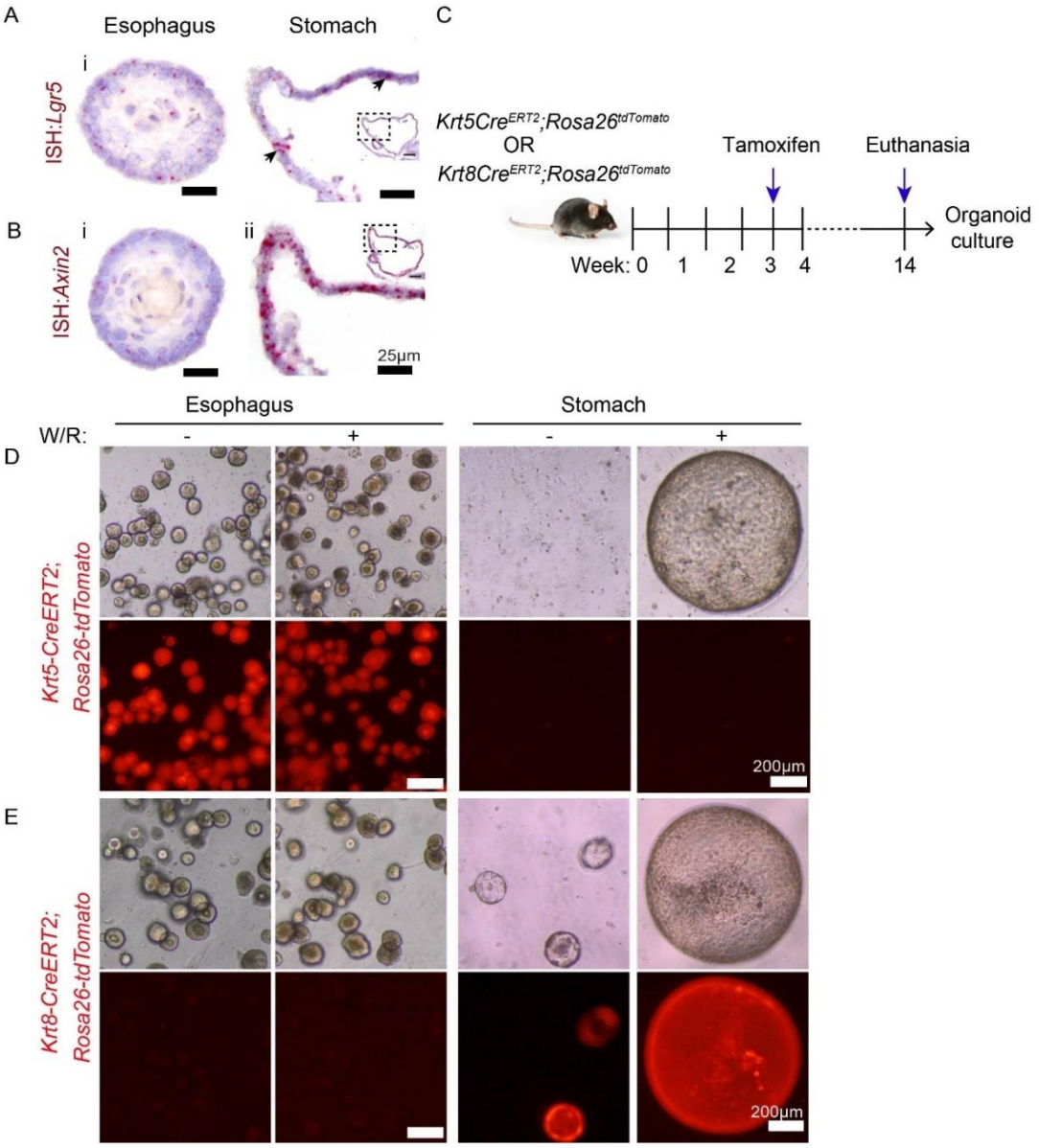

Figure 17. Alternation of Wnt conditioned media doesn't induce transdifferentiation between KRT5+ esophageal and KRT8+ stomach adult epithelial stem cells (A-B) smRNA-ISH for mouse esophagus and stomach organoids probed for *Lgr5* (A) and *Axin2* (B). **(C)** Schematic representation of Tamoxifen treatment for lineage tracing of mice epithelial cells either expressing *Krt5-CreERT2; Rosa26-tdTomato* **(D)** or *Krt8-CreERT2; Rosa26-tdTomato* **(E)**. Lineage in epithelial cells in mice was induced by activating Cre recombinase by administering tamoxifen intraperitoneally at the age of 4 weeks on two consecutive days. Mice were euthanized in the 14th week, and gastroesophageal epithelial cells were cultured in the absence or presence of WNT3A and RSPO1 conditioned media.

7.10 Bulk transcriptomic analysis reveals distinct transcriptional signatures of esophagus and stomach epithelial cells

To understand the molecular difference between esophagus and stomach epithelial cell types of the GEJ region, bulk transcriptomic analysis was performed on the esophageal squamous and stomach columnar organoid-derived epithelial cells from 3 mice. Among 34393 unique genes, 8030 were differentially regulated between columnar and squamous epithelium (Figure 18 A). To find differences in biological processes and molecular functions between esophagus and stomach epithelial cells, gene ontology was performed for all differentially expressed genes. The top 20 differentially expressed genes between the esophagus and stomach organoid epithelial cells showed enrichment of pathways related to the respective tissue types (Figure 18 B). Pathway related to the epidermal cell development, keratinocyte differentiation, transcription and translation, and regulation of cell-cell adhesion was highly enriched in the esophageal epithelial cells signifying higher cell turnover and degree of cellular differentiation of squamous epithelium. In the case of stomach epithelial cells, metabolic processes related to lipid, ion transport, and digestive system processes were enriched, suggesting the role in the absorption of short-chain fatty acids, fluid, secretion of acids, and hormones involved in food digestion (Figure 18 B). To support the enriched GO terms, periodic acid–Schiff (PAS) staining was performed on the organoid and GEJ tissue to detect secreted mucus and glycolipids. Stomach organoids and the GEJ tissue showed intense PAS staining in the columnar epithelium, indicating high expression and secretion of glycoproteins, glycolipids, and mucins compared to the stratified epithelium of the esophagus (Figure 18 C). Pathway related to epithelial cell proliferation, cell junction assembly, and cell-substrate adhesion was similarly regulated between the two epithelial cell types. Transcriptomic analysis of cytokeratins which are intermediate filaments that enable cells to withstand mechanical stress also showed distinct expressions specific to cell types. Cytokeratin *Krt14, Krt15, Krt17, Krt5, Krt4, Krt13, Krt6a, Krt6b,* and *Krt16* were highly expressed in the squamous epithelial cells while *Krt8, Krt18, Krt7, Krt19, Krt20* are highly expressed in the columnar epithelial cells (Figure 18 D). Thus, GO term pathways provide

structural, functional, and molecular similarity between organoid and its *in vivo* tissue of origin and the dissimilarity between squamous and columnar epithelium.

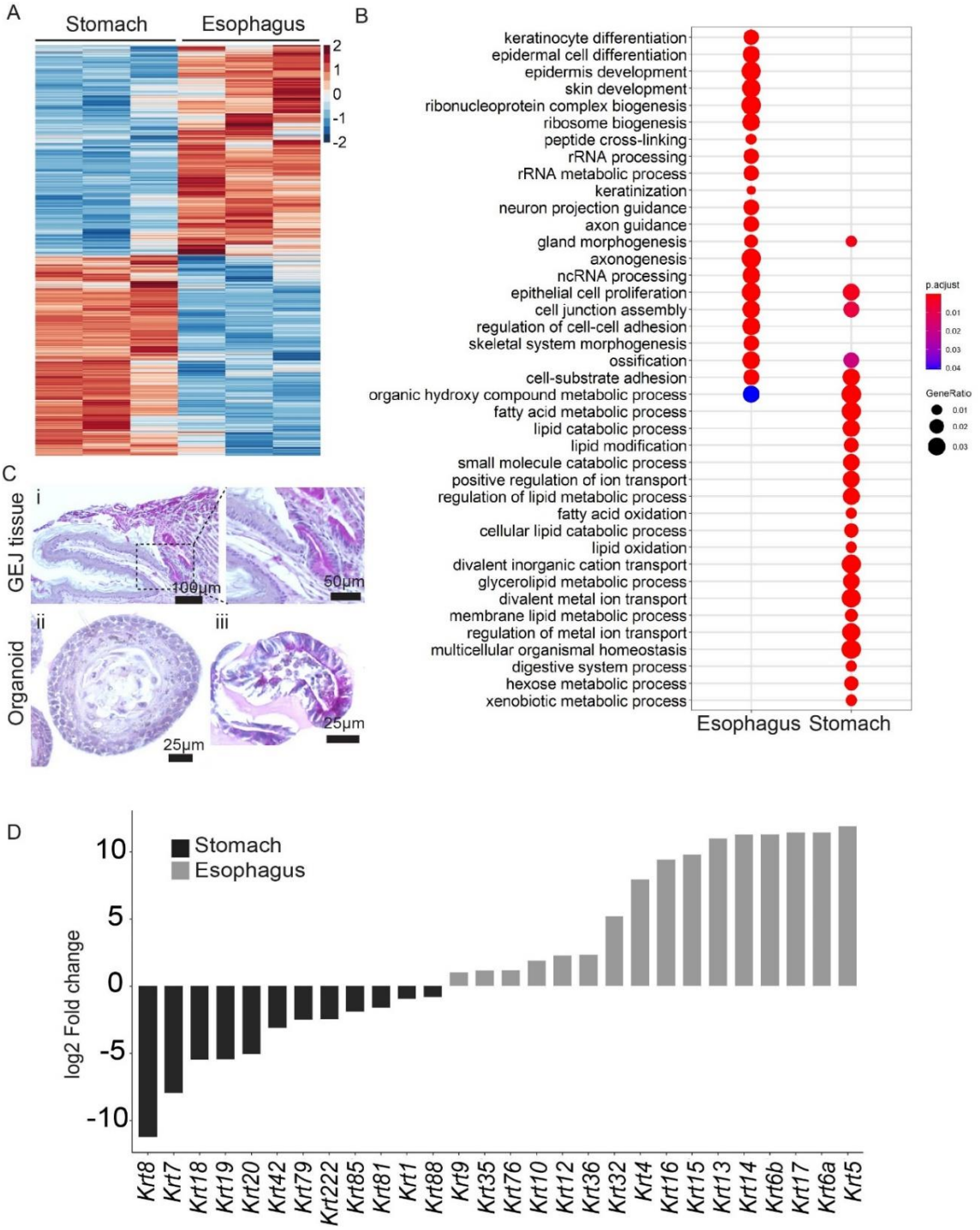

Figure 18. Bulk transcriptomic analysis of mouse esophagus and stomach organoids revealing lineage-specific gene signatures and biological processes. (A) Heat map showing differentially expressed genes (DEG) between esophagus and stomach organoids. Columns represent gene signatures derived from an individual mouse. The color bar represents

z-scored gene expression. **(B)** Image showing top 20 enriched gene ontology (GO) terms related to DEG between esophageal and stomach organoids. **(C)** Brightfield image for PAS stained mouse GEJ tissue section (i), esophageal organoid (ii), and stomach organoid (iii). **(D)** Bar plot revealing distinct cytokeratin expression profile between mouse esophagus and stomach organoids as depicted by Log_2FC of differentially expressed cytokeratin genes.

7.11 Single-cell RNA seq reveals cellular heterogeneity and transcriptional signatures of esophagus and stomach epithelial cells

Single-cell RNA sequencing (scRNA-seq) was performed for the epithelial cells derived from the esophagus and stomach organoids to understand cellular types and cell type-specific gene expression patterns. Organoids were cultured from esophagus and stomach epithelial cells in their respective media. The isolated single cells were used for the cDNA library preparation and RNA sequencing. The cell-type-specific gene expression patterns, cell states, and the cellular developmental trajectories of the epithelium were analyzed from RNA-seq data. Initially, RNA seq data were processed for quality control, de-multiplexing, and clustering by FindNeighbors and FindClusters functions using the R program (Figure 19 A).

Initially, to determine the overall expression difference between epithelial cell types, a combined cluster analysis of esophagus and stomach epithelial cells was performed using unsupervised clustering by dimensionality reduction and visualization by uniform manifold approximation and projection (UMAP). UMAP analysis projected two major clusters related to esophagus and stomach epithelial cells. This shows major transcriptional differences between these two epithelial cell types (Figure 19 B). Further, cluster analysis was performed to characterize the cellular heterogeneity and identify subpopulations within each epithelial type. Sub-clustering of epithelial cells generated seven transcriptionally distinct sub-clusters. These include two clusters from columnar epithelial cells from the stomach (ST-Co1, ST-Co2) and 4 subclusters from the squamous epithelial cells from the esophagus (ES-Sq1, ES-Sq2A, ES-Sq2B, ES-Sq3A, and Sq3B) (Figure 19 B). Cell type annotation was performed based on the genes uniquely or differentially expressed among the sub-

clusters. Next, the plot of the average gene expression and percentage of cells expressing annotated genes across the subcultures was generated to assign the cell types.

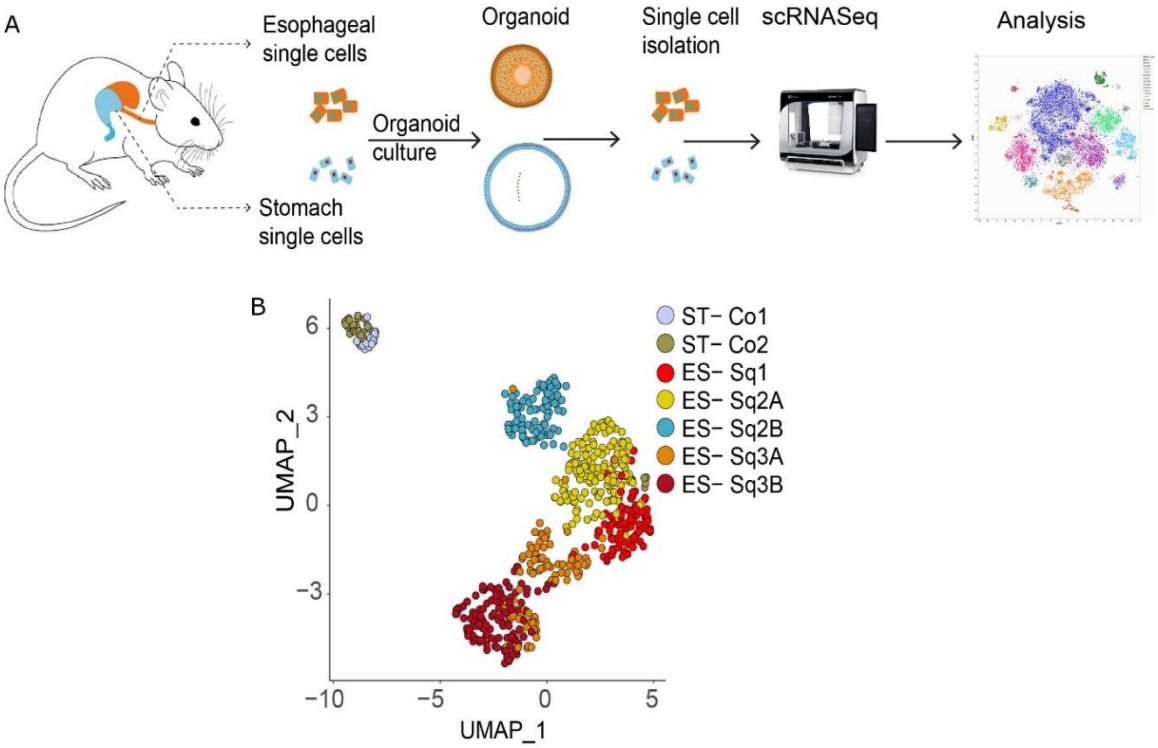

Figure 19. Single-cell RNA seq analysis of mouse esophagus and stomach organoid epithelial cells. (A) Schematic representation of epithelial cell isolation, organoid culture, single-cell isolation, and scRNA-seq analysis. **(B)** UMAP of scRNA-seq data depicting esophagus and stomach epithelial cell clusters. Individual cells are color-coded by cluster annotation (ST, stomach; ES, esophagus; Co, columnar; Sq, squamous)

7.12 Subcellular composition of stomach epithelial cells

To delineate the cellular composition of stomach sub-clusters, a dot plot for the average expression of annotated marker genes was analyzed (Figure 20 A). Stomach sub-cluster ST-Co1 enriched for the expression of well-known stomach stems cell markers such as *Lgr5* (Figure 20 B, C)*, Aqp5,* and *Axin2* (Xiao and Zhou 2020)*,* indicating the presence of stem cells in this cluster. The key markers of cells present in the neck and isthmus region of the stomach gland, including *Pgc* (Figure 20 B, E), *Muc6, Gkn3,* and *Atp4a* expression, were found in St-Co1. These sub-cluster cells also expressed high levels of

proliferation markers, including *Mki67* (Figure 20 B, D)*, Pcna, Top2a*, and *Stmn1* (Figure 20 B, F). The second sub-cluster of stomach cells, ST-Co2, was found to express high levels of, *Gkn1, Gkn2, and Tff1* (Figure 20 B, F) representing the pit cells of the gastric gland (Han et al. 2019), (Busslinger et al. 2021). Overall scRNA-seq analysis of stomach organoids reveals the presence of different cell types in the stomach gland.

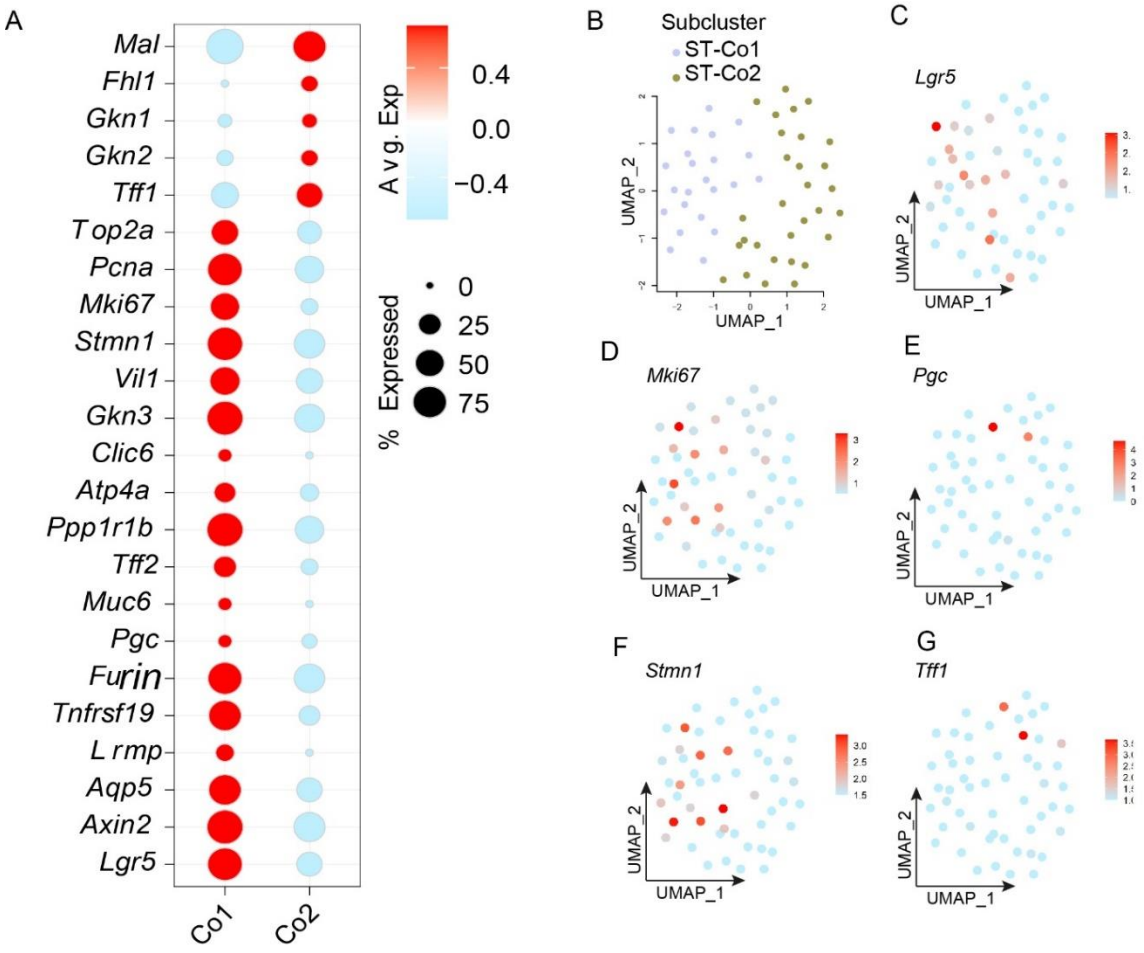

Figure 20. Single-cell RNA seq analysis of stomach organoids showing cell types representing stomach gland. (A) Dot plot image depicting the expression of selected marker genes for epithelial cell types found in the stomach gland. Circle size indicates the percentage of cells expressing indicated genes. The fill color depicts the normalized and scaled mean expression levels from high (red) to low (blue). **(B)** UMAP of stomach epithelial cells showing subclusters. **(C-G)** Normalized expression values of selected marker genes color-coded on UMAP representing stomach epithelial subclusters.

7.13 Subcellular composition of esophagus epithelial cells

In contrast to the stomach, the characteristics of stem cells and differentiating cells of the multilayered squamous epithelial organoids of the esophagus are not well studied. Thus, I analyzed the key marker genes representing the sub-clusters of esophageal epithelial cells (Figure 21 A, B). The ES-Sq1 subcluster expresses *Col7a1, Timm9, Trp63,* and *Krt17* markers known to express in the stem cells of the squamous epithelium, representing the basal cell population of the stratified epithelium (Figure 21 B, C, D). The expression of *Fau, Cav1, Jun, Btg2 Atf3* is highly enriched in the ES-Sq2A sub-cluster cells(Figure 21 B, E). In comparison, the expression of proliferation markers including *Mki67, Top2a, and Pcna* was highly expressed in the ES-Sq2A but also showed reduced expression in the ES-Sq1 and ES-Sq2B (Figure 21 A). It indicates that ES-Sq2A represents parabasal cells that contain proliferative cells with the reduced characteristic of stem cell property. The subcluster ES-Sq2B was enriched for the *Atf3, Cav1, Ybx1, Cald1,* and *Sox4* genes, representing the second population of parabasal cells devoid of many stem cell markers but expressing low levels of proliferation markers (Figure 21 A, B, F). The expression of differentiation marker genes *Rhov, Cstb, Krt6a, Krt13, Anxa1, Tgm1, Spink5, Krt4, Sprr3,* and *Elf5* was gradually increased from the sub-cluster ES-Sq3A to ES-Sq3B (Figure 21 B, G). These clusters didn’t express any stem cell and proliferation marker genes representing suprabasal and terminally differentiated cells.

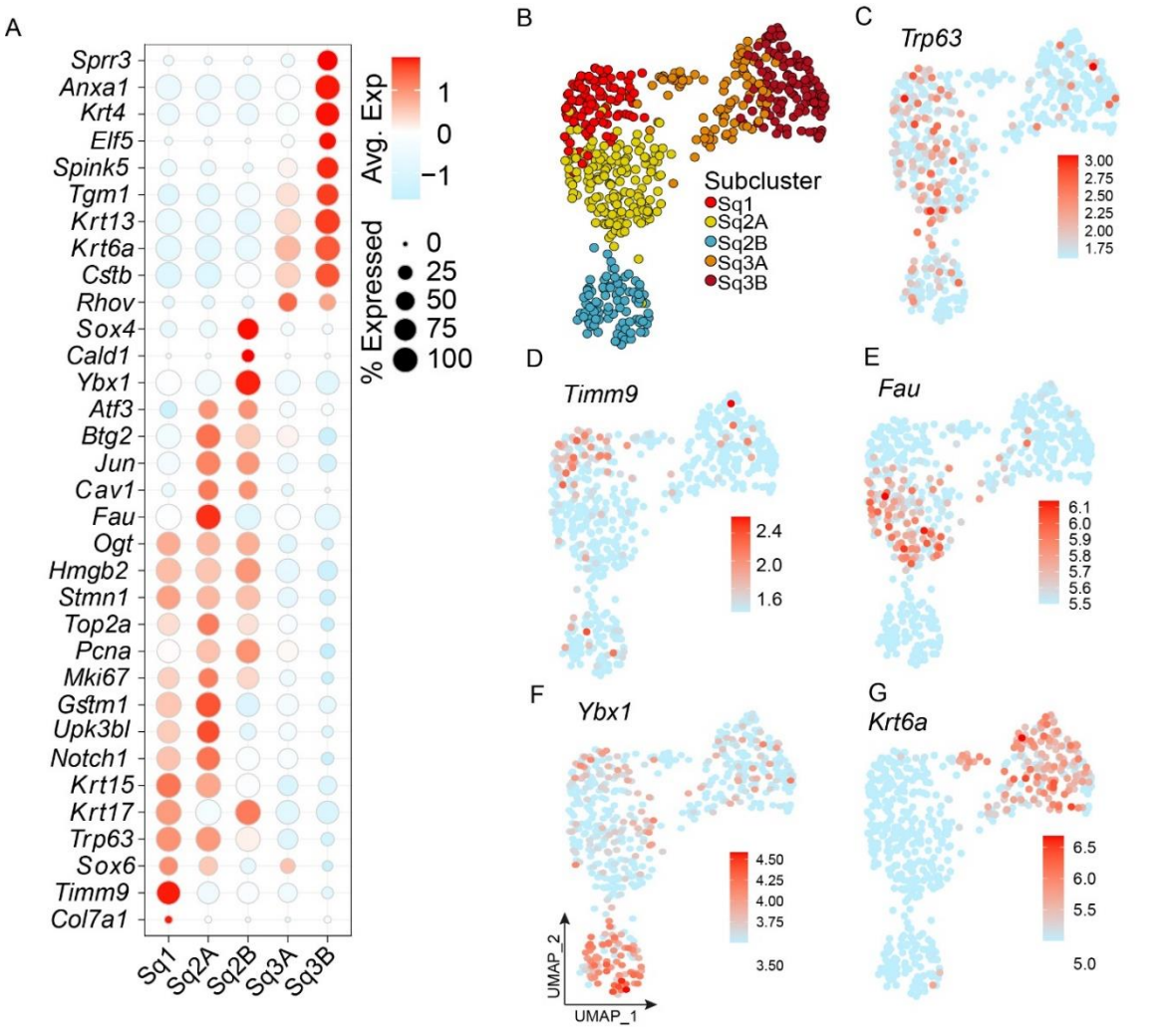

Figure 21. Single-cell RNA seq analysis of esophagus organoids reveals distinct cell types of stratified squamous layers. (A) Dot plot image depicting the expression of selected marker genes specific for epithelial cell types found in the esophagus stratified layers. Circle size indicates the percentage of cells expressing indicated genes. The fill color depicts the normalized and scaled mean expression levels from high (red) to low (blue). **(B)** UMAP of esophagus organoid epithelial cells showing subclusters. **(C-G)** Normalized expression values of selected marker genes color-coded on UMAP representing esophagus epithelial subclusters.

The spatial expression pattern was verified using the Human Protein Atlas (HPA) database to confirm annotated marker genes' authenticity. As predicted, it revealed the ES-Sq1 subcluster gene proteins are restricted to the basal cells of the esophageal multi-layered epithelium. ES-Sq2A and ES-Sq2 B-related proteins were expressed in the parabasal cell region, excluding the basal and fully differentiated cells. The ES-Sq3A subcluster proteins were expressed predominantly in the suprabasal cells, while the ES-Sq3B subcluster proteins marked the terminally differentiated layers of the esophageal epithelium.

Since stem cells were predicted to be present in the basal cell layers of the esophageal epithelium (Zhang et al. 2021), I analyzed the putative stem cell marker from the basal population of scRNA-seq data. One of the candidate genes, *Krt17* expressing cells usually highly expressed in the squamous precancerous lesion and cancer cells and involved in the wound repair process (Zhang, Yin, and Zhang 2019, Liu et al. 2020, Mitoyan et al. 2021), marks stem cell population. Jun family proteins are known to be involved in the proliferation, anti-apoptotic, and differentiation of squamous epithelial cells and may represent the parabasal cell population (Piechaczyk and Farràs 2008). Based on the expression pattern in the scRNA sequence data, *Krt17*^{hi}/*Jun*^{low} population was found to be the stem cell population in the esophageal epithelial cells. To validate its expression pattern in tissue and organoids, immunostaining for the KRT17, JUN and KRT6 was performed, revealing exclusive KRT17^{high}/JUN^{low} basal stem cells while the parabasal cells above expressed both KRT17 and JUN, and the differentiated cells expressed high levels of KRT6 (Figure 22 A, B).

To understand the hierarchical relationship between sub-cluster types and assign the progression of the stem cells and the path of differentiation of their descendants, pseudotime analysis was performed using the slingshot lineage inference tool. Pseudo-temporal modeling facilitates the reconstruction of differentiation trajectories based on gene expression transition when cells change from one state to the next. It displayed two trajectories; the first trajectory starts from basal cells (ES-Sq1), transitions through parabasal (ES-Sq2A), suprabasal (Es-Sq3A), and finally reaches terminally differentiated cells (ES-Sq3B). The second trajectory moves from basal cells to parabasal (ES-Sq2A) and parabasal (ES-Sq2B) (Figure 22 C). It suggested the presence of different cell states with two types of differentiation processes. In conclusion, the sub-cluster annotation and lineage trajectory recapitulate the differentiation stages of the stratified esophageal epithelial cells from the GEJ.

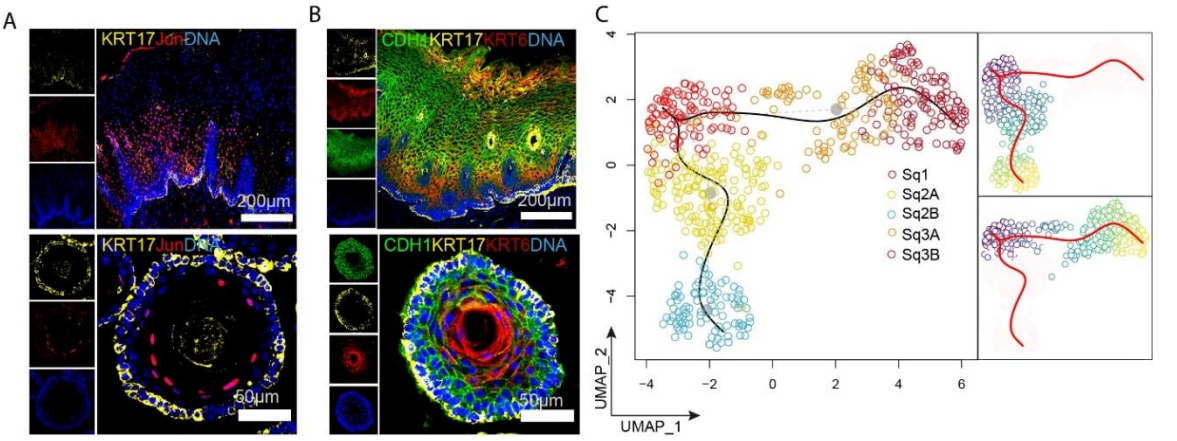

Figure 22. Esophageal stem cell compartment and lineage trajectory. (A-B) Confocal immunofluorescence images of human GEJ tissue and mouse organoids stained with KRT17 (yellow), Jun (red), and nuclei labeled with DAPI (blue) (A); CDH1 (red), KRT17 (yellow), KRT6 (red), and nuclei labeled with DAPI (blue) (B). **(C)** UMAP showing the reconstruction of pseudo time trajectories in esophagus epithelial subclusters originating from Sq1. The right panel shows individual trajectories originating from the Sq1 cluster, trajectory-1 (Upper panel), and trajectory-2 (lower panel).

7.14 Divergent canonical and non-canonical Wnt pathways regulate gastroesophageal epithelial homeostasis

In vitro analysis of tissue and organoids revealed the importance of the canonical Wnt pathway in regulating GEJ epithelial cells. However, the involvement of other non-canonical Wnt pathways in the homeostasis of junctional cells in the GEJ is not well studied. Next, I aimed to understand the differential expression of genes involved in the canonical Wnt/β catenin pathway, non-canonical Wnt/PCP pathway, and Wnt/Ca^{2+} pathway. The Canonical Wnt/β catenin pathway is involved in the stem cell maintenance of various cells from development to the adult stage through the stabilization of β catenin mediated by Wnt ligands (Clevers 2006). While the noncanonical Wnt pathway involves Wnt ligands and Frizzled receptors mediated through β catenin independent pathway (Carreira-Barbosa and Nunes 2020). The non-canonical Wnt/PCP pathway regulates the actin cytoskeleton for the polarized organization of cell structures, while the non-canonical Wnt/Ca^{2+} pathway regulates cell fate and cell migration (Yang and Mlodzik 2015, Q. Wang et al. 2010). Analysis of differentially expressed genes from bulk transcriptomic data

showed enrichment of canonical Wnt pathway and non-canonical Wnt/Ca^{2+} pathway genes in the stomach cells, while esophagus epithelial cells were enriched for the non-canonical Wnt/PCP pathway genes (Figure 23 A).

Further, to evaluate in detail of expression pattern of canonical and non-canonical Wnt pathway genes in the subpopulation of epithelial cells, scRNA-seq data were analyzed. The genes coding for key proteins mediating canonical Wnt signaling *Ctnnb1, Axin2, Lrp5, Lrp6,* and transcription factor *Tcf7* were highly expressed in the columnar epithelial cell clusters of the stomach. Also, the non-canonical Wnt/Ca^{2+} pathway genes, including *Camk2b, Camk2d,* and *Nfatc2* were specifically expressed at higher levels in the stomach epithelial sub-clusters. In contrast, only non-canonical Wnt/PCP pathway genes *Scrib, Rac1, Serpinb5, Daam1,* and *Vangl1* were highly expressed in the esophagus squamous epithelial cell clusters (Figure 23 B).

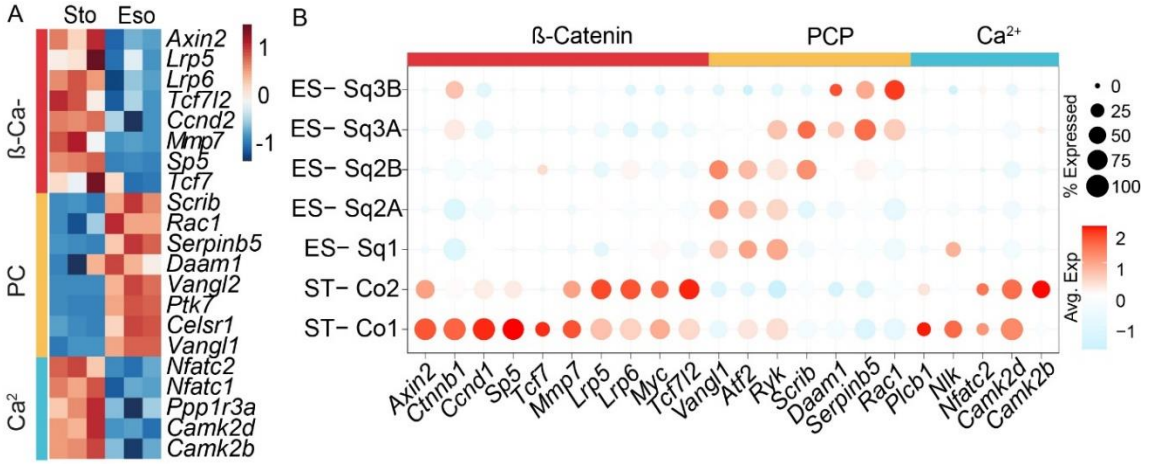

Figure 23. GEJ epithelial cell homeostasis is regulated by canonical and noncanonical Wnt pathways. (A) Heat map showing expression of differentially regulated canonical and noncanonical Wnt signaling pathway genes in the esophagus versus stomach epithelial organoids. Columns represent organoids derived from 3 biological replicates. The color bar represents z-scored gene expression. **(B)** Dot plot depicting expression of canonical and non-canonical Wnt pathway-associated genes in the stomach and esophagus epithelial subclusters. Circle size indicates the percentage of cells expressing an indicated gene. The filled color depicts the normalized and scaled mean expression levels from high (red) to low (blue).

The intrinsic canonical Wnt signaling driven by secreted canonical Wnt ligands can regulate epithelial stem cell regeneration. To check if esophageal epithelial cells depend on intrinsic Wnt signaling, they were grown in the presence and

absence of WNT3A/RSPO1 conditioned media. In addition, the organoids were either treated or untreated with 5 µM Wnt secretion inhibitor IWP2. Additionally, similarly treated stomach stem cells were taken as a control. The organoid size and differentiation pattern was analyzed. The absence or presence of WNT3A/RSPO1 or IWP2 didn't influence the growth and organoid size of esophagus organoids (Figure 24 A, B). In contrast, adding IWP2 in the presence of WNT3A/RSPO1 conditioned media reduced the size of the stomach organoid (Figure 24 A, C). These results suggest that in addition to exogenous Wnt ligands, secreted Wnt ligands play a role in the regeneration of stomach stem cells. To test if inhibition of intrinsic Wnt signaling induces differentiation in the stomach, organoids were stained for mucus (MUC5Ac) that is only secreted by differentiated cells. Despite the presence of WNT3A/RSPO1 conditioned media, IWP2 treatment led to accelerated differentiation of stomach organoids with increased secretion of MUC5Ac (Figure 24 D). Thus, distinct Wnt signaling dependency contributes to the differential regeneration of gastro-esophageal epithelial stem cells at GEJ.

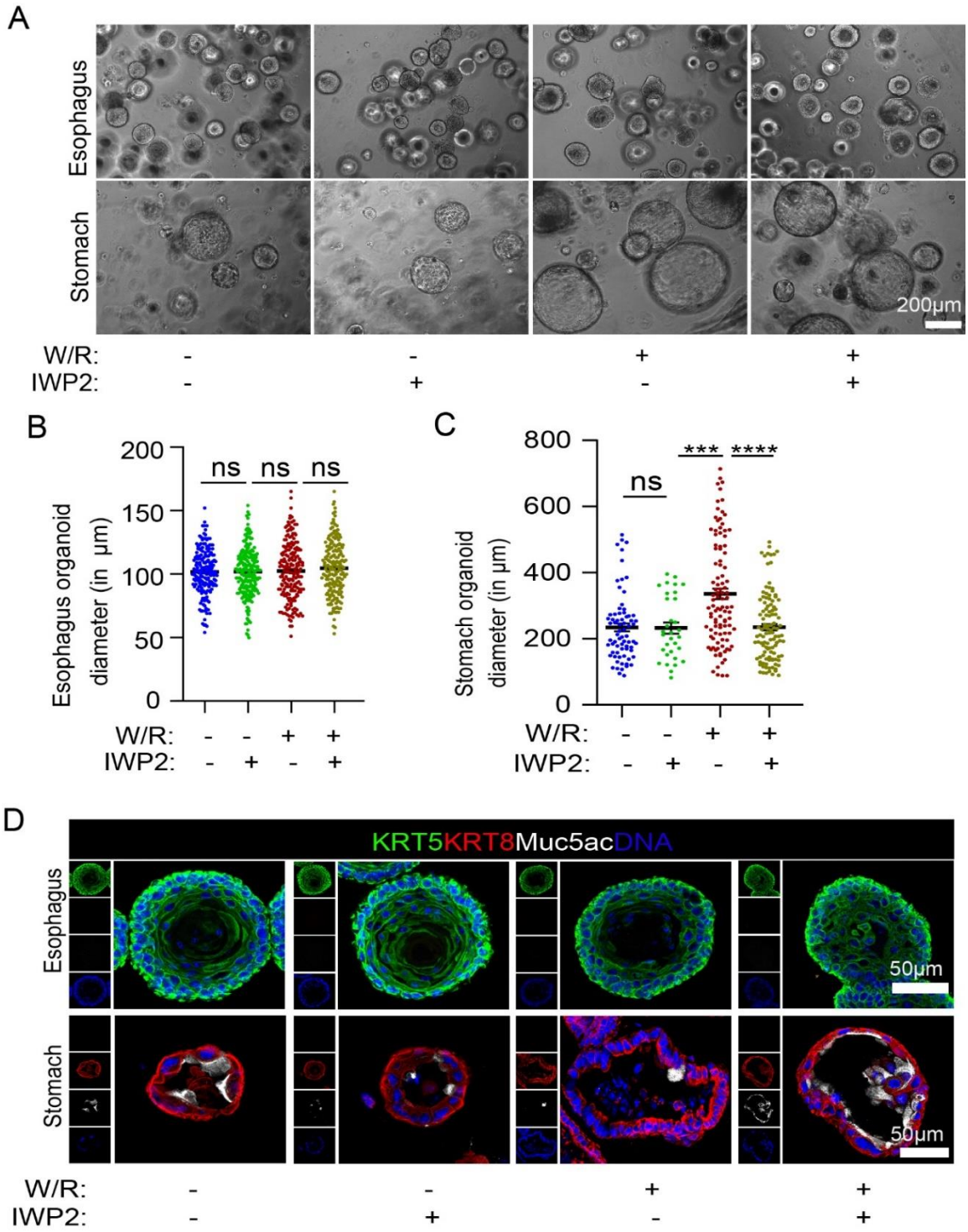

Figure 24. Wnt secretion inhibition does not affect squamous epithelial cells but induces differentiation in stomach epithelial cells. (A) Bright-field images of esophagus and stomach organoids grown in the presence or absence of WNT3A and RSPO1 and either treated or untreated with 5 µM Wnt secretion inhibitor IWP2. **(B-C)** Quantification of organoid size in diameter was measured for esophageal squamous organoids, n ≥ 183 (B), and stomach columnar organoids, n ≥ 32 (C). n= number of organoids measured from 3 biological replicates. ns= Non significant, *** =p<.01, ****=p<.0001. **(D)** Confocal images of esophageal organoid

and stomach organoid immunolabeled with KRT5 (green), KRT8 (Red), Muc5ac (white), and nuclei stained with DAPI (blue).

7.15 Stomach epithelial cells show enriched Retinoic acid activity genes

RA is the active metabolite derived from dietary Vitamin A (retinol), essential for normal vision and immune function development. Low-level dietary intake of Vitamin A is one of the risk factors associated with the development of BE (Lukić et al. 2012). RA activity is known to increase during BE development. However, it decreases as BE progresses to dysplasia and adenocarcinoma (Chang et al. 2007, Chang et al. 2008). To understand how RA pathway genes are regulated in the GEJ epithelial cells, gene set enrichment analysis was performed using the bulk transcriptomic data of esophagus and stomach epithelial organoids. The investigation revealed that the retinoic acid-related genes were highly enriched in the stomach epithelial cells compared to the esophagus (Figure 25 A, B). To obtain insights at the single-cell level, dot plot analysis was performed for single-cell RNA seq data of control esophagus and stomach epithelial cells. The cellular receptor for retinol *Stra6*, the main enzymes involved in the RA metabolism, including retinol dehydrogenase enzyme *Rdh10*, aldehyde dehydrogenase *Aldh1a1,* and reversible enzyme dehydrogenase/reductase 3 *dhsr3* were highly upregulated in the stomach epithelial cells. The stomach epithelial cells also express high nuclear retinoic acid receptor *Rara*, *Rarb*, and Nuclear Receptor Coactivator 1 (*Ncoa1*) genes. The RA degradation enzyme *Cyp26b1* involved in feedback regulation is highly expressed in the stomach, indicating higher RA synthesizing activity in the stomach epithelial cells. Esophageal epithelial cells were enriched for the other receptors and synthesizing enzymes, including *Crabp1, Crabp2*, *Rdh5, Rdh12,* and *Aldh1a3*. However, these genes were expressed in a few epithelial cells. Interestingly, Nuclear Receptor repressor protein 1 gene *Ncor1,* nuclear receptors *Rarg*, *Rxrb* are highly expressed in the esophagus. NCOR1 protein mediates transcriptional repression of retinoic acid receptors by promoting chromatin condensation and thereby impeding the access of transcription factors (Xu, Glass, and Rosenfeld 1999) (Figure 25 C). This indicates that the esophagus actively inhibits RA signaling. Thus, these results suggest that RA

signaling has an active role in stomach homeostasis while inhibition of RA is essential for esophageal epithelial homeostasis regulation.

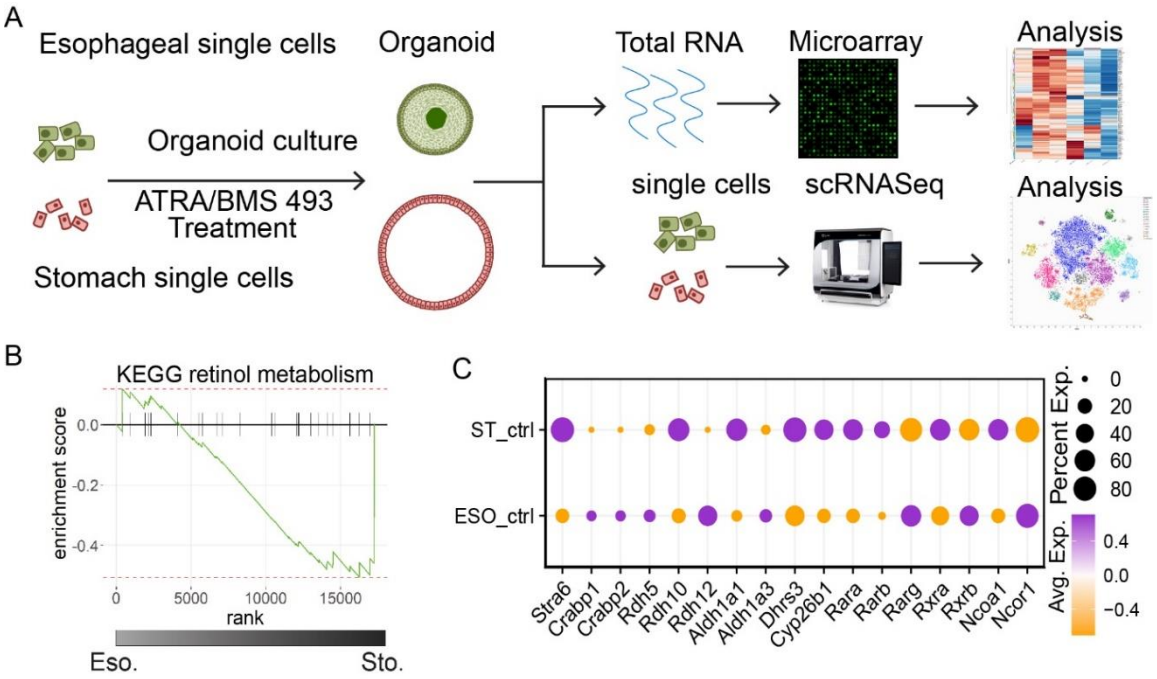

Figure 25. Stomach epithelial cells were enriched for RA pathway genes. (A) Schematic diagram showing epithelial cells growing into organoids with treatments of either ATRA or BMS 493 and process of generation of bulk RNA transcriptomic and single-cell RNA sequence data. **(B)** GSEA enrichment plot showing enrichment of KEGG retinol metabolism pathway genes in the normal stomach organoids compared to the normal esophagus organoids. **(C)** Single-cell RNA sequence dot plot showing the expression pattern of RA pathway-related genes. Dot size represents the percentage of cells expressing the genes, and the gradient color represents the average expression value of the gene.

To understand how RA regulates GEJ epithelial cell homeostasis and if altered RA signaling has any implications for BE development, I cultured esophageal and stomach epithelial cells into organoids in the presence of all-trans-retinoic acid (ATRA) that activate RA signaling (represent RA proficiency) and pan-retinoic acid receptor (pan-RAR) inverse agonist BMS 493 (represents RA deficiency). First, to optimize the functional concentration of ATRA, esophagus, and stomach epithelial cells were grown into organoids in the presence of 100 nM and 1 μM ATRA, and the organoids were analyzed on day 7. In both ATRA concentrations, esophageal organoids showed reduced size, but no change in the size of stomach organoids was observed (Figure 26 A).

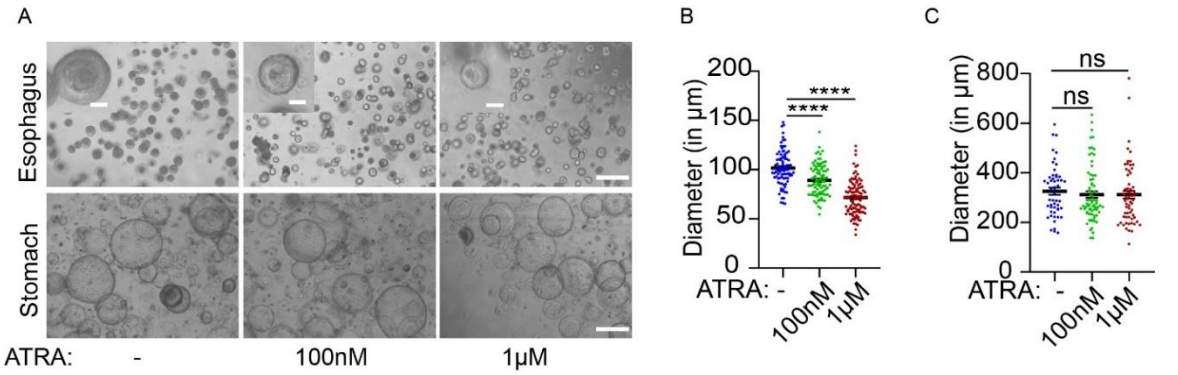

Figure 26. Concentration-dependent effect of RA on GEJ organoids: (A) Representative bright-field image of mouse esophageal and stomach organoids grown in the presence of 100 nM and 1 µM ATRA for 7 days. Scale bar: 500 µm. The inset shows a magnified individual organoid, inset scale bar: 50 µm. (**B-C**) Quantification of the size of organoids by measurement of organoid diameter for the esophageal organoids (B, n ≥ 86, n represents the number of organoids) and stomach organoids (D, n ≥ 51, n represents the number of organoids) from the representative of 3 biological replicates. ns= non-significant, ****=p<.0001.

This result was further confirmed by the quantification of the diameters of organoids, revealing a significant decrease in the size of esophageal organoids in the presence of ATRA in a concentration-dependent manner; on the contrary, stomach organoid size was unchanged (Figure 26 B, C). To see whether the ATRA effect was reversible, epithelial cells were cultured additionally with BMS 493. The presence of BMS 493 reversed the ATRA-induced reduction of the esophageal organoid size, whereas treatment with BMS 493 alone didn't affect the size of organoids (Figure 27 A, B). Interestingly, culturing stomach epithelial cells in the presence of BMS 493 alone significantly reduced the stomach organoid size. This effect was reversed by additional treatment of BMS 493 treated stomach organoids with ATRA (Figure 27 A, C). Further, to understand the long-term impact of RA signaling on GEJ epithelial cells, organoids were passaged in the presence or absence of ATRA and BMS 493. Treatment of ATRA reduced the passaging ability of esophageal organoids, which was reversed by the presence of BMS 493. Interestingly, despite BMS 493-induced reduction in stomach organoid size, there is no difference in the passaging ability either in the presence or absence of ATRA and BMS 493 (Figure 27 D). These results suggest that high RA activity reduces the stemness of esophageal epithelia but has no impact on the stemness of the stomach epithelium. To check the effect on cell proliferation, immunofluorescence staining was performed for proliferation marker Ki-67 and

squamous stem cell marker p63. ATRA treatment reduced the proliferation of cells in the esophageal organoids, corroborating previously observed reduction in the size of organoids, whereas stomach organoids increased the proliferating cells (Figure 27 E). p63, which is involved in the stemness and stratification of squamous epithelial cells, is expressed in cells in the basal and parabasal layers. Upon ATRA treatment, the p63 expression level was reduced (Figure 27 E). It implies that cells maintain stem cell signatures but are unable to proliferate. In the absence of RA, the basal cell number in esophageal organoids increased with the higher expression level of p63 and Ki-67, suggesting increased stem cell turnover.

This result indicates that squamous and columnar epithelial cells in the GEJ respond differentially to the RA signaling, suggesting RA may play a critical role in maintaining adult GEJ homeostasis.

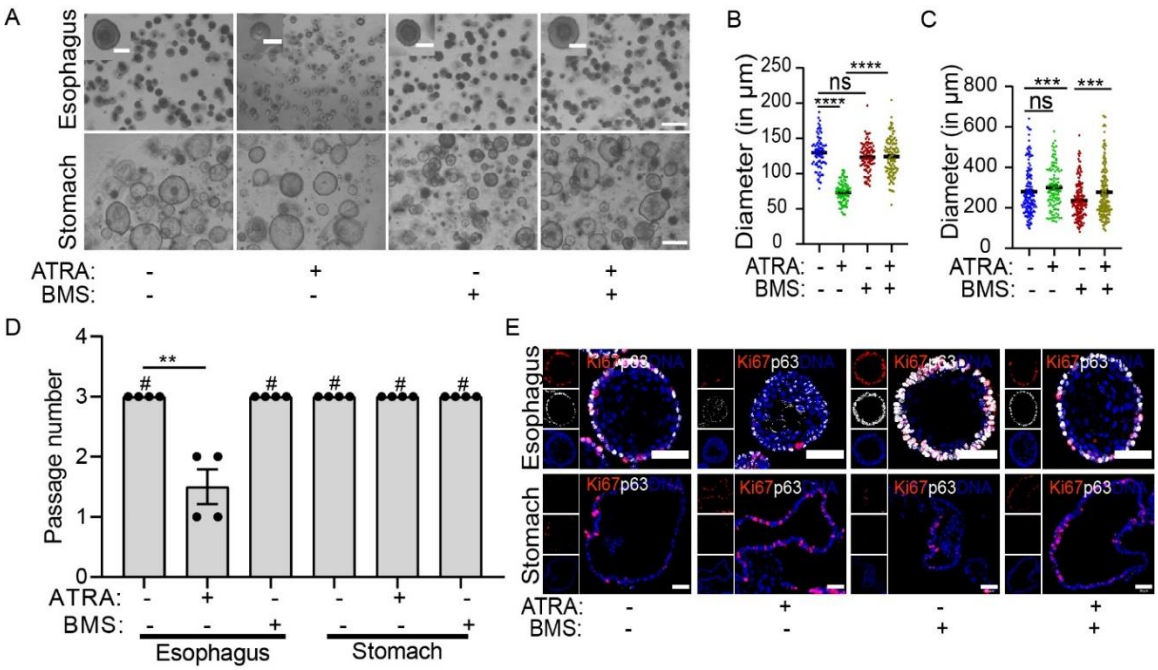

Figure 27. RA alters normal homeostasis in the esophagus and stomach organoids. (A) Bright filed images of esophagus and stomach organoids grown in combinations of either ATRA (1µM) or BMS 493 (1µM) and both. The inset shows the magnified image of a single organoid. Scale bar: 500 µm, inset- 100 µm. **(B-C)** Quantification of the size of organoids by measuring the organoid diameter for esophageal organoids (B, n ≥ 76, n represents the number of organoids) and stomach organoids (C, n ≥ 111, n represents the number of organoids) from a representative of 3 biological replicates. ns= non-significant, *** =p<.001, ****=p<.0001. **(D)** Longevity assay for the passaging ability of esophageal and stomach organoids treated with

ATRA, BMS 493 at equal splitting ratio. 6000 single cells per well were used for passage 0 in all treatments and controls. For subsequent passages 1 to 3, 6000 cells were seeded for the control. For the treated organoids, single cells were made, and the cell number was counted for each condition in each passage. The seeding cell number was kept equivalent to the number of cells corresponding to the splitting ratio of control from passages 1 to 3. Data representative of two independent biological replicates. ns= non-significant, *** =p<.001, **** =p<.0001. # indicates the organoids culture terminated at passage 3. (**E**) Confocal images for the esophageal organoids (upper row) and stomach organoids (lower row) were treated with ATRA, BMS 493, stained with Ki67 (red), p63 (white), and nuclei stained with DAPI (blue). Scale bar 50 µm. Images are representative of 2 independent biological replicates.

7.16 RA induces a distinct transcriptional signature in the GEJ epithelial cells

Since proficiency or deficiency of RA had a differential effect on the GEJ epithelial organoids morphology and homeostasis, I decided to understand in-depth gene expression changes that occurred at the global level. For this, epithelial cells were grown into organoids in the presence or absence of ATRA and BMS 493 for 7 days. Total RNA was isolated from the harvested organoids and performed microarray expression analysis. PCA analysis of bulk transcriptomic data revealed the distinct expression pattern between tissue types. Between treatment types, clusters were separated in the esophageal organoids, whereas in stomach organoids, control and ATRA-treated cells formed one group compared to the BMS 493 treated cells (Figure 28 A). Overall a smaller number of differentially regulated genes were found in control vs. ATRA-treated stomach cells. In contrast, ATRA treatment was found to have a more significant impact on the transcriptional profile of the esophageal organoids (Figure 28 A, C).

In both tissue types, a higher number of differentially regulated genes was found in BMS 493 compared to control-treated cells (Figure 28 B). To identify the cellular processes induced with ATRA and BMS 493 treatment, over-representation analysis (ORA) of top 5 gene ontology (GO) annotations for the oppositely regulated genes was performed (Figure 28 D). RA metabolic pathway-related genes in the stomach organoids were enriched upon ATRA treatment. Genes related to the fatty acid pathway were increased in the stomach epithelial cells upon BMS 493 treatment indicating RA deficiency in the stomach epithelial cells induces a more secretory phenotype. In the

esophagus, genes were enriched for the negative regulation of cell development, axon guidance, glycoprotein metabolic process, and gland development upon ATRA treatment. BMS 493 treated cells were enriched for the keratinocyte differentiation and epidermal cell development pathway genes. Studies suggested that RA alters the expression profiles of terminally differentiated epithelial cells (Fuchs and Green 1981, Szymański et al. 2020). Similar to these studies, genes in the epidermal differentiation complex (EDC) locus were differentially expressed between ATRA and BMS 493 treated epithelial cells in the esophagus organoids (Figure 28 E). Overall results suggest that RA proficiency in the esophageal epithelial cells induces stem cell inhibitory state and alteration in the terminal differentiation pattern. In contrast, RA deficiency causes higher homeostatic status in the esophagus. As opposed to the esophagus, stomach epithelial cells require RA activity for their normal homeostasis, and RA deficiency induces changes in the cell phenotype.

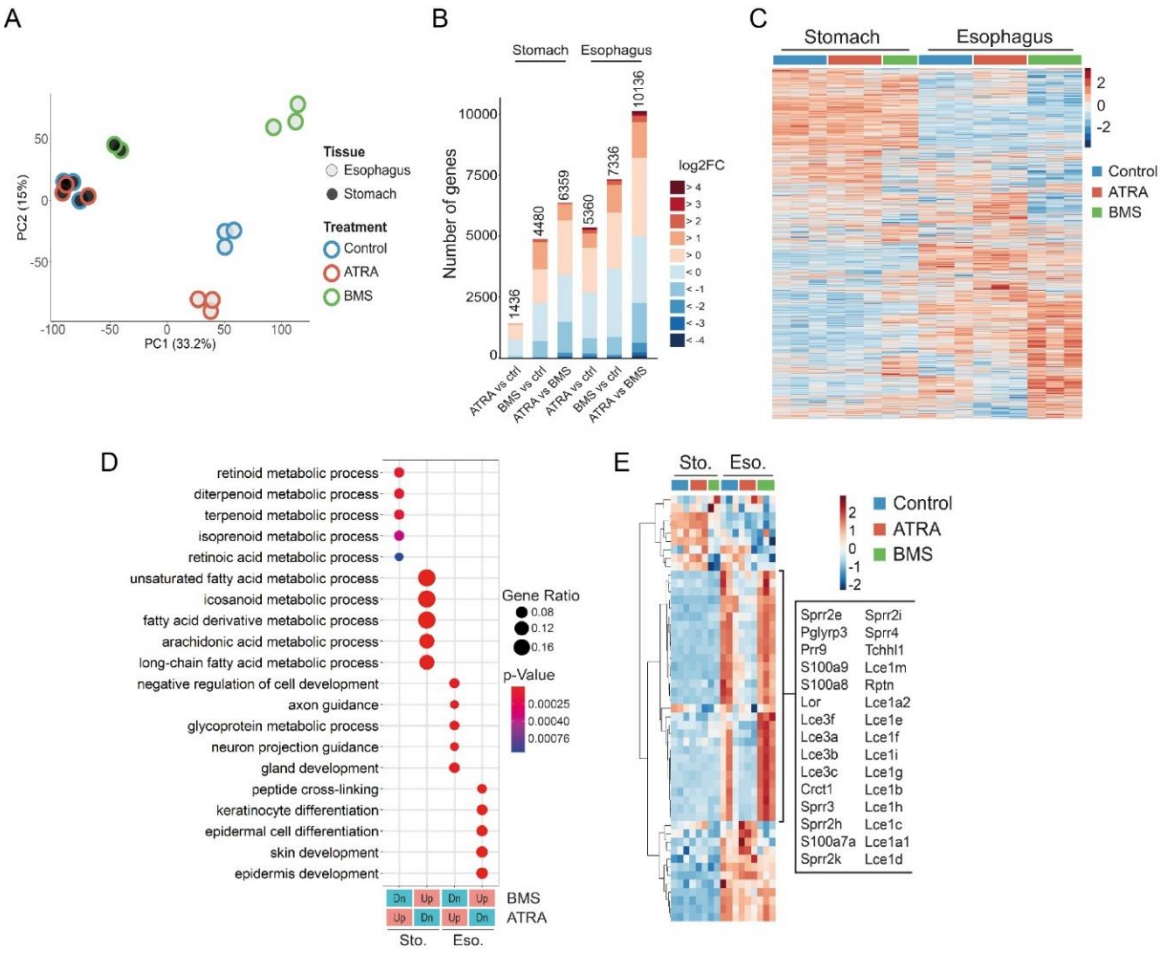

Figure 28. Bulk transcriptomic data showing differential regulation in the esophagus and stomach epithelial cells. (A) PCA plot of differentially expressed genes from esophagus and stomach organoids either treated with ATRA or BMS 493 or control. The plot shows expression patterns related to the tissue differences and treatment types. The inner color of the circle indicates tissue types, esophagus (grey), stomach (black), and the outer circle color indicates the treatment types, control (blue), ATRA (red), and BMS 493 (green). **(B)** The bar plot represents the number of genes differentially expressed in the esophageal and stomach organoids between the two treatment groups. The number on top of the bar graph indicates the number of differentially expressed genes between two conditions, and the color gradient represents the log2FC change. **(C)** Heat map for the bulk transcriptomic data showing expression of differentially expressed genes in the esophagus and stomach organoids either treated with ATRA or BMS 493 or control. Each column represents the individual biological replicate. The Colour bar represents scaled expression values. **(D)** Top 5 enriched GO terms for oppositely regulated genes between treatments in esophagus and stomach organoids. **(E)** Heat map showing EDC locus gene expression pattern differences in the esophagus and stomach organoids treated with ATRA, BMS 493, or control.

7.17 RA alters cytokeratin expression patterns in the organoids

Cytokeratins in the epithelial cells form the intermediate filament of the cell cytoskeleton, whose expression depends on the type of epithelial cell, stage of development, tissue site, and pathological conditions. RA alters the expression pattern of different cytokeratins in the epithelial cells (Törmä 2011). As shown (Figure 29 A), GEJ squamous and columnar epithelial cells show distinct cytokeratin expression. I wanted to analyze if RA induces any changes in the cytokeratin expression pattern specific to epithelial cell types and transdifferentiation of one epithelial type to another. Bulk transcriptomic data revealed that the cytokeratins, usually present in the normal columnar epithelial cells (*Krt7, Krt18, Krt19, Krt20*), were highly upregulated in the ATRA-treated esophagus squamous epithelial cells. BMS 493 treatment reduced the expression of *Krt7, Krt18, Krt19,* and *Krt20* cytokeratin, indicating that RA regulates the expression of these cytokeratins. The expression of squamous-specific cytokeratin was not altered in both ATRA and BMS 493 treatment conditions in esophagus organoids. Most of the cytokeratin expression remained unaltered in the stomach organoids except for *Krt81, Krt85*, and *Krt222,* which were reduced in the presence of BMS 493. The western blot analysis confirmed RA-specific alteration in KRT7, and KRT8 and

KRT5 expressions were analyzed as controls for squamous and columnar lineage-specific markers (Figure 29 D). Further, gene expression of *Krt7* and *Krt8* in the ATRA and BMS 493 treated organoids was confirmed by qRT PCR. *Krt7* expression was increased in the esophagus in the presence of RA as determined by qRT PCR and western blot (Figure 29 B, D). There was a slight increase in the *Krt8* expression at the mRNA level in the esophagus in ATRA-treated cells; however, it did not lead to increased KRT8 protein as determined by the western blot (Figure 29 C, D). Immunofluorescence staining was performed to identify the cellular location of expression of altered cytokeratins in the organoids. Squamous-specific KRT5 was expressed only in the esophagus, and columnar-specific KRT8 was only expressed in the stomach organoids. Treatment with RA and BMS 493 didn't alter the KRT5 and KRT8 expression in both epithelial cell types (Figure 29 E).

.

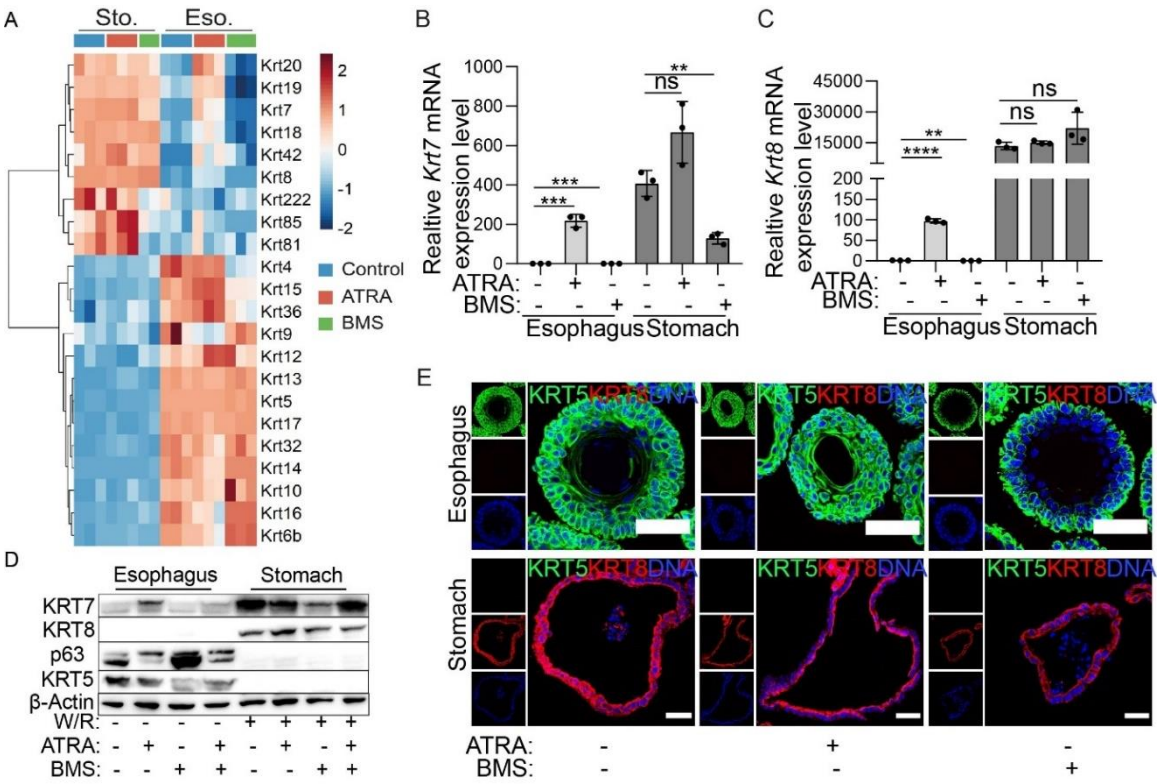

Figure 29. RA increases the KRT7 expression. (A) Heat map showing the selected cytokeratin gene expression in esophagus and stomach organoids treated with either ATRA or BMS 493 or untreated. The Colour bar represents scaled expression values. **(B-C)** Quantitative reverse transcription- RTPCR (qRTPCR) for the *Krt7* (B) and *Krt8* (C) expression in the esophageal and stomach organoids treated with ATRA, BMS 493 compared to the control. For esophagus and stomach treatments, fold expression was calculated from esophagus control. Data are representative of 2 biological replicates. (n=3, n represents technical replicates. ns=

non-significant, ** =p<.01, *** =p<.001, **** =p<.0001). **(D)** Western blot for the KRT5, p63, KRT8, and KRT7 protein expression in the esophagus and stomach organoids treated with either ATRA or BMS 493 or untreated. Beta-actin was used as a loading control. The esophagus and stomach organoids were cultured in the absence of Wnt (W-/R-) and the presence of Wnt (W+/R+) media, respectively. **(E)** Confocal images for the esophageal organoids (upper row) and stomach organoids (lower row) were treated with either ATRA or BMS 493 or kept untreated. Organoids were stained with KRT5(green), KRT8(red), and nuclei were stained with DAPI (blue). Scale bar: 50μm. Images are representative of 2 independent biological replicates.

To examine whether ATRA-induced KRT7 expression in esophageal squamous organoids is long-lasting, organoids were treated with ATRA or BMS 493. In the following passage, the treated organoids were split into two sets. One set of organoids was kept untreated (ATRA release), and another set was kept under continued treatment. Western blot analysis of KRT7 showed that ATRA release reduced the expression of KRT7, confirming RA specifically induced the KRT7 expression and is reversible in the esophageal epithelium (Figure 30 A). However, the presence or absence of Wnt components in the media didn't induce KRT7 expression in the esophagus organoids. To further confirm the spatially localized expression of KRT7 in the organoids, immunofluorescence analysis was performed. ATRA treatment induced the expression of KRT7 in the esophagus epithelium, and KRT7 levels are intrinsically high in the stomach, and additional treatment with ATRA shows a further increase. However, inhibition of RA by BMS 493 treatment reduced KRT7 levels in both the stomach and esophageal organoids (Figure 30 B). Irrespective of Wnt growth factors, ATRA-treated squamous organoids show increased KRT7 expression in the differentiated cells facing the lumen but not in the basal stem cells (Figure 30 A, B, upper panel). This indicates that RA signaling regulates the expression of KRT7 irrespective of Wnt signaling.

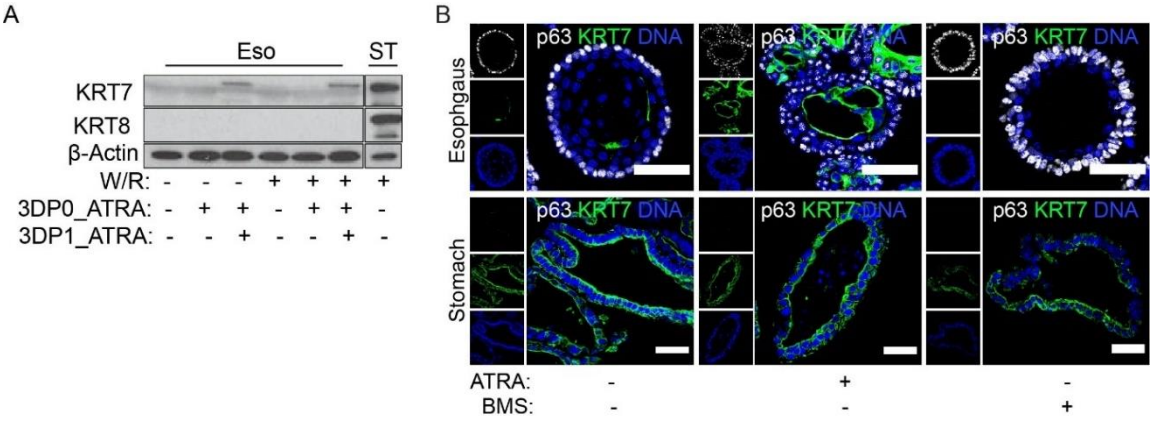

Figure 30. RA reversibly induces KRT7 expression in the GEJ epithelial cells. (A) Western blot image for the KRT7 and KRT8 protein expression in the 3D passage 1 (3DP1) esophageal organoids either untreated or treated with ATRA, BMS 493. Beta-actin was used as a loading control. In 3D passage 0, organoids were treated either with ATRA or BMS 493 in the 3D passage 0. In a subsequent passage 3DP1, these organoids were treated with either ATRA or BMS 493 or kept untreated. **(B)** Confocal images for the esophageal organoids (upper row) and stomach organoids (lower row) treated with ATRA, BMS 493, stained with KRT7 (green), p63 (white), and nuclei stained DAPI (blue). Scale bar 50 µm. Images are representative of 2 independent biological replicates.

7.18 RA upregulates BE marker genes in the squamous epithelium but doesn't lead to transdifferentiation into the columnar epithelium

The expression of *Krt7* and *Krt20* were implicated in the BE (Kosoff et al. 2012, Korbut et al. 2020) and these genes were upregulated in the ATRA-treated esophageal organoids. Studies also hypothesized that KRT7-expressing transitional cells are the precursor for BE development (Wang et al. 2011, Jiang et al. 2017). Here I investigated if the expression of KRT7 indicates the transdifferentiation of squamous esophageal cells to BE-like cells. To test this, with the help of a bioinformatician, I have compared bulk transcriptome data from ATRA, and BMS 493 treated organoids with differentially regulated genes in BE derived from publicly available data (Hyland et al. 2014). Irrespective of treatments, genes from the stomach organoids and BE gene signatures were similarly regulated, indicating the transcriptional similarity of BE with stomach epithelial cells (Figure 31 A). Interestingly, some genes known to be highly expressed in the BE (*Id2, Krt20, Bmp2, Krt18, Sox9, Agr2, Krt8*) were similarly

upregulated in the ATRA-treated esophageal organoids. The reason could be that these genes might contain the retinoid-responsive element upstream of their promotor (Rachelle E Kosoff et al. 2012, Törmä 2011). Further, the expression of these genes in esophageal epithelium might indicate or induce transdifferentiation of squamous epithelium to the columnar or BE epithelium. To test whether RA induces transdifferentiation from squamous to columnar epithelium, epithelial cells from mice either expressing *Krt5-CreErt2/Rosa26-tdTomato* or *Krt8-CreErt2/Rosa26-tdTomato* were cultured in the presence of either ATRA and BMS 493. Lineage tracing was induced from the beginning of treatment by adding tamoxifen into the culture media. Only cells marked for KRT5 developed squamous organoids but didn't develop into stomach organoids. Further treatment with ATRA and BMS 493 does not affect the KRT5 lineage development. Similarly, KRT8 lineage was traced only in stomach organoids, and ATRA or BMS 493 treatment didn't induce transdifferentiation to the esophagus organoids. This suggests that RA can induce genes associated with columnar/ BE epithelial cells in the esophagus, but it doesn't transdifferentiate committed squamous epithelial lineage into the columnar epithelial lineage (Figure 31 B).

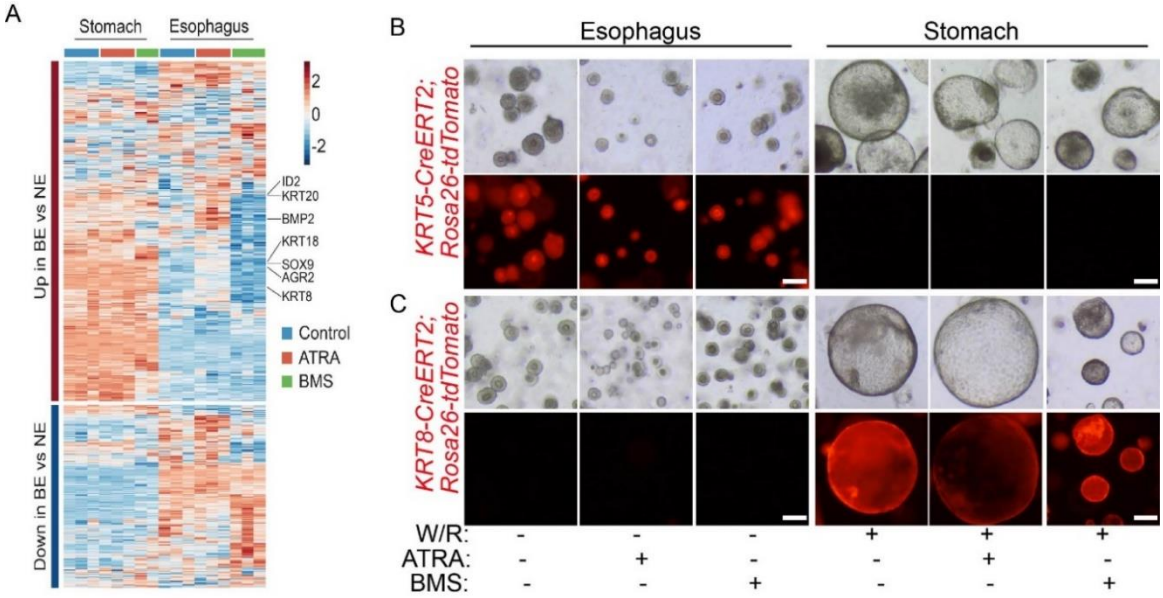

Figure 31. Higher RA doesn't induce trans-differentiation of esophagus squamous epithelium to columnar epithelium. (A) Heat map showing differentially expressed genes between the normal esophagus and BE (Hyland et al. 2014), compared with the gene expression signature of esophagus and stomach organoids treated with either ATRA or BMS or untreated. The color bar represents scaled expression values. **(B-C)** Fluorescence images showing in-vitro

lineage tracing for the organoids derived from the mouse *Krt5-CreErt2/Rosa26-tdTomato* epithelia (B) and *Krt8-CreErt2/Rosa26-tdTomato* epithelia (C) treated either with ATRA or BMS 493 or untreated. The esophagus and stomach organoids were cultured in the absence of Wnt (W-R-) and the presence of Wnt (W+R+) conditioned media, respectively. Scale bar: 500 µm.

7.19 RA deficiency alters epithelial cell lineage in the stomach organoids

As observed above, RA deficiency induces a reduction in the stomach organoids, but still, they have passaging abilities. Previously studies reported the upregulation of the RA degradation enzyme gene *Cyp26a1* in the BE tissue samples (Chang et al. 2008). This indicates that localized RA deprivation exists in the BE tissue indicating RA might play a role in the differentiation of BE epithelial cells. To check this possibility, bulk transcriptomic data of ATRA and BMS 493 treated stomach epithelial cells were analyzed for any changes in the epithelial cell type markers. The analysis showed that the marker genes associated with stomach and BE epithelial cells were dysregulated. The stomach stem cell marker gene *Lgr5* expression was reduced in the absence of RA while *Sox2* expression increased (Figure 32 A, B, C). The reduced expression of *Lgr5* didn't diminish the long-term expansion of BMS 493 treated organoids suggesting epithelial homeostasis maintenance by alternative stem cells. Upregulation of marker genes of enteroendocrine lineage (*Neurog3, Sct, Ghrl, Nts*) intestinal specific epithelial cells (*Cdx2, Tff3, Pdx1*) were observed in the BMS 493 treated stomach epithelial cells (Figure 32 A). This shows that RA deficiency could play a role in the differentiation of BE-like epithelial lineage by upregulating intestinal and enteroendocrine lineage marker genes in the stomach epithelial cells.

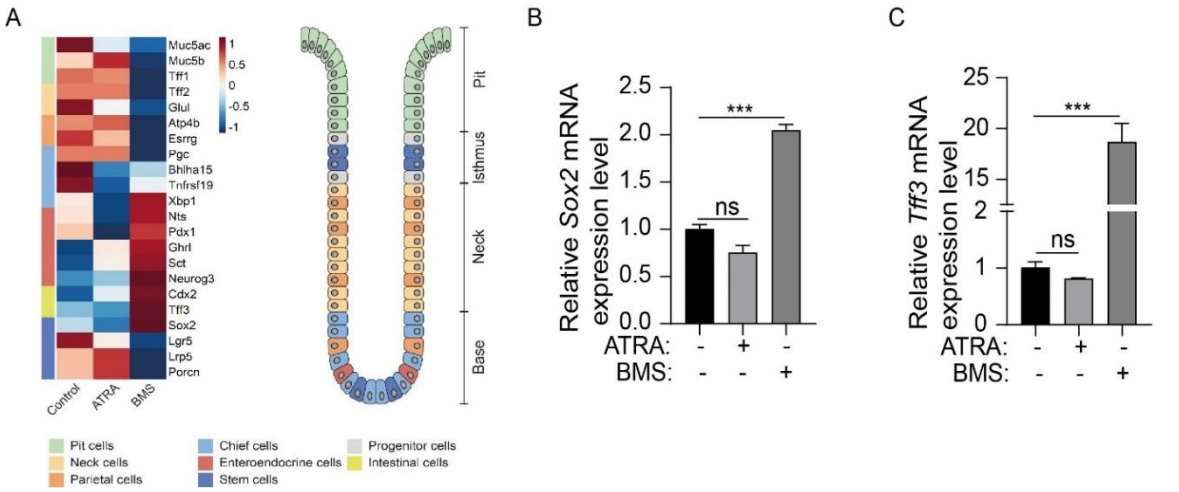

Figure 32. RA deficiency induces intestinal and enteroendocrine marker gene expression in the stomach epithelial cells. (A) Heat map showing mean expression for the selected gastric and intestinal cells type marker genes for stomach organoids treated with either ATRA or BMS 493 or untreated. The color bar represents scaled expression values. **(B-C)** Quantitative-RT-PCR for the *Sox2, Tff3* gene expression in the stomach organoids treated with either ATRA or BMS 493 compared to control. Data are representative of 2 biological replicates. (n=3, n represents technical replicates. ns= non-significant, **** =p<.0001).

To understand the changes occurring at the level of cell lineage, single-cell RNA sequencing was performed using "multiplexing using lipid-tagged indices for single-cell and single-nucleus RNA sequencing" (MULTI-seq) analysis. This method involves the lipid-tagged barcoding of cells from different samples, which can be pooled later and sequenced as one sample. This allows minimal sample processing, preserving cell viability and endogenous gene expression patterns, doublet identification, and recovery of cells with low RNA content (McGinnis et al. 2019). For this, epithelial cells from the stomach were grown into organoids in the presence of either ATRA or BMS 493, and untreated cells were kept as control (in triplicates). Isolated single cells from the organoids were lipid barcoded for each treatment, pooled, and subjected to single-cell RNA sequencing using 10X genomics technology. The resulting output was de-multiplexed, and data visualization was done by dimensionality reduction using Uniform Manifold Approximation and Projection (UMAP). This analysis showed that the epithelial cell clusters from the control and ATRA treatment overlapped, whereas BMS 493-specific epithelial cells formed a distinct cluster (Figure 33 A). As observed from bulk transcriptomic data, RA deficiency had a higher effect on the stomach epithelial transcriptional signature than the higher

RA levels. Dot plot analysis of scRNA-seq data revealed that the stem cell marker gene *Lgr5* and *Axin2* were enriched in control and ATRA-treated epithelial cells compared to the BMS 493 treated cells (Figure 33 D). The markers associated with proliferating zone called the isthmus region of the stomach gland, such as *Stmn1, Runx1,* and *Sox2*, were enriched in the BMS 493 treated stomach epithelial cells (Figure 33 D).

Interestingly, the gene markers of intestinal-specific cells and enteroendocrine cells were also enriched in RA deficiency, suggesting the role of RA signaling in the regulation of the lineage of stomach epithelial cells. These results are recapitulated with the earlier bulk transcriptomic data (Figure 32 A). To understand the cell cluster types and cell of origin for all the lineages present in the treatments, cells from the treatments were combined for clustering and pseudo-time trajectory analysis. Pseudo-time trajectory analysis provides information on the differentiation process undergone by the lineages with time which can be used for inferring the early and later stages of epithelial lineage. Combined clustering analysis provided 4 clusters (Co1, Co2, Co3, and Co4) with two lineages. Both lineages have shared one origin cluster (Co1), which is enriched for the *Lgr5* stem cell marker (Figure 33 C), which gave rise to Co2 and Co3 clusters in one lineage and Co4 clusters in a second lineage (Figure 33 B). To analyze the contribution of cells from each treatment to the clusters, a Sankey diagram analysis was performed (Figure 33 E). This analysis shows that the Co1 cluster contains the cells shared by all the treatments suggesting a stem cell compartment with a common origin for the lineages. The Co2 clusters were majorly shared by the control and ATRA-treated epithelial cells, whereas the Co3 cluster was equally shared by the cells from all the treatments. The Co4 formed the distinct cluster, which was majorly represented by the BMS 493 treated epithelial cells, which include cells expressing intestinal and enteroendocrine cell lineages. To further support this observation, the aggregate score of the markers genes of intestinal and enteroendocrine cells lineage was highly enriched in the BMS 493 treated epithelial cells cluster (Figure 33 F). To further verify the mouse data obtained from the human normal and BE data, gene expression data sets from the treatments were compared with the recently published human data set (Nowicki-Osuch et al. 2021). The genes associated with BE, which are

upregulated in the BMS 493 treated epithelial cells, were similarly regulated to the genes differentially expressed between human BE compared to the normal gastric gene expression data set (Nowicki-Osuch et al. 2021) (Figure 33 G). The overall results suggest RA deficiency has a role in the cell lineage alteration in the BE.

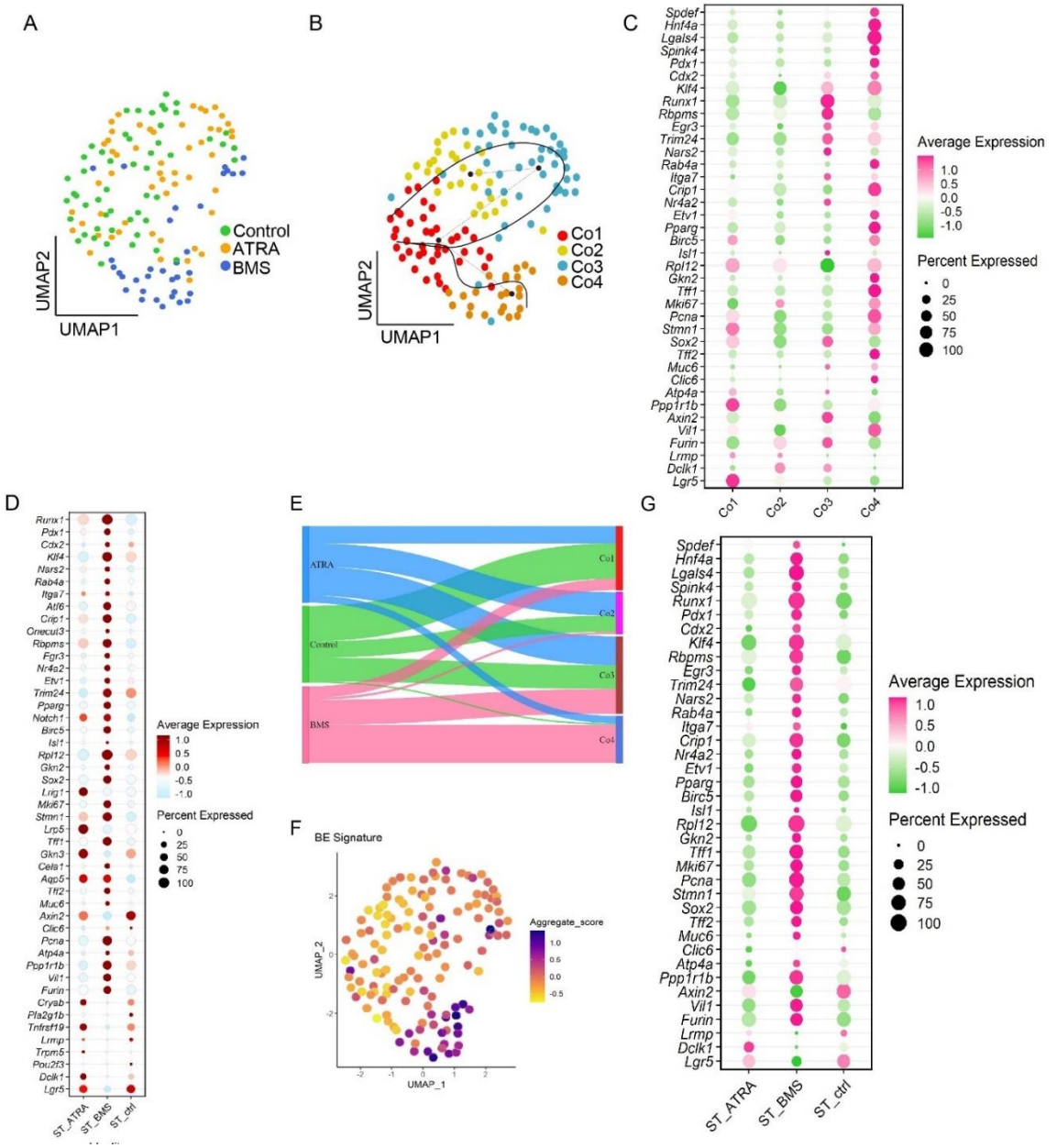

Figure 33. Single-cell RNA sequence reveals that the stomach epithelial cells under RA deficiency conditions express BE marker genes. **(A)** UMAP plot for the combined stomach epithelial cells from control, ATRA, and BMS 493 treated organoids. The dot color represents treatment conditions. **(B)** UMAP plot showing lineage inference and pseudo time analysis using Slingshot for combined stomach epithelial cells from control, ATRA, and BMS 493 treated organoid. The dot color represents epithelial cell cluster types. **(C)** Dot plot for the average

expression of marker genes of stomach epithelial cell types and BE cells for epithelial sub-clusters. **(D)** Dot plot for the average expression of marker genes and percentage of cells representing epithelial cell types in the treatment group. **(E)** Sankey diagram illustrating the contribution of cells in each subcluster from the treatment conditions. **(F)** The UMAP plot represents the aggregate score for the selected gene expression associated with BE signature genes. **(G)** Dot plot for the average expression of marker genes of stomach epithelial cell types and BE cells for the treatment conditions.

7.20 Higher RA induces esophageal epithelial cells to undergo a quiescence state

The ATRA-induced smaller size of esophageal organoids, reduced organoids passaging ability, and enrichment of negative cell cycle regulation genes made me speculate that the higher RA induces a quiescence state specifically in the esophageal epithelial cells but not in the stomach epithelial cells. To identify whether higher RA signaling affected the cell state, GSEA enrichment analysis for the dormancy-associated genes was performed for the differentially regulated genes between ATRA and BMS 493 treated cells (Figure 34 A). The presence of ATRA upregulated the genes related to retinol metabolism, TGF-β signaling, p53 pathway, Notch signaling, and hypoxia pathways which are known to be overrepresented in the dormancy (Dunaway et al. 2019, Prunier et al. 2019, Cabezas-Wallscheid et al. 2017) while down-regulated in RA deficiency. By contrast, genes related to the normal cell cycle processes such as ribosome biogenesis, translational initiation, purine metabolism, and DNA repair were downregulated in higher RA and upregulated in RA deficiency. To validate, the genes from the TGF-β pathway (*Tgfb3, Bmp2, Id2*) and retinol acid pathway (*Cyp26b1, Rarb*) were quantified with RT-PCR (Figure 34 B-F). These genes were upregulated in ATRA treated and down-regulated in the RA deficiency.

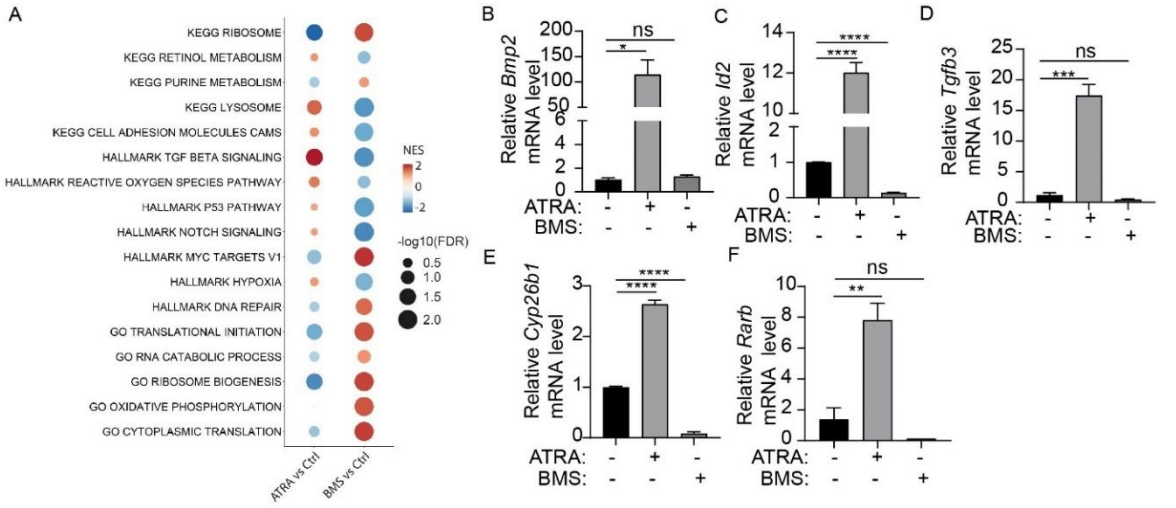

Figure 34. RA upregulates TGF beta and dormancy pathway. (A) Bubble plot derived from bulk transcriptomic data showing GSEA enrichment of selected dormancy-related gene set for esophageal organoids treated with ATRA and BMS 493. Bubble size represents the –log10 (FDR), and color represents the normalized enrichment score. **(B-F)** Quantitative RTPCR for the TGF-β and RA pathway genes *Bmp2, Id2, Tgfb3, Cyp26b1, and Rarb,* in the esophagus organoids treated with either ATRA or BMS 493 compared to the control. Data are representative of 2 biological replicates. (n=3, n represents technical replicates).

Single-cell RNA sequence analysis was performed, as mentioned above, to understand the RA effect on esophageal epithelial cells. A combined cluster analysis was performed to ascertain the relationship between the treated clusters. UMAP analysis showed that the control and BMS 493 treated epithelial cells formed adjacent clusters. In contrast, ATRA-treated cells formed distinct cell clusters implicating a more prominent effect of increased RA signaling on squamous epithelial cells compared to the control. To determine the sub-cluster types in the combined treatment analysis, the expression pattern of gene signatures of basal cells, parabasal cells, and differentiated cells were analyzed. Gene sets from each cell type formed distinct expression patterns in the combined cluster. Based on the cell type-specific gene annotation, 8 clusters were (Sq-I, Sq-II, Sq-III, Sq-IV, Sq-V, Sq-VI, Sq-VII, Sq-VIII) generated (Figure 35 A-C). Lineage analysis was performed to find the origin of clusters and differentiation patterns. Pseudotime analysis by slingshot showed that cluster Sq1 forms the origin (Figure 35 B). The analysis generated 5 independent lineage trajectories representing diverse cell types with different degrees of differentiation. Two lineages represent control and BMS-treated epithelial cell differentiation pattern. In comparison, the other three lineages

include only ATRA-treated epithelial cells suggesting RA induces broader transcriptomic changes in the esophageal squamous epithelial cells (Figure 35 B). The gene aggregate score plot for the basal, parabasal, and differentiated marker genes was shown a distinct pattern of expression in all the treatment conditions suggesting retention of cell heterogeneity similar to the control (Figure 35 D-F). However, ATRA-treated epithelial cell clusters showed higher expression of TGF-β pathway genes (Figure 35 G).

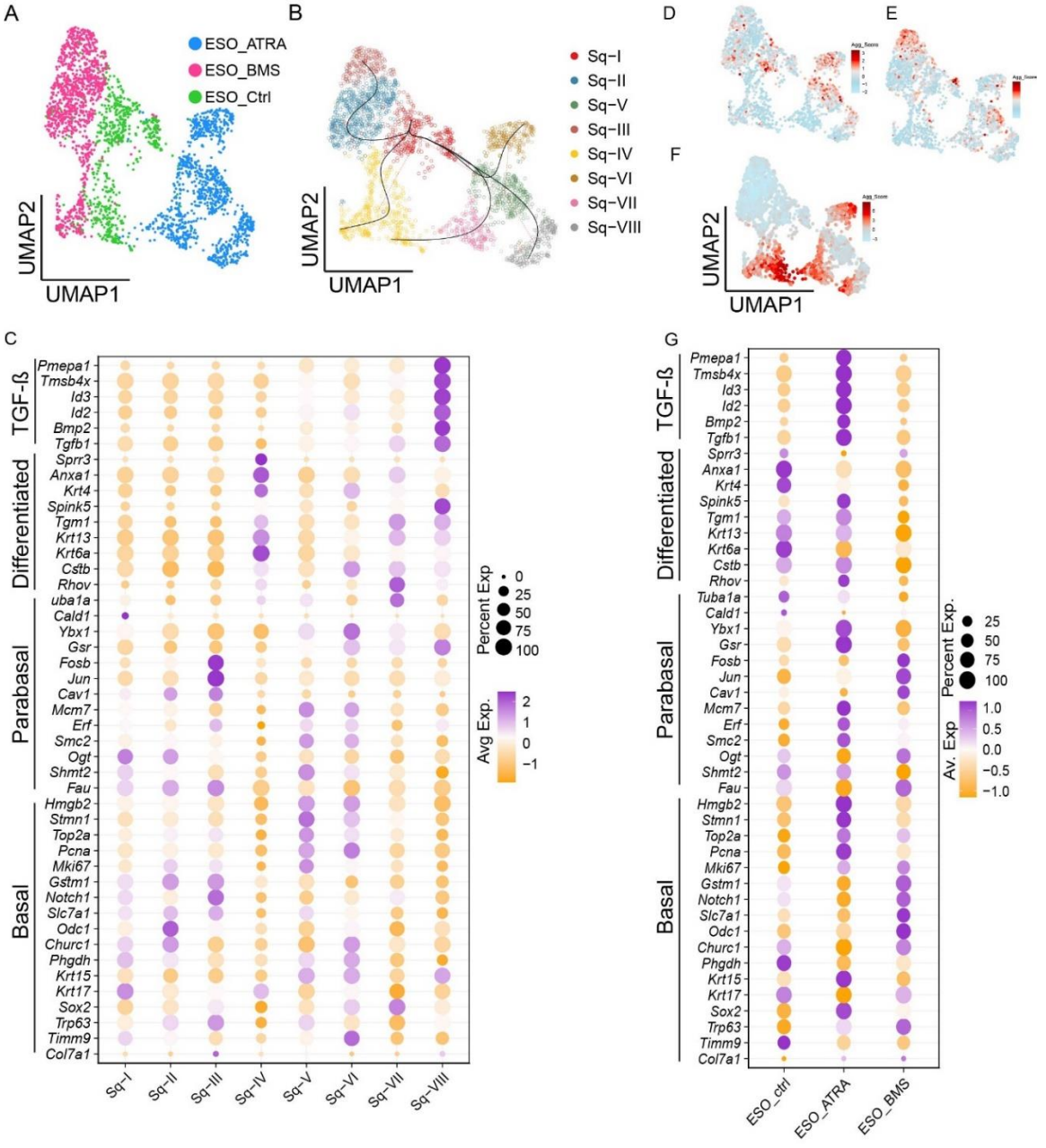

Figure 35. Distinct squamous epithelial cell cluster emerges in the presence of higher RA. (A) UMAP plot for the combined esophageal cells from control, ATRA, and BMS 493 treated esophagus organoids. The dot color represents treatment conditions. **(B)** UMAP showing lineage inference and pseudotime analysis using Slingshot for combined esophageal cells from control,

ATRA, and BMS treatment. The dot color represents cluster types. **(C)** Dot plot for the average expression and percentage of cells expressing genes representing epithelial subtypes in treatment groups. **(D-F)** UMAP shows the distribution of aggregate scores for the expression of genes specific to basal (n=8) (D), parabasal (n=9) (E), and differentiated (n=7) (F) epithelial cells. **(G)** Dot plot for the average expression and percentage of cells expressing genes representing epithelial cell cluster subtypes.

Sankey diagram shows that the control is shared by the clusters Sq1 and SqIV, while BMS 493 treated cells are shared by the clusters SqII, SqIII, and SqIV. Sq V to SqVIII clusters formed independent clusters and was only shared by the cells from ATRA-treated epithelial cells (Figure 36 A). Sq V to SqVIII clusters includes basal, parabasal, and differentiated cell clusters, which specifically show enhanced expression of the TGF-β pathway, RA pathway, cell cycle inhibition genes, and dormancy-associated genes as shown in aggregated gene set expression score plot (Figure 34 B, 36 B-D) (Prunier et al. 2019, Cabezas-Wallscheid et al. 2017, Kanehisa and Goto 2000, Sadasivam and DeCaprio 2013).

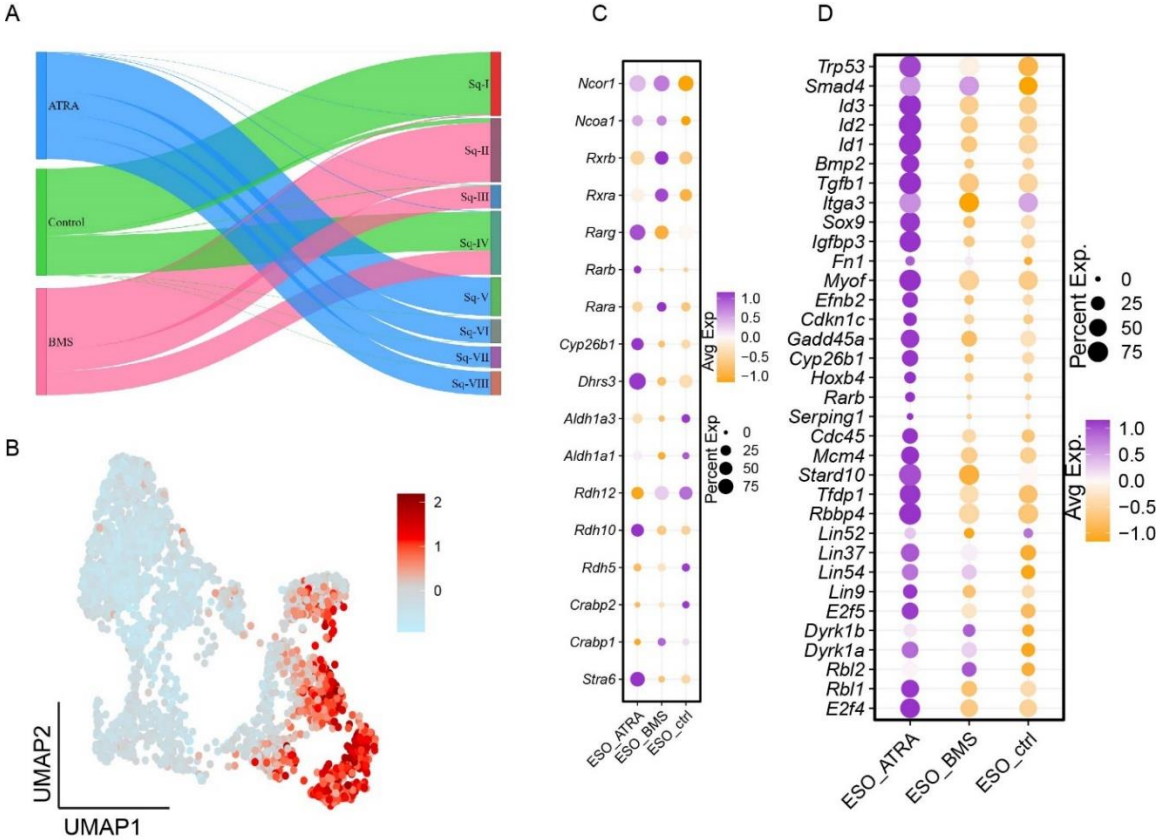

Figure 36. Distinct squamous epithelial cell cluster enriched with dormancy-associated genes. (A) Sankey diagram representing the contribution of cells in each epithelial subcluster from the treatment conditions. **(B)** UMAP plot represents the aggregate score for the selected

genes (n=34) expression associated with cellular dormancy. **(C)** Dot plot for the average expression and percentage of cells expressing RA pathway genes in treatment conditions. **(D)**Dot plot for the average expression and percentage of cells expressing dormancy-related genes in the treatment conditions.

Next, I asked whether the RA-induced effect was reversible or persisted for the long term in the esophageal epithelial cells. For this, the esophageal cells were either grown in the presence or absence of ATRA and BMS 493. In the following passage, single cells were generated from these organoids; one set was continued with treatment as before, and another set of cells was left untreated (RA release) (Figure 37 A). The organoids from these conditions were analyzed for size and stained with KRT5 and differentiation marker KRT6. The data revealed that the presence of ATRA reduced the organoid size, and the removal of ATRA in the subsequent passage reversed the organoid size equivalent to control untreated organoids (Figure 37 C). Moreover, differentiation marker KRT6 was not observed in the ATRA-treated organoids indicating the presence of early cells in a quiescent state (Figure 37 B). To check the percentage of cells in the quiescent state, FACS analysis was performed for ATRA-treated epithelial cells. These treated cells were permeabilized and stained with proliferation marker KI67 and DNA stain 7-ADD. The cycle analysis revealed a higher number of cells in G0 (quiescent state) in the ATRA-treated cells, compared to the control and BMS 493-treated cells (Figure 37 E). Collectively increased RA signaling induces quiescence in the esophageal epithelial cells, and RA deficiency causes a more homeostatic phenotype.

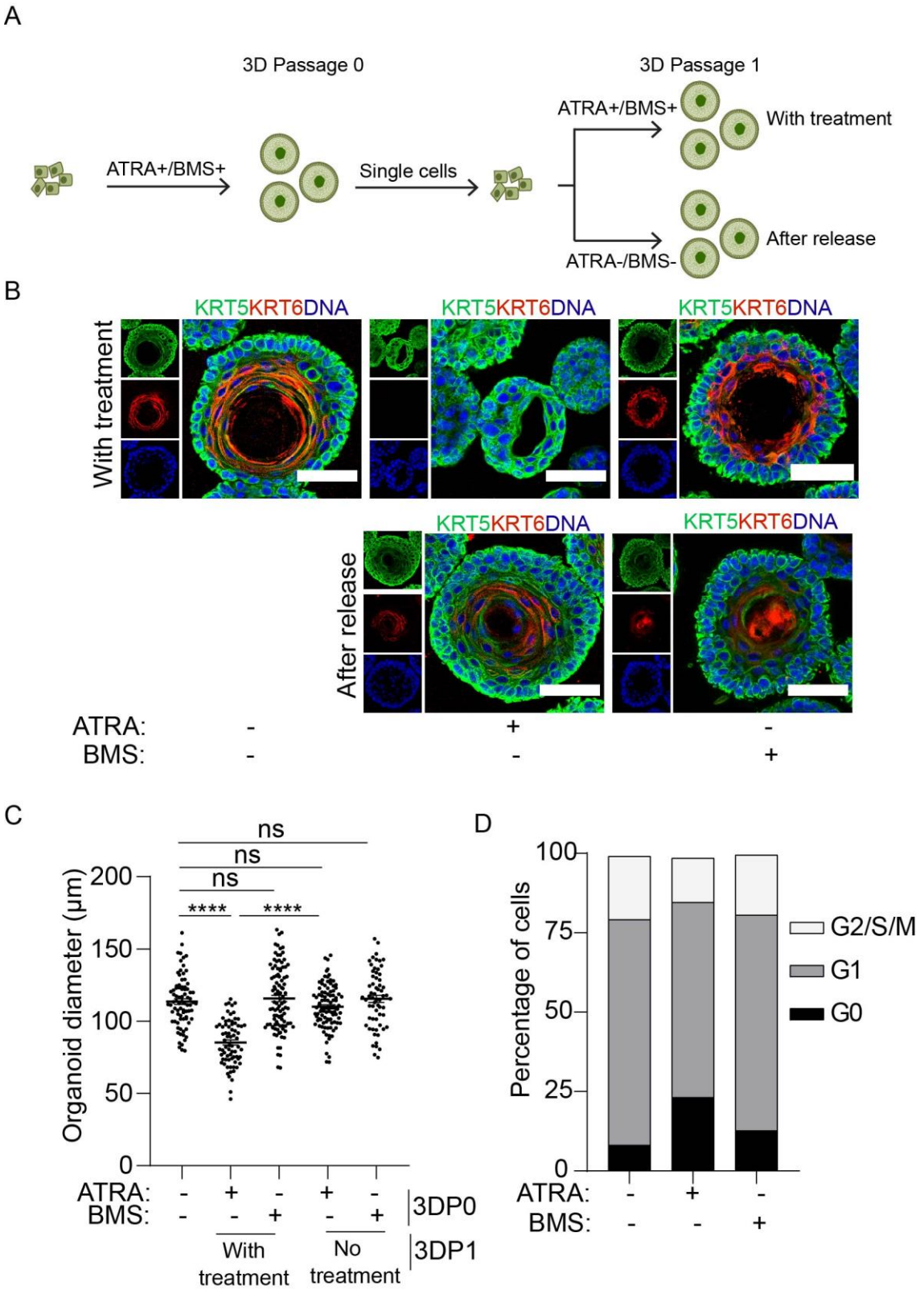

Figure 37. Distinct squamous epithelial cell cluster enriched with dormancy-associated genes upon ATRA treatment. (A) Schematic representation showing ATRA and BMS 493 treatment and release assay. Organoids were treated with ATRA and BMS 493 in 3D passage 0. In the following passage 1, treated organoids were cultured either the presence or absence of ATRA and BMS 493. **(B)** Confocal images for the esophageal 3D organoid passage 1 with

treatment and after the release of ATRA and BMS 493, were stained with KRT5 (green), KRT6 (red), and nuclei stained with DAPI (blue). Scale bar 50 μm. Images are representative of 2 independent biological replicates. **(C)** Measurement of 3D passage 1 day 7 organoid diameter in the treatment and release assay with ATRA and BMS 493 for esophageal organoids ($n \geq 59$, n represents the number of organoids measured). **D)** Cell cycle phase analysis for esophageal organoids, representing the percentage of cells in the G0, G1, and G2/M phases upon treatment with ATRA and BMS 493. All data are representative of 2-3 biological replicates. ns= non-significant, **** =p<.0001.

8 Discussion

8.1 Epithelial cell types and their organization at the gastroesophageal junction

The SCJ at GEJ formed by the esophagus' squamous epithelial cells and the stomach's columnar epithelium is a boundary of two functionally distinct epithelial cell types. The multilayered squamous epithelial cells of the esophagus provide a mechanical barrier, and mucous-secreting columnar epithelial cells of the stomach protect from abnormal external stimuli. At the same time, the location and architecture of GEJ make it vulnerable to persistent stress induced by mechanical stress or GERD, which in turn impact the distinct microenvironments underlying the GEJ epithelia. The persistence of damage-inducing stimuli causes an adaptive phenomenon in the GEJ region called BE to cope with abnormal triggers. During BE development, the GEJ region undergoes alterations in various processes, including wound healing, tissue regeneration, inflammation, and composition of the microbiome, which potentiate the initiation of cancer development. Therefore, it is essential to understand in-depth how normal homeostasis maintained the GEJ boundary, which forms the basis for deciphering mechanisms deregulated during disease development. Hence my first objective was to investigate the epithelial composition and mechanisms regulating the homeostasis of GEJ.

The GI tract is shown to develop from the endodermal cells called primitive gut tubes. The spatial expression of lineage-restricted transcription factors SOX2, PDX1, and CDX2 divides the endoderm into foregut, midgut, and hindgut regions (Sherwood, Chen, and Melton 2009). The early foregut region is lined by columnar-type primitive epithelial cells. The transcription factor SOX2 in the esophagus and GATA4 in the stomach establish the boundary between committed squamous and columnar epithelium (Sankoda et al. 2021, DeLaForest et al. 2021). Before the commitment of adult epithelial cells, the primitive epithelium lined by the esophagus and stomach has the characteristics of development into either squamous type or columnar type epithelial cells depending on the type of transcription factor it expresses. Using *Sox2* and *Gata4* knockout models, the existence of columnar type epithelium in the esophagus region and p63 expressing squamous epithelium in the stomach region of the respective model was demonstrated (Sankoda et al.

2021, DeLaForest et al. 2021). In line with this, in our data from mouse embryonic day E13.5, similar primitive epithelial cells could be observed. Further, these were observed to undergo differentiation into squamous epithelium from the anterior esophagus region. These cells express columnar marker KRT7/KRT8, as also observed by others (Wang et al. 2011).

The ability of GATA4-expressing cells to differentiate into p63-positive cells diminishes after mouse embryonic day E15.5 (Sankoda et al. 2021). This coincides with the inhibition of the BMP signaling pathway between E10.5 and E14.5 by stromal secretion of Noggin, which induces the stratification of epithelial cells in the esophagus (Rodriguez et al. 2010). A similar observation was also made in the p63 null mouse, where the absence of p63 results in a columnar type of epithelial cells. Since p63 null mice are nonviable after birth, the properties of committed esophageal epithelial cells from adult p63 null mice are unknown (Yang et al. 1999, Wang et al. 2011). Though the single-layered cells of the esophagus in p63 null mice did not show any differentiation into stomach epithelial cell types, instead, they undergo terminal differentiation (Yang et al. 1999). Using an in-vitro culture system, Yu et al. showed that the KRT8 expressing primitive columnar type epithelial cells could trans-differentiate into KRT14 expressing squamous epithelium through a direct conversion process without involving apoptosis or proliferation (Yu, Slack, and Tosh 2005). This suggests that the lineage commitment of primitive cells was defined by the timely expression of transcription factors and the microenvironmental signal from underlying stromal cells.

During embryonic development, I could see KRT7, and KRT8 expression persists in the primitive cells, which undergo trans-differentiation. The non-dividing primitive cells are repositioned above the newly proliferating basal squamous epithelial cells. In comparison with primitive cells, the basal squamous epithelial cells show decreased expression of KRT7 and KRT8 but an increased expression of p63 and KRT5. This suggests that in the early embryonic esophagus, epithelial cells undergo pseudo-stratification, where some basal cells acquire squamous lineage, and other primitive cells expressing KRT7 and KRT8 move above the basal cells (Yu et al. 2005). It indicates that not all primitive epithelial cells differentiate into squamous epithelial cells. Our data revealed a precise boundary between squamous and

columnar epithelial cells after the E-19 day creating GEJ. The KRT5 and p63 expressing squamous epithelial cells demarcated the border with the KRT8 expressing columnar epithelial cells of the stomach by E-19. However, on day E-19, the KRT7 and KRT8 expressing primitive columnar cells in the esophagus which aligned with the columnar epithelial cells in the stomach detach from the esophageal and forestomach region.

The process of single-layered epithelium undergoing glandular architecture in the stomach was evident from day E-16. Previously, transcription factor GATA4 and transcriptional co-activator FOG1/2 were shown to be involved in this process (Jacobsen et al. 2002). Further, no expression of p63 or KRT5 was seen in the primitive stomach epithelial cells. This suggests the lineage commitment of the epithelial cells meeting at the GEJ is regulated by a distinct external signal by the stromal cells underlying the respective epithelial cells. Our data revealed a nonoverlapping SCJ border in the adult human and mouse GEJ. KRT5, KRT8, and p63 expression by immunohistochemistry and smRNA-ISH analysis showed that squamous markers p63 and KRT5 were only expressed in the esophagus, and columnar-specific marker KRT8 was only expressed in the columnar stomach epithelial cells. Although KRT7 expression was found predominantly in the stomach epithelial cells, it is also expressed in the esophageal cells near SCJ. Interestingly, higher levels of KRT7 expression were found in the squamous epithelial cells and the first gland of stomach epithelial cells at the protein level. While at the mRNA level, higher expression was found in the stomach epithelial cells.

Previous studies have shown the presence of residual embryonic epithelial stem cells and specialized transitional basal epithelial cells at the GEJ (Wang et al. 2011), (Jiang et al. 2017). Wang et al. have shown that p63-KRT7+ expressing embryonic cells are only found as the discrete population in the adult SCJ. Authors show that these residual embryonic cells possess the property of stem cells and can replace the injured squamous epithelial cells with a columnar type of cell, creating BE metaplasia (Wang et al. 2011). Similarly, Jiang et al. showed the presence of KRT5+p63+KRT7+ non-keratinized basal transitional epithelial cells in the SCJ, distinct from the residual embryonic stem cells. The presence of such cells has been reported in other anatomical SCJ sites, such as the Ecto-Endo cervix and anorectum (Jiang

et al. 2017). Further, these transitional basal cells at GEJ attained expression of columnar metaplasia-related marker genes when *Cdx2* was ectopically expressed under the *Krt5* promotor (Jiang et al. 2017). Here I could see in the adult stage the presence of P63+KRT5+KRT7+ expressing committed squamous epithelial lineage cells present in the SCJ of GEJ mouse.

I could also find the presence of such cellular populations in other regions of the mouse esophagus by smRNA-ISH, suggesting that they are not restricted to SCJ. While in the case of normal human GEJ, no such population was found in our IHC study. Although I could find few KRT7-positive cells in the differentiated epithelial layers, the differentiation status of such cells excludes the possibility of the stem cell nature for these KRT7+ cells. A recent study of human GEJ showed the presence of p63+KRT5+KRT7+ expressing cells in the submucosal gland neck epithelial cells (Nowicki-Osuch et al. 2021). So, the squamous and columnar epithelial cells may be intercalated with each other in the ductal region of the submucosal glands. Thus, it may not be an accurate representation of SCJ transitional cells. Since mice are devoid of the submucosal gland, such a specially organized population is unlikely to be present in the mouse GEJ. And the expression of KRT7 is shown in the multilayered epithelial cells in the disease condition (Glickman et al. 2001). Since the expression of KRT7 is modulated by differentiation morphogens such as retinoids, and BMP4 (Amita et al. 2013, Törmä 2011, Feng et al. 2016) both squamous and columnar epithelial cells show increased levels of KRT7 in the BE, likely due to the altered niche signals and probably not due to trans-differentiation of squamous to columnar epithelium.

Our data in the adult mouse and human tissue with p63, KRT5, and KRT8 markers revealed a clear distinction between the squamous and columnar epithelium at the GEJ. This was further supported by the smRNA-ISH expression pattern of KRT5 and KRT8 in the mouse GEJ. These results suggest the presence of two distinct squamous and columnar epithelial-specific stem cells. Lineage tracing in the adult mouse using KRT8 or KRT5 marker genes enabled us to determine the uni-lineage nature of epithelial stem cells of GEJ. Further, our analysis did not reveal any epithelial cells in the GEJ region whose lineage was traced for both squamous and columnar marker proteins. The limitation of our lineage tracing approach was using a single marker gene in a

mouse. However, this can be overcome by lineage tracing by utilizing mice expressing both KRT5 and KRT8 lineage markers. Similar to our observation in GEJ, previously, the squamous epithelium of ectocervix and columnar epithelial cells of the endo-cervix that meet at the cervical SCJ were traced for KRT5 and KRT8 lineage, respectively (Chumduri et al. 2021).

Together, our data show that the squamous epithelium of the esophagus and columnar epithelium of the stomach originate from columnar precursor cells in the embryonic stage. In the adult, the committed epithelial cells at the GEJ arise from two distinct epithelial stem cells. Further, the expression of KRT7 doesn't define the epithelial cell types; rather, it represents the differentiation status of epithelial cells.

8.2 Regulation of gastroesophageal junction homeostasis

Regulation of stem cells depends on autocrine and paracrine signals from the surrounding niche, which includes differentiated cells, stromal cells, immune cells, and extracellular substrates (Scadden 2006). During development from the foregut region, esophagus and stomach epithelial cells are derived from different developmental signals (Zhang et al. 2021, Willet and Mills 2016). The epithelial-stromal interaction plays a crucial role in establishing epithelial homeostasis. Several signaling pathways, including Wnt, BMP, and Notch, play an important role in the regulation of stem cells in the stomach glands (Fischer and Sigal 2019, Todisco 2017, Demitrack et al. 2017). However, no detailed study has been performed on the regulation of esophageal stem cells and epithelial cells at the GEJ. In this study, I could show the existence of a gradient Wnt signaling microenvironment in the stromal region of the esophagus and stomach that regulates epithelial homeostasis. *Lgr5* was initially established as a stem cell marker in the intestinal epithelial cells and later in different tissues lined by columnar type of epithelial cells (Barker et al. 2007, Schindler, Watanabe, and Howell 2018). As shown by others, the gastrointestinal stem cell marker *Lgr5* is only expressed in the base of stomach glands (Barker et al. 2010), (Phesse and Sansom 2017). Here I found that *Lgr5* is not expressed in the esophagus epithelial cells indicating squamous epithelial cells possess different stem cells than stomach columnar epithelial cells. The *Axin2* component of the beta-catenin destruction complex and downstream target

gene of the Wnt pathway is known to be expressed in the basal cell region of the stomach gland (Barker et al. 2010). *Axin2*-positive cells were postulated as stem cells that drive tissue regeneration under a normal homeostatic state and during tissue injury (Sigal et al. 2017). *Axin2* was expressed in the same region where *Lgr5* expression was found in the stomach gland and sporadically in the muscularis mucosa layer of the esophagus and stomach regions. Since *Axin2* is a downstream target gene of canonical beta-catenin-mediated Wnt signaling, it suggests that canonical Wnt signaling is active in the stomach epithelial cells. This observation was supported by the lineage tracing of *Axin2* in the epithelial cells of stomach glands from the base and sporadically in the muscularis layer. This observation suggests that active Wnt activation is not involved in the stem cell homeostasis of esophageal epithelial cells.

Stromal cells lying below epithelial cells play an essential role in the regulation of homeostasis of epithelial cells by singling cross-talk through the secretion of various factors (Lei et al. 2014). These include agonistic and antagonistic factors of Wnt and BMP signaling pathways (Gregorieff et al. 2005, Kosinski et al. 2007). The R-spondins enhance the Wnt signaling molecule by binding to LGR receptors and inhibiting the function of Wnt inhibitory ubiquitinase RNF43/ZNRF3. The R-spondins are secreted by the stromal cells and act as Wnt activating paracrine signals for the stomach epithelial stem cells. Similar to other observations (Sigal et al. 2017), our data revealed that R-spondin 3 is expressed in the myofibroblast cells adjacent to the stomach glands, thus supporting the self-renewal of stem cells of the stomach epithelial cells.

Interestingly, these myofibroblast cells in the esophagus lie below the stromal cells. The spatial distribution of R-spondin 3 (*Rspo3*) by smRNA-ISH shows that *Rspo3* expressing myofibroblast cells are separated from esophageal basal squamous epithelial cells by the presence of stromal cells between them. Hence the R-spondin 3 secreted by the myofibroblast in the esophagus is inaccessible to the basal stem cells. Overall, the fibroblast cells in the esophagus and stomach provide a gradient of Wnt activation signals from lower to higher in the esophagus and stomach region, respectively.

The Wnt antagonist Dickkopf (DKK) related proteins are known to regulate canonical Wnt signaling by binding to Kremen1/2 and Wnt receptor LRP5/6 (Mao et al. 2001). The DKK family includes DKK1, DKK2, DKK3, and DKK4,

which regulate Wnt/beta-catenin signaling, except for DKK3, which regulates the TGF beta and FGF pathways (Pinho and Niehrs 2007). Analysis of micro-dissected intestinal tissue showed the enrichment of Wnt inhibitor molecules *Sfrp1*, *Sfrp2*, *Dkk2*, and *Dkk3* genes expression in the mesenchyme compartment compared to the epithelial compartment (Li et al. 2007). Our observation of higher *Dkk2* expression in the stromal cells below esophageal epithelial cells indicates a higher level of Wnt inhibitory microenvironment in the esophagus compared to the stomach. This is parallel to the observation in the ectocervix, where *Dkk2* is highly expressed in the stromal layer below the squamous stem cells. In vitamin A-deficient mice, a higher expression of *Dkk2* was found in the stromal region of the endocervix and the development of squamous metaplasia (Chumduri et al. 2021). This suggests that high Wnt signaling suppresses the proliferation of squamous stem cells by unknown mechanisms. In organotypic tissue culture, studies have shown the formation of invaginating papillae from the esophageal epithelial cells when cultured with esophagus tissue-derived stromal tissue but not with skin stromal tissue (Seery and Watt 2000). Therefore, the spatial establishment of stromal cells below the GEJ epithelial cells with Wnt activating and inhibitory factors define the squamocolumnar junction.

8.3 Esophagus and stomach 3D organoids mimic the *in vivo* niche factor requirement

By knowing the importance of differential Wnt signaling for GEJ epithelial homeostasis *in vivo*, the 3D organoid model was used to determine the significance of Wnt signaling factors for an *in-vitro* culture of primary epithelial cells. Both esophagus and stomach epithelial cells were grown into 3D organoids in basement membrane preparation Matrigel, which supports cell attachment, polarisation, and differentiation of cell types mimicking tissue of origin. This feature of Matrigel was achieved due to the presence of extracellular matrix proteins such as laminin, collagen IV, heparin sulfate proteoglycans, entactin, and other growth factors (Vukicevic et al. 1992, Hughes, Postovit, and Lajoie 2010). The growth-supporting factors FGF10, EGF, B27, and N2 supplements were essential for both epithelial organoid growth. Further, inhibition of the BMP and TGF-β pathway by Noggin and TGF-

β inhibitors were required for the development of both types of epithelial organoids.

The 3D organoid model for stomach epithelial cells was established previously for the mouse (Barker et al. 2010, Stange et al. 2013), and humans (Schlaermann et al. 2016). Wnt and R-spondin were indispensable for stomach epithelial organoid formation and long-term expansion. Our observation supported that the absence of WNT3A and RSPO1 in the media culture didn't support the generation of columnar organoids from the stomach epithelial cells. In parallel, the addition of IWP2, an inhibitory molecule of Wnt secretion by inhibiting porcupine (Porcn), a member of the membrane-bound O-acyltransferases (MBOAT) protein family (Wang et al. 2013), reduced the stomach organoid size and induced differentiation. The possible reason could be the requirement of Wnt ligands secreted by the epithelial cells (Flanagan et al. 2018), other than additionally provided in the culture media. The protein Casein kinase 1δ (CK1 δ) is involved in the activation of Wnt by beta-catenin stabilization through phosphorylation of Wnt co-receptor LRP5/6, disheveled (DVL), and destruction of complex component Axin (Davidson et al. 2005, Peters et al. 1999, Cheong et al. 2011). The study has shown that IWP2 can inhibit the CK1δ suggesting the reduction in the stomach organoid size is not only due to inhibition in the WNT secretion but also the inhibition of Wnt pathway signaling (García-Reyes et al. 2018).

In the case of mouse esophageal organoids, I found that the presence of Wnt-activating components was not essential for the initial growth of the organoids. Further, the long-term expansion ability of mouse esophageal organoids was decreased in the presence of Wnt-activating components. Interestingly, inhibition of Wnt secretion by IWP2 treatment didn't change the growth of esophageal organoids. This observation was interesting since the organoids from other tissues, such as the stomach, intestine, colon, and endocervix, require Wnt signals for growth and propagation. This difference could be attributed to the fact that esophageal epithelial cells are squamous type, similar to the ectocervix, anus, and skin, and require different signals for stem cell maintenance and self-renewal. It was shown that the Wnt signal is dispensable for the growth of ectocervical organoids (Chumduri et al. 2021).

My data show similar mechanisms that might be present in the esophagus epithelial stem cells.

Interestingly, none of the four biological replicates of human esophageal stem cells grew into organoids in the presence of Wnt activation components. This observation was similar to the previous report that Wnt-containing media optimized for intestinal organoids didn't support human esophageal organoid growth (Sato et al. 2011). The keratinocyte media (KSFMC) supported human esophageal organoid growth until a limited number of passages (Kasagi et al. 2018). Our observation corroborated with the previous result, where human squamous ectocervical epithelial cells could not grow in the presence of Wnt-activating media components (Chumduri et al. 2021).

A previous study *in vitro* has shown that inhibition of canonical Wnt signaling in human pluripotent stem cells was required to induce dorsal foregut formation and subsequent generation of esophageal organoids (Trisno et al. 2018). Further, in a retinoic acid-deficient mouse model, it was shown that the development of squamous metaplasia in columnar epithelial lined endocervix was supported by the high expression of Wnt inhibitor *Dkk2* in the stromal cells below the metaplastic tissue (Chumduri et al. 2021). However, esophageal organoids can only be passaged up to 4 to 5 passages indicating the additional requirement of optimization in the growth media components. The addition of hydrocortisone, similar to ectocervical organoid culture (Chumduri et al. 2021), increased cell numbers but not the passaging ability of esophagus organoids.

I also showed that squamous organoids do not express *Lgr5*, the receptor for Wnt activating protein R-spondin (de Lau et al. 2014), downstream target gene *Axin2,* and hence no further activation of canonical Wnt compared to the stomach organoids. Several studies have shown the high expression of columnar epithelial-related genes, including *Krt7*, in the esophagus region of BE epithelium (Korbut et al. 2020, Glickman et al. 2001, van Baal et al. 2005) and thus propose that the BE epithelium is derived via trans-differentiation. In the lineage-trace epithelial organoid model, I could show that the presence of Wnt doesn't induce trans-differentiation of squamous to columnar epithelium. Taken together, our model of organoid generation from the esophagus and stomach recapitulated the tissue epithelial stem cell niche and can be used to study the disease development at the GEJ.

8.4 Subcellular composition of the esophagus and stomach organoid epithelial cells and underlying signaling

To better understand the metaplasia and disease development in the GEJ epithelial cells, it is essential to analyze the epithelial cellular subtypes and the regulation of their differentiation. This was investigated using bulk transcriptomic and scRNA-seq analysis of esophagus and stomach organoids. The bulk transcriptomic analysis revealed the structural and functional difference between esophageal squamous and stomach columnar epithelial organoids. Squamous epithelial cells are enriched for genes related to epithelial development and differentiation and stratification to provide mechanical barrier and strength to the esophagus. In comparison, stomach epithelial cells were enriched for the fatty acid metabolic process and regulation of ion transport, suggesting a role in the secretion of hormones and the digestion process (Ito et al. 2021, Yuan et al. 2020). Thus, the data indicates that our organoid model retains the functional characteristics of the esophagus and stomach epithelium, similar to the *in vivo* condition.

scRNA-seq of stomach organoid epithelial cells revealed the subcellular composition within the epithelium, including stem cells and differentiated cell types found in the stomach gland (Choi et al. 2014). The stem cell markers *Lgr5, Aqp5,* and *Axin2* (Barker et al. 2010, Tan et al. 2020, Sigal et al. 2017) expressing cells were detected at the single-cell level. Further, neck region-specific chief cells, parietal cells, and enteroendocrine cell marker-expressing cells were also found at the single-cell level. This indicates that stomach organoids retain functional roles of the cells, such as secretion of gastric acid, digestion and growth hormones, and mucous (Arin et al. 2017, Gribble and Reimann 2019). Although stem cells are present in the base of glands of the stomach, the proliferating cells are usually present in the isthmus region of the stomach gland, which is enriched for the cells expressing proliferation markers including *Mki67, Top2a, Stmn1* (Han et al. 2019). In our scRNA-seq analysis, the cells expressing markers related to the base, neck, and isthmus regions were clustered together. However, the terminally differentiated pit cells were found in a different cluster showing the transcriptional difference between early and late lineage cells. Overall scRNA-seq analysis shows that stomach

organoids could retain stemness and differentiate into other cell types of the stomach gland during long-term expansion.

Owing to the presence of distinct epithelial layers in the esophagus, scRNA-seq revealed different sub-cellular clusters based on the differentiation status of epithelial cells (Yu, Slack, and Tosh 2005). The basal stem cell (Sq1), proliferative (Sq2A, Sq2B), and differentiated (Sq3A, Sq3B) layers were found in our analysis. The mouse has single-layered basal epithelial cells with proliferative and non-proliferative stem cells. Whereas in humans, most of the proliferative cells exist above the basal stem cell layer (Jiang et al. 2015, Barbera et al. 2015). I found the expression of stem cell-related protein gene *Trp63* and proliferation marker *Mki67* in Sq1 and Sq2 cell clusters of mouse esophagus organoids. Two kinds of theories exist regarding stem cells in the esophagus, i.e., homogenous basal cells and heterogeneous basal cell populations (Zhang et al. 2021). The mathematical model was shown by using a transgenic label-retaining cell (LRC) assay that in the absence of slow-cycling basal cells, the basal cells divide equally into proliferative and differentiating daughter cells indicating homogenous basal stem cells (Doupé et al. 2012). While several studies postulated different markers for the esophageal stem cells based on the label retention property of quiescent stem cells and lineage tracing. Among them, *Itga6*^{hi} *CD71*^{lo} (Croagh et al. 2007), *Sox2*$^{+}$*Itgb4*^{hi}*Itga6*^{hi}*CD73*^{hi} (DeWard et al. 2014), *Krt15*+ basal cells (Giroux et al. 2017), *CD34*^{hi} (Kalabis et al. 2008), *p75*^{NTR} (Okumura et al. 2003), markers represent the heterogenous population of basal stem cells. However, a reliable stem cell marker for esophageal epithelium is not currently available due to the altered cell behavior and proliferation to wounding response during *in vivo* and *in vitro* manipulation (Barbera et al. 2015). Since the organoid model resembles the *in vivo* tissue architecture, the scRNA-seq analysis will enable us to determine the stem cell composition of esophageal squamous organoids. The stem cell populations (Sq1) are enriched for the *TRP63*, *Col7a1,* a type VII collagen fibril expressed in the basal cells for anchoring to the basement membrane (Regauer et al. 1990), *Krt15, Krt17* marker genes. Recent studies employing scRNA-seq analysis of human esophagus epithelial cells have shown *Col17a1*^{high} *Krt15*^{high} population represents the quiescent stem cell/progenitor cell population. However, our scRNA-seq analysis and immunochemistry found

Krt17^{high} *Jun*^{low} cells representing the stem cell region in the esophageal tissue and organoids. Even though *Krt17* expression is low in normal conditions, it is known to be activated during wound repair (Mazzalupo et al. 2003, Kim, Wong, and Coulombe 2006) and highly up-regulated in the carcinoma of the cervix (Escobar-Hoyos et al. 2014), esophagus (Liu et al. 2020) and breast (van de Rijn et al. 2002) indicating potential stem cell role of *Krt17* expressing cells. Recently it was shown that *Krt17* expressing basal cells in the anorectal junction plays a role in normal homeostasis. Similarly, *c-Jun*, a component of the AP-1 transcription factor regulating cell growth and differentiation in response to growth factors (Shaulian and Karin 2002), is expressed in the proliferative compartment (Sq2a, Sq2b) but not in the stem cell compartment. This suggests the presence of gradient distribution of stem cells and differentiating epithelial cells create stratification of esophageal cells in the organoids and tissue. This is also supported by our observation of the increased expression of the *Notch1* receptor, an inducer of differentiation (Ohashi et al. 2010), from the stem cell compartment (Sq1) to the proliferation cell compartment (Sq2A).

Wnt pathways have been shown as an important regulator in the development of the esophagus and lung, where the former requires the inactivation of the Wnt pathway while later requires *Wnt2/2b* mediated signaling (Woo et al. 2011), (Goss et al. 2009). The canonical and non-canonical WNT signals are crucial pathways in stomach epithelial cell homeostasis and cancer (Flanagan et al. 2018). While the role of the Wnt pathway is not much explored in the adult esophagus, the expression of Wnt pathway genes in the human esophagus was reported (Ali et al. 2009). In our transcriptomic and scRNA-seq analysis, I observed overexpression of canonical Wnt and non-canonical Wnt/Ca^{2+} pathway genes in the stomach epithelial cells compared to the esophagus epithelial cells. While non-canonical Wnt/PCP pathway genes were over-expressed in the esophagus epithelial cells. This supports the canonical WNT3a requirement for stomach organoid generation and higher *Dkk2* (inhibitor of canonical WNT signaling) expression in the stromal cells below the esophageal basal epithelial cells. Since I couldn't observe the higher expression of canonical Wnt target genes, *Lgr5* and *Axin2*, I theorized that only non-canonical Wnt/PCP pathways regulated in the esophagus induce

differentiation and stratification of squamous epithelial cells. The stromal RSPO3 binds LGR5 and maintains stemness in the stomach epithelial cells (Sigal et al. 2017). However, *Rspo3* expression is far from basal epithelial cells in the esophagus tissue; diffused *Rspo3* might activate Wnt/PCP pathway rather than the canonical Wnt Pathway (Ohkawara, Glinka, and Niehrs 2011). Overall, our analysis of the tissue and organoid model highlights the differential requirement of canonical and non-canonical Wnt signaling for the esophagus and stomach epithelial homeostasis.

8.5 Retinoic acid signaling in the gastroesophageal epithelial cells

Our transcriptomic analysis revealed enrichment of RA pathway genes in the stomach compared to the esophagus. Previously, ATRA treatment was shown to induce the proliferation of gastric epithelial progenitors, reduce pit cells, and increase chief cells (Karam et al. 2005). Further, *Aldh1a1* (*Raldh1*) is expressed mainly in the proliferating and differentiating cells in the developing esophagus and stomach (Niederreither et al. 2002). Here I observed higher *Aldh1a1* expression in the adult stomach than in the esophagus. Moreover, human gastric epithelial cells can synthesize RA and regulate gastric immune interaction (Bimczok et al. 2015). It suggests that RA might play a role in the homeostasis of gastric epithelial cells and protection from infection by autocrine RA biosynthesis. In the case of the esophagus, RA is necessary during the developmental process for the differentiation of the foregut from the endoderm (Wang et al. 2006).

Further, RARg is required for the differentiation of esophageal epithelial cells from foregut-derived hiPSC (Koterazawa et al. 2020). I found a higher expression of *Rarg* in the esophagus, indicating its functional role in stratification. Since I observed a relatively smaller number of esophageal epithelial cells expressing RA biosynthesis pathway genes, it implies a low RA activity requirement for normal esophagus epithelial homeostasis. This is further confirmed by *in vitro* treatment of organoids with ATRA, where higher concentrations reduced organoid size and longevity. In contrast, RA inhibition reduces the stomach organoid size, while in the esophagus, RA inhibition

increases organoid size and proliferation, suggesting a distinct role for RA in these two epithelial cell types. This is similar to the other observation where the absence of RA biosynthesis enzyme ALDH6 induces cell proliferation and tumorigenesis in the breast cancer cell line (Rexer, Zheng, and Ong 2001). It was shown that RA inhibition increased lung epithelial organoids through YAP and FGF pathway signaling in the fibroblast-organoid culture model (Ng-Blichfeldt et al. 2018). Since our organoids were grown without fibroblasts, other pathways related to cell proliferation might have been induced. GO term analysis of esophageal cells also confirmed this observation where the epidermal cell developmental pathway was enriched in the absence of RA.

8.6 RA signaling in esophagus epithelia

In the mouse esophagus, highly differentiated squamous epithelial cells in the outermost layer are present as enucleated and undergo cornification and act as a physical barrier to incoming food. I observed that esophageal organoids treated with ATRA are devoid of cornified layers. Further transcriptomic data revealed reduced expression of esophagus epithelial differentiation complex (EDC) genes (Rothnagel et al. 1994, Mischke 1998), including involucrin, loricrin, small proline-rich protein family (SPRRs), etc., upon ATRA treatment. However, RA inhibition increased epithelial proliferation and cornification. This is similar to observations in the squamous epithelial cells of the oral and esophageal mucosa, where loricrin expression decreased, and *Cldn1* and *KRT4* expression increased in response to RA (Miyazono et al. 2020). This effect was reversed by RA inhibition, suggesting an optimum concentration of RA is required for epidermal morphogenesis (Asselineau et al. 1989). Interestingly, I observed the induction of cytokeratins such as *Krt7, Krt18, Krt19, and Krt20* upon ATRA treatment in the esophageal organoids. During the initiation of BE, the multilayered epithelium (MLE) of squamous and columnar cells precedes the metaplasia (Shields et al. 1993). Our results could be correlated to the epithelial intermediate phenotypic changes during the initiation of BE, where the presence of MLE expresses both squamous and columnar marker genes (Glickman et al. 2001). However, in skin keratinocytes, a similar increased level of other cytokeratins was reported, which is attributed to the presence of

retinoic acid response element (RARE) under the promotor region of cytokeratin genes or other RARE independent mechanisms (Törmä 2011), suggesting abrupt induction of cytokeratin by pathology-associated signals or increased RA activity in the early stages of BE (Chang et al. 2008). Intriguingly, other BE-related genes (*Id2, Bmp2, Krt18, Sox9, Agr2, Krt8*) were up-regulated in the human BE tissues (Hyland et al. 2014) as well as in our ATRA-treated esophagus organoids. BE epithelia was hypothesized to arise by trans-differentiation of the esophagus squamous epithelial cells during BE development, based on the increased expression of columnar epithelia-related genes (Clemons et al. 2012, Vega et al. 2014, Minacapelli et al. 2017, Milano et al. 2007, D. H. Wang et al. 2010, Wang et al. 2014, Kong et al. 2011, Colleypriest et al. 2017). In contrast, in our invitro organoid lineage tracing after treatment with ATRA, columnar epithelial growth media didn't trans-differentiate squamous epithelium to columnar epithelium. However, I could see increased expression of columnar/BE-related *Krt7* upon ATRA treatment in the differentiated layers of squamous epithelium. Overall, based on *in vivo* epithelial lineage tracing and IHC analysis, our data suggests that squamous and columnar epithelial cells are lineage-committed. Further, our data show that the squamous epithelial cells do not trans-differentiate to columnar epithelial cells during BE initiation. Instead, BE initiation occurs in a columnar type of epithelial cells either derived from the stomach cardia or submucosal gland of the esophagus as previously proposed by other groups as well (Nowicki-Osuch et al. 2021, Lee et al. 2017, Quante et al. 2012, O'Neil, Christine P. Petersen, et al. 2017, Leedham et al. 2008, Owen et al. 2018).

Interestingly, RA signaling inhibition increased the expression of p63 and cornification-related genes in esophageal organoids. Western blot analysis revealed increased expression of the lower molecular weight isoform of p63 (ΔNp63, without an amino-terminal transactivation domain) compared to the higher molecular weight p63 (TAP63, with an amino-terminal transactivation domain) (Yang et al. 1998). ΔNp63 expressed in the basal cells accelerates proliferation by binding to p53 binding sites in the p21 and 14-3-3σ promoters (Westfall et al. 2003). TAP63 is known to induce stratification and cornification (Koster et al. 2004) partly through the regulation of Notch signaling (Srivastava et al. 2018). However, ATRA treatment retained the same level of

TAP63 expression but reduced ΔNp63 expression. Similar down-regulation of p63 by ATRA was reported in the nasopharyngeal epithelial cells, suggesting a role of the RA pathway in regulating p63 expression and squamous epithelial stemness and homeostasis (Yip and Tsao 2008). However, I could see the expression of p63 in the basal and parabasal epithelial cell layer in the ATRA-treated organoids. This might indicate that RA treatment induces early differentiation of esophagus epithelial cells or promotes the slow recycling of quiescent epithelial cells (Dunaway et al. 2019).

Interestingly bulk transcriptomic data revealed the up-regulation of quiescence-related pathway genes in the presence of RA, while RA inhibition enriched the genes related to cell proliferation. One of the up-regulated pathways, TGF beta signaling, is shown to induce quiescence in the keratinocytes, intestinal crypt stem cells, and cancer cells (Booth et al. 2000, Lin and Yang 2013, Reiss and Sartorelli 1987, Prunier et al. 2019). Similarly, dormant hematopoietic stem cells have up-regulated expression of retinoic acid pathway genes, low levels of *Myc,* and low levels of essential biosynthetic process genes (Cabezas-Wallscheid et al. 2017). Further, our cell cycle analysis revealed an increased percentage of cells in the G0 state in high RA conditions. Our scRNA-seq analysis also revealed that ATRA-treated esophageal cells formed distinct clusters and higher aggregate expression of quiescence-related genes in the basal and parabasal cell populations. Moreover, removal of RA inhibition could revert the quiescence of esophageal epithelial cells suggesting that ATRA treatment didn't induce terminal differentiation or senescence of epithelial cells, rather ATRA removal allowed normal epithelial cell proliferation and organoid formation.

8.7 RA signaling in the stomach

During BE progression, metaplastic epithelial cells in the GEJ attain intestinal-type epithelial features such as the presence of MUC2-producing goblet cells, Paneth cells, enterocytes, and enteroendocrine cells (Schreiber, Apstein, and Hermos 1978), (Sbarbati et al. 2002), (Wong et al. 2000). Depending on the metaplastic stage, BE epithelial cells express *Cdx2, Villin, Tff3, and Muc2,* which are usually expressed in the intestinal epithelial cells (McDonald, Graham, et al. 2015). Interestingly our transcriptomic and scRNA-seq data

from RA-inhibited stomach organoid, epithelial cells showed enriched expression of genes related to the intestinal type epithelial cells like a goblet and enteroendocrine cells. Since I found higher regulation of the RA pathway in the stomach compared to the esophagus, I theorized that RA deficiency might induce stomach epithelial cells to attain intestinal-type epithelial phenotype. Although I could not detect goblet or enteroendocrine epithelial cells by immunofluorescence in the organoids treated with RA inhibitor, the gene expression could indicate early-stage lineage differentiation. This observation implicates that RA depletion leads to the emergence of the intestinal type of epithelial cells in the metaplastic GEJ. Studies have shown decreased expression of retinoic acid receptors *Rara* and *Rarb* during the progression from normal to intestinal metaplasia (IM) and cancer in gastric cells (Jiang et al. 1999).

Similarly, *Rarb* expression decreased in oral, head and neck, and lung cancers(Lotan 1997). Further, increased RA activity in the early stage of BE tissue and decreased RA activity in the EAC were observed (Chang et al. 2008). This was related to the high expression of RA catabolizing enzyme *Cyp26a1*, which causes intra-cellular RA depletion and proliferation of epithelial cells. The increased expression of *Cyp26a1* is partly due to canonical Wnt pathway activation (Shelton et al. 2006, Clément, Jablons, and Benhattar 2007). This is further corroborated by a study that found the development of IM at the late stage of BE increased the risk of EAC development due to an increase in Wnt pathway signaling (Chaves et al. 2002, González et al. 1997). This implies that local reduction in the level of RA modulates metaplastic stomach epithelial cells to differentiate into intestinal epithelial cell lineages. It was demonstrated that depletion of *Rara* in the intestinal epithelial cells increased the goblet cell number and paneth cells (Jijon et al. 2018). A recent study in colorectal cancer organoids also showed that RAR inhibition increased paneth cell and enteroendocrine lineage while RXR inhibition increased the number of goblet cells (Wester et al. 2021). Even though stomach epithelial cells are not genetically similar to intestine epithelial cells, the RA could similarly regulate many genes. Our observation also indicates that alteration in lineage-defining proteins such as CDX2 is necessary for differentiating stomach metaplastic epithelial cells to specialized intestinal cells, which usually takes 2 to 10 years

in BE individuals (Phillips, Frierson, and Moskaluk 2003, Seno et al. 2002, Chaves et al. 2002, O'Riordan et al. 2004).

Overall results indicate that RA activity is a gradient in the GEJ from a lower level in the esophagus to a higher level in the stomach epithelial cells. This also implies that stromal cells could regulate this RA gradient in the GEJ, as observed in the Müllerian duct during the development of the uterus and vagina (Nakajima et al. 2019). During GERD, erosion of squamous epithelial cells begins the epithelial wound repair by adjacent stomach epithelial cells by the creeping movement into the esophagus. Further, the local low RA environment of the esophagus and/or mutation in the RA regulating enzymes induces metaplastic differentiation of epithelial cells into intestinal cell types.

9 Concluding remarks

In conclusion, in this study, I have shown that two distinct committed epithelial stem cells give rise to postnatal squamous epithelia of the esophagus and columnar epithelia of the stomach, which meet at the GEJ. I elucidated the differences in these two epithelial stem cell lineages by employing organoid models, *in vitro* lineage tracing, immunohistochemistry, and sc-RNA seq. The Wnt signals from the underlying stromal compartment are found to be critical in esophagus squamous and stomach columnar epithelial stem cell homeostasis. Using organoids cultures, I demonstrated that these two epithelial cells are maintained by opposing Wnt signaling modulating factors with Wnt deficient environment regulating esophagus squamous epithelial stem cells, while a Wnt proficient environment regulating the stomach columnar epithelial stem cells. Interestingly scRNA-seq analysis revealed that stem cells of columnar epithelium of GEJ express canonical Wnt pathway genes and differentiated cells express Ca^{2+}dependent non-canonical Wnt pathway genes. Distinctly oesophageal squamous epithelium subpopulation express structurally associated noncanonical Wnt pathway genes. Further, I have shown the differential regulation of RA signaling in these two epithelial cells employing organoid models and sc-RNA sequencing. This comprehensive study provides an understanding of mechanisms regulating GEJ epithelial homeostasis in healthy tissue, which offers new insights to study the development of BE.

Thus far, most studies proposed either trans-differentiation of squamous epithelium or the specialized type of epithelial cells present in the SCJ as the cells of origin for BE development. In my research, I found that RA treatment of squamous epithelia although induces the expression of a few gene markers usually related to the columnar epithelial cells, RA didn’t induce trans-differentiation of squamous epithelial lineage to the columnar epithelial lineage. This observation clarifies long-standing ambiguity about the role of RA in transdifferentiating squamous to columnar type epithelia at GEJ.

Instead, I found for the first time that RA plays a role in the induction of dormancy or drives stem cells toward specific differentiated cell types within the two epithelial lineages. Higher RA induces a quiescent phenotype in the squamous epithelium while inhibition of RA induces increased squamous

epithelial proliferation. While in the stomach, columnar epithelial cells, RA deficiency-induced differentiation towards the intestinal epithelial cells by inducing expression of genes such as CDX2. This study provides a novel understanding of the role of RA in developing intestinal-type metaplasia during BE progression. Nevertheless, spatial Wnt and RA regulation and changes occurring during the transition from normal human epithelial cells at the SCJ to BE needs further investigation.

10 Supplement

10.1 List of figures

10.2 List of tables

10.3 Abbreviations

2D	2 dimension
3D	Three dimension
7 AAD	7-amino-actinomycin D
ADF	advanced DMEM/F12
ALDH	Aldehyde Dehydrogenase
AMP	Amplification probe
Anxa1	Annexin A1
APS	ammonium persulfate
Aqp5	Aquaporin 5
Atf3	Activating Transcription Factor 3
Atp4a	ATPase H+/K+ Transporting Subunit Alpha
ATRA	all-trans-retinoic acid
Axin2	axis inhibition protein 2
BD	Becton Dickinson
BE	Barrett's esophagus
Bmp2	Bone Morphogenetic Protein 2
BMS 493	Pan-retinoic Acid Receptor (pan-RAR) Inverse Agonist.
bp	base pair
BP	Biological process
BSA	Bovine serum albumin
BTG2	BTG Anti-Proliferation Factor 2
C57bl/6	C57 black 6
cald1	Caldesmon 1
CamK	Calcium/Calmodulin Dependent Protein Kinase
Cav1	Caveolin 1
CDH1	Cadherin 1
cDNA	complementary DNA
CDX2	Caudal Type Homeobox 2
Co	Columnar
Col7a1	Collagen Type VII Alpha 1 Chain
Cre	Cyclization recombinase
Cryo-SFM	Cryo serum-free medium
Cstb	Cystatin B
Ctnnb1	Catenin Beta 1
Cyp26b1	Cytochrome P450 Family 26 Subfamily B Member 1
Daam1	Disheveled Associated Activator Of Morphogenesis 1
DapB	dihydrodipicolinate reductase
DAPI	4’,6-diamidino-2-phenylindole
DEG	differentially expressed genes
Dkk2	Dickkopf-related protein 2
DMEM	Dulbecco's Modified Eagle Medium
DMSO	Dimethyl Sulfoxide
DNA	Deoxyribonucleic acid
DNase	deoxyribonuclease
dNTPs	Deoxynucleotide Triphosphates

E	Embryonic
ECL	enhanced chemiluminescence
EDC	epidermal differentiation complex
EGF	Epidermal growth factor
Elf5	E74 Like ETS Transcription Factor 5
Ep	Epithelia
ER	Estrogen receptor
ES	Esophagus
Eso	Esophagus
FACS	Fluorescence-Activated Cell Sorting
Fau	FBR-MuSV-Associated Ubiquitously Expressed
FC	Fold change
FCS	fetal calf serum
FDR	false discovery rate
FGF10	Fibroblast growth factor 10
FGSEA	Fast Gene Set Enrichment Analysis
Fig	Figure
FITC	Fluorescein isothiocyanate
FSC	forward scatter
FW	Forward
GEJ	Gastroesophageal junction
GEMs	Gel-Bead-In-EMulsions
GERD	Gastroesophageal reflux disease
Ghrl	Ghrelin
GKN	Gastrokine
GO	Gene ontology
GSEA	Gene set enrichment analysis
H2O	Water
HBBS	Hank’s balanced salt solution
HCl	hydrogen chloride
HEPES	(4-(2-hydroxyethyl)-1-piperazineethanesulfonic acid)
HPA	Human Protein Atlas
HRP	horseradish peroxidase
Id2	Inhibitor Of DNA Binding 2
IF	Immunofluorescence
ISH	In situ hybridization
IWP2	Inhibitor of Wnt Production-2
Jun	Jun Proto-Oncogene, AP-1 Transcription Factor Subunit
KCl	Potassium chloride
KH2PO4	potassium dihydrogenphosphate
KRT	Cytokeratin
KSFMC	Complete Keratinocyte Serum-Free Medium
Lgr5	Leucine-rich repeat-containing G-protein coupled receptor 5
LRP	LDL Receptor-Related Protein
MgCl2	Magnesium chloride
Mki67	Marker Of Proliferation Ki-67
Mm	Mus musculus
MSigDB	Molecular Signature Database

Muc6	Mucin 6
My	Myofibroblast
Na2HPO4	Disodium hydrogen phosphate
NaCl	Sodium chloride
NaCl	N-acetyl-L-cysteine
Ncoa1	Nuclear Receptor Coactivator 1
Neurog3	Neurogenin 3
Nfatc	Nuclear Factor Of Activated T Cells
NIC	Nicotinamide mononucleotide
Nts	Neurotensin
OCT	Optimal cutting temperature
ORA	over-representation analysis
P	Passage
PAS	periodic acid–Schiff
PBS	phosphate-buffered saline
PCA	Principal component analysis
PCNA	Proliferating Cell Nuclear Antigen
PCP	planar cell polarity
PCR	polymerase chain reaction
Pdx1	Pancreatic And Duodenal Homeobox 1
PFA	Paraformaldehyde
Pgc	Progastricsin
Ppib	Peptidyl-prolyl cis-trans isomerase B
PVDF	Polyvinylidene fluoride
qRT-PCR	Quantitative Reverse Transcription polymerase chain reaction
RA	Retinoic acid
Rac1	Rac Family Small GTPase 1
RAR	retinoic acid receptor
Rarb	Retinoic Acid Receptor Beta
RDH	Retinol Dehydrogenase
Rhov	Ras Homolog Family Member V
RNA	Ribonucleic acid
RNase	Ribonuclease
ROCK	rho-associated protein kinase
Rosa26	Reverse Oriented Splice Acceptor, Clone 26
RSPO	R-spondin
RT	Room temperature
Runx1	RUNX Family Transcription Factor 1
RV	Reverse
SCJ	Squamo-columnar Junction
Scrib	Scribble Planar Cell Polarity Protein
scRNA-seq	Single-cell RNA sequence
Sct	Secretin
SDS	Sodium dodecyl sulfate
SDS-PAGE	Sodium dodecyl sulfate polyacrylamide gel electrophoresis
SERPINB5	Serpin Family B Member 5
smRNA-ISH	single-molecule Ribonucleic acid in situ hybridization
Sox2	SRY-Box Transcription Factor 2

Sox4	SRY-Box Transcription Factor 4
Spink5	Serine Peptidase Inhibitor Kazal Type 5
sprr3	Small Proline Rich Protein 3
Sq	Squamous
SSC	side scatter
SSC	saline-sodium citrate
St	Stomach
Stmn1	Stathmin 1
Sto	Stomach
STRA6	Stimulated By Retinoic Acid Gene 6 Homolog
TBS	Tris-buffered saline
TCF	Transcription Factor
tdTomato	Tandem dimer Tomato
TEMED	Tetramethylethylenediamine
Tff	Trefoil Factor
Tfgb3	Transforming growth factor, beta 3
Tgmn1	Transglutaminase 1
Timm9	Translocase Of Inner Mitochondrial Membrane 9
Top2a	DNA Topoisomerase II Alpha
Trp63	Transformation-Related Protein 63
UMAP	uniform manifold approximation and projection
UV	ultraviolet
Vangl1	Vang-Like Protein 1
W/R	WNT3A/RSPO1
WB	Western blot
WNT3A	Wingless-Type MMTV Integration Site Family, Member 3A
Ybx1	Y-Box Binding Protein 1
α-SMA	microfilament α-smooth muscle actin
ΔΔCt	Delta Delta threshold cycle
w/v	Weight/Volume
v/v	Volume/Volume

Units

Gy	Gray
%	Percent
°C	degree Celsius
µg	microgram (s)
µL	microlitre (s)
µM	micro molar
µm	micrometer (s)
cm	centimeter (s)
cm2	centimeter square
g	gram (s)
g/L	gram/litre
hr	hour (s)
kDa	kilodalton

L	liter (s)
M	molar
mA	milliampere (s)
mg	milligram (s)
min	minute (s)
mL	milliliter (s)
mM	milli molar
mm	millimeter (s)
ng	nanogram (s)
nM	nanomolar
nm	nanometer (s)
pH	potential of hydrogen
rpm	rotation per minute
sec	Second (s)
V	volt
Xg	relative centrifugal force

10.4 Publication list

10.4.1 In Preparation

1. Spatial organisation and homeostasis of epithelial lineages at the gastroesophageal junction is regulated by the divergent Wnt mucosal microenvironment.
2. Retinoic acid-mediated regulation of gastro-esophageal epithelial cells and development of Barrett's esophagus.

10.4.2 Publications during doctoral study

1. Koster, S., Gurumurthy, R. K., **Kumar, N**., Prakash, P. G., Dhanraj, J., Bayer, S., Berger, H., Kurian, S. M., Drabkina, M., Mollenkopf, H.-J., Goosmann, C., Brinkmann, V., Nagel, Z., Mangler, M., Meyer, T. F., & Chumduri, C. (2022). Modelling Chlamydia and HPV co-infection in patient-derived ectocervix organoids reveals distinct cellular reprogramming. Nature Communications, 13(1), 1030. https://doi.org/10.1038/s41467-022-28569-1
2. Gurumurthy, R. K., Koster, S., **Kumar, N**., Meyer, T. F., & Chumduri, C. (2022). Patient-derived and mouse endo-ectocervical organoid generation, genetic manipulation and applications to model infection. Nature Protocols, 17(7), 16581690. https://doi.org/10.1038/s41596-022-00695-6
3. Gurumurthy, R. K., **Kumar, N**., & Chumduri, C. (2021). Optimized protocol for isolation of high-quality single cells from the female mouse reproductive tract tissues for single-cell RNA sequencing. STAR Protocols, 2(4), 100970. https://doi.org/10.1016/j.xpro.2021.100970
4. Gurumurthy, R. K., **Kumar, N**., & Chumduri, C. (2021). Spatial analysis of organ-wide RNA, protein expression, and lineage tracing in the female mouse reproductive tract. STAR Protocols, 2(4), 100969. https://doi.org/10.1016/j.xpro.2021.100969
5. **Kumar, N**., Gurumurthy, R. K., Prakash, P. G., Kurian, S. M., Wentland, C., Brinkmann, V., Mollenkopf, H.-J., Krammer, T., Toussaint, C., Saliba, A.-E., Biebl, M., Juergensen, C., Wiedenmann, B., Meyer, T. F., & Chumduri, C. (2021). Spatial organisation and homeostasis of epithelial

lineages at the gastroesophageal junction is regulated by the divergent Wnt mucosal microenvironment. BioRxiv, 2021.08.05.455222. https://doi.org/10.1101/2021.08.05.455222

6. Chumduri, C., Gurumurthy, R. K., Berger, H., Dietrich, O., **Kumar, N**., Koster, S., Brinkmann, V., Hoffmann, K., Drabkina, M., Arampatzi, P., Son, D., Klemm, U., Mollenkopf, H.-J., Herbst, H., Mangler, M., Vogel, J., Saliba, A.-E., & Meyer, T. F. (2021). Opposing Wnt signals regulate cervical squamocolumnar homeostasis and emergence of metaplasia. Nature Cell Biology, 23(2), 184–197. https://doi.org/10.1038/s41556-020-00619-0
7. Sepe, L. P., Hartl, K., Iftekhar, A., Berger, H., **Kumar, N**., Goosmann, C., Chopra, S., Schmidt, S. C., Gurumurthy, R. K., Meyer, T. F., & Boccellato, F. (2020). Genotoxic Effect of Salmonella Paratyphi A Infection on Human Primary Gallbladder Cells. MBio, 11(5). https://doi.org/10.1128/mBio.01911-20

10.5 Affidavit

Affidavit

I hereby confirm that my thesis entitled "Mechanistic regulation of gastroesophageal junction and role of retinoic acid in the development of Barrett's esophagus" is the result of my own work. I did not receive any help or support from commercial consultants. All sources and/or materials applied are listed and specified in the thesis.

Furthermore, I confirm that this thesis has not yet been submitted as part of another examination process neither in identical nor in similar form.

Place, Date Signature

Eidesstattliche Erklärung

Hiermit erkläre ich an Eides statt, die Dissertation "Mechanistische Regulierung des gastroösophagealen Übergangs und die Rolle der Retinsäure bei der Entwicklung des Barrett-Ösophagus" eigenständig, d.h. insbesondere selbständig und ohne Hilfe eines kommerziellen Promotionsberaters, angefertigt und keine anderen als die von mir angegebenen Quellen und Hilfsmittel verwendet zu haben. Ich erkläre außerdem, dass die Dissertation weder in gleicher noch in ähnlicher Form bereits in einem anderen Prüfungsverfahren vorgelegen hat.

Ort, Datum Unterschrift

10.6 Curriculam vitae

10.7 Acknowledgment

First of all, I would like to thank my supervisor Dr. Cindrilla Chumduri for her instructive supervision, guidance, scientific support, assistance, and encouragement during the years of my doctoral study. I will always be immensely grateful for being a part of her research group.

I thank Dr. Rajendra Kumar Gurumurthy for his co-supervision, fruitful scientific discussions, and for providing me constructive feedback on my work. I would also like to thank my thesis committee members for their valuable scientific feedback and support.

I would like to thank Prof. Dr. Thomas F. Meyer for providing me an opportunity to initiate my Ph.D. work in MPIIB and the lab research facility. I thank all the former colleagues of MPIIB who directly or indirectly supported my work, especially technician Marina Drabkina. I thank MPIIB Microscopy Core Facility, Microarray facility, and Animal facility members for their help with my project.

I would like to extend my thanks to all team members of Chumduri lab. Special thanks to Pon Ganish Prakash for single-cell RNA seq data analysis and fruitful discussions. I thank past lab members Dr. Stefanie Koster, Christian Wentland, Philip Nkemdirim Mbonu, Dajung Son, Jaya Bhuvaneshwari, and Shilpa Mary Kurian for their support in carrying out my experiments. I am also thankful to all my colleagues in the Chair of Microbiology, Wurzburg, for their valuable input, assistance, and support.

Above all, I express my gratitude to my family and friends. I am deeply thankful to my parents for their motivation and endless support in achieving my goal. I would like to thank my wife, Deepthi Vijaya Kulal always being understanding, encouraging, and infinitely supportive.

11 References

Abnet, Christian C., You-Lin Qiao, Sanford M. Dawsey, Dennis W. Buckman, Chung S. Yang, William J. Blot, Zhi-Wei Dong, Philip R. Taylor, and Steven D. Mark. 2003. "Prospective Study of Serum Retinol, Beta-Carotene, Beta-Cryptoxanthin, and Lutein/Zeaxanthin and Esophageal and Gastric Cancers in China." *Cancer Causes & Control : CCC* 14(7):645–55. doi: 10.1023/a:1025619608851.

Agoston, Agoston T., Thai H. Pham, Robert D. Odze, David H. Wang, Kiron M. Das, Stuart J. Spechler, and Rhonda F. Souza. 2018. "Columnar-Lined Esophagus Develops via Wound Repair in a Surgical Model of Reflux Esophagitis." *Cellular and Molecular Gastroenterology and Hepatology* 6(4):389–404. doi: 10.1016/j.jcmgh.2018.06.007.

Ali, Irshad, Parvaneh Rafiee, Yue Zheng, Christopher Johnson, Banani Banerjee, George Haasler, Howard Jacob, and Reza Shaker. 2009. "Intramucosal Distribution of WNT Signaling Components in Human Esophagus." *Journal of Clinical Gastroenterology* 43(4):327–37. doi: 10.1097/mcg.0b013e31816256ff.

Amita, Mitsuyoshi, Katsuyuki Adachi, Andrei P. Alexenko, Sunilima Sinha, Danny J. Schust, Laura C. Schulz, R. Michael Roberts, and Toshihiko Ezashi. 2013. "Complete and Unidirectional Conversion of Human Embryonic Stem Cells to Trophoblast by BMP4." *Proceedings of the National Academy of Sciences of the United States of America* 110(13):E1212-21. doi: 10.1073/pnas.1303094110.

Arendt, Detlev, Jacob M. Musser, Clare V. H. Baker, Aviv Bergman, Connie Cepko, Douglas H. Erwin, Mihaela Pavlicev, Gerhard Schlosser, Stefanie Widder, Manfred D. Laubichler, and Günter P. Wagner. 2016. "The Origin and Evolution of Cell Types." *Nature Reviews. Genetics* 17(12):744–57. doi: 10.1038/nrg.2016.127.

Arin, Rosa M., Adriana Gorostidi, Hiart Navarro-Imaz, Yuri Rueda, Olatz Fresnedo, and Begoña Ochoa. 2017. "Adenosine: Direct and Indirect Actions on Gastric Acid Secretion." *Frontiers in Physiology* 8:737. doi: 10.3389/fphys.2017.00737.

Arnold, Melina, Mathieu Laversanne, Linda Morris Brown, Susan S. Devesa, and Freddie Bray. 2017. "Predicting the Future Burden of Esophageal Cancer by Histological Subtype: International Trends in Incidence up to 2030." *The American Journal of Gastroenterology* 112(8):1247–55. doi: 10.1038/ajg.2017.155.

Asselineau, D., B. A. Bernard, C. Bailly, and M. Darmon. 1989. "Retinoic Acid Improves Epidermal Morphogenesis." *Developmental Biology* 133(2):322–35. doi: 10.1016/0012-1606(89)90037-7.

Aubin, Josée, Ugo Déry, Margot Lemieux, Pierre Chailler, and Lucie Jeannotte. 2002. "Stomach Regional Specification Requires Hoxa5-Driven Mesenchymal-Epithelial Signaling." *Development (Cambridge, England)* 129(17):4075–87. doi: 10.1242/dev.129.17.4075.

van Baal, Jantine W. P. M., Francesca Milano, Agnieszka M. Rygiel, Jacques J. G. H. M. Bergman, Wilda D. Rosmolen, Sander J. H. van Deventer, Kenneth K. Wang, Maikel P. Peppelenbosch, and Kausilia K. Krishnadath. 2005. "A Comparative Analysis by SAGE of Gene Expression Profiles of Barrett's Esophagus, Normal Squamous Esophagus, and Gastric Cardia." *Gastroenterology* 129(4):1274–81. doi: 10.1053/j.gastro.2005.07.026.

Barber, Teresa, Guillermo Esteban-Pretel, María Pilar Marín, and Joaquín Timoneda. 2014. "Vitamin a Deficiency and Alterations in the Extracellular Matrix." *Nutrients* 6(11):4984–5017. doi: 10.3390/nu6114984.

Barbera, Mariagnese, Massimiliano di Pietro, Elaine Walker, Charlotte Brierley, Shona MacRae, Benjamin D. Simons, Phil H. Jones, John Stingl, and Rebecca C. Fitzgerald. 2015. "The Human Squamous Oesophagus Has Widespread Capacity for Clonal Expansion from Cells at Diverse Stages of Differentiation." *Gut* 64(1):11–19. doi: 10.1136/gutjnl-2013-306171.

Barker, Nick, Johan H. van Es, Jeroen Kuipers, Pekka Kujala, Maaike van den Born, Miranda Cozijnsen, Andrea Haegebarth, Jeroen Korving, Harry Begthel, Peter J. Peters, and Hans Clevers. 2007. "Identification of Stem Cells in Small Intestine and Colon by Marker Gene Lgr5." *Nature* 449(7165):1003–7. doi: 10.1038/nature06196.

Barker, Nick, Meritxell Huch, Pekka Kujala, Marc van de Wetering, Hugo J. Snippert, Johan H. van Es, Toshiro Sato, Daniel E. Stange, Harry Begthel, Maaike van den Born, Esther Danenberg, Stieneke van den Brink, Jeroen Korving, Arie Abo, Peter J. Peters, Nick Wright, Richard Poulsom, and Hans Clevers. 2010. "Lgr5(+ve) Stem Cells Drive Self-Renewal in the Stomach and Build Long-Lived Gastric Units in Vitro." *Cell Stem Cell* 6(1):25–36. doi: 10.1016/j.stem.2009.11.013.

BARRETT, N. R. 1950. “Chronic Peptic Ulcer of the Oesophagus and ‘Oesophagitis’.” *The British Journal of Surgery* 38(150):175–82. doi: 10.1002/bjs.18003815005.

Benjamini, Yoav, and Yosef Hochberg. 1995. “Controlling the False Discovery Rate: A Practical and Powerful Approach to Multiple Testing.” *Journal of the Royal Statistical Society: Series B (Methodological)* 57(1):289–300. doi: 10.1111/j.2517-6161.1995.tb02031.x.

Bimczok, D., J. Y. Kao, M. Zhang, S. Cochrun, P. Mannon, S. Peter, C. M. Wilcox, K. E. Mönkemüller, P. R. Harris, J. M. Grams, R. D. Stahl, P. D. Smith, and L. E. Smythies. 2015. “Human Gastric Epithelial Cells Contribute to Gastric Immune Regulation by Providing Retinoic Acid to Dendritic Cells.” *Mucosal Immunology* 8(3):533–44. doi: 10.1038/mi.2014.86.

Bohn, Torsten, Charles Desmarchelier, Sedef N. El, Jaap Keijer, Evert van Schothorst, Ralph Rühl, and Patrick Borel. 2019. “β-Carotene in the Human Body: Metabolic Bioactivation Pathways - from Digestion to Tissue Distribution and Excretion.” *The Proceedings of the Nutrition Society* 78(1):68–87. doi: 10.1017/S0029665118002641.

Booth, D., J. D. Haley, A. M. Bruskin, and C. S. Potten. 2000. “Transforming Growth Factor-B3 Protects Murine Small Intestinal Crypt Stem Cells and Animal Survival after Irradiation, Possibly by Reducing Stem-Cell Cycling.” *International Journal of Cancer* 86(1):53–59. doi: 10.1002/(sici)1097-0215(20000401)86:1<53::aid-ijc8>3.0.co;2-z.

Bovolenta, Paola, Pilar Esteve, Jose Maria Ruiz, Elsa Cisneros, and Javier Lopez-Rios. 2008. “Beyond Wnt Inhibition: New Functions of Secreted Frizzled-Related Proteins in Development and Disease.” *Journal of Cell Science* 121(Pt 6):737–46. doi: 10.1242/jcs.026096.

Bray, Freddie, Jacques Ferlay, Isabelle Soerjomataram, Rebecca L. Siegel, Lindsey A. Torre, and Ahmedin Jemal. 2018. “Global Cancer Statistics 2018: GLOBOCAN Estimates of Incidence and Mortality Worldwide for 36 Cancers in 185 Countries.” *CA: A Cancer Journal for Clinicians* 68(6):394–424. doi: 10.3322/caac.21492.

Breuer, Christian, Winfried L. Neuhuber, and Jürgen Wörl. 2004. “Development of Neuromuscular Junctions in the Mouse Esophagus: Morphology Suggests a Role for Enteric Coinnervation during Maturation of Vagal Myoneural Contacts.” *The Journal of Comparative Neurology* 475(1):47–69. doi: 10.1002/cne.20156.

Buenrostro, Jason D., Beijing Wu, Ulrike M. Litzenburger, Dave Ruff, Michael L. Gonzales, Michael P. Snyder, Howard Y. Chang, and William J. Greenleaf. 2015. “Single-Cell Chromatin Accessibility Reveals Principles of Regulatory Variation.” *Nature* 523(7561):486–90. doi: 10.1038/nature14590.

Bugter, Jeroen M., Nicola Fenderico, and Madelon M. Maurice. 2021. “Mutations and Mechanisms of WNT Pathway Tumour Suppressors in Cancer.” *Nature Reviews. Cancer* 21(1):5–21. doi: 10.1038/s41568-020-00307-z.

Busslinger, Georg A., Bas L. A. Weusten, Auke Bogte, Harry Begthel, Lodewijk A. A. Brosens, and Hans Clevers. 2021. “Human Gastrointestinal Epithelia of the Esophagus, Stomach, and Duodenum Resolved at Single-Cell Resolution.” *Cell Reports* 34(10):108819. doi: 10.1016/j.celrep.2021.108819.

Cabezas-Wallscheid, Nina, Florian Buettner, Pia Sommerkamp, Daniel Klimmeck, Luisa Ladel, Frederic B. Thalheimer, Daniel Pastor-Flores, Leticia P. Roma, Simon Renders, Petra Zeisberger, Adriana Przybylla, Katharina Schönberger, Roberta Scognamiglio, Sandro Altamura, Carolina M. Florian, Malak Fawaz, Dominik Vonficht, Melania Tesio, Paul Collier, Dinko Pavlinic, Hartmut Geiger, Timm Schroeder, Vladimir Benes, Tobias P. Dick, Michael A. Rieger, Oliver Stegle, and Andreas Trumpp. 2017. “Vitamin A-Retinoic Acid Signaling Regulates Hematopoietic Stem Cell Dormancy.” *Cell*. doi: 10.1016/j.cell.2017.04.018.

Cabibi, Daniela, Eugenio Fiorentino, Gianni Pantuso, Achille Mastrosimone, Cosimo Callari, Matilde Cacciatore, Maria Campione, and Francesco Aragona. 2009. “Keratin 7 Expression as an Early Marker of Reflux-Related Columnar Mucosa without Intestinal Metaplasia in the Esophagus.” *Medical Science Monitor : International Medical Journal of Experimental and Clinical Research* 15(5):CR203-210.

Carreira-Barbosa, Filipa, and Sofia C. Nunes. 2020. “Wnt Signaling: Paths for Cancer Progression.” *Advances in Experimental Medicine and Biology* 1219:189–202. doi: 10.1007/978-3-030-34025-4_10.

Chandrasoma, P. 2005. “Controversies of the Cardiac Mucosa and Barrett’s Oesophagus.” *Histopathology* 46(4):361–73. doi: 10.1111/j.1365-2559.2005.02088.x.

Chang, C. L., E. Hong, P. Lao-Sirieix, and R. C. Fitzgerald. 2008. “A Novel Role for the Retinoic Acid-Catabolizing Enzyme CYP26A1 in Barrett’s Associated Adenocarcinoma.” *Oncogene* 27(21):2951–60. doi: 10.1038/sj.onc.1210969.

Chang, Chih-Long, Pierre Lao-Sirieix, Vicki Save, Guillermo de La Cueva Mendez, Ron Laskey, and Rebecca C. Fitzgerald. 2007. "Retinoic Acid-Induced Glandular Differentiation of the Oesophagus." *Gut* 56(7):906–17. doi: 10.1136/gut.2006.097915.

Chang, Tao-Hsin, Fu-Lien Hsieh, Matthias Zebisch, Karl Harlos, Jonathan Elegheert, and E. Yvonne Jones. 2015. "Structure and Functional Properties of Norrin Mimic Wnt for Signalling with Frizzled4, Lrp5/6, and Proteoglycan." *ELife* 4. doi: 10.7554/eLife.06554.

Chaudhry SR, Liman MNP, Peterson DC. 2021. "Anatomy, Abdomen and Pelvis, Stomach." Treasure Island (FL): StatPearls Publishing

Chaves, P., A. Dias Pereira, C. Cruz, A. Suspiro, J. C. Mendes de Almeida, C. N. Leitão, and J. Soares. 2002. "Recurrent Columnar-Lined Esophageal Segments--Study of the Phenotypic Characteristics Using Intestinal Markers." *Diseases of the Esophagus : Official Journal of the International Society for Diseases of the Esophagus* 15(4):282–86. doi: 10.1046/j.1442-2050.2002.00264.x.

Chen, Geng, Baitang Ning, and Tieliu Shi. 2019. "Single-Cell RNA-Seq Technologies and Related Computational Data Analysis." *Frontiers in Genetics* 10:317. doi: 10.3389/fgene.2019.00317.

Cheong, J. K., T. H. Nguyen, H. Wang, P. Tan, P. M. Voorhoeve, S. H. Lee, and D. M. Virshup. 2011. "IC261 Induces Cell Cycle Arrest and Apoptosis of Human Cancer Cells via CK1δ/ε and Wnt/β-Catenin Independent Inhibition of Mitotic Spindle Formation." *Oncogene* 30(22):2558–69. doi: 10.1038/onc.2010.627.

Choi, Eunyoung, Joseph T. Roland, Brittney J. Barlow, Ryan O'Neal, Amy E. Rich, Ki Taek Nam, Chanjuan Shi, and James R. Goldenring. 2014. "Cell Lineage Distribution Atlas of the Human Stomach Reveals Heterogeneous Gland Populations in the Gastric Antrum." *Gut* 63(11):1711–20. doi: 10.1136/gutjnl-2013-305964.

Choi, Yeon Sook, Yuhang Zhang, Mingang Xu, Yongguang Yang, Mayumi Ito, Tien Peng, Zheng Cui, Andras Nagy, Anna-Katerina Hadjantonakis, Richard A. Lang, George Cotsarelis, Thomas Andl, Edward E. Morrisey, and Sarah E. Millar. 2013. "Distinct Functions for Wnt/β-Catenin in Hair Follicle Stem Cell Proliferation and Survival and Interfollicular Epidermal Homeostasis." *Cell Stem Cell* 13(6):720–33. doi: 10.1016/j.stem.2013.10.003.

Chumduri, Cindrilla, Rajendra Kumar Gurumurthy, Hilmar Berger, Oliver Dietrich, Naveen Kumar, Stefanie Koster, Volker Brinkmann, Kirstin Hoffmann, Marina Drabkina, Panagiota Arampatzi, Dajung Son, Uwe Klemm, Hans-Joachim Mollenkopf, Hermann Herbst, Mandy Mangler, Jörg Vogel, Antoine-Emmanuel Saliba, and Thomas F. Meyer. 2021. "Opposing Wnt Signals Regulate Cervical Squamocolumnar Homeostasis and Emergence of Metaplasia." *Nature Cell Biology* 23(2):184–97. doi: 10.1038/s41556-020-00619-0.

Clark, Stephen J., Ricard Argelaguet, Chantriolnt-Andreas Kapourani, Thomas M. Stubbs, Heather J. Lee, Celia Alda-Catalinas, Felix Krueger, Guido Sanguinetti, Gavin Kelsey, John C. Marioni, Oliver Stegle, and Wolf Reik. 2018. "ScNMT-Seq Enables Joint Profiling of Chromatin Accessibility DNA Methylation and Transcription in Single Cells." *Nature Communications* 9(1):781. doi: 10.1038/s41467-018-03149-4.

Clément, Geneviève, David M. Jablons, and Jean Benhattar. 2007. "Targeting the Wnt Signaling Pathway to Treat Barrett's Esophagus." *Expert Opinion on Therapeutic Targets* 11(3):375–89. doi: 10.1517/14728222.11.3.375.

Clemons, Nicholas J., David H. Wang, Daniel Croagh, Anjali Tikoo, Christina M. Fennell, Carmel Murone, Andrew M. Scott, D. Neil Watkins, and Wayne A. Phillips. 2012. "Sox9 Drives Columnar Differentiation of Esophageal Squamous Epithelium: A Possible Role in the Pathogenesis of Barrett's Esophagus." *American Journal of Physiology. Gastrointestinal and Liver Physiology* 303(12):G1335-46. doi: 10.1152/ajpgi.00291.2012.

Clevers, Hans. 2006. "Wnt/Beta-Catenin Signaling in Development and Disease." *Cell* 127(3):469–80. doi: 10.1016/j.cell.2006.10.018.

Clevers, Hans. 2016. "Modeling Development and Disease with Organoids." *Cell* 165(7):1586–97. doi: 10.1016/j.cell.2016.05.082.

Colleypriest, Benjamin J., Zoë D. Burke, Leonard P. Griffiths, Yu Chen, Wei-Yuan Yu, Ramiro Jover, Michael Bock, Leigh Biddlestone, Jonathan M. Quinlan, Stephen G. Ward, J. Mark Farrant, Jonathan M. W. Slack, and David Tosh. 2017. "Hnf4α Is a Key Gene That Can Generate Columnar Metaplasia in Oesophageal Epithelium." *Differentiation; Research in Biological Diversity* 93:39–49. doi: 10.1016/j.diff.2016.11.001.

Cook, Michael B., and Aaron P. Thrift. 2021. “Epidemiology of Barrett’s Esophagus and Esophageal Adenocarcinoma: Implications for Screening and Surveillance.” *Gastrointestinal Endoscopy Clinics of North America* 31(1):1–26. doi: 10.1016/j.giec.2020.08.001.

Costantini, Lara, Romina Molinari, Barbara Farinon, and Nicolò Merendino. 2020. “Retinoic Acids in the Treatment of Most Lethal Solid Cancers.” *Journal of Clinical Medicine* 9(2). doi: 10.3390/jcm9020360.

Croagh, Daniel, Wayne A. Phillips, Rick Redvers, Robert J. S. Thomas, and Pritinder Kaur. 2007. “Identification of Candidate Murine Esophageal Stem Cells Using a Combination of Cell Kinetic Studies and Cell Surface Markers.” *Stem Cells (Dayton, Ohio)* 25(2):313–18. doi: 10.1634/stemcells.2006-0421.

Curtius, Kit, Joel H. Rubenstein, Amitabh Chak, and John M. Inadomi. 2020. “Computational Modelling Suggests That Barrett’s Oesophagus May Be the Precursor of All Oesophageal Adenocarcinomas.” *Gut*. doi: 10.1136/gutjnl-2020-321598.

Davidson, Gary, Wei Wu, Jinlong Shen, Josipa Bilic, Ursula Fenger, Peter Stannek, Andrei Glinka, and Christof Niehrs. 2005. “Casein Kinase 1 Gamma Couples Wnt Receptor Activation to Cytoplasmic Signal Transduction.” *Nature* 438(7069):867–72. doi: 10.1038/nature04170.

DeLaForest, Ann, Bridget M. Kohlnhofer, Olivia D. Franklin, Roman Stavniichuk, Cayla A. Thompson, Kirthi Pulakanti, Sridhar Rao, and Michele A. Battle. 2021. “GATA4 Controls Epithelial Morphogenesis in the Developing Stomach to Promote Establishment of Glandular Columnar Epithelium.” *Cellular and Molecular Gastroenterology and Hepatology* 12(4):1391–1413. doi: 10.1016/j.jcmgh.2021.05.021.

Demitrack, Elise S., Gail B. Gifford, Theresa M. Keeley, Nobukatsu Horita, Andrea Todisco, D. Kim Turgeon, Christian W. Siebel, and Linda C. Samuelson. 2017. “NOTCH1 and NOTCH2 Regulate Epithelial Cell Proliferation in Mouse and Human Gastric Corpus.” *American Journal of Physiology. Gastrointestinal and Liver Physiology* 312(2):G133–44. doi: 10.1152/ajpgi.00325.2016.

Deo, Priya Nimish, and Revati Deshmukh. 2018. “Pathophysiology of Keratinization.” *Journal of Oral and Maxillofacial Pathology : JOMFP* 22(1):86–91. doi: 10.4103/jomfp.JOMFP_195_16.

DeWard, Aaron D., Julie Cramer, and Eric Lagasse. 2014. “Cellular Heterogeneity in the Mouse Esophagus Implicates the Presence of a Nonquiescent Epithelial Stem Cell Population.” *Cell Reports* 9(2):701–11. doi: 10.1016/j.celrep.2014.09.027.

Domyan, Eric T., Elisabetta Ferretti, Kurt Throckmorton, Yuji Mishina, Silvia K. Nicolis, and Xin Sun. 2011. “Signaling through BMP Receptors Promotes Respiratory Identity in the Foregut via Repression of Sox2.” *Development (Cambridge, England)* 138(5):971–81. doi: 10.1242/dev.053694.

Doupé, David P., Maria P. Alcolea, Amit Roshan, Gen Zhang, Allon M. Klein, Benjamin D. Simons, and Philip H. Jones. 2012. “A Single Progenitor Population Switches Behavior to Maintain and Repair Esophageal Epithelium.” *Science (New York, N.Y.)* 337(6098):1091–93. doi: 10.1126/science.1218835.

Duijster, Janneke W., Eelco Franz, Jacques Neefjes, and Lapo Mughini-Gras. 2021. “Bacterial and Parasitic Pathogens as Risk Factors for Cancers in the Gastrointestinal Tract: A Review of Current Epidemiological Knowledge.” *Frontiers in Microbiology* 12:790256. doi: 10.3389/fmicb.2021.790256.

Dunaway, Spencer, Alexandra Rothaus, Yuhang Zhang, Ana Luisa Kadekaro, Thomas Andl, and Claudia D. Andl. 2019. “Divide and Conquer: Two Stem Cell Populations in Squamous Epithelia, Reserves and the Active Duty Forces.” *International Journal of Oral Science* 11(3):26. doi: 10.1038/s41368-019-0061-2.

Dye, Briana R., David R. Hill, Michael A. H. Ferguson, Yu-Hwai Tsai, Melinda S. Nagy, Rachel Dyal, James M. Wells, Christopher N. Mayhew, Roy Nattiv, Ophir D. Klein, Eric S. White, Gail H. Deutsch, and Jason R. Spence. 2015. “In Vitro Generation of Human Pluripotent Stem Cell Derived Lung Organoids.” *ELife* 4. doi: 10.7554/eLife.05098.

Eberle, Julia Anna-Maria, Patric Richter, Patricia Widmayer, Vladimir Chubanov, Thomas Gudermann, and Heinz Breer. 2013. “Band-like Arrangement of Taste-like Sensory Cells at the Gastric Groove: Evidence for Paracrine Communication.” *Frontiers in Physiology* 4:58. doi: 10.3389/fphys.2013.00058.

Eleftheriadis, Nicholas, Haruhiro Inoue, Haruo Ikeda, Manabu Onimaru, Akira Yoshida, Toshihisa Hosoya, Roberta Maselli, and Shin-Ei Kudo. 2013. “Endocytoscopic Visualization of Squamous Cell Islands within Barrett’s Epithelium.” *World Journal of Gastrointestinal Endoscopy* 5(4):174–79. doi: 10.4253/wjge.v5.i4.174.

Escobar-Hoyos, Luisa F., Jie Yang, Jiawen Zhu, Julie-Ann Cavallo, Haiyan Zhai, Stephanie Burke, Antonius Koller, Emily I. Chen, and Kenneth R. Shroyer. 2014. "Keratin 17 in Premalignant and Malignant Squamous Lesions of the Cervix: Proteomic Discovery and Immunohistochemical Validation as a Diagnostic and Prognostic Biomarker." *Modern Pathology : An Official Journal of the United States and Canadian Academy of Pathology, Inc* 27(4):621–30. doi: 10.1038/modpathol.2013.166.

Farin, Henner F., Johan H. van Es, and Hans Clevers. 2012. "Redundant Sources of Wnt Regulate Intestinal Stem Cells and Promote Formation of Paneth Cells." *Gastroenterology* 143(6):1518-1529.e7. doi: 10.1053/j.gastro.2012.08.031.

Feng, Lingling, Brandoch Cook, Su-Yi Tsai, Ting Zhou, Brooke LaFlamme, Todd Evans, and Shuibing Chen. 2016. "Discovery of a Small-Molecule BMP Sensitizer for Human Embryonic Stem Cell Differentiation." *Cell Reports* 15(9):2063–75. doi: 10.1016/j.celrep.2016.04.066.

Fischer, Anne-Sophie, and Michael Sigal. 2019. "The Role of Wnt and R-Spondin in the Stomach During Health and Disease." *Biomedicines* 7(2). doi: 10.3390/biomedicines7020044.

Fitzgerald, Rebecca C., Massimiliano di Pietro, Krish Ragunath, Yeng Ang, Jin-Yong Kang, Peter Watson, Nigel Trudgill, Praful Patel, Philip v Kaye, Scott Sanders, Maria O'Donovan, Elizabeth Bird-Lieberman, Pradeep Bhandari, Janusz A. Jankowski, Stephen Attwood, Simon L. Parsons, Duncan Loft, Jesper Lagergren, Paul Moayyedi, Georgios Lyratzopoulos, John de Caestecker, and British Society of Gastroenterology. 2014. "British Society of Gastroenterology Guidelines on the Diagnosis and Management of Barrett's Oesophagus." *Gut* 63(1):7–42. doi: 10.1136/gutjnl-2013-305372.

Flanagan, Dustin J., Chloe R. Austin, Elizabeth Vincan, and Toby J. Phesse. 2018. "Wnt Signalling in Gastrointestinal Epithelial Stem Cells." *Genes* 9(4). doi: 10.3390/genes9040178.

Franch-Marro, Xavier, Franz Wendler, Janice Griffith, Madelon M. Maurice, and Jean-Paul Vincent. 2008. "In Vivo Role of Lipid Adducts on Wingless." *Journal of Cell Science* 121(Pt 10):1587–92. doi: 10.1242/jcs.015958.

Fu, Dah-Jiun, Lianghai Wang, Fouad K. Chouairi, Ian M. Rose, Danysh A. Abetov, Andrew D. Miller, Robert J. Yamulla, John C. Schimenti, Andrea Flesken-Nikitin, and Alexander Yu Nikitin. 2020. "Gastric Squamous-Columnar Junction Contains a Large Pool of Cancer-Prone Immature Osteopontin Responsive Lgr5-CD44+ Cells." *Nature Communications* 11(1):84. doi: 10.1038/s41467-019-13847-2.

Fuchs, E., and H. Green. 1981. "Regulation of Terminal Differentiation of Cultured Human Keratinocytes by Vitamin A." *Cell* 25(3):617–25. doi: 10.1016/0092-8674(81)90169-0.

von Furstenberg, Richard J., Joy Li, Christina Stolarchuk, Rachel Feder, Alexa Campbell, Leandi Kruger, Liara M. Gonzalez, Anthony T. Blikslager, Diana M. Cardona, Shannon J. McCall, Susan J. Henning, and Katherine S. Garman. 2017. "Porcine Esophageal Submucosal Gland Culture Model Shows Capacity for Proliferation and Differentiation." *Cellular and Molecular Gastroenterology and Hepatology* 4(3):385–404. doi: 10.1016/j.jcmgh.2017.07.005.

Gao, Nan, Peter White, and Klaus H. Kaestner. 2009. "Establishment of Intestinal Identity and Epithelial-Mesenchymal Signaling by Cdx2." *Developmental Cell* 16(4):588–99. doi: 10.1016/j.devcel.2009.02.010.

García-Reyes, Balbina, Lydia Witt, Björn Jansen, Ebru Karasu, Tanja Gehring, Johann Leban, Doris Henne-Bruns, Christian Pichlo, Elena Brunstein, Ulrich Baumann, Fabian Wesseler, Bernd Rathmer, Dennis Schade, Christian Peifer, and Uwe Knippschild. 2018. "Discovery of Inhibitor of Wnt Production 2 (IWP-2) and Related Compounds As Selective ATP-Competitive Inhibitors of Casein Kinase 1 (CK1) δ/ε." *Journal of Medicinal Chemistry* 61(9):4087–4102. doi: 10.1021/acs.jmedchem.8b00095.

Gharahkhani, Puya, Rebecca C. Fitzgerald, Thomas L. Vaughan, Claire Palles, Ines Gockel, Ian Tomlinson, Matthew F. Buas, Andrea May, Christian Gerges, Mario Anders, Jessica Becker, Nicole Kreuser, Tania Noder, Marino Venerito, Lothar Veits, Thomas Schmidt, Hendrik Manner, Claudia Schmidt, Timo Hess, Anne C. Böhmer, Jakob R. Izbicki, Arnulf H. Hölscher, Hauke Lang, Dietmar Lorenz, Brigitte Schumacher, Andreas Hackelsberger, Rupert Mayershofer, Oliver Pech, Yogesh Vashist, Katja Ott, Michael Vieth, Josef Weismüller, Markus M. Nöthen, Barrett's and Esophageal Adenocarcinoma Consortium (BEACON), Esophageal Adenocarcinoma GenEtics Consortium (EAGLE), Wellcome Trust Case Control Consortium 2 (WTCCC2), Stephen Attwood, Hugh Barr, Laura Chegwidden, John de Caestecker, Rebecca Harrison, Sharon B. Love, David MacDonald, Paul Moayyedi, Hans Prenen, R. G. Peter Watson, Prasad G. Iyer, Lesley A. Anderson, Leslie Bernstein, Wong-Ho Chow, Laura J. Hardie, Jesper Lagergren, Geoffrey Liu, Harvey A. Risch, Anna H. Wu, Weimin Ye, Nigel C. Bird, Nicholas J. Shaheen, Marilie D. Gammon, Douglas A. Corley, Carlos Caldas, Susanne Moebus, Michael Knapp, Wilbert H. M. Peters, Horst Neuhaus, Thomas

Rösch, Christian Ell, Stuart MacGregor, Paul Pharoah, David C. Whiteman, Janusz Jankowski, and Johannes Schumacher. 2016. "Genome-Wide Association Studies in Oesophageal Adenocarcinoma and Barrett's Oesophagus: A Large-Scale Meta-Analysis." *The Lancet. Oncology* 17(10):1363–73. doi: 10.1016/S1470-2045(16)30240-6.

Ghyselinck, Norbert B., and Gregg Duester. 2019. "Retinoic Acid Signaling Pathways." *Development (Cambridge, England)* 146(13). doi: 10.1242/dev.167502.

Gilbert, Erin W., Renato A. Luna, Vincent L. Harrison, and John G. Hunter. 2011. "Barrett's Esophagus: A Review of the Literature." *Journal of Gastrointestinal Surgery : Official Journal of the Society for Surgery of the Alimentary Tract* 15(5):708–18. doi: 10.1007/s11605-011-1485-y.

Gillen, P., P. Keeling, P. J. Byrne, A. B. West, and T. P. Hennessy. 1988. "Experimental Columnar Metaplasia in the Canine Oesophagus." *The British Journal of Surgery* 75(2):113–15. doi: 10.1002/bjs.1800750208.

Giroux, Véronique, Ashley A. Lento, Mirazul Islam, Jason R. Pitarresi, Akriti Kharbanda, Kathryn E. Hamilton, Kelly A. Whelan, Apple Long, Ben Rhoades, Qiaosi Tang, Hiroshi Nakagawa, Christopher J. Lengner, Adam J. Bass, E. Paul Wileyto, Andres J. Klein-Szanto, Timothy C. Wang, and Anil K. Rustgi. 2017. "Long-Lived Keratin 15+ Esophageal Progenitor Cells Contribute to Homeostasis and Regeneration." *The Journal of Clinical Investigation* 127(6):2378–91. doi: 10.1172/JCI88941.

Glickman, J. N., Y. Y. Chen, H. H. Wang, D. A. Antonioli, and R. D. Odze. 2001. "Phenotypic Characteristics of a Distinctive Multilayered Epithelium Suggests That It Is a Precursor in the Development of Barrett's Esophagus." *The American Journal of Surgical Pathology* 25(5):569–78. doi: 10.1097/00000478-200105000-00002.

Gnecchi, Massimiliano, Zhiping Zhang, Aiguo Ni, and Victor J. Dzau. 2008. "Paracrine Mechanisms in Adult Stem Cell Signaling and Therapy." *Circulation Research* 103(11):1204–19. doi: 10.1161/CIRCRESAHA.108.176826.

Goldblum, John R. 2003. "Barrett's Esophagus and Barrett's-Related Dysplasia." *Modern Pathology : An Official Journal of the United States and Canadian Academy of Pathology, Inc* 16(4):316–24. doi: 10.1097/01.MP.0000062996.66432.12.

González, M. v, M. L. Artímez, L. Rodrigo, C. López-Larrea, M. J. Menéndez, V. Alvarez, R. Pérez, M. F. Fresno, M. J. Pérez, A. Sampedro, and E. Coto. 1997. "Mutation Analysis of the P53, APC, and P16 Genes in the Barrett's Oesophagus, Dysplasia, and Adenocarcinoma." *Journal of Clinical Pathology* 50(3):212–17. doi: 10.1136/jcp.50.3.212.

Goss, Ashley M., Ying Tian, Tadasuke Tsukiyama, Ethan David Cohen, Diane Zhou, Min Min Lu, Terry P. Yamaguchi, and Edward E. Morrisey. 2009. "Wnt2/2b and Beta-Catenin Signaling Are Necessary and Sufficient to Specify Lung Progenitors in the Foregut." *Developmental Cell* 17(2):290–98. doi: 10.1016/j.devcel.2009.06.005.

Gregorieff, Alex, Daniel Pinto, Harry Begthel, Olivier Destrée, Menno Kielman, and Hans Clevers. 2005. "Expression Pattern of Wnt Signaling Components in the Adult Intestine." *Gastroenterology* 129(2):626–38. doi: 10.1016/j.gastro.2005.06.007.

Gribble, Fiona M., and Frank Reimann. 2019. "Function and Mechanisms of Enteroendocrine Cells and Gut Hormones in Metabolism." *Nature Reviews. Endocrinology* 15(4):226–37. doi: 10.1038/s41574-019-0168-8.

Gross, Andre, Jonas Schoendube, Stefan Zimmermann, Maximilian Steeb, Roland Zengerle, and Peter Koltay. 2015. "Technologies for Single-Cell Isolation." *International Journal of Molecular Sciences* 16(8):16897–919. doi: 10.3390/ijms160816897.

Hafemeister, Christoph, and Rahul Satija. 2019. "Normalization and Variance Stabilization of Single-Cell RNA-Seq Data Using Regularized Negative Binomial Regression." *Genome Biology* 20(1):296. doi: 10.1186/s13059-019-1874-1.

Han, Lu, Praneet Chaturvedi, Keishi Kishimoto, Hiroyuki Koike, Talia Nasr, Kentaro Iwasawa, Kirsten Giesbrecht, Phillip C. Witcher, Alexandra Eicher, Lauren Haines, Yarim Lee, John M. Shannon, Mitsuru Morimoto, James M. Wells, Takanori Takebe, and Aaron M. Zorn. 2020. "Single Cell Transcriptomics Identifies a Signaling Network Coordinating Endoderm and Mesoderm Diversification during Foregut Organogenesis." *Nature Communications* 11(1):4158. doi: 10.1038/s41467-020-17968-x.

Han, Seungmin, Juergen Fink, David J. Jörg, Eunmin Lee, Min Kyu Yum, Lemonia Chatzeli, Sebastian R. Merker, Manon Josserand, Teodora Trendafilova, Amanda Andersson-Rolf, Catherine Dabrowska, Hyunki Kim, Ronald Naumann, Ji-Hyun Lee, Nobuo Sasaki, Richard Lester Mort, Onur Basak, Hans Clevers, Daniel E. Stange, Anna Philpott, Jong

Kyoung Kim, Benjamin D. Simons, and Bon-Kyoung Koo. 2019. “Defining the Identity and Dynamics of Adult Gastric Isthmus Stem Cells.” *Cell Stem Cell* 25(3):342-356.e7. doi: 10.1016/j.stem.2019.07.008.

Han, Xiaoping, Ziming Zhou, Lijiang Fei, Huiyu Sun, Renying Wang, Yao Chen, Haide Chen, Jingjing Wang, Huanna Tang, Wenhao Ge, Yincong Zhou, Fang Ye, Mengmeng Jiang, Junqing Wu, Yanyu Xiao, Xiaoning Jia, Tingyue Zhang, Xiaojie Ma, Qi Zhang, Xueli Bai, Shujing Lai, Chengxuan Yu, Lijun Zhu, Rui Lin, Yuchi Gao, Min Wang, Yiqing Wu, Jianming Zhang, Renya Zhan, Saiyong Zhu, Hailan Hu, Changchun Wang, Ming Chen, He Huang, Tingbo Liang, Jianghua Chen, Weilin Wang, Dan Zhang, and Guoji Guo. 2020. “Construction of a Human Cell Landscape at Single-Cell Level.” *Nature* 581(7808):303–9. doi: 10.1038/s41586-020-2157-4.

Hao, Huai-Xiang, Yang Xie, Yue Zhang, Olga Charlat, Emma Oster, Monika Avello, Hong Lei, Craig Mickanin, Dong Liu, Heinz Ruffner, Xiaohong Mao, Qicheng Ma, Raffaella Zamponi, Tewis Bouwmeester, Peter M. Finan, Marc W. Kirschner, Jeffery A. Porter, Fabrizio C. Serluca, and Feng Cong. 2012. “ZNRF3 Promotes Wnt Receptor Turnover in an R-Spondin-Sensitive Manner.” *Nature* 485(7397):195–200. doi: 10.1038/nature11019.

Hao, Yuhan, Stephanie Hao, Erica Andersen-Nissen, William M. Mauck, Shiwei Zheng, Andrew Butler, Maddie J. Lee, Aaron J. Wilk, Charlotte Darby, Michael Zager, Paul Hoffman, Marlon Stoeckius, Efthymia Papalexi, Eleni P. Mimitou, Jaison Jain, Avi Srivastava, Tim Stuart, Lamar M. Fleming, Bertrand Yeung, Angela J. Rogers, Juliana M. McElrath, Catherine A. Blish, Raphael Gottardo, Peter Smibert, and Rahul Satija. 2021. “Integrated Analysis of Multimodal Single-Cell Data.” *Cell* 184(13):3573-3587.e29. doi: 10.1016/j.cell.2021.04.048.

Harris-Johnson, Kelley S., Eric T. Domyan, Chad M. Vezina, and Xin Sun. 2009. “Beta-Catenin Promotes Respiratory Progenitor Identity in Mouse Foregut.” *Proceedings of the National Academy of Sciences of the United States of America* 106(38):16287–92. doi: 10.1073/pnas.0902274106.

Haumaitre, C., E. Barbacci, M. Jenny, M. O. Ott, G. Gradwohl, and S. Cereghini. 2005. “Lack of TCF2/VHNF1 in Mice Leads to Pancreas Agenesis.” *Proceedings of the National Academy of Sciences of the United States of America* 102(5):1490–95. doi: 10.1073/pnas.0405776102.

Hayakawa, Yoku, Hiroshi Nakagawa, Anil K. Rustgi, Jianwen Que, and Timothy C. Wang. 2021. “Stem Cells and Origins of Cancer in the Upper Gastrointestinal Tract.” *Cell Stem Cell* 28(8):1343–61. doi: 10.1016/j.stem.2021.05.012.

He, Di, Di Wang, Ping Lu, Nan Yang, Zhigang Xue, Xianmin Zhu, Peng Zhang, and Guoping Fan. 2021. “Single-Cell RNA Sequencing Reveals Heterogeneous Tumor and Immune Cell Populations in Early-Stage Lung Adenocarcinomas Harboring EGFR Mutations.” *Oncogene* 40(2):355–68. doi: 10.1038/s41388-020-01528-0.

He, Shuai, Lin-He Wang, Yang Liu, Yi-Qi Li, Hai-Tian Chen, Jing-Hong Xu, Wan Peng, Guo-Wang Lin, Pan-Pan Wei, Bo Li, Xiaojun Xia, Dan Wang, Jin-Xin Bei, Xiaoshun He, and Zhiyong Guo. 2020. “Single-Cell Transcriptome Profiling of an Adult Human Cell Atlas of 15 Major Organs.” *Genome Biology* 21(1):294. doi: 10.1186/s13059-020-02210-0.

Huch, Meritxell, and Bon-Kyoung Koo. 2015. “Modeling Mouse and Human Development Using Organoid Cultures.” *Development (Cambridge, England)* 142(18):3113–25. doi: 10.1242/dev.118570.

Hughes, Chris S., Lynne M. Postovit, and Gilles A. Lajoie. 2010. “Matrigel: A Complex Protein Mixture Required for Optimal Growth of Cell Culture.” *Proteomics* 10(9):1886–90. doi: 10.1002/pmic.200900758.

Hunsu, Victoria O., Caroline O. B. Facey, Jeremy Z. Fields, and Bruce M. Boman. 2021. “Retinoids as Chemo-Preventive and Molecular-Targeted Anti-Cancer Therapies.” *International Journal of Molecular Sciences* 22(14). doi: 10.3390/ijms22147731.

Hur, Chin, Melecia Miller, Chung Yin Kong, Emily C. Dowling, Kevin J. Nattinger, Michelle Dunn, and Eric J. Feuer. 2013. “Trends in Esophageal Adenocarcinoma Incidence and Mortality.” *Cancer* 119(6):1149–58. doi: 10.1002/cncr.27834.

Hyland, Paula L., Nan Hu, Melissa Rotunno, Hua Su, Chaoyu Wang, Lemin Wang, Ruth M. Pfeiffer, Barbara Gherman, Carol Giffen, Cathy Dykes, Sanford M. Dawsey, Christian C. Abnet, Kathryn M. Johnson, Ruben D. Acosta, Patrick E. Young, Brooks D. Cash, and Philip R. Taylor. 2014. “Global Changes in Gene Expression of Barrett’s Esophagus Compared to Normal Squamous Esophagus and Gastric Cardia Tissues.” *PloS One* 9(4):e93219. doi: 10.1371/journal.pone.0093219.

Ito, Takao, Yuta Yamamoto, Naoko Yamagishi, and Yoshimitsu Kanai. 2021. “Stomach Secretes Estrogen in Response to the Blood Triglyceride Levels.” *Communications Biology* 4(1):1364. doi: 10.1038/s42003-021-02901-9.

Jacobsen, Christina M., Naoko Narita, Malgorzata Bielinska, Andrew J. Syder, Jeffrey I. Gordon, and David B. Wilson. 2002. "Genetic Mosaic Analysis Reveals That GATA-4 Is Required for Proper Differentiation of Mouse Gastric Epithelium." *Developmental Biology* 241(1):34–46. doi: 10.1006/dbio.2001.0424.

Jho, Eek-hoon, Tong Zhang, Claire Domon, Choun-Ki Joo, Jean-Noel Freund, and Frank Costantini. 2002. "Wnt/Beta-Catenin/Tcf Signaling Induces the Transcription of Axin2, a Negative Regulator of the Signaling Pathway." *Molecular and Cellular Biology* 22(4):1172–83. doi: 10.1128/MCB.22.4.1172-1183.2002.

Jiang, Ming, Wei Yao Ku, Zhongren Zhou, Evan S. Dellon, Gary W. Falk, Hiroshi Nakagawa, Mei Lun Wang, Kuancan Liu, Jun Wang, David A. Katzka, Jeffrey H. Peters, Xiaopeng Lan, and Jianwen Que. 2015. "BMP-Driven NRF2 Activation in Esophageal Basal Cell Differentiation and Eosinophilic Esophagitis." *Journal of Clinical Investigation*. doi: 10.1172/JCI78850.

Jiang, Ming, Haiyan Li, Yongchun Zhang, Ying Yang, Rong Lu, Kuancan Liu, Sijie Lin, Xiaopeng Lan, Haikun Wang, Han Wu, Jian Zhu, Zhongren Zhou, Jianming Xu, Dong-Kee Lee, Lanjing Zhang, Yuan-Cho Lee, Jingsong Yuan, Julian A. Abrams, Timothy C. Wang, Antonia R. Sepulveda, Qi Wu, Huaiyong Chen, Xin Sun, Junjun She, Xiaoxin Chen, and Jianwen Que. 2017. "Transitional Basal Cells at the Squamous-Columnar Junction Generate Barrett's Oesophagus." *Nature* 550(7677):529–33. doi: 10.1038/nature24269.

Jiang, S. Y., S. R. Shen, R. Y. Shyu, J. C. Yu, H. J. Harn, M. Y. Yeh, M. M. Lee, and Y. C. Chang. 1999. "Expression of Nuclear Retinoid Receptors in Normal, Premalignant and Malignant Gastric Tissues Determined by in Situ Hybridization." *British Journal of Cancer* 80(1–2):206–14. doi: 10.1038/sj.bjc.6690340.

Jijon, H. B., L. Suarez-Lopez, O. E. Diaz, S. Das, J. de Calisto, M. Parada-kusz, M. B. Yaffe, M. J. Pittet, J. R. Mora, Y. Belkaid, R. J. Xavier, and E. J. Villablanca. 2018. "Intestinal Epithelial Cell-Specific RARα Depletion Results in Aberrant Epithelial Cell Homeostasis and Underdeveloped Immune System." *Mucosal Immunology* 11(3):703–15. doi: 10.1038/mi.2017.91.

Johansson, Johan, Hans-Olof Håkansson, Lennart Mellblom, Antti Kempas, Karl-Erik Johansson, Fredrik Granath, and Olof Nyrén. 2005. "Prevalence of Precancerous and Other Metaplasia in the Distal Oesophagus and Gastro-Oesophageal Junction." *Scandinavian Journal of Gastroenterology* 40(8):893–902. doi: 10.1080/00365520510015692.

Jovic, Dragomirka, Xue Liang, Hua Zeng, Lin Lin, Fengping Xu, and Yonglun Luo. 2022. "Single-Cell RNA Sequencing Technologies and Applications: A Brief Overview." *Clinical and Translational Medicine* 12(3):e694. doi: 10.1002/ctm2.694.

Kalabis, Jiri, Kenji Oyama, Takaomi Okawa, Hiroshi Nakagawa, Carmen Z. Michaylira, Douglas B. Stairs, Jose-Luiz Figueiredo, Umar Mahmood, J. Alan Diehl, Meenhard Herlyn, and Anil K. Rustgi. 2008. "A Subpopulation of Mouse Esophageal Basal Cells Has Properties of Stem Cells with the Capacity for Self-Renewal and Lineage Specification." *The Journal of Clinical Investigation* 118(12):3860–69. doi: 10.1172/JCI35012.

Kanehisa, M., and S. Goto. 2000. "KEGG: Kyoto Encyclopedia of Genes and Genomes." *Nucleic Acids Research* 28(1):27–30. doi: 10.1093/nar/28.1.27.

Kang, Hyun Min, Meena Subramaniam, Sasha Targ, Michelle Nguyen, Lenka Maliskova, Elizabeth McCarthy, Eunice Wan, Simon Wong, Lauren Byrnes, Cristina M. Lanata, Rachel E. Gate, Sara Mostafavi, Alexander Marson, Noah Zaitlen, Lindsey A. Criswell, and Chun Jimmie Ye. 2018. "Multiplexed Droplet Single-Cell RNA-Sequencing Using Natural Genetic Variation." *Nature Biotechnology* 36(1):89–94. doi: 10.1038/nbt.4042.

Karam, Sherif M., Rony John, David H. Alpers, and Abdul Samad Ponery. 2005. "Retinoic Acid Stimulates the Dynamics of Mouse Gastric Epithelial Progenitors." *Stem Cells (Dayton, Ohio)* 23(3):433–41. doi: 10.1634/stemcells.2004-0178.

Kasagi, Yuta, Prasanna M. Chandramouleeswaran, Kelly A. Whelan, Koji Tanaka, Veronique Giroux, Medha Sharma, Joshua Wang, Alain J. Benitez, Maureen DeMarshall, John W. Tobias, Kathryn E. Hamilton, Gary W. Falk, Jonathan M. Spergel, Andres J. Klein-Szanto, Anil K. Rustgi, Amanda B. Muir, and Hiroshi Nakagawa. 2018. "The Esophageal Organoid System Reveals Functional Interplay Between Notch and Cytokines in Reactive Epithelial Changes." *Cellular and Molecular Gastroenterology and Hepatology* 5(3):333–52. doi: 10.1016/j.jcmgh.2017.12.013.

Kessler, Mirjana, Karen Hoffmann, Volker Brinkmann, Oliver Thieck, Susan Jackisch, Benjamin Toelle, Hilmar Berger, Hans-Joachim Mollenkopf, Mandy Mangler, Jalid Sehouli, Christina Fotopoulou, and Thomas F. Meyer. 2015. "The Notch and Wnt Pathways Regulate Stemness and Differentiation in Human Fallopian Tube Organoids." *Nature Communications* 6:8989. doi: 10.1038/ncomms9989.

van Keymeulen, Alexandra, Ana Sofia Rocha, Marielle Ousset, Benjamin Beck, Gaëlle Bouvencourt, Jason Rock, Neha Sharma, Sophie Dekoninck, and Cédric Blanpain. 2011. "Distinct Stem Cells Contribute to Mammary Gland Development and Maintenance." *Nature* 479(7372):189–93. doi: 10.1038/nature10573.

Kim, Eugene, Ming Jiang, Huachao Huang, Yongchun Zhang, Natalie Tjota, Xia Gao, Jacques Robert, Nikesha Gilmore, Lin Gan, and Jianwen Que. 2019. "Isl1 Regulation of Nkx2.1 in the Early Foregut Epithelium Is Required for Trachea-Esophageal Separation and Lung Lobation." *Developmental Cell* 51(6):675-683.e4. doi: 10.1016/j.devcel.2019.11.002.

Kim, Jihoon, Bon-Kyoung Koo, and Juergen A. Knoblich. 2020. "Human Organoids: Model Systems for Human Biology and Medicine." *Nature Reviews. Molecular Cell Biology* 21(10):571–84. doi: 10.1038/s41580-020-0259-3.

Kim, Seyun, Pauline Wong, and Pierre A. Coulombe. 2006. "A Keratin Cytoskeletal Protein Regulates Protein Synthesis and Epithelial Cell Growth." *Nature* 441(7091):362–65. doi: 10.1038/nature04659.

Kleinman, H. K., M. L. McGarvey, J. R. Hassell, V. L. Star, F. B. Cannon, G. W. Laurie, and G. R. Martin. 1986. "Basement Membrane Complexes with Biological Activity." *Biochemistry* 25(2):312–18. doi: 10.1021/bi00350a005.

Kolterud, Asa, Ann S. Grosse, William J. Zacharias, Katherine D. Walton, Katherine E. Kretovich, Blair B. Madison, Meghna Waghray, Jennifer E. Ferris, Chunbo Hu, Juanita L. Merchant, Andrzej A. Dlugosz, Andreas H. Kottmann, and Deborah L. Gumucio. 2009. "Paracrine Hedgehog Signaling in Stomach and Intestine: New Roles for Hedgehog in Gastrointestinal Patterning." *Gastroenterology* 137(2):618–28. doi: 10.1053/j.gastro.2009.05.002.

Komekado, Hideyuki, Hideki Yamamoto, Tsutomu Chiba, and Akira Kikuchi. 2007. "Glycosylation and Palmitoylation of Wnt-3a Are Coupled to Produce an Active Form of Wnt-3a." *Genes to Cells : Devoted to Molecular & Cellular Mechanisms* 12(4):521–34. doi: 10.1111/j.1365-2443.2007.01068.x.

Kong, Jianping, Mary Ann Crissey, Shinsuke Funakoshi, James L. Kreindler, and John P. Lynch. 2011. "Ectopic Cdx2 Expression in Murine Esophagus Models an Intermediate Stage in the Emergence of Barrett's Esophagus." *PloS One* 6(4):e18280. doi: 10.1371/journal.pone.0018280.

Korbut, Edyta, Vincent T. Janmaat, Mateusz Wierdak, Jerzy Hankus, Dagmara Wójcik, Marcin Surmiak, Katarzyna Magierowska, Tomasz Brzozowski, Maikel P. Peppelenbosch, and Marcin Magierowski. 2020. "Molecular Profile of Barrett's Esophagus and Gastroesophageal Reflux Disease in the Development of Translational Physiological and Pharmacological Studies." *International Journal of Molecular Sciences* 21(17). doi: 10.3390/ijms21176436.

Kosinski, Cynthia, Vivian S. W. Li, Annie S. Y. Chan, Ji Zhang, Coral Ho, Wai Yin Tsui, Tsun Leung Chan, Randy C. Mifflin, Don W. Powell, Siu Tsan Yuen, Suet Yi Leung, and Xin Chen. 2007. "Gene Expression Patterns of Human Colon Tops and Basal Crypts and BMP Antagonists as Intestinal Stem Cell Niche Factors." *Proceedings of the National Academy of Sciences of the United States of America* 104(39):15418–23. doi: 10.1073/pnas.0707210104.

Kosoff, Rachelle E., Kristin L. Gardiner, Lauren M. F. Merlo, Kirill Pavlov, Anil K. Rustgi, and Carlo C. Maley. 2012. "Development and Characterization of an Organotypic Model of Barrett's Esophagus." *Journal of Cellular Physiology*. doi: 10.1002/jcp.23007.

Koster, Maranke I., Soeun Kim, Alea A. Mills, Francesco J. DeMayo, and Dennis R. Roop. 2004. "P63 Is the Molecular Switch for Initiation of an Epithelial Stratification Program." *Genes & Development* 18(2):126–31. doi: 10.1101/gad.1165104.

Koterazawa, Yasufumi, Michiyo Koyanagi-Aoi, Keiichiro Uehara, Yoshihiro Kakeji, and Takashi Aoi. 2020. "Retinoic Acid Receptor γ Activation Promotes Differentiation of Human Induced Pluripotent Stem Cells into Esophageal Epithelium." *Journal of Gastroenterology* 55(8):763–74. doi: 10.1007/s00535-020-01695-7.

Kubo, Ai, and Douglas A. Corley. 2007. "Meta-Analysis of Antioxidant Intake and the Risk of Esophageal and Gastric Cardia Adenocarcinoma." *The American Journal of Gastroenterology* 102(10):2323–30; quiz 2331. doi: 10.1111/j.1572-0241.2007.01374.x.

de Lau, Wim, Weng Chuan Peng, Piet Gros, and Hans Clevers. 2014. "The R-Spondin/Lgr5/Rnf43 Module: Regulator of Wnt Signal Strength." *Genes & Development* 28(4):305–16. doi: 10.1101/gad.235473.113.

Lee, Yoomi, Aleksandra M. Urbanska, Yoku Hayakawa, Hongshan Wang, Andrew S. Au, Aesis M. Luna, Wenju Chang, Guangchun Jin, Govind Bhagat, Julian A. Abrams, Richard A. Friedman, Andrea Varro, Kenneth K. Wang, Malcolm Boyce, Anil K. Rustgi, Antonia R. Sepulveda, Michael Quante, and Timothy C. Wang. 2017. "Gastrin Stimulates a

Cholecystokinin-2-Receptor-Expressing Cardia Progenitor Cell and Promotes Progression of Barrett's-like Esophagus." *Oncotarget* 8(1):203–14. doi: 10.18632/oncotarget.10667.

Leedham, S. J., S. L. Preston, S. A. C. McDonald, G. Elia, P. Bhandari, D. Poller, R. Harrison, M. R. Novelli, J. A. Jankowski, and N. A. Wright. 2008. "Individual Crypt Genetic Heterogeneity and the Origin of Metaplastic Glandular Epithelium in Human Barrett's Oesophagus." *Gut* 57(8):1041–48. doi: 10.1136/gut.2007.143339.

Lei, Nan Ye, Ziyad Jabaji, Jiafang Wang, Vaidehi S. Joshi, Garrett J. Brinkley, Hassan Khalil, Fengchao Wang, Artur Jaroszewicz, Matteo Pellegrini, Linheng Li, Michael Lewis, Matthias Stelzner, James C. Y. Dunn, and Martín G. Martín. 2014. "Intestinal Subepithelial Myofibroblasts Support the Growth of Intestinal Epithelial Stem Cells." *PloS One* 9(1):e84651. doi: 10.1371/journal.pone.0084651.

Leushacke, Marc, Si Hui Tan, Angeline Wong, Yada Swathi, Amin Hajamohideen, Liang Thing Tan, Jasmine Goh, Esther Wong, Simon L. I. J. Denil, Kazuhiro Murakami, and Nick Barker. 2017. "Lgr5-Expressing Chief Cells Drive Epithelial Regeneration and Cancer in the Oxyntic Stomach." *Nature Cell Biology* 19(7):774–86. doi: 10.1038/ncb3541.

Levine, David M., Weronica E. Ek, Rui Zhang, Xinxue Liu, Lynn Onstad, Cassandra Sather, Pierre Lao-Sirieix, Marilie D. Gammon, Douglas A. Corley, Nicholas J. Shaheen, Nigel C. Bird, Laura J. Hardie, Liam J. Murray, Brian J. Reid, Wong-Ho Chow, Harvey A. Risch, Olof Nyrén, Weimin Ye, Geoffrey Liu, Yvonne Romero, Leslie Bernstein, Anna H. Wu, Alan G. Casson, Stephen J. Chanock, Patricia Harrington, Isabel Caldas, Irene Debiram-Beecham, Carlos Caldas, Nicholas K. Hayward, Paul D. Pharoah, Rebecca C. Fitzgerald, Stuart Macgregor, David C. Whiteman, and Thomas L. Vaughan. 2013. "A Genome-Wide Association Study Identifies New Susceptibility Loci for Esophageal Adenocarcinoma and Barrett's Esophagus." *Nature Genetics* 45(12):1487–93. doi: 10.1038/ng.2796.

Li, Na, Liwen Wei, Xiaoyu Liu, Hongjun Bai, Yvonne Ye, Dan Li, Nan Li, Ulrich Baxa, Qun Wang, Ling Lv, Yun Chen, Mingqian Feng, Byungkook Lee, Wei Gao, and Mitchell Ho. 2019. "A Frizzled-Like Cysteine-Rich Domain in Glypican-3 Mediates Wnt Binding and Regulates Hepatocellular Carcinoma Tumor Growth in Mice." *Hepatology (Baltimore, Md.)* 70(4):1231–45. doi: 10.1002/hep.30646.

Li, Xiaofeng, Yazhou Zhang, Heeseog Kang, Wenzhong Liu, Peng Liu, Jianghong Zhang, Stephen E. Harris, and Dianqing Wu. 2005. "Sclerostin Binds to LRP5/6 and Antagonizes Canonical Wnt Signaling." *The Journal of Biological Chemistry* 280(20):19883–87. doi: 10.1074/jbc.M413274200.

Li, Xing, Blair B. Madison, William Zacharias, Asa Kolterud, David States, and Deborah L. Gumucio. 2007. "Deconvoluting the Intestine: Molecular Evidence for a Major Role of the Mesenchyme in the Modulation of Signaling Cross Talk." *Physiological Genomics* 29(3):290–301. doi: 10.1152/physiolgenomics.00269.2006.

Lin, Hsien-Yi, and Liang-Tung Yang. 2013. "Differential Response of Epithelial Stem Cell Populations in Hair Follicles to TGF-β Signaling." *Developmental Biology* 373(2):394–406. doi: 10.1016/j.ydbio.2012.10.021.

Liu, Zhun, Shaobin Yu, Shuting Ye, Zhimin Shen, Lei Gao, Ziyang Han, Peipei Zhang, Fei Luo, Sui Chen, and Mingqiang Kang. 2020. "Keratin 17 Activates AKT Signalling and Induces Epithelial-Mesenchymal Transition in Oesophageal Squamous Cell Carcinoma." *Journal of Proteomics* 211:103557. doi: 10.1016/j.jprot.2019.103557.

Livak, K. J., and T. D. Schmittgen. 2001. "Analysis of Relative Gene Expression Data Using Real-Time Quantitative PCR and the 2(-Delta Delta C(T)) Method." *Methods (San Diego, Calif.)* 25(4):402–8. doi: 10.1006/meth.2001.1262.

Lojk, Jasna, and Janja Marc. 2021. "Roles of Non-Canonical Wnt Signalling Pathways in Bone Biology." *International Journal of Molecular Sciences* 22(19). doi: 10.3390/ijms221910840.

Lörinc, Ester, and Stefan Öberg. 2012. "Submucosal Glands in the Columnar-Lined Oesophagus: Evidence of an Association with Metaplasia and Neosquamous Epithelium." *Histopathology* 61(1):53–58. doi: 10.1111/j.1365-2559.2012.04180.x.

Lotan, R. 1997. "Retinoids and Chemoprevention of Aerodigestive Tract Cancers." *Cancer Metastasis Reviews* 16(3–4):349–56. doi: 10.1023/a:1005808429176.

Luciano, L., and E. Reale. 1992. "The 'Limiting Ridge' of the Rat Stomach." *Archives of Histology and Cytology* 55 Suppl:131–38. doi: 10.1679/aohc.55.suppl_131.

Lukić, Marko, Ana Segec, Igor Segec, Ljerka Pinotić, Kregimir Pinotić, Bruno Atalić, Kresiimir Solić, and Aleksandar Vcev. 2012. "The Impact of the Vitamins A, C and E in the Prevention of Gastroesophageal Reflux Disease, Barrett's Oesophagus and Oesophageal Adenocarcinoma." *Collegium Antropologicum* 36(3):867–72.

Macosko, Evan Z., Anindita Basu, Rahul Satija, James Nemesh, Karthik Shekhar, Melissa Goldman, Itay Tirosh, Allison R. Bialas, Nolan Kamitaki, Emily M. Martersteck, John J. Trombetta, David A. Weitz, Joshua R. Sanes, Alex K. Shalek, Aviv Regev, and Steven A. McCarroll. 2015. "Highly Parallel Genome-Wide Expression Profiling of Individual Cells Using Nanoliter Droplets." *Cell* 161(5):1202–14. doi: 10.1016/j.cell.2015.05.002.

Madisen, Linda, Theresa A. Zwingman, Susan M. Sunkin, Seung Wook Oh, Hatim A. Zariwala, Hong Gu, Lydia L. Ng, Richard D. Palmiter, Michael J. Hawrylycz, Allan R. Jones, Ed S. Lein, and Hongkui Zeng. 2010. "A Robust and High-Throughput Cre Reporting and Characterization System for the Whole Mouse Brain." *Nature Neuroscience* 13(1):133–40. doi: 10.1038/nn.2467.

Mao, B., W. Wu, Y. Li, D. Hoppe, P. Stannek, A. Glinka, and C. Niehrs. 2001. "LDL-Receptor-Related Protein 6 Is a Receptor for Dickkopf Proteins." *Nature* 411(6835):321–25. doi: 10.1038/35077108.

Mao, Bingyu, and Christof Niehrs. 2003. "Kremen2 Modulates Dickkopf2 Activity during Wnt/LRP6 Signaling." *Gene* 302(1–2):179–83. doi: 10.1016/s0378-1119(02)01106-x.

Marshall, R. E., A. Anggiansah, C. L. Anggiansah, W. A. Owen, and W. J. Owen. 1999. "Esophageal Body Length, Lower Esophageal Sphincter Length, Position and Pressure in Health and Disease." *Diseases of the Esophagus : Official Journal of the International Society for Diseases of the Esophagus* 12(4):297–302. doi: 10.1046/j.1442-2050.1999.00060.x.

Matsumoto, Michinaga, Hirokazu Yokoyama, Hidekazu Suzuki, Haruko Shiraishi-Yokoyama, and Toshifumi Hibi. 2005. "Retinoic Acid Formation from Retinol in the Human Gastric Mucosa: Role of Class IV Alcohol Dehydrogenase and Its Relevance to Morphological Changes." *American Journal of Physiology. Gastrointestinal and Liver Physiology* 289(3):G429-33. doi: 10.1152/ajpgi.00502.2004.

Mazzalupo, Stacy, Pauline Wong, Paul Martin, and Pierre A. Coulombe. 2003. "Role for Keratins 6 and 17 during Wound Closure in Embryonic Mouse Skin." *Developmental Dynamics : An Official Publication of the American Association of Anatomists* 226(2):356–65. doi: 10.1002/dvdy.10245.

McDonald, Stuart A. C., Trevor A. Graham, Danielle L. Lavery, Nicholas A. Wright, and Marnix Jansen. 2015. "The Barrett's Gland in Phenotype Space." *Cellular and Molecular Gastroenterology and Hepatology* 1(1):41–54. doi: 10.1016/j.jcmgh.2014.10.001.

McDonald, Stuart A. C., Danielle Lavery, Nicholas A. Wright, and Marnix Jansen. 2015. "Barrett Oesophagus: Lessons on Its Origins from the Lesion Itself." *Nature Reviews. Gastroenterology & Hepatology* 12(1):50–60. doi: 10.1038/nrgastro.2014.181.

McGinnis, Christopher S., David M. Patterson, Juliane Winkler, Daniel N. Conrad, Marco Y. Hein, Vasudha Srivastava, Jennifer L. Hu, Lyndsay M. Murrow, Jonathan S. Weissman, Zena Werb, Eric D. Chow, and Zev J. Gartner. 2019. "MULTI-Seq: Sample Multiplexing for Single-Cell RNA Sequencing Using Lipid-Tagged Indices." *Nature Methods* 16(7):619–26. doi: 10.1038/s41592-019-0433-8.

Mikels, A. J., and R. Nusse. 2006. "Wnts as Ligands: Processing, Secretion and Reception." *Oncogene* 25(57):7461–68. doi: 10.1038/sj.onc.1210053.

Milano, Francesca, Jantine W. P. M. van Baal, Navtej S. Buttar, Agnieszka M. Rygiel, Floor de Kort, Cathrine J. DeMars, Wilda D. Rosmolen, Jacques J. G. H. M. Bergman, Jan van Marle, Kenneth K. Wang, Maikel P. Peppelenbosch, and Kausilia K. Krishnadath. 2007. "Bone Morphogenetic Protein 4 Expressed in Esophagitis Induces a Columnar Phenotype in Esophageal Squamous Cells." *Gastroenterology* 132(7):2412–21. doi: 10.1053/j.gastro.2007.03.026.

Minacapelli, Carlos D., Manisha Bajpai, Xin Geng, Christina L. Cheng, Abhishek A. Chouthai, Rhonda Souza, Stuart J. Spechler, and Kiron M. Das. 2017. "Barrett's Metaplasia Develops from Cellular Reprograming of Esophageal Squamous Epithelium Due to Gastroesophageal Reflux." *American Journal of Physiology. Gastrointestinal and Liver Physiology* 312(6):G615–22. doi: 10.1152/ajpgi.00268.2016.

Mischke, D. 1998. "The Complexity of Gene Families Involved in Epithelial Differentiation. Keratin Genes and the Epidermal Differentiation Complex." *Sub-Cellular Biochemistry* 31:71–104.

Mitoyan, Louciné, Véronique Chevrier, Hector Hernandez-Vargas, Alexane Ollivier, Zeinab Homayed, Julie Pannequin, Flora Poizat, Cécile de Biasi-Cador, Emmanuelle Charafe-Jauffret, Christophe Ginestier, and Géraldine Guasch. 2021. "A Stem Cell Population at the Anorectal Junction Maintains Homeostasis and Participates in Tissue Regeneration." *Nature Communications* 12(1):2761. doi: 10.1038/s41467-021-23034-x.

Miyazono, Shoji, Takahito Otani, Kayoko Ogata, Norio Kitagawa, Hiroshi Iida, Yuko Inai, Takashi Matsuura, and Tetsuichiro Inai. 2020. "The Reduced Susceptibility of Mouse Keratinocytes to Retinoic Acid May Be Involved in the Keratinization of Oral and Esophageal Mucosal Epithelium." *Histochemistry and Cell Biology* 153(4):225–37. doi: 10.1007/s00418-020-01845-1.

Moon, Hyeongsun, Jerry Zhu, Leanne R. Donahue, Eunju Choi, and Andrew C. White. 2019. "Krt5+/Krt15+ Foregut Basal Progenitors Give Rise to Cyclooxygenase-2-Dependent Tumours in Response to Gastric Acid Stress." *Nature Communications* 10(1):2225. doi: 10.1038/s41467-019-10194-0.

Moreb, Jan S., Amir Gabr, Govind R. Vartikar, Santosh Gowda, James R. Zucali, and Dagmara Mohuczy. 2005. "Retinoic Acid Down-Regulates Aldehyde Dehydrogenase and Increases Cytotoxicity of 4-Hydroperoxycyclophosphamide and Acetaldehyde." *The Journal of Pharmacology and Experimental Therapeutics* 312(1):339–45. doi: 10.1124/jpet.104.072496.

Mylka, Viacheslav, Irina Matetovici, Suresh Poovathingal, Jeroen Aerts, Niels Vandamme, Ruth Seurinck, Kevin Verstaen, Gert Hulselmans, Silvie van den Hoecke, Isabelle Scheyltjens, Kiavash Movahedi, Hans Wils, Joke Reumers, Jeroen van Houdt, Stein Aerts, and Yvan Saeys. 2022. "Comparative Analysis of Antibody- and Lipid-Based Multiplexing Methods for Single-Cell RNA-Seq." *Genome Biology* 23(1):55. doi: 10.1186/s13059-022-02628-8.

Nakajima, Tadaaki, Tomomi Sato, Taisen Iguchi, and Noboru Takasugi. 2019. "Retinoic Acid Signaling Determines the Fate of the Uterus from the Mouse Müllerian Duct." *Reproductive Toxicology (Elmsford, N.Y.)* 86:56–61. doi: 10.1016/j.reprotox.2019.03.006.

Ng-Blichfeldt, John-Poul, Anneke Schrik, Rosa K. Kortekaas, Jacobien A. Noordhoek, Irene H. Heijink, Pieter S. Hiemstra, Jan Stolk, Melanie Königshoff, and Reinoud Gosens. 2018. "Retinoic Acid Signaling Balances Adult Distal Lung Epithelial Progenitor Cell Growth and Differentiation." *EBioMedicine* 36:461–74. doi: 10.1016/j.ebiom.2018.09.002.

Nguyen, P. H., J. Giraud, C. Staedel, L. Chambonnier, P. Dubus, E. Chevret, H. Bœuf, X. Gauthereau, B. Rousseau, M. Fevre, I. Soubeyran, G. Belleannée, S. Evrard, D. Collet, F. Mégraud, and C. Varon. 2016. "All-Trans Retinoic Acid Targets Gastric Cancer Stem Cells and Inhibits Patient-Derived Gastric Carcinoma Tumor Growth." *Oncogene* 35(43):5619–28. doi: 10.1038/onc.2016.87.

Niederreither, Karen, Valérie Fraulob, Jean-Marie Garnier, Pierre Chambon, and Pascal Dollé. 2002. "Differential Expression of Retinoic Acid-Synthesizing (RALDH) Enzymes during Fetal Development and Organ Differentiation in the Mouse." *Mechanisms of Development* 110(1–2):165–71. doi: 10.1016/s0925-4773(01)00561-5.

Niehrs, C. 2006. "Function and Biological Roles of the Dickkopf Family of Wnt Modulators." *Oncogene* 25(57):7469–81. doi: 10.1038/sj.onc.1210054.

Nowicki-Osuch, Karol, Lizhe Zhuang, Sriganesh Jammula, Christopher W. Bleaney, Krishnaa T. Mahbubani, Ginny Devonshire, Annalise Katz-Summercorn, Nils Eling, Anna Wilbrey-Clark, Elo Madissoon, John Gamble, Massimiliano di Pietro, Maria O'Donovan, Kerstin B. Meyer, Kourosh Saeb-Parsy, Andrew D. Sharrocks, Sarah A. Teichmann, John C. Marioni, and Rebecca C. Fitzgerald. 2021. "Molecular Phenotyping Reveals the Identity of Barrett's Esophagus and Its Malignant Transition." *Science (New York, N.Y.)* 373(6556):760–67. doi: 10.1126/science.abd1449.

Nyeng, Pia, Gitte Anker Norgaard, Sune Kobberup, and Jan Jensen. 2007. "FGF10 Signaling Controls Stomach Morphogenesis." *Developmental Biology* 303(1):295–310. doi: 10.1016/j.ydbio.2006.11.017.

Odze, Robert D. 2005. "Unraveling the Mystery of the Gastroesophageal Junction: A Pathologist's Perspective." *The American Journal of Gastroenterology* 100(8):1853–67. doi: 10.1111/j.1572-0241.2005.50096.x.

Odze, Robert, Stuart J. Spechler, Eitan Podgaetz, Anh Nguyen, Vani Konda, and Rhonda F. Souza. 2021. "Histologic Study of the Esophagogastric Junction of Organ Donors Reveals Novel Glandular Structures in Normal Esophageal and Gastric Mucosae." *Clinical and Translational Gastroenterology* 12(5):e00346. doi: 10.14309/ctg.0000000000000346.

Offield, M. F., T. L. Jetton, P. A. Labosky, M. Ray, R. W. Stein, M. A. Magnuson, B. L. Hogan, and C. v Wright. 1996. "PDX-1 Is Required for Pancreatic Outgrowth and Differentiation of the Rostral Duodenum." *Development (Cambridge, England)* 122(3):983–95. doi: 10.1242/dev.122.3.983.

Ohashi, Shinya, Mitsuteru Natsuizaka, Yumi Yashiro-Ohtani, Ross A. Kalman, Momo Nakagawa, Lizi Wu, Andres J. Klein-Szanto, Meenhard Herlyn, J. Alan Diehl, Jonathan P. Katz, Warren S. Pear, John T. Seykora, and Hiroshi Nakagawa. 2010. "NOTCH1 and NOTCH3 Coordinate Esophageal Squamous Differentiation through a CSL-Dependent Transcriptional Network." *Gastroenterology* 139(6):2113–23. doi: 10.1053/j.gastro.2010.08.040.

Ohkawara, Bisei, Andrei Glinka, and Christof Niehrs. 2011. "Rspo3 Binds Syndecan 4 and Induces Wnt/PCP Signaling via Clathrin-Mediated Endocytosis to Promote Morphogenesis." *Developmental Cell* 20(3):303–14. doi: 10.1016/j.devcel.2011.01.006.

Okumura, Tomoyuki, Yutaka Shimada, Masayuki Imamura, and Shigeru Yasumoto. 2003. "Neurotrophin Receptor P75(NTR) Characterizes Human Esophageal Keratinocyte Stem Cells in Vitro." *Oncogene* 22(26):4017–26. doi: 10.1038/sj.onc.1206525.

O'Neil, Andrew, Christine P Petersen, Eunyoung Choi, Amy C. Engevik, and James R. Goldenring. 2017. "Unique Cellular Lineage Composition of the First Gland of the Mouse Gastric Corpus." *The Journal of Histochemistry and Cytochemistry : Official Journal of the Histochemistry Society* 65(1):47–58. doi: 10.1369/0022155416678182.

O'Riordan, J. M., O. N. Tucker, P. J. Byrne, G. S. A. McDonald, N. Ravi, P. W. N. Keeling, and J. v Reynolds. 2004. "Factors Influencing the Development of Barrett's Epithelium in the Esophageal Remnant Postesophagectomy." *The American Journal of Gastroenterology* 99(2):205–11. doi: 10.1111/j.1572-0241.2004.04057.x.

Owen, Richard Peter, Michael Joseph White, David Tyler Severson, Barbara Braden, Adam Bailey, Robert Goldin, Lai Mun Wang, Carlos Ruiz-Puig, Nicholas David Maynard, Angie Green, Paolo Piazza, David Buck, Mark Ross Middleton, Chris Paul Ponting, Benjamin Schuster-Böckler, and Xin Lu. 2018. "Single Cell RNA-Seq Reveals Profound Transcriptional Similarity between Barrett's Oesophagus and Oesophageal Submucosal Glands." *Nature Communications* 9(1):4261. doi: 10.1038/s41467-018-06796-9.

Palles, Claire, Laura Chegwidden, Xinzhong Li, John M. Findlay, Garry Farnham, Francesc Castro Giner, Maikel P. Peppelenbosch, Michal Kovac, Claire L. Adams, Hans Prenen, Sarah Briggs, Rebecca Harrison, Scott Sanders, David MacDonald, Chris Haigh, Art Tucker, Sharon Love, Manoj Nanji, John deCaestecker, David Ferry, Barrie Rathbone, Julie Hapeshi, Hugh Barr, Paul Moayyedi, Peter Watson, Barbara Zietek, Neera Maroo, Laura Gay, Tim Underwood, Lisa Boulter, Hugh McMurtry, David Monk, Praful Patel, Krish Ragunath, David al Dulaimi, Iain Murray, Konrad Koss, Andrew Veitch, Nigel Trudgill, Chuka Nwokolo, Bjorn Rembacken, Paul Atherfold, Elaine Green, Yeng Ang, Ernst J. Kuipers, Wu Chow, Stuart Paterson, Sudarshan Kadri, Ian Beales, Charles Grimley, Paul Mullins, Conrad Beckett, Mark Farrant, Andrew Dixon, Sean Kelly, Matthew Johnson, Shahjehan Wajed, Anjan Dhar, Elinor Sawyer, Rebecca Roylance, Lynn Onstad, Marilie D. Gammon, Douglas A. Corley, Nicholas J. Shaheen, Nigel C. Bird, Laura J. Hardie, Brian J. Reid, Weimin Ye, Geoffrey Liu, Yvonne Romero, Leslie Bernstein, Anna H. Wu, Alan G. Casson, Rebecca Fitzgerald, David C. Whiteman, Harvey A. Risch, David M. Levine, Tom L. Vaughan, Auke P. Verhaar, Jan van den Brande, Eelke L. Toxopeus, Manon C. Spaander, Bas P. L. Wijnhoven, Luc J. W. van der Laan, Kausilia Krishnadath, Cisca Wijmenga, Gosia Trynka, Ross McManus, John v Reynolds, Jacintha O'Sullivan, Padraic MacMathuna, Sarah A. McGarrigle, Dermot Kelleher, Severine Vermeire, Isabelle Cleynen, Raf Bisschops, Ian Tomlinson, and Janusz Jankowski. 2015. "Polymorphisms near TBX5 and GDF7 Are Associated with Increased Risk for Barrett's Esophagus." *Gastroenterology* 148(2):367–78. doi: 10.1053/j.gastro.2014.10.041.

Persson, Christina, Shizuka Sasazuki, Manami Inoue, Norie Kurahashi, Motoki Iwasaki, Tsutomu Miura, Weimin Ye, Shoichiro Tsugane, and JPHC Study Group. 2008. "Plasma Levels of Carotenoids, Retinol and Tocopherol and the Risk of Gastric Cancer in Japan: A Nested Case-Control Study." *Carcinogenesis* 29(5):1042–48. doi: 10.1093/carcin/bgn072.

Peters, J. M., R. M. McKay, J. P. McKay, and J. M. Graff. 1999. "Casein Kinase I Transduces Wnt Signals." *Nature* 401(6751):345–50. doi: 10.1038/43830.

Phesse, Toby J., and Owen J. Sansom. 2017. "Lgr5 Joins the Club of Gastric Stem Cell Markers in the Corpus." *Nature Cell Biology* 19(7):752–54. doi: 10.1038/ncb3567.

Phillips, Roy W., Henry F. Frierson, and Christopher A. Moskaluk. 2003. "Cdx2 as a Marker of Epithelial Intestinal Differentiation in the Esophagus." *The American Journal of Surgical Pathology* 27(11):1442–47. doi: 10.1097/00000478-200311000-00006.

Piechaczyk, Marc, and Rosa Farràs. 2008. "Regulation and Function of JunB in Cell Proliferation." *Biochemical Society Transactions* 36(Pt 5):864–67. doi: 10.1042/BST0360864.

Pinho, Sonia, and Christof Niehrs. 2007. “Dkk3 Is Required for TGF-Beta Signaling during Xenopus Mesoderm Induction.” *Differentiation; Research in Biological Diversity* 75(10):957–67. doi: 10.1111/j.1432-0436.2007.00185.x.

Plasschaert, Lindsey W., Rapolas Žilionis, Rayman Choo-Wing, Virginia Savova, Judith Knehr, Guglielmo Roma, Allon M. Klein, and Aron B. Jaffe. 2018. “A Single-Cell Atlas of the Airway Epithelium Reveals the CFTR-Rich Pulmonary Ionocyte.” *Nature* 560(7718):377–81. doi: 10.1038/s41586-018-0394-6.

Poturnajova, M., Z. Kozovska, and M. Matuskova. 2021. “Aldehyde Dehydrogenase 1A1 and 1A3 Isoforms - Mechanism of Activation and Regulation in Cancer.” *Cellular Signalling* 87:110120. doi: 10.1016/j.cellsig.2021.110120.

Prunier, Chloé, David Baker, Peter ten Dijke, and Laila Ritsma. 2019. “TGF-β Family Signaling Pathways in Cellular Dormancy.” *Trends in Cancer* 5(1):66–78. doi: 10.1016/j.trecan.2018.10.010.

Quante, Michael, Govind Bhagat, Julian A. Abrams, Frederic Marache, Pamela Good, Michele D. Lee, Yoomi Lee, Richard Friedman, Samuel Asfaha, Zinaida Dubeykovskaya, Umar Mahmood, Jose-Luiz Figueiredo, Jan Kitajewski, Carrie Shawber, Charles J. Lightdale, Anil K. Rustgi, and Timothy C. Wang. 2012. “Bile Acid and Inflammation Activate Gastric Cardia Stem Cells in a Mouse Model of Barrett-like Metaplasia.” *Cancer Cell* 21(1):36–51. doi: 10.1016/j.ccr.2011.12.004.

Que, Jianwen. 2015. “The Initial Establishment and Epithelial Morphogenesis of the Esophagus: A New Model of Tracheal-Esophageal Separation and Transition of Simple Columnar into Stratified Squamous Epithelium in the Developing Esophagus.” *Wiley Interdisciplinary Reviews: Developmental Biology* 4(4):419–30. doi: 10.1002/wdev.179.

Que, Jianwen, Murim Choi, Joshua W. Ziel, John Klingensmith, and Brigid L. M. Hogan. 2006. “Morphogenesis of the Trachea and Esophagus: Current Players and New Roles for Noggin and Bmps.” *Differentiation; Research in Biological Diversity* 74(7):422–37. doi: 10.1111/j.1432-0436.2006.00096.x.

Que, Jianwen, Tadashi Okubo, James R. Goldenring, Ki-Taek Nam, Reiko Kurotani, Edward E. Morrisey, Olena Taranova, Larysa H. Pevny, and Brigid L. M. Hogan. 2007. “Multiple Dose-Dependent Roles for Sox2 in the Patterning and Differentiation of Anterior Foregut Endoderm.” *Development (Cambridge, England)* 134(13):2521–31. doi: 10.1242/dev.003855.

Raghoebir, Lalini, Elvira R. M. Bakker, Jason C. Mills, Sigrid Swagemakers, Marjon Buscop-van Kempen, Anne Boerema-de Munck, Siska Driegen, Dies Meijer, Frank Grosveld, Dick Tibboel, Ron Smits, and Robbert J. Rottier. 2012. “SOX2 Redirects the Developmental Fate of the Intestinal Epithelium toward a Premature Gastric Phenotype.” *Journal of Molecular Cell Biology* 4(6):377–85. doi: 10.1093/jmcb/mjs030.

Ramalho-Santos, M., D. A. Melton, and A. P. McMahon. 2000. “Hedgehog Signals Regulate Multiple Aspects of Gastrointestinal Development.” *Development (Cambridge, England)* 127(12):2763–72. doi: 10.1242/dev.127.12.2763.

Rankin, Scott A., Lu Han, Kyle W. McCracken, Alan P. Kenny, Christopher T. Anglin, Emily A. Grigg, Calyn M. Crawford, James M. Wells, John M. Shannon, and Aaron M. Zorn. 2016. “A Retinoic Acid-Hedgehog Cascade Coordinates Mesoderm-Inducing Signals and Endoderm Competence during Lung Specification.” *Cell Reports* 16(1):66–78. doi: 10.1016/j.celrep.2016.05.060.

Regauer, S., G. R. Seiler, Y. Barrandon, K. W. Easley, and C. C. Compton. 1990. “Epithelial Origin of Cutaneous Anchoring Fibrils.” *The Journal of Cell Biology* 111(5 Pt 1):2109–15. doi: 10.1083/jcb.111.5.2109.

Reid, Brian J., Rumen Kostadinov, and Carlo C. Maley. 2011. “New Strategies in Barrett’s Esophagus: Integrating Clonal Evolutionary Theory with Clinical Management.” *Clinical Cancer Research : An Official Journal of the American Association for Cancer Research* 17(11):3512–19. doi: 10.1158/1078-0432.CCR-09-2358.

Reiss, M., and A. C. Sartorelli. 1987. “Regulation of Growth and Differentiation of Human Keratinocytes by Type Beta Transforming Growth Factor and Epidermal Growth Factor.” *Cancer Research* 47(24 Pt 1):6705–9.

Rexer, B. N., W. L. Zheng, and D. E. Ong. 2001. “Retinoic Acid Biosynthesis by Normal Human Breast Epithelium Is via Aldehyde Dehydrogenase 6, Absent in MCF-7 Cells.” *Cancer Research* 61(19):7065–70.

Rheinwald, J. G., and H. Green. 1975. “Serial Cultivation of Strains of Human Epidermal Keratinocytes: The Formation of Keratinizing Colonies from Single Cells.” *Cell* 6(3):331–43. doi: 10.1016/s0092-8674(75)80001-8.

van de Rijn, Matt, Charles M. Perou, Rob Tibshirani, Phillippe Haas, Olli Kallioniemi, Juha Kononen, Joachim Torhorst, Guido Sauter, Markus Zuber, Ossi R. Köchli, Frank Mross, Holger Dieterich, Rob Seitz, Doug Ross, David Botstein, and Pat Brown. 2002. "Expression of Cytokeratins 17 and 5 Identifies a Group of Breast Carcinomas with Poor Clinical Outcome." *The American Journal of Pathology* 161(6):1991–96. doi: 10.1016/S0002-9440(10)64476-8.

Ritchie, Matthew E., Belinda Phipson, Di Wu, Yifang Hu, Charity W. Law, Wei Shi, and Gordon K. Smyth. 2015. "Limma Powers Differential Expression Analyses for RNA-Sequencing and Microarray Studies." *Nucleic Acids Research* 43(7):e47. doi: 10.1093/nar/gkv007.

Roberts, Catherine. 2020. "Regulating Retinoic Acid Availability during Development and Regeneration: The Role of the CYP26 Enzymes." *Journal of Developmental Biology* 8(1). doi: 10.3390/jdb8010006.

Rock, Jason R., Mark W. Onaitis, Emma L. Rawlins, Yun Lu, Cheryl P. Clark, Yan Xue, Scott H. Randell, and Brigid L. M. Hogan. 2009. "Basal Cells as Stem Cells of the Mouse Trachea and Human Airway Epithelium." *Proceedings of the National Academy of Sciences of the United States of America* 106(31):12771–75. doi: 10.1073/pnas.0906850106.

Rodriguez, P., S. da Silva, L. Oxburgh, F. Wang, B. L. M. Hogan, and J. Que. 2010. "BMP Signaling in the Development of the Mouse Esophagus and Forestomach." *Development*. doi: 10.1242/dev.056077.

Rothnagel, J. A., M. A. Longley, D. S. Bundman, S. L. Naylor, P. A. Lalley, N. A. Jenkins, D. J. Gilbert, N. G. Copeland, and D. R. Roop. 1994. "Characterization of the Mouse Loricrin Gene: Linkage with Profilaggrin and the Flaky Tail and Soft Coat Mutant Loci on Chromosome 3." *Genomics* 23(2):450–56. doi: 10.1006/geno.1994.1522.

Roulis, Manolis, and Richard A. Flavell. 2016. "Fibroblasts and Myofibroblasts of the Intestinal Lamina Propria in Physiology and Disease." *Differentiation; Research in Biological Diversity* 92(3):116–31. doi: 10.1016/j.diff.2016.05.002.

Sadasivam, Subhashini, and James A. DeCaprio. 2013. "The DREAM Complex: Master Coordinator of Cell Cycle-Dependent Gene Expression." *Nature Reviews. Cancer* 13(8):585–95. doi: 10.1038/nrc3556.

Sankoda, Nao, Wataru Tanabe, Akito Tanaka, Hirofumi Shibata, Knut Woltjen, Tsutomu Chiba, Hironori Haga, Yoshiharu Sakai, Masaki Mandai, Takuya Yamamoto, Yasuhiro Yamada, Shinji Uemoto, and Yoshiya Kawaguchi. 2021. "Epithelial Expression of Gata4 and Sox2 Regulates Specification of the Squamous-Columnar Junction via MAPK/ERK Signaling in Mice." *Nature Communications* 12(1):560. doi: 10.1038/s41467-021-20906-0.

Sarosiek, J., and R. W. McCallum. 2000. "Mechanisms of Oesophageal Mucosal Defence." *Bailliere's Best Practice & Research. Clinical Gastroenterology* 14(5):701–17. doi: 10.1053/bega.2000.0119.

Sato, Toshiro, Daniel E. Stange, Marc Ferrante, Robert G. J. Vries, Johan H. van Es, Stieneke van den Brink, Winan J. van Houdt, Apollo Pronk, Joost van Gorp, Peter D. Siersema, and Hans Clevers. 2011. "Long-Term Expansion of Epithelial Organoids from Human Colon, Adenoma, Adenocarcinoma, and Barrett's Epithelium." *Gastroenterology* 141(5):1762–72. doi: 10.1053/j.gastro.2011.07.050.

Sato, Toshiro, Robert G. Vries, Hugo J. Snippert, Marc van de Wetering, Nick Barker, Daniel E. Stange, Johan H. van Es, Arie Abo, Pekka Kujala, Peter J. Peters, and Hans Clevers. 2009. "Single Lgr5 Stem Cells Build Crypt-Villus Structures in Vitro without a Mesenchymal Niche." *Nature* 459(7244):262–65. doi: 10.1038/nature07935.

Sbarbati, A., N. Faccioli, F. Ricci, F. Merigo, D. Benati, G. Castaldini, C. Cordiano, and F. Osculati. 2002. "Ultrastructural Phenotype of 'Intestinal-Type' Cells in Columnar-Lined Esophagus." *Ultrastructural Pathology* 26(2):107–11. doi: 10.1080/01913120252959281.

Scadden, David T. 2006. "The Stem-Cell Niche as an Entity of Action." *Nature* 441(7097):1075–79. doi: 10.1038/nature04957.

Schindler, Adam J., Arisa Watanabe, and Stephen B. Howell. 2018. "LGR5 and LGR6 in Stem Cell Biology and Ovarian Cancer." *Oncotarget* 9(1):1346–55. doi: 10.18632/oncotarget.20178.

Schlaermann, Philipp, Benjamin Toelle, Hilmar Berger, Sven C. Schmidt, Matthias Glanemann, Jürgen Ordemann, Sina Bartfeld, Hans J. Mollenkopf, and Thomas F. Meyer. 2016. "A Novel Human Gastric Primary Cell Culture System for Modelling Helicobacter Pylori Infection in Vitro." *Gut* 65(2):202–13. doi: 10.1136/gutjnl-2014-307949.

Schreiber, D. S., M. Apstein, and J. A. Hermos. 1978. "Paneth Cells in Barrett's Esophagus." *Gastroenterology* 74(6):1302–4.

Schutgens, Frans, and Hans Clevers. 2020. “Human Organoids: Tools for Understanding Biology and Treating Diseases.” *Annual Review of Pathology* 15:211–34. doi: 10.1146/annurev-pathmechdis-012419-032611.

Seery, J. P., and F. M. Watt. 2000. “Asymmetric Stem-Cell Divisions Define the Architecture of Human Oesophageal Epithelium.” *Current Biology : CB* 10(22):1447–50. doi: 10.1016/s0960-9822(00)00803-4.

Seno, H., M. Oshima, M. A. Taniguchi, K. Usami, T. O. Ishikawa, T. Chiba, and M. M. Taketo. 2002. “CDX2 Expression in the Stomach with Intestinal Metaplasia and Intestinal-Type Cancer: Prognostic Implications.” *International Journal of Oncology* 21(4):769–74. doi: 10.3892/ijo.21.4.769.

Shaheen, Nicholas J., Gary W. Falk, Prasad G. Iyer, Lauren B. Gerson, and American College of Gastroenterology. 2016. “ACG Clinical Guideline: Diagnosis and Management of Barrett’s Esophagus.” *The American Journal of Gastroenterology* 111(1):30–50; quiz 51. doi: 10.1038/ajg.2015.322.

Shaulian, Eitan, and Michael Karin. 2002. “AP-1 as a Regulator of Cell Life and Death.” *Nature Cell Biology* 4(5):E131-6. doi: 10.1038/ncb0502-e131.

Shelton, Dawne N., Imelda T. Sandoval, Annie Eisinger, Stephanie Chidester, Anokha Ratnayake, Chris M. Ireland, and David A. Jones. 2006. “Up-Regulation of CYP26A1 in Adenomatous Polyposis Coli-Deficient Vertebrates via a WNT-Dependent Mechanism: Implications for Intestinal Cell Differentiation and Colon Tumor Development.” *Cancer Research* 66(15):7571–77. doi: 10.1158/0008-5472.CAN-06-1067.

Sherwood, Richard I., Tzong-Yang Albert Chen, and Douglas A. Melton. 2009. “Transcriptional Dynamics of Endodermal Organ Formation.” *Developmental Dynamics : An Official Publication of the American Association of Anatomists* 238(1):29–42. doi: 10.1002/dvdy.21810.

Shields, H. M., S. J. Rosenberg, F. R. Zwas, B. J. Ransil, A. J. Lembo, and R. Odze. 2001. “Prospective Evaluation of Multilayered Epithelium in Barrett’s Esophagus.” *The American Journal of Gastroenterology* 96(12):3268–73. doi: 10.1111/j.1572-0241.2001.05324.x.

Shields, H. M., F. Zwas, D. A. Antonioli, W. G. Doos, S. Kim, and S. J. Spechler. 1993. “Detection by Scanning Electron Microscopy of a Distinctive Esophageal Surface Cell at the Junction of Squamous and Barrett’s Epithelium.” *Digestive Diseases and Sciences* 38(1):97–108. doi: 10.1007/BF01296780.

Sigal, Michael, Catriona Y. Logan, Marta Kapalczynska, Hans-Joachim Mollenkopf, Hilmar Berger, Bertram Wiedenmann, Roeland Nusse, Manuel R. Amieva, and Thomas F. Meyer. 2017. “Stromal R-Spondin Orchestrates Gastric Epithelial Stem Cells and Gland Homeostasis.” *Nature* 548(7668):451–55. doi: 10.1038/nature23642.

Singh, Harshabad, Davide Seruggia, Shariq Madha, Madhurima Saxena, Ankur K. Nagaraja, Zhong Wu, Jin Zhou, Aaron J. Huebner, Adrianna Maglieri, Juliette Wezenbeek, Konrad Hochedlinger, Stuart H. Orkin, Adam J. Bass, Jason L. Hornick, and Ramesh A. Shivdasani. 2022. “Transcription Factor-Mediated Intestinal Metaplasia and the Role of a Shadow Enhancer.” *Genes & Development* 36(1–2):38–52. doi: 10.1101/gad.348983.121.

Snider, Erik J., Griselda Compres, Daniel E. Freedberg, Hossein Khiabanian, Yael R. Nobel, Stephania Stump, Anne-Catrin Uhlemann, Charles J. Lightdale, and Julian A. Abrams. 2019. “Alterations to the Esophageal Microbiome Associated with Progression from Barrett’s Esophagus to Esophageal Adenocarcinoma.” *Cancer Epidemiology, Biomarkers & Prevention : A Publication of the American Association for Cancer Research, Cosponsored by the American Society of Preventive Oncology* 28(10):1687–93. doi: 10.1158/1055-9965.EPI-19-0008.

Souza, Rhonda F., and Stuart J. Spechler. 2022. “Mechanisms and Pathophysiology of Barrett Oesophagus.” *Nature Reviews. Gastroenterology & Hepatology* 19(9):605–20. doi: 10.1038/s41575-022-00622-w.

Spechler, Stuart J., Prateek Sharma, Rhonda F. Souza, John M. Inadomi, Nicholas J. Shaheen, and American Gastroenterological Association. 2011. “American Gastroenterological Association Technical Review on the Management of Barrett’s Esophagus.” *Gastroenterology* 140(3):e18-52; quiz e13. doi: 10.1053/j.gastro.2011.01.031.

Spechler, Stuart J., and Rhonda F. Souza. 2014. “Barrett’s Esophagus.” *The New England Journal of Medicine* 371(9):836–45. doi: 10.1056/NEJMra1314704.

Spencer-Dene, Bradley, Frederic G. Sala, Saverio Bellusci, Stephen Gschmeissner, Gordon Stamp, and Clive Dickson. 2006. “Stomach Development Is Dependent on Fibroblast Growth Factor 10/Fibroblast Growth Factor Receptor 2b-Mediated Signaling.” *Gastroenterology* 130(4):1233–44. doi: 10.1053/j.gastro.2006.02.018.

Srivastava, Saumya S., Hunain Alam, Sonam J. Patil, Rashmi Shrinivasan, Sweta Raikundalia, Pratik Rajeev Chaudhari, and Milind M. Vaidya. 2018. "Keratin 5/14-mediated Cell Differentiation and Transformation Are Regulated by TAp63 and Notch-1 in Oral Squamous Cell Carcinoma-derived Cells." *Oncology Reports* 39(5):2393–2401. doi: 10.3892/or.2018.6298.

Stachler, Matthew D., Amaro Taylor-Weiner, Shouyong Peng, Aaron McKenna, Agoston T. Agoston, Robert D. Odze, Jon M. Davison, Katie S. Nason, Massimo Loda, Ignaty Leshchiner, Chip Stewart, Petar Stojanov, Sara Seepo, Michael S. Lawrence, Daysha Ferrer-Torres, Jules Lin, Andrew C. Chang, Stacey B. Gabriel, Eric S. Lander, David G. Beer, Gad Getz, Scott L. Carter, and Adam J. Bass. 2015. "Paired Exome Analysis of Barrett's Esophagus and Adenocarcinoma." *Nature Genetics* 47(9):1047–55. doi: 10.1038/ng.3343.

Staller, Kyle, and Braden Kuo. 2013. "Development, Anatomy, and Physiology of the Esophagus." Pp. 269–86 in *Principles of Deglutition*. New York, NY: Springer New York.

Stange, Daniel E., Bon-Kyoung Koo, Meritxell Huch, Greg Sibbel, Onur Basak, Anna Lyubimova, Pekka Kujala, Sina Bartfeld, Jan Koster, Jessica H. Geahlen, Peter J. Peters, Johan H. van Es, Marc van de Wetering, Jason C. Mills, and Hans Clevers. 2013. "Differentiated Troy+ Chief Cells Act as Reserve Stem Cells to Generate All Lineages of the Stomach Epithelium." *Cell* 155(2):357–68. doi: 10.1016/j.cell.2013.09.008.

Street, Kelly, Davide Risso, Russell B. Fletcher, Diya Das, John Ngai, Nir Yosef, Elizabeth Purdom, and Sandrine Dudoit. 2018. "Slingshot: Cell Lineage and Pseudotime Inference for Single-Cell Transcriptomics." *BMC Genomics* 19(1):477. doi: 10.1186/s12864-018-4772-0.

Su, Zhan, Laura J. Gay, Amy Strange, Claire Palles, Gavin Band, David C. Whiteman, Francesco Lescai, Cordelia Langford, Manoj Nanji, Sarah Edkins, Anouk van der Winkel, David Levine, Peter Sasieni, Céline Bellenguez, Kimberley Howarth, Colin Freeman, Nigel Trudgill, Art T. Tucker, Matti Pirinen, Maikel P. Peppelenbosch, Luc J. W. van der Laan, Ernst J. Kuipers, Joost P. H. Drenth, Wilbert H. Peters, John v Reynolds, Dermot P. Kelleher, Ross McManus, Heike Grabsch, Hans Prenen, Raf Bisschops, Kausila Krishnadath, Peter D. Siersema, Jantine W. P. M. van Baal, Mark Middleton, Russell Petty, Richard Gillies, Nicola Burch, Pradeep Bhandari, Stuart Paterson, Cathryn Edwards, Ian Penman, Kishor Vaidya, Yeng Ang, Iain Murray, Praful Patel, Weimin Ye, Paul Mullins, Anna H. Wu, Nigel C. Bird, Helen Dallal, Nicholas J. Shaheen, Liam J. Murray, Konrad Koss, Leslie Bernstein, Yvonne Romero, Laura J. Hardie, Rui Zhang, Helen Winter, Douglas A. Corley, Simon Panter, Harvey A. Risch, Brian J. Reid, Ian Sargeant, Marilie D. Gammon, Howard Smart, Anjan Dhar, Hugh McMurtry, Haythem Ali, Geoffrey Liu, Alan G. Casson, Wong-Ho Chow, Matt Rutter, Ashref Tawil, Danielle Morris, Chuka Nwokolo, Peter Isaacs, Colin Rodgers, Krish Ragunath, Chris MacDonald, Chris Haigh, David Monk, Gareth Davies, Saj Wajed, David Johnston, Michael Gibbons, Sue Cullen, Nicholas Church, Ruth Langley, Michael Griffin, Derek Alderson, Panos Deloukas, Sarah E. Hunt, Emma Gray, Serge Dronov, Simon C. Potter, Avazeh Tashakkori-Ghanbaria, Mark Anderson, Claire Brooks, Jenefer M. Blackwell, Elvira Bramon, Matthew A. Brown, Juan P. Casas, Aiden Corvin, Audrey Duncanson, Hugh S. Markus, Christopher G. Mathew, Colin N. A. Palmer, Robert Plomin, Anna Rautanen, Stephen J. Sawcer, Richard C. Trembath, Ananth C. Viswanathan, Nicholas Wood, Gosia Trynka, Cisca Wijmenga, Jean-Baptiste Cazier, Paul Atherfold, Anna M. Nicholson, Nichola L. Gellatly, Deborah Glancy, Sheldon C. Cooper, David Cunningham, Tore Lind, Julie Hapeshi, David Ferry, Barrie Rathbone, Julia Brown, Sharon Love, Stephen Attwood, Stuart MacGregor, Peter Watson, Scott Sanders, Weronica Ek, Rebecca F. Harrison, Paul Moayyedi, John de Caestecker, Hugh Barr, Elia Stupka, Thomas L. Vaughan, Leena Peltonen, Chris C. A. Spencer, Ian Tomlinson, Peter Donnelly, Janusz A. Z. Jankowski, Esophageal Adenocarcinoma Genetics Consortium, and Wellcome Trust Case Control Consortium 2. 2012. "Common Variants at the MHC Locus and at Chromosome 16q24.1 Predispose to Barrett's Esophagus." *Nature Genetics* 44(10):1131–36. doi: 10.1038/ng.2408.

Subramanian, Aravind, Pablo Tamayo, Vamsi K. Mootha, Sayan Mukherjee, Benjamin L. Ebert, Michael A. Gillette, Amanda Paulovich, Scott L. Pomeroy, Todd R. Golub, Eric S. Lander, and Jill P. Mesirov. 2005. "Gene Set Enrichment Analysis: A Knowledge-Based Approach for Interpreting Genome-Wide Expression Profiles." *Proceedings of the National Academy of Sciences of the United States of America* 102(43):15545–50. doi: 10.1073/pnas.0506580102.

Surmann-Schmitt, Cordula, Nathalie Widmann, Uwe Dietz, Bernhard Saeger, Nicole Eitzinger, Yukio Nakamura, Marianne Rattel, Richard Latham, Christine Hartmann, Helga von der Mark, Georg Schett, Klaus von der Mark, and Michael Stock. 2009. "Wif-1 Is Expressed at Cartilage-Mesenchyme Interfaces and Impedes Wnt3a-Mediated Inhibition of Chondrogenesis." *Journal of Cell Science* 122(Pt 20):3627–37. doi: 10.1242/jcs.048926.

Szymański, Łukasz, Rafał Skopek, Małgorzata Palusińska, Tino Schenk, Sven Stengel, Sławomir Lewicki, Leszek Kraj, Paweł Kamiński, and Arthur Zelent. 2020. "Retinoic Acid and Its Derivatives in Skin." *Cells* 9(12). doi: 10.3390/cells9122660.

Tamai, Keiko, Xin Zeng, Chunming Liu, Xinjun Zhang, Yuko Harada, Zhijie Chang, and Xi He. 2004. “A Mechanism for Wnt Coreceptor Activation.” *Molecular Cell* 13(1):149–56. doi: 10.1016/s1097-2765(03)00484-2.

Tan, Si Hui, Yada Swathi, Shawna Tan, Jasmine Goh, Ryo Seishima, Kazuhiro Murakami, Masanobu Oshima, Toshikatsu Tsuji, Phyllis Phuah, Liang Thing Tan, Esther Wong, Aliya Fatehullah, Taotao Sheng, Shamaine Wei Ting Ho, Heike I. Grabsch, Supriya Srivastava, Ming Teh, Simon L. I. J. Denil, Seri Mustafah, Patrick Tan, Asim Shabbir, Jimmy So, Khay Guan Yeoh, and Nick Barker. 2020. “AQP5 Enriches for Stem Cells and Cancer Origins in the Distal Stomach.” *Nature* 578(7795):437–43. doi: 10.1038/s41586-020-1973-x.

Tang, Fuchou, Catalin Barbacioru, Yangzhou Wang, Ellen Nordman, Clarence Lee, Nanlan Xu, Xiaohui Wang, John Bodeau, Brian B. Tuch, Asim Siddiqui, Kaiqin Lao, and M. Azim Surani. 2009. “MRNA-Seq Whole-Transcriptome Analysis of a Single Cell.” *Nature Methods* 6(5):377–82. doi: 10.1038/nmeth.1315.

Tang, Xiao-Han, and Lorraine J. Gudas. 2011. “Retinoids, Retinoic Acid Receptors, and Cancer.” *Annual Review of Pathology* 6:345–64. doi: 10.1146/annurev-pathol-011110-130303.

al Tanoury, Ziad, Aleksandr Piskunov, and Cécile Rochette-Egly. 2013. “Vitamin A and Retinoid Signaling: Genomic and Nongenomic Effects.” *Journal of Lipid Research* 54(7):1761–75. doi: 10.1194/jlr.R030833.

Tata, Aleksandra, Ryan D. Chow, and Purushothama Rao Tata. 2021. “Epithelial Cell Plasticity: Breaking Boundaries and Changing Landscapes.” *EMBO Reports* 22(7):e51921. doi: 10.15252/embr.202051921.

The Gene Ontology Consortium. 2019. “The Gene Ontology Resource: 20 Years and Still GOing Strong.” *Nucleic Acids Research* 47(D1):D330–38. doi: 10.1093/nar/gky1055.

Todisco, Andrea. 2017. “Regulation of Gastric Metaplasia, Dysplasia, and Neoplasia by Bone Morphogenetic Protein Signaling.” *Cmgh* 3(3):339–47. doi: 10.1016/j.jcmgh.2017.01.014.

Törmä, Hans. 2011. “Regulation of Keratin Expression by Retinoids.” *Dermato-Endocrinology* 3(3):136–40. doi: 10.4161/derm.3.3.15026.

Tosh, David, and Jonathan M. W. Slack. 2002. “How Cells Change Their Phenotype.” *Nature Reviews. Molecular Cell Biology* 3(3):187–94. doi: 10.1038/nrm761.

Trisno, Stephen L., Katherine E. D. Philo, Kyle W. McCracken, Emily M. Catá, Sonya Ruiz-Torres, Scott A. Rankin, Lu Han, Talia Nasr, Praneet Chaturvedi, Marc E. Rothenberg, Mohammad A. Mandegar, Susanne I. Wells, Aaron M. Zorn, and James M. Wells. 2018. “Esophageal Organoids from Human Pluripotent Stem Cells Delineate Sox2 Functions during Esophageal Specification.” *Cell Stem Cell* 23(4):501-515.e7. doi: 10.1016/j.stem.2018.08.008.

Upton, Melissa P., Norman S. Nishioka, Bernard J. Ransil, Stanley J. Rosenberg, William P. Puricelli, Felice R. Zwas, and Helen M. Shields. 2006. “Multilayered Epithelium May Be Found in Patients with Barrett’s Epithelium and Dysplasia or Adenocarcinoma.” *Digestive Diseases and Sciences* 51(10):1783–90. doi: 10.1007/s10620-006-9243-9.

Vega, Maria E., Véronique Giroux, Mitsuteru Natsuizaka, Mingen Liu, Andres J. Klein-Szanto, Douglas B. Stairs, Hiroshi Nakagawa, Kenneth K. Wang, Timothy C. Wang, John P. Lynch, and Anil K. Rustgi. 2014. “Inhibition of Notch Signaling Enhances Transdifferentiation of the Esophageal Squamous Epithelium towards a Barrett’s-like Metaplasia via KLF4.” *Cell Cycle (Georgetown, Tex.)* 13(24):3857–66. doi: 10.4161/15384101.2014.972875.

Vercauteren Drubbel, Alizée, Sheleya Pirard, Simon Kin, Benjamin Dassy, Anne Lefort, Frédérick Libert, Sachiyo Nomura, and Benjamin Beck. 2021. “Reactivation of the Hedgehog Pathway in Esophageal Progenitors Turns on an Embryonic-like Program to Initiate Columnar Metaplasia.” *Cell Stem Cell* 28(8):1411-1427.e7. doi: 10.1016/j.stem.2021.03.019.

Vo, Daniella T., MacKenzie R. Fuller, Courtney Tindle, Mahitha Shree Anandachar, Soumita Das, Debashis Sahoo, and Pradipta Ghosh. 2021. “SPT6 Loss Permits the Transdifferentiation of Keratinocytes into an Intestinal Fate That Resembles Barrett’s Metaplasia.” *IScience* 24(10):103121. doi: 10.1016/j.isci.2021.103121.

Vukicevic, S., H. K. Kleinman, F. P. Luyten, A. B. Roberts, N. S. Roche, and A. H. Reddi. 1992. “Identification of Multiple Active Growth Factors in Basement Membrane Matrigel Suggests Caution in Interpretation of Cellular Activity Related to Extracellular Matrix Components.” *Experimental Cell Research* 202(1):1–8. doi: 10.1016/0014-4827(92)90397-q.

Wang, David H., Nicholas J. Clemons, Tomoharu Miyashita, Adam J. Dupuy, Wei Zhang, Anette Szczepny, Ian M. Corcoran-Schwartz, Daniel L. Wilburn, Elizabeth A. Montgomery, Jean S. Wang, Nancy A. Jenkins, Neal A. Copeland, John W. Harmon, Wayne A. Phillips, and D. Neil Watkins. 2010. "Aberrant Epithelial-Mesenchymal Hedgehog Signaling Characterizes Barrett's Metaplasia." *Gastroenterology* 138(5):1810–22. doi: 10.1053/j.gastro.2010.01.048.

Wang, David H., Anjana Tiwari, Monica E. Kim, Nicholas J. Clemons, Nanda L. Regmi, William A. Hodges, David M. Berman, Elizabeth A. Montgomery, D. Neil Watkins, Xi Zhang, Qiuyang Zhang, Chunfa Jie, Stuart J. Spechler, and Rhonda F. Souza. 2014. "Hedgehog Signaling Regulates FOXA2 in Esophageal Embryogenesis and Barrett's Metaplasia." *The Journal of Clinical Investigation* 124(9):3767–80. doi: 10.1172/JCI66603.

Wang, Qiao-Li, Shao-Hua Xie, Karl Wahlin, and Jesper Lagergren. 2018. "Global Time Trends in the Incidence of Esophageal Squamous Cell Carcinoma." *Clinical Epidemiology* 10:717–28. doi: 10.2147/CLEP.S166078.

Wang, Qin, Andrew J. Symes, Corrina A. Kane, Alex Freeman, Joseph Nariculam, Philippa Munson, Christopher Thrasivoulou, John R. W. Masters, and Aamir Ahmed. 2010. "A Novel Role for Wnt/Ca2+ Signaling in Actin Cytoskeleton Remodeling and Cell Motility in Prostate Cancer." *PloS One* 5(5):e10456. doi: 10.1371/journal.pone.0010456.

Wang, Xia, Hong Ouyang, Yusuke Yamamoto, Pooja Ashok Kumar, Tay Seok Wei, Rania Dagher, Matthew Vincent, Xin Lu, Andrew M. Bellizzi, Khek Yu Ho, Christopher P. Crum, Wa Xian, and Frank McKeon. 2011. "Residual Embryonic Cells as Precursors of a Barrett's-like Metaplasia." *Cell* 145(7):1023–35. doi: 10.1016/j.cell.2011.05.026.

Wang, Xiaolei, Jesung Moon, Michael E. Dodge, Xinchao Pan, Lishu Zhang, Jordan M. Hanson, Rubina Tuladhar, Zhiqiang Ma, Heping Shi, Noelle S. Williams, James F. Amatruda, Thomas J. Carroll, Lawrence Lum, and Chuo Chen. 2013. "The Development of Highly Potent Inhibitors for Porcupine." *Journal of Medicinal Chemistry* 56(6):2700–2704. doi: 10.1021/jm400159c.

Wang, Zengxin, Pascal Dollé, Wellington v Cardoso, and Karen Niederreither. 2006. "Retinoic Acid Regulates Morphogenesis and Patterning of Posterior Foregut Derivatives." *Developmental Biology* 297(2):433–45. doi: 10.1016/j.ydbio.2006.05.019.

Wani, Sachin, Srinivas R. Puli, Nicholas J. Shaheen, Brenda Westhoff, Sanjeev Slehria, Ajay Bansal, Amit Rastogi, Hari Sayana, and Prateek Sharma. 2009. "Esophageal Adenocarcinoma in Barrett's Esophagus after Endoscopic Ablative Therapy: A Meta-Analysis and Systematic Review." *The American Journal of Gastroenterology* 104(2):502–13. doi: 10.1038/ajg.2008.31.

Wester, Roelof A., Lisa van Voorthuijsen, Hannah K. Neikes, Jelmer J. Dijkstra, Lieke A. Lamers, Siebren Frölich, Maarten van der Sande, Colin Logie, Rik G. H. Lindeboom, and Michiel Vermeulen. 2021. "Retinoic Acid Signaling Drives Differentiation toward the Absorptive Lineage in Colorectal Cancer." *IScience* 24(12):103444. doi: 10.1016/j.isci.2021.103444.

Westfall, Matthew D., Deborah J. Mays, Joseph C. Sniezek, and Jennifer A. Pietenpol. 2003. "The Delta Np63 Alpha Phosphoprotein Binds the P21 and 14-3-3 Sigma Promoters in Vivo and Has Transcriptional Repressor Activity That Is Reduced by Hay-Wells Syndrome-Derived Mutations." *Molecular and Cellular Biology* 23(7):2264–76. doi: 10.1128/MCB.23.7.2264-2276.2003.

Weusten, Bas, Raf Bisschops, Emanuel Coron, Mário Dinis-Ribeiro, Jean-Marc Dumonceau, José-Miguel Esteban, Cesare Hassan, Oliver Pech, Alessandro Repici, Jacques Bergman, and Massimiliano di Pietro. 2017. "Endoscopic Management of Barrett's Esophagus: European Society of Gastrointestinal Endoscopy (ESGE) Position Statement." *Endoscopy* 49(2):191–98. doi: 10.1055/s-0042-122140.

Willert, Karl, Jeffrey D. Brown, Esther Danenberg, Andrew W. Duncan, Irving L. Weissman, Tannishtha Reya, John R. Yates, and Roel Nusse. 2003. "Wnt Proteins Are Lipid-Modified and Can Act as Stem Cell Growth Factors." *Nature* 423(6938):448–52. doi: 10.1038/nature01611.

Willert, Karl, and Roel Nusse. 2012. "Wnt Proteins." *Cold Spring Harbor Perspectives in Biology* 4(9):a007864. doi: 10.1101/cshperspect.a007864.

Willet, Spencer G., and Jason C. Mills. 2016. "Stomach Organ and Cell Lineage Differentiation: From Embryogenesis to Adult Homeostasis." *Cellular and Molecular Gastroenterology and Hepatology* 2(5):546–59. doi: 10.1016/j.jcmgh.2016.05.006.

Wong, W. M., G. W. Stamp, G. Elia, R. Poulsom, and N. A. Wright. 2000. "Proliferative Populations in Intestinal Metaplasia: Evidence of Deregulation in Paneth and Goblet Cells, but Not Endocrine Cells." *The Journal of Pathology* 190(1):107–13. doi: 10.1002/(SICI)1096-9896(200001)190:1<107::AID-PATH504>3.0.CO;2-V.

Woo, Janghee, Isabelle Miletich, Byeong-Moo Kim, Paul T. Sharpe, and Ramesh A. Shivdasani. 2011. "Barx1-Mediated Inhibition of Wnt Signaling in the Mouse Thoracic Foregut Controls Tracheo-Esophageal Septation and Epithelial Differentiation." *PloS One* 6(7):e22493. doi: 10.1371/journal.pone.0022493.

Xiao, Shiyu, and Liya Zhou. 2020. "Gastric Stem Cells: Physiological and Pathological Perspectives." *Frontiers in Cell and Developmental Biology* 8:571536. doi: 10.3389/fcell.2020.571536.

Xie, Fa-Jun, Yi-Ping Zhang, Qiu-Qing Zheng, Hong-Chuan Jin, Fa-Liang Wang, Ming Chen, Lan Shao, De-Hong Zou, Xin-Min Yu, and Wei-Min Mao. 2013. "Helicobacter Pylori Infection and Esophageal Cancer Risk: An Updated Meta-Analysis." *World Journal of Gastroenterology* 19(36):6098–6107. doi: 10.3748/wjg.v19.i36.6098.

Xu, L., C. K. Glass, and M. G. Rosenfeld. 1999. "Coactivator and Corepressor Complexes in Nuclear Receptor Function." *Current Opinion in Genetics & Development* 9(2):140–47. doi: 10.1016/S0959-437X(99)80021-5.

Yamamoto, Yusuke, Xia Wang, Denis Bertrand, Florian Kern, Ting Zhang, Marcin Duleba, Supriya Srivastava, Chiea Chuen Khor, Yuanyu Hu, Lane H. Wilson, Hagen Blaszyk, Daniil Rolshud, Ming Teh, Jianjun Liu, Brooke E. Howitt, Matthew Vincent, Christopher P. Crum, Niranjan Nagarajan, Khek Yu Ho, Frank McKeon, and Wa Xian. 2016. "Mutational Spectrum of Barrett's Stem Cells Suggests Paths to Initiation of a Precancerous Lesion." *Nature Communications* 7:10380. doi: 10.1038/ncomms10380.

Yang, A., M. Kaghad, Y. Wang, E. Gillett, M. D. Fleming, V. Dötsch, N. C. Andrews, D. Caput, and F. McKeon. 1998. "P63, a P53 Homolog at 3q27-29, Encodes Multiple Products with Transactivating, Death-Inducing, and Dominant-Negative Activities." *Molecular Cell* 2(3):305–16. doi: 10.1016/s1097-2765(00)80275-0.

Yang, A., R. Schweitzer, D. Sun, M. Kaghad, N. Walker, R. T. Bronson, C. Tabin, A. Sharpe, D. Caput, C. Crum, and F. McKeon. 1999. "P63 Is Essential for Regenerative Proliferation in Limb, Craniofacial and Epithelial Development." *Nature* 398(6729):714–18. doi: 10.1038/19539.

Yang, Liying, Xiaohua Lu, Carlos W. Nossa, Fritz Francois, Richard M. Peek, and Zhiheng Pei. 2009. "Inflammation and Intestinal Metaplasia of the Distal Esophagus Are Associated with Alterations in the Microbiome." *Gastroenterology* 137(2):588–97. doi: 10.1053/j.gastro.2009.04.046.

Yang, Min, Min Wang, Xianping Li, Yixin Xie, Xiaomeng Xia, Jingjing Tian, Kan Zhang, and Aiguo Tang. 2018. "Wnt Signaling in Cervical Cancer?" *Journal of Cancer* 9(4):659–68. doi: 10.7150/jca.22005.

Yang, Yingzi, and Marek Mlodzik. 2015. "Wnt-Frizzled/Planar Cell Polarity Signaling: Cellular Orientation by Facing the Wind (Wnt)." *Annual Review of Cell and Developmental Biology* 31:623–46. doi: 10.1146/annurev-cellbio-100814-125315.

al Yassin, T. M., and P. G. Toner. 1977. "Fine Structure of Squamous Epitheilum and Submucosal Glands of Human Oesophagus." *Journal of Anatomy* 123(Pt 3):705–21.

Yazaki, E., and D. Sifrim. 2012. "Anatomy and Physiology of the Esophageal Body." *Diseases of the Esophagus : Official Journal of the International Society for Diseases of the Esophagus* 25(4):292–98. doi: 10.1111/j.1442-2050.2011.01180.x.

Yip, Y. L., and S. W. Tsao. 2008. "Regulation of P63 Expression in Primary and Immortalized Nasopharyngeal Epithelial Cells." *International Journal of Oncology* 33(4):713–24. doi: 10.3892/ijo_00000057.

Yu, Wei-Yuan, Jonathan M. W. Slack, and David Tosh. 2005. "Conversion of Columnar to Stratified Squamous Epithelium in the Developing Mouse Oesophagus." *Developmental Biology* 284(1):157–70. doi: 10.1016/j.ydbio.2005.04.042.

Yuan, Dumin, Zhiyuan Ma, Biguang Tuo, Taolang Li, and Xuemei Liu. 2020. "Physiological Significance of Ion Transporters and Channels in the Stomach and Pathophysiological Relevance in Gastric Cancer." *Evidence-Based Complementary and Alternative Medicine : ECAM* 2020:2869138. doi: 10.1155/2020/2869138.

Zagami, Claudia, Diana Papp, Alice Anna Daddi, and Francesco Boccellato. 2022. "Morphogen Signals Shaping the Gastric Glands in Health and Disease." *International Journal of Molecular Sciences* 23(7). doi: 10.3390/ijms23073632.

Zhan, T., N. Rindtorff, and M. Boutros. 2017. “Wnt Signaling in Cancer.” *Oncogene* 36(11):1461–73. doi: 10.1038/onc.2016.304.

Zhang, Xiaowei, Meimei Yin, and Ling-Juan Zhang. 2019. “Keratin 6, 16 and 17-Critical Barrier Alarmin Molecules in Skin Wounds and Psoriasis.” *Cells* 8(8). doi: 10.3390/cells8080807.

Zhang, Xinjun, Seong-Moon Cheong, Nathalia G. Amado, Alice H. Reis, Bryan T. MacDonald, Matthias Zebisch, E. Yvonne Jones, Jose Garcia Abreu, and Xi He. 2015. “Notum Is Required for Neural and Head Induction via Wnt Deacylation, Oxidation, and Inactivation.” *Developmental Cell* 32(6):719–30. doi: 10.1016/j.devcel.2015.02.014.

Zhang, Yongchun, Dominique Bailey, Patrick Yang, Eugene Kim, and Jianwen Que. 2021. “The Development and Stem Cells of the Esophagus.” *Development (Cambridge, England)* 148(6). doi: 10.1242/dev.193839.

Zhang, Yongchun, Ming Jiang, Eugene Kim, Sijie Lin, Kuancan Liu, Xiaopeng Lan, and Jianwen Que. 2017. “Development and Stem Cells of the Esophagus.” *Seminars in Cell & Developmental Biology* 66:25–35. doi: 10.1016/j.semcdb.2016.12.008.

Zhang, Yongchun, and Jianwen Que. 2020. “BMP Signaling in Development, Stem Cells, and Diseases of the Gastrointestinal Tract.” *Annual Review of Physiology* 82:251–73. doi: 10.1146/annurev-physiol-021119-034500.

Zhou, Gang, Yong-Gang Sun, Hong-Bin Wang, Wei-Qiang Wang, Xing-Wei Wang, and Dian-Chun Fang. 2009. “Acid and Bile Salt Up-Regulate BMP4 Expression in Human Esophageal Epithelium Cells.” *Scandinavian Journal of Gastroenterology* 44(8):926–32. doi: 10.1080/00365520902998661.

Zhu, Weidong, Ichiro Shiojima, Yuzuru Ito, Zhi Li, Hiroyuki Ikeda, Masashi Yoshida, Atsuhiko T. Naito, Jun-ichiro Nishi, Hiroo Ueno, Akihiro Umezawa, Tohru Minamino, Toshio Nagai, Akira Kikuchi, Makoto Asashima, and Issei Komuro. 2008. “IGFBP-4 Is an Inhibitor of Canonical Wnt Signalling Required for Cardiogenesis.” *Nature* 454(7202):345–49. doi: 10.1038/nature07027.